



Synthesis of Highly Structured and Receptor-Selective Tetradecapeptidic Analogs of Somatostatin:

Fine-tuning the non-covalent interactions among their aromatic residues

Pablo Martín-Gago

ADVERTIMENT. La consulta d'aquesta tesi queda condicionada a l'acceptació de les següents condicions d'ús: La difusió d'aquesta tesi per mitjà del servei TDX (www.tdx.cat) i a través del Dipòsit Digital de la UB (diposit.ub.edu) ha estat autoritzada pels titulars dels drets de propietat intel·lectual únicament per a usos privats emmarcats en activitats d'investigació i docència. No s'autoritza la seva reproducció amb finalitats de lucre ni la seva difusió i posada a disposició des d'un lloc aliè al servei TDX ni al Dipòsit Digital de la UB. No s'autoritza la presentació del seu contingut en una finestra o marc aliè a TDX o al Dipòsit Digital de la UB (framing). Aquesta reserva de drets afecta tant al resum de presentació de la tesi com als seus continguts. En la utilització o cita de parts de la tesi és obligat indicar el nom de la persona autora.

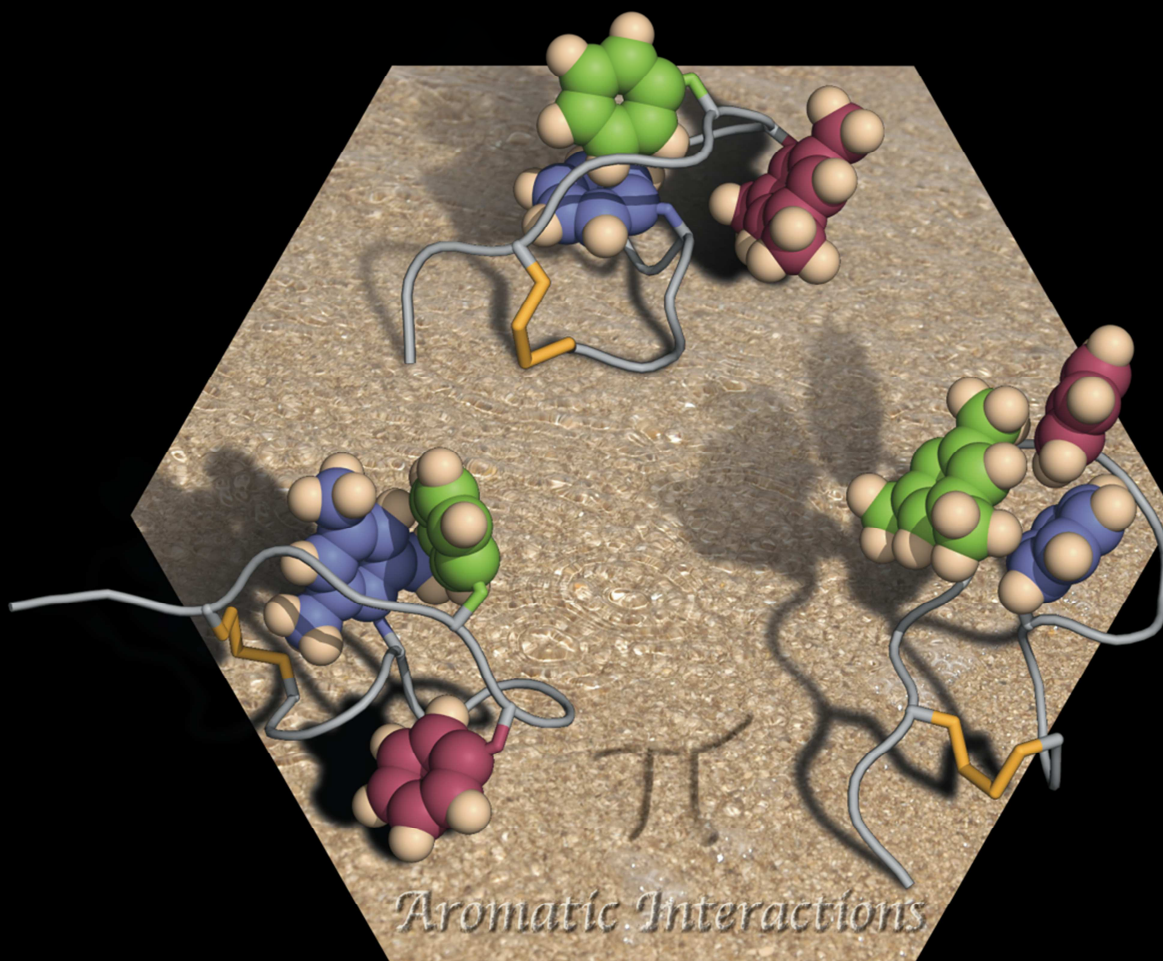
ADVERTENCIA. La consulta de esta tesis queda condicionada a la aceptación de las siguientes condiciones de uso: La difusión de esta tesis por medio del servicio TDR (www.tdx.cat) y a través del Repositorio Digital de la UB (diposit.ub.edu) ha sido autorizada por los titulares de los derechos de propiedad intelectual únicamente para usos privados enmarcados en actividades de investigación y docencia. No se autoriza su reproducción con finalidades de lucro ni su difusión y puesta a disposición desde un sitio ajeno al servicio TDR o al Repositorio Digital de la UB. No se autoriza la presentación de su contenido en una ventana o marco ajeno a TDR o al Repositorio Digital de la UB (framing). Esta reserva de derechos afecta tanto al resumen de presentación de la tesis como a sus contenidos. En la utilización o cita de partes de la tesis es obligado indicar el nombre de la persona autora.

WARNING. On having consulted this thesis you're accepting the following use conditions: Spreading this thesis by the TDX (www.tdx.cat) service and by the UB Digital Repository (diposit.ub.edu) has been authorized by the titular of the intellectual property rights only for private uses placed in investigation and teaching activities. Reproduction with lucrative aims is not authorized nor its spreading and availability from a site foreign to the TDX service or to the UB Digital Repository. Introducing its content in a window or frame foreign to the TDX service or to the UB Digital Repository is not authorized (framing). Those rights affect to the presentation summary of the thesis as well as to its contents. In the using or citation of parts of the thesis it's obliged to indicate the name of the author.

Doctoral Thesis
2013

Synthesis of Highly Structured and Receptor-Selective Tetradecapeptidic Analogs of Somatostatin:

Fine-tuning the non-covalent interactions
among their aromatic residues.



UNIVERSITAT DE BARCELONA



Pablo Martín-Gago

**Synthesis of Highly Structured and Receptor-Selective
Tetradecapeptidic Analogs of Somatostatin:
Fine-tuning the non-covalent interactions among their aromatic
residues.**

Pablo Martín-Gago

Programa de doctorado: Química Orgánica Bienio 2010-2012

Director de tesis: Antoni Riera Escalé

Facultad de Química

Departamento de Química Orgánica

Memoria presentada por Pablo Martín-Gago para optar al grado de doctor por la
Universitat de Barcelona

Pablo Martín-Gago

Revisada por:

Dr. Antoni Riera Escalé

Barcelona, septiembre de 2013

Este trabajo se ha realizado con el soporte económico del Ministerio de Ciencia e Innovación (beca predoctoral del programa nacional de Formación de Profesorado Universitario, FPU). El trabajo ha sido financiado mediante los proyectos de investigación MEC (CTQ 2008-00763), MICINN (CTQ2011-23620) y DGR (SGR-2009-00901).

El trabajo experimental se ha llevado a cabo en el laboratorio de la “Research Unit on Asymmetric Synthesis” del “Institute for Research in Biomedicine” (IRB Barcelona), ubicado en el Parque Científico de Barcelona.

Acknowledgments

Quisiera mostrar mi más sincero agradecimiento al doctor Antoni Riera por haberme brindado la oportunidad de trabajar en su grupo de investigación así como por su interés, dedicación e ideas brillantes durante estos años. También especial mención a la Dra. María Macías, mi co-directora de tesis off the record, por su constante apoyo y por su impecable trato a nivel profesional como personal. También quisiera agradecerle al Dr. Xavier Verdaguer el interés y la ayuda mostrada durante estos años.

Quisiera agradecer también la colaboración que me han prestado los servicios técnicos del Parque Científico de Barcelona en la realización de este trabajo, especialmente a Ester y Belén de Enantia S. L por su ayuda en los análisis por HPLC.

I am particularly thankful to Prof. Gregory Fu at the California Institute of Technology, for giving me the opportunity to work in his group. I thank everybody in the Fu group: Dan, Andrea, Alex B. meatspin.com, Shara's leather jacket, Closed Eyes Albert, Ash lil Judas, JC, Sue, Jose, Moralla (I'll see you in Dortmund!), Yufan, Hien... I learned lots from you guys. An especial thanks to Shosho, who made my short-research stay one of the best times of my entire life.

Y, como no, a mis compañeros de laboratorio que forman parte fundamental de este trabajo. A los primeros y que no se olvidan: Cati, Jean-Claude, María, etc. A los más recientes: Charo (la que comenzó la andadura con la somatostatina), Marc Réves (con lo bueno que eres chico! Plas, plas!) y Thierry (can we have a beer? de hecho, el ránking nunca ha vuelto a ser igual). A Pau y Eric, por ayudarme siempre que lo he necesitado con el imán y los cálculos computacionales. Y a los URSA presentes: Á...Álex (el hombre de negocios que siempre lleva polos con el mejor parecido razonable de la historia), a Núria (menos mal que estabas aquí cuando necesitaba gestiones burocráticas), a Héléa (por sus masajes mientras se hace el café), al patillas (bueno, a este no le agradezco nada en verdad, por favor intenta no destruir el proyecto que tanto me ha costado llevar al éxito ;-)), a Happy Days Chris (por la profesionalidad que ha traído a URSA) y a (acento súper catalán) Sílviiiia (mi última compañera de vitrina, aunque no me hacías las capas finas ha sido un placer trabajar a tu lado). Especial mención de agradecimiento para los URSA que han hecho que mi vida fuera del lab en Bcn sea casi igual de genial que en Salamanca (The Small City of Dreams): al quedao de Edgar (pero qué bueno eres chico!, a ver si vienes ya de Oxford porque vaya canteo majete...), a Seán (mi alumno de español del que estoy más orgulloso, que aún protagonices el 40% de mis profile pics en Facebook refleja que aún estás con nosotros!), a Agus (por esas noches de copas con Ana y por esas grandes ideas sobre química, sobre todo la del enlace -CF₂-, que te voy a robar como no te des prisa), a mi chinita preferida Chen (por las valoraciones de tu ropa, cortarme las capas finas, momentos de movidas, enseñarme más de la mitad de lo que sé de experimental por compartir vitrina contigo y por esas dos

visitas en San Diego en las que me has hecho sentir como si estuviera en casa), a Súper Daniel Byrom (por su presencia e interés constante y por amenizarme cada tarde al salir del lab con cervezas en el chino, en el precio único o donde haga falta, si no hubiera sido por ti este último año hubiera dado un lachi de kilo) y a Ana Mari (la persona más especial durante mi estancia en Barcelona, aunque te mereces una hoja entera de agradecimientos te tendrás que conformar con esto: GRACIAS).

También tengo que agradecer a la gente de fuera del lab que ha contribuido a que me haya sentido como en casa durante estos años: a Luca (esas barbacoas), a Marta vestiditos (sabes que realmente te aprecio a saco), Anna-Iris (por todas las ayudas prestadas), a Rodo (a ver si se va Patito ya y volvemos a liarlas ;-)), a Kader, Michael, Andrey, Mili, Laura, Lorena, Aitor, etc. (por los viejos tiempos), a la parejita de moda Susana-Paula (a.k.a. la sin flow y la sevillana, porque estos últimos meses las hemos liado MUY a saco), a Iri (for the not-so-old times), a Gonzalo (con el que, de hecho, me he sentido en casa durante los dos primeros años y hemos compartido mil viajes irrepetibles), a Peter (no sabría decidirme por nuestro mejor momento juntos; el choque Goku-Vegeta contra Pitbull, el último Nasty Mondays, el 100% Mexican-Irish, Edward weird-hands, tus BBQ's y lo de después...). Verás como me olvido de alguien y me la viene a dar fresca...

A los que han estado ahí toda la vida, Chanclas, Angulo y Gomas, porque aún sin saberlo han sido un pilar fundamental durante todos estos años lejos de casa. Lo que nosotros hemos vivimos juntos está al alcance de muy muy muy pocos, qué bueno! También a los demás, Mankis, Tendencias, Sory, Bea sonrisas (best oral ever), Teresita, Miguel y Rocío, por hacer que mis visitas a Salamanca se conviertan en depresiones a mi vuelta.

AL PhD CHAT, otro de los pilares fundamentales durante estos cuatro años. No se puede decir nada más que BRUTAL chateros, BRUTAL.

A Ly, porque ha sido la persona que más ha contribuido mi felicidad durante mi estancia en Barcelona.

Y por último, quisiera dar las gracias a mis padres y hermana, por darme una vida tan fácil. Esta tesis está dedicada a vosotros.

“If we assume we have arrived, we stop searching, we stop developing”

Jocelyn Bell Burnell

Content

List of Abbreviations

Chapter 1. Introduction, background and objectives	1
Chapter 2. Enantioselective syntheses of non-natural aromatic amino acids	
2.1 Introduction.....	13
2.2. Dehydroamino acid syntheses	15
2.2.1. The Horner-Wadsworth-Emmons olefination	18
2.2.2. The Heck and Suzuki cross-coupling reactions	20
2.2.3. The Azlactone route.....	23
2.2.4. The Perkin reaction.....	25
2.3. Rhodium-Catalyzed Asymmetric Hydrogenation	
2.3.1. Introduction.....	27
2.3.2. DuPHOS and DIPAMP as ligands	28
2.3.3. The Rh(I)-MaxPHOS system	29
2.4 Hydrolysis and Fmoc-protection.....	32
Chapter 3. Somatostatin analogs containing the Msa amino acid	
3.1. Introduction: Aromatic interactions in peptides and proteins	35
3.2. Somatostatin analogs containing Msa residues.....	39
3.2.1. Synthesis.....	39
3.2.2. Serum stability studies.....	41
3.2.3. Receptor-subtype selectivity assays.....	42
3.2.4. Structure.....	44
3.3. Conclusions.....	54
Chapter 4. SRIF analogs containing the Tmp residue	
4.1. Introduction: The Msa versus the Tmp amino acid	59
4.2. SRIF analogs containing the Tmp residue	60
4.2.1. Receptor-subtype selectivity	60
4.2.2. Structure.....	62
4.3. Msa and Tmp in position 7 and SSTR2-selectivity	66
4.4. Conclusions.....	69

Chapter 5. Linear 14-residue SRIF analogs containing the L-Msa7_D-Trp8 motif	
5.1. Introduction: Searching for SSTR2-selective analogs	73
5.2. Linear [D-Trp8]-SRIF analogs bearing Msa7	74
5.2.1. Structure.....	74
5.2.2. Binding affinity to SSTR1-5.....	77
5.3. Conclusions.....	79
Chapter 6. Tetradecapeptidic SRIF analogs bearing Dfp residues	
6.1. Introduction: The role of fluorine substituents in aromatic interactions	83
6.2. 14-Residue SRIF analogs containing Dfp residues	88
6.2.1. Receptor-subtype selectivity	88
6.2.2. Structure.....	89
6.3. Conclusions.....	95
Chapter 7. Somatostatin derivatives containing Cha residues	
7.1. Introduction: The Cha amino acid	99
7.2. Structural data and radioligand binding assays	102
7.3. Conclusions	107
Chapter 8. [L-Msa7_D-Trp8]- SRIF analogs containing Tmp and Dfp residues	
8.1. Introduction: Multiple residue substitutions for SSTR2-selectivity	111
8.2. [L-Msa7_D-Trp8]-SRIF analogs containing Tmp and Dfp residues	111
8.2.1. Receptor-subtype selectivity	112
8.2.2. Structure.....	113
8.3. Conclusions.....	118
Chapter 9. Global conclusions	123
Chapter 10. Experimental section	
10.1. Experimental section for the synthesis of amino acids	
10.1.1. General methods and instrumentation	127
10.1.2. Compounds from the HWE olefination	128
10.1.3. Compounds from the Heck reaction.....	132
10.1.4. Compounds from the azlactone route.....	133
10.1.5. Compounds from the Perkin reaction	134
10.1.6. Rh-Catalyzed Asymmetric Hydrogenations	135
10.1.7. Compounds obtained after hydrolysis	139
10.1.8. Compounds subjected to Fmoc-protection	140
10.2. Experimental section for the synthesis of SRIF analogs	

10.2.1. General methods and instrumentation	143
10.2.2. General considerations for the SPPS	145
10.2.3. General methods for the synthesis of SRIF analogs.....	146
10.2.4. 14-Residue SRIF analogs (in order of appearance)	147
10.3. Computational methods.....	153
10.4. Receptor-subtype selectivity assays	153
10.5. Serum stability assays.....	155

The attached CD contains:

Appendix I: ¹H-NMR Spectra of the final Fmoc-protected amino acids.

Appendix II: Full characterization of SRIF analogs.

TOCSY and NOESY spectra of SRIF, [D-Trp8]-SRIF and SRIF analogs.

Structural statistics from the computational calculations.

Appendix I: Summary in Spanish	159
Appendix II: Index of SRIF analogs (in order of appearance).....	189

List of abbreviations

aa	amino acid	DMSO	dimethylsulfoxide
Ac	acetyl	e.e.	enantiomeric excess
AcOEt	ethyl acetate	eq.	equivalent
ACN	acetonitrile	ESI	electrospray ionization
AD	asymmetric dihydroxylation	Et	ethyl
°C	degree Celsius	EWG	electron-withdrawing group
δ	NMR chemical shift	^{19}F	fluorine NMR
λ	wavelength	Fmoc	9-fluorenylmethoxycarbonyl
Bn	benzyl	g	gram
Boc	<i>tert</i> -butoxycarbonyl	GC-MS	gas chromatography-mass spectroscopy
BSA	bovine serum albumin	h	hour(s)
^tBu	<i>tert</i> -butyl	HOBt	1-hydroxybenzotriazole
^{13}C	carbon NMR	HPLC	High-Performance Liquid Chromatography
calcd.	calculated	HRMS	High Resolution Mass Spectrum
cat.	catalyst	HSQC	Heteronuclear Single Quantum Correlation
Cbz	carboxybenzyl	i.e.	id est, that is
d	doublet	IR	infrared (spectroscopy or spectrum)
dd	doublet of doublets	J	coupling constant
dt	doublet of triplets	K_i	inhibition constant
DBU	1,8-diazabicyclo[5.4.0.]undec-7-ene	kcal mol $^{-1}$	kilocalories per mole
DIEA	N,N-diisopropylethylamine	m	multiplet
DMAP	4-(dimethylamino)pyridine	M	molar
DME	dimethoxyethane	Me	methyl
DMF	<i>N,N</i> -dimethylformamide	mg	milligram

List of abbreviations

min	minute	SPPS	solid-phase peptide synthesis
mL	millilitre	SRIF	somatotropin release-inhibiting factor
mmol	millimole	SSTR	somatostatin subtype receptor
mol	mole	r.t.	room temperature
m.p.	melting point	t	triplet
MS	mass spectrometry	$t_{1/2}$	half-life
m/z	mass to charge ratio	T°	temperature
NMR	nuclear magnetic resonance	^t Bu	tert-butyl
NOE	nuclear Overhauser effect	T_c	coalescence temperature
NOESY	nuclear Overhauser effect spectroscopy	TBAF	tetrabutylammonium fluoride
<i>o</i>	<i>ortho</i>	TBS	<i>tert</i> -butyldimethylsilyl
<i>p</i>	<i>para</i>	TFA	trifluoroacetic acid
PEG	polyethylene glycol	TFE	trifluoroethanol
PES	potential energy surface	TIPS	triisopropylsilyl
Ph	phenyl	Tf	trifluoromethanesulfonyl
PPh ₃	triphenylphosphine	THF	tetrahydrofuran
ppm	parts per million	TLC	thin layer chromatography
py	pyridine	TMS	trimethylsilyl
q	quartet	TIS	triisopropylsilane
quant.	quantitative	TOCSY	total correlation spectroscopy
s	singlet	T_R	retention time
S _N 1	unimolecular nucleophilic substitution	UV	ultraviolet (spectroscopy or spectrum)
S _N 2	bimolecular nucleophilic substitution	vs.	versus

1

Introduction, background and objectives

Somatostatin, a peptidic hormone also known as somatotropin release-inhibiting factor (SRIF), was first discovered in hypothalamic extracts in 1973 as an active form of 14 amino acids (Figure 1.1).¹ Since its initial isolation, new forms of variable length have been identified.² Thus, the name somatostatins refers to a family of cyclopeptides (SRIFs) that are produced mainly by normal endocrine, gastrointestinal, immune and neuronal cells, as well as by certain tumors. The highly potent somatostatin peptide SRIF-14 (Figure 1.1) is generated as a C-terminal product from prosomatostatin.

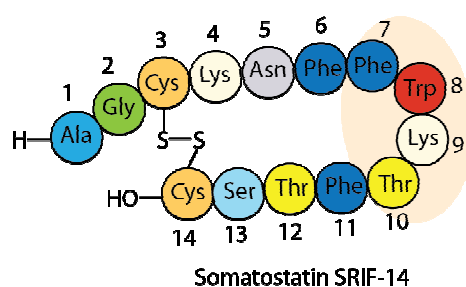


Figure 1.1. Amino acid sequence of somatostatin, showing its pharmacophore.

SRIFs are implicated in multiple biological functions, mediated by direct interaction of the peptides with a family of structurally related, G-protein coupled transmembrane receptors (GPCRs), named SSTR1-5. These receptors differ in their tissue distribution and pharmacological properties.³ By binding to these GPCRs on target cells, SRIFs act as neuromodulators and neurotransmitters, as well as potent inhibitors of various secretory processes and cell proliferation.⁴ SRIFs are unique in their broad inhibitory effects on both endocrine secretion —of growth hormone, insulin, glucagon, gastrin, etc. — and exocrine secretion —of gastric acid, intestinal fluid and pancreatic enzymes—.⁵ This pan-antisecretory profile has led to

1 a) P. Brazeau, W. Vale, R. Burgus, N. Ling, M. Butcher, J. Rivier, R. Guillemin, *Science* **1973**, *179*, 77-79; b) R. Burgus, N. Ling, M. Butcher, R. Guillemin, *Proc. Natl. Acad. Sci. U S A* **1973**, *70*, 684-688.

2 M. A. Sheridan, J. D. Kittilson, B. J. Slagter, *Am. Zool.* **2000**, *40*, 269-286.

3 D. Hoyer, G. I. Bell, M. Berelowitz, J. Epelbaum, W. Feniuk, P. P. A. Humphrey, A. O'Carroll, Y. C. Patel, A. Schonbrunn, et al *Trends Pharmacol. Sci.* **1995**, *16*, 86-88.

4 a) G. Weckbecker, F. Raulf, B. Stolz, C. Bruns, *Pharmacol. Ther.* **1993**, *60*, 245-264; b) G. Gillies, *Trends Pharmacol. Sci.* **1997**, *18*, 87-95.

5 a) S. Reichlin, *N. Engl. J. Med.* **1983**, *309*, 1495-1501; b) S. Reichlin, *N. Engl. J. Med.* **1983**, *309*, 1556-1563.

exploratory clinical trials of natural SRIF-14 for the treatment of a range of dysfunctions, including diabetes type I and II, hypersecretory tumors, such as growth hormone-secreting pituitary adenomas and gastrinomas, and gastrointestinal disorders, including bleeding gastric ulcers or pancreatitis.⁵ However, full therapeutic potential of SRIF cannot be further exploited owing to its short half-life of <3 min in plasma and its lack of selectivity against all receptors. Rapid degradation makes constant infusion of the drug necessary, and its broad spectrum of biological activity leads to barely optimized treatments.

With the aim to overcome these limitations, many SRIF analogs containing key modifications have been synthesized over recent decades. The primary contributions of a number of researchers, including Brazeau, Coy, Rivier, Schally and Vale, provided the foundation for the discovery of SRIF and early SRIF analogs.^{1a,6} Bauer and colleagues at Novartis (previously Sandoz) synthesized octreotide, a metabolically stabilized cyclooctapeptide derivative of SRIF that potently inhibits the secretion of a number of hormones.⁷ Octreotide (Sandostatin®), lanreotide (Somatuline®),⁸ vapreotide (Sanvar®)⁹ and pasireotide (Signifor®)¹⁰ are the four synthetic analogs that have reached the market so far (Figure 1.2). Octreotide, lanreotide and vapreotide are octapeptides, while pasireotide is a hexapeptide, thus they contain a shorter and more rigid ring than somatostatin. Consequently, they are long-acting analogs with increased receptor selectivity. Also, they share a similar fragment including residues Phe/Thr7-D-Trp8-Lys9-Thr/Val10, which populates beta-turn conformations and has been proposed to be the pharmacophore of the hormone.^{6a}

6 a) J. Rivier, M. Brown, C. Rivier, N. Ling, W. Vale, *Pept. , Proc. Eur. Pept. Symp. , 14th* **1976**, 427-51; b) D. H. Coy, E. J. Coy, A. Arimura, A. V. Schally, *Biochem. Biophys. Res. Commun.* **1973**, *54*, 1267-1273.

7 a) W. Bauer, U. Briner, W. Doepfner, R. Haller, R. Huguenin, P. Marbach, T. J. Petcher, J. Pless *Life Sci.* **1982**, *31*, 1133-1140.

8 J. Marek, V. Hána, M. Kršek, V. Justová, F. Catus, F. Thomas, *Eur.J. Endocrinol.* **1994**, *131*, 20-26.

9 P. M. Girard, E. Goldschmidt, D. Vittecoq, P. Massip, J. Gastiaburu, M. C. Meyohas, J. P. Coulaud, A. V. Schally, *AIDS* **1992**, *6*, 715-718.

10 For SOM230 (Signifor, recently approved for the treatment of Cushing's disease) see: C. Bruns, I. Lewis, U. Briner, G. Meno-Tetang, G. Weckbecker, *Eur. J. Endocrinol.* **2002**, *146*, 707-716.

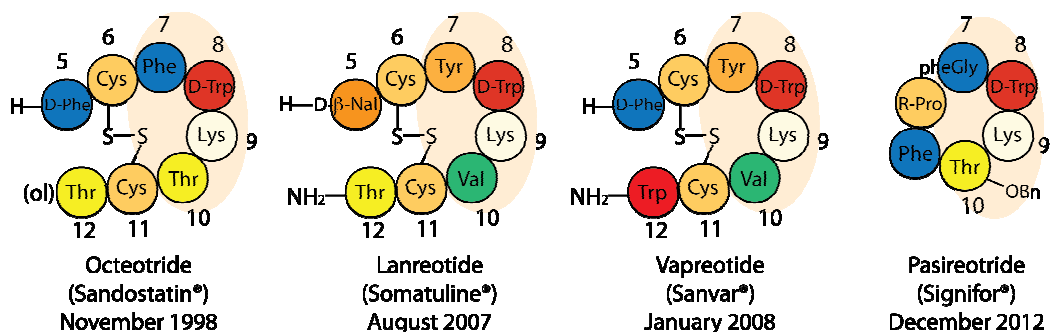


Figure 1.2. Amino acid sequences of marketed short-ring analogs of somatostatin, showing their respective pharmacophores and the first approved date of the FDA (please note that Sanvar® is not fully approved yet). R-Pro = [(2-aminoethyl)aminocarbonyloxy]-L-proline.

The discovery of the five SRIF receptor subtypes (SSRT1-5) in the early 1990s^{3,11} triggered intensive research into their binding properties and coupling to multiple signaling pathways. This research also revealed that the clinically used SRIF analogs octreotide and lanreotide are preferential ligands of the SSTR2 receptor subtype, thus leading to rational approaches to develop peptide and non-peptide SRIF analogs that bind selectively or more broadly ('universally') to the SRIF receptor subtypes. Research focused mainly on the synthesis and study of derivatives of octreotide, a potential hit-to-lead in drug discovery. While only a few tetradecapeptidic analogs have been synthesized, many octapeptides containing crucial modifications have been reported: exchange of amino acids, ring size adjustment, disulfide bridge modification, multiple N-methylations or site-specific PEGylation.¹² Several of these analogs improved the “drug-like” properties of the natural hormone.

Recent advances in peptide solid-phase synthesis prompted us to revisit the full-length SRIF-14 scaffold to design new analogs with enriched stability and receptor selectivity. Thus, we would minimize an intrinsic drawback of octapeptidic derivatives, namely the loss of activity in certain receptors. Furthermore,

11 Y. C. Patel, C. B. Srikant, *Endocrinology* **1994**, *135*, 2814-2817.

12 a) C. R. R. Grace, J. Erchegyi, S. C. Koerber, J. C. Reubi, J. Rivier, R. Riek, *J. Med. Chem.* **2006**, *49*, 4487-4496. b) A. Di Cianni, A. Carotenuto, D. Brancaccio, E. Novellino, J. C. Reubi, K. Beetschen, A. M. Papini, M. Ginanneschi, *J. Med. Chem.* **2010**, *53*, 6188-6197. c) J. Chatterjee, B. Laufer, J. G. Beck, Z. Helyes, E. Pintér, J. Szolcsányi, A. Horvath, J. Mandl, J. C. Reubi, G. Kéri, H. Kessler, *ACS Med. Chem. Lett.* **2011**, *2*, 509-514. d) M. Morpurgo, C. Monfardini, L. J. Hofland, M. Sergi, P. Orsolini, J. M. Dumont, F. M. Veronese, *Bioconjugate Chem.* **2002**, *13*, 1238-1243.

tetrapeptidic analogs are structurally closer to the natural hormone than octapeptides: highly SSTR-selective, structurally non-flexible 14-residue somatostatin analogs would ideally allow us to characterize the main conformation of SRIF when it binds to its five receptors.

The 3D structure of somatostatin has been a matter of debate during the last three decades. Many studies have provided information about the inherent high flexibility of SRIF in solution.¹³ Attempts to characterize its structure in detail have been unsuccessful, and the native structure of somatostatin is currently considered an ensemble of several interconverting conformations in equilibrium, a few of which are partially structured.¹⁴

Early studies uncovered the possibility that an aromatic interaction between Phe6, Phe7 or Phe11 plays a key role in the structural stabilization of the hormone.¹⁵ Exchanging the Phe6 and Phe11 amino acids for alanine led to a SRIF analog with 98% reduced efficacy.^{16,17} However, when Phe6 and Phe11 were replaced by a cystine, the correspondent peptide retained its biological activity,¹⁵ thereby suggesting close spatial proximity through “hydrophobic bonding” between these residues in some of the biologically active SRIF conformations.^{13a} This hypothesis was supported by pioneering NMR experiments carried out by Arison *et al.*¹⁸ The marked temperature dependence in the chemical shift suggested that the Phe6 protons

13 a) M. Knappenberg, A. Michel, A. Scarso, J. Brison, J. Zanen, K. Hallenga, P. Deschrijver, G. Van Binst, *Biochim.Biophys.Acta, Protein Struct. Mol. Enzymol.* **1982**, 700, 229-246; b) K. Hallenga, G. Van Binst, A. Scarso, A. Michel, M. Knappenberg, C. Dremier, J. Brison, J. Dirx, *FEBS Lett.* **1980**, 119, 47-52; c) L. A. Buffington, V. Garsky, J. Rivier, W. A. Gibbons *Biophys. J.* **1983**, 41, 299-304; d) L. A. Buffington, V. Garsky, J. Rivier, W. A. Gibbons, *Int. J. Pept. Protein Res.* **1983**, 21, 231-241.

14 A. Kaerner, K. H. Weaver, D. L. Rabenstein, *Magn. Reson. Chem.* **1996**, 34, 587-594.

15 a) J. E. Rivier, M. R. Brown, W. W. Vale, *J. Med. Chem.* **1976**, 19, 1010-1013; b) D. F. Veber, F. W. Holly, W. J. Paleveda, R. F. Nutt, S. J. Bergstrand, M. Torchiana, M. S. Glitzer, R. Saperstein, R. Hirschmann, *Proc. Natl. Acad. Sci. U. S. A.* **1978**, 75, 2636-2640.

16 W. W. Vale, C. Rivier, M. R. Brown, J. E. Rivier *Hypothalamic Peptide Hormones and Pituitary Regulation, Advances in Experimental Medicine and Biology.* Plenum Press **1977**, pp 123-156.

17 Analogs were compared to somatostatin in their ability to decrease the levels of portal vein glucagon and insulin in anesthetized rats.

18 B. H. Arison, R. Hirschmann, W. J. Paleveda, S. F. Brady, D. F. Veber, *Biochem. Biophys. Res. Commun.* **1981**, 100, 1148-115

were in the shielding cone of an aromatic ring. NMR studies of both SRIF and a shorter analog carried out by Cutnell *et al.* provided geometric information about this non-covalent interaction.¹⁹ The temperature effect on the Phe6 proton shifts was not consistent with parallel stacking, so a perpendicular aromatic interaction was proposed (with *o*- and *m*-H of Phe6 pointing near the center of a second aromatic ring). The authors also showed that replacement of Phe7 with alanine in this smaller analog retained the up-field *o*-H resonance of (presumably) Phe6, whilst Phe11 substitution with alanine eliminated this shift. This observation supported the hypothesis that Phe11 shields Phe6 in this proposed “perpendicular” aromatic interaction, and it stabilizes the active conformations in the natural counterpart (Figure 1.3).

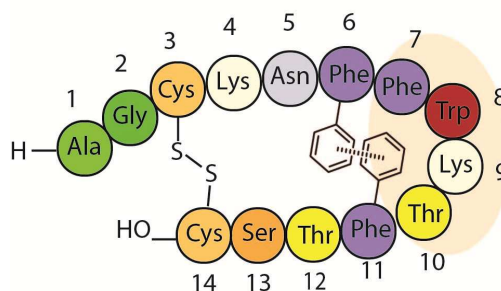


Figure 1.3. Proposed Phe6-Phe11 aromatic stabilizing interaction.

However, four years later this subject was re-examined and, after 2D NOESY NMR studies, no proton-proton NOE's between Phe11 and any of the other aromatic rings were detected.²⁰ Van Binst and co-workers concluded that the Phe6-Phe11 interaction was not significantly present in the main conformations of SRIF in aqueous solution, and orientation of Phe7 towards the Phe6 aromatic protons was proposed. In the same regard, the substitution of every residue by Tyr (“Tyr-Scan”) in SRIF that Rivier *et al.*²¹ carried out, suggested that Phe6 is functionally involved in

19 J. D. Cutnell, G. N. La Mar, J. L. Dallas, P. Hug, H. Ring, G. Rist, *Biochim.Biophys.Acta, Protein Struct.Mol.Enzymol.* **1982**, 700, 59-66.

20 a) A. W. H. Jans, K. Hallenga, G. Van Binst, A. Michel, A. Scarso, J. Zanen, *Biochim.Biophys.Acta, Protein Struct.Mol.Enzymol.* **1985**, 827, 447-452. b) E. M. M. Van den Berg, A. W. H. Jans, G. Van Binst, *Biopolymers* **1986**, 25, 1895-1908.

21 J. E. Rivier, M. R. Brown, W. W. Vale, *J. Med. Chem.* **1976**, 19, 1010-1013.

receptor activation process, whereas Phe7 is involved in the internal stabilization of SRIF tertiary structure through the stacking of aromatic rings. These hypotheses have not been proved or refuted so far, since it has not been possible to obtain detailed NMR or X-ray data on the 3D structure of the peptide. The “octapeptidic boom” that started in the 90’s led to the disregard of this topic and the attention was shifted to the cyclooctapeptidic template, which contains a disulfide bond as a surrogate of the putative Phe6-Phe11 aromatic interaction (see Figures 1.2 and 1.3).

We considered that exploring the presumed aromatic interactions that stabilize some bioactive conformations in SRIF would be a unique way to obtain analogs with enhanced stability and conformational rigidity, and improved biological activity. For this purpose, we decided to incorporate specific non-natural aromatic amino acids in the 14-residue SRIF scaffold. If key non-covalent interactions are intensified, we will reduce the conformational flexibility of SRIF, and the 3D structure of these tetradecapeptides would be susceptible to characterization by NMR techniques for the first time. Ideally, these highly structured analogs will be more stable and receptor-selective than the natural counterpart, and their main conformation in solution may shed light on the particular conformations SRIF adopts when it binds to its five receptors subtypes. These highly stable SSTR-selective somatostatin analogs could have an interesting therapeutic potential.

Thus, in this doctoral thesis, we explore the substitution of the natural Phe6, Phe7 and Phe11 residues that are present in the sequence of SRIF by three specific non-natural amino acids (Figure 1.4): 3-mesitylalanine (Msa), 3-(3',4',5'-trimethylphenyl)-alanine (Tmp) and 3-(3',5'-difluorophenyl)-alanine (Dfp). We selected these residues on the basis of their high hydrophobicity (in comparison to tha of Phe) and their particular steric and electronic properties.

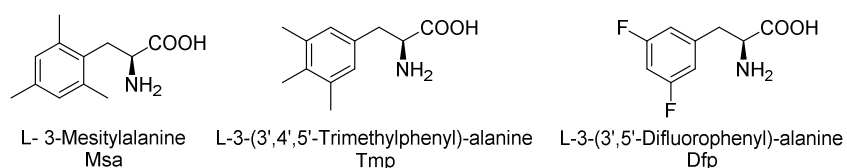


Figure 1.4. Selected non-natural aromatic amino acids that will be introduced in the natural sequence of somatostatin.

The present doctoral thesis has been organized as follows:

The asymmetric syntheses of these unnatural aromatic amino acids are described in **Chapter 2**.

In **Chapter 3**, we describe our first approach devoted to the exploration of the aromatic interactions in somatostatin. In this section, we study ten SRIF analogs containing the non-natural 3-mesitylalanine (Msa) amino acid, which were synthesized by Rosario Ramón in her PhD thesis. We first chose the Msa residue on the basis of the higher hydrophobicity and electronic density that the methyl groups confer upon the aromatic moiety, and of the reduced conformational mobility of the mesityl ring relative to Phe. We found that the introduction of one Msa residue, in position 6, 7 or 11, provides analogs with a high conformational rigidity, due to the enhancement of certain non-covalent interactions between aromatic residues.

In **Chapter 4**, we discuss whether the structural impact caused by the Msa amino acid is a result of its higher electron-density or its intrinsic side-chain rigidity (the *ortho*-methyl substitution limits the mobility of its side-chain, an effect that may be extended to the whole peptidic architecture). To do so, we explore three SRIF analogs in which the natural Phe6, Phe7 or Phe11 were replaced by one Tmp residue. Despite the shape difference, this non-natural amino acid displays similar hydrophobic and electronic properties to those of Msa, although the three methyl groups barely restrict the mobility of its aromatic side-chain.

At this point, excellent results were found when the natural Phe7 was substituted by Msa or Tmp residues. In **Chapter 5** we explore the scope of this modification in the absence of the intrinsic disulfide bond, by studying two linear SRIF analogs containing an Msa residue in position 7. This work allowed us to develop the two first linear 14-residue SRIF analogs that display a high SSTR2-activity and -selectivity.

Chapter 6 covers the exploration of SRIF analogs containing 3-(3',5'-difluorophenyl)-alanine (Dfp) residues. We considered that this amino acid, containing a fluorinated and electron-poor aromatic moiety, represented an ideal

way to further prove and study polar- π interactions in SRIF analogs, due to the small steric yet large electronic impact that it implies.

The results obtained in previous chapters led us to investigate, separately, the relative contributions of hydrophobic and electronic factors to the aromatic interactions in SRIF. In **Chapter 7**, we study four different SRIF analogs in which the Phe6, Phe7 or Phe11 were replaced by the commercially available 3-cyclohexylalanine (Cha) residue. We selected the Cha amino acid because it has a similar hydrophobicity and polarity than the natural Phe, but it lacks the ability to participate in aromatic interactions driven by electronic factors.

Finally, we describe four tetradecapeptidic SRIF analogs containing more than two non-natural residues at the same time (*i.e.* Msa, Tmp and Dfp). The combined and synergistic effect of these aromatic amino acids in the structure, serum stability and receptor-subtype selectivity of SRIF analogs is discussed in **Chapter 9**.

From the methodological point of view, the main objectives of my PhD work can be summarized as follows:

- 1- To scale up the asymmetric synthesis of non-natural aromatic amino acids containing particular electronic and/or steric properties.
- 2- To synthesize new site-directed modified somatostatin analogs containing those non-natural residues in the SRIF sequence.
- 3- To examine the 3D structure of these synthetic tetradecapeptides by NMR and computational techniques. In the case of highly structured SRIF analogs, their main conformation will be carefully characterized and discussed.
- 4- To determine whether an aromatic interaction that stabilizes some bioactive conformations of SRIF's exists and, if so, to identify the residues involved.
- 5- To obtain the K_i values of the new analogs by radioligand binding assays for the five somatostatin receptors.
- 6- To determine the half-life of the newly designed compounds in human serum and to relate the serum stability with the structural modifications.

- 7- To gain insight into structure-activity relationships of somatostatin and its analogs: to identify, by analogy, the active conformations of the natural hormone when it binds to any particular receptor and to determine essential structural motifs or properties that are required for the affinity of SRIF and SRIF analogs for SSTR1-5.

2

Enantioselective syntheses of non-natural aromatic amino acids

Chapter 2. Enantioselective syntheses of non-natural aromatic amino acids

2.1 Introduction.....	13
2.2. Dehydroamino acid syntheses	15
2.2.1. The Horner-Wadsworth-Emmons olefination	18
2.2.2. The Heck and Suzuki cross-coupling reactions	20
2.2.3. The Azlactone route.....	23
2.2.4. The Perkin reaction.....	25
2.3. Rhodium-Catalyzed Asymmetric Hydrogenation	
2.3.1. Introduction	27
2.3.2. DuPHOS and DIPAMP as ligands	28
2.3.3. The Rh(I)-MaxPHOS system	29
2.4 Hydrolysis and Fmoc-protection	32

2.1. The Msa, Tmp and Dfp residues

Non-natural amino acids, the non-genetically-coded amino acids, have become very important tools for modern drug discovery research.¹ In particular, synthetic α -amino acids play a key role in protein and peptide research. Due to their structural diversity and functional versatility, these building blocks have been extensively used in the construction of protein and peptide analogs to modify specific characteristics of the parent compound: different folding, conformational flexibility, hydrophobicity, enzymatic stability, receptor affinity and selectivity, etc.² These modifications may improve the 'drug-like' (pharmacokinetic and pharmacodynamic) properties of the analogs, relative to those of the parent compound.

Considerable effort has been dedicated to the syntheses of non-natural α -amino acids in recent decades. Because of their distinct functional groups, shapes and properties, different amino acids require different optimized synthetic strategies. Although many enantioselective routes leading to α -amino acids have been described,³ the syntheses of a large number of pharmacologically important amino acids are still performed by enzymatic, chemical or chromatographic resolution.⁴

Given our interest in introducing these compounds into the somatostatin sequence, we planned to develop efficient asymmetric syntheses that provide straightforward access to the conveniently protected amino acids in a multigram scale. In this manner, both enantiomers of the desired product would be easily available in sufficient quantities.

Some projects previously done by our research group focused on the enantiomeric synthesis of α -amino acids. During her thesis, Rosario Ramón carried out the asymmetric synthesis of the Msa and Qla amino acids by means of two key

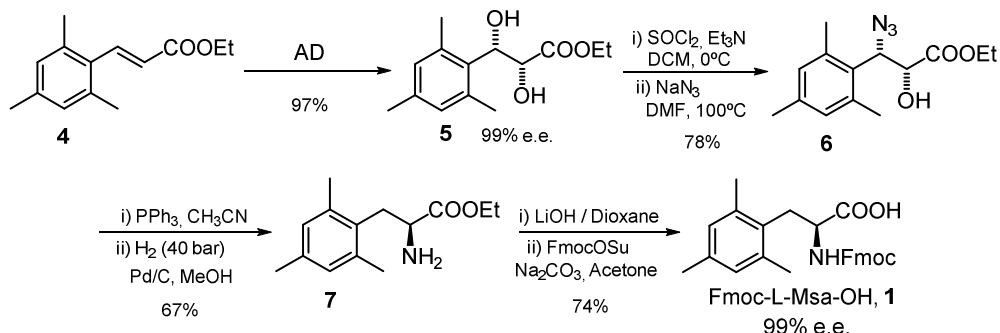
1 a) J. Xie, P. G. Schultz, *Nat. Rev. Mol. Cell Biol.* **2006**, *7*, 775-782; b) J. S. Ma, *Chim. Oggi* **2003**, *21*, 65-68.

2 R. M. J. Liskamp, D. T. S. Rijkers, J. A. W. Kruijtzter, J. Kemmink, *ChemBioChem* **2011**, *12*, 1626-1653.

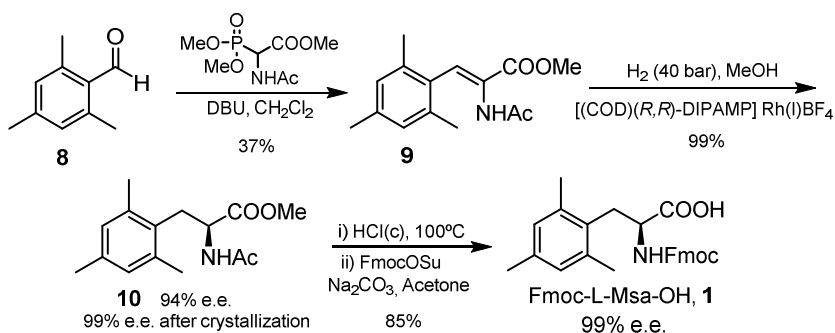
3 A. Perdih, M. S. Dolenc, *Curr. Org. Chem.* **2011**, *15*, 3750-3799.

4 J. Z. Crich, R. Brieva, P. Marquart, R. L. Gu, S. Flemming, C. J. Sih, *J. Org. Chem.* **1993**, *58*, 3252-3258.

reactions as source of chirality: a Sharpless Asymmetric Dihydroxylation (Scheme 2.1) and a Rhodium-Catalyzed Asymmetric Hydrogenation (Scheme 2.2).⁵



Scheme 2.1. Synthesis of Fmoc-L-Msa-OH by using a Sharpless Asymmetric Dihydroxylation reaction to introduce chirality.

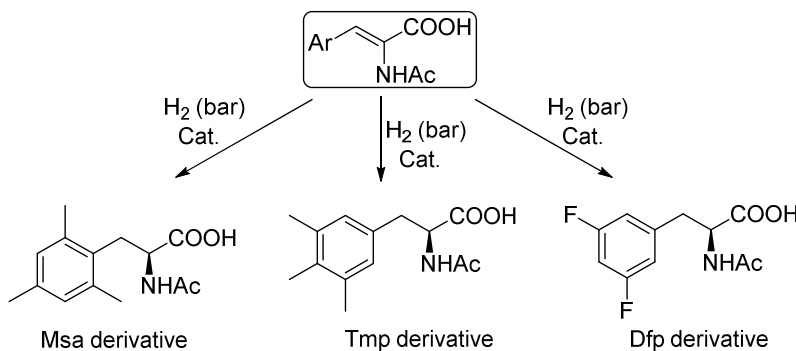


Scheme 2.2. Synthesis of Fmoc-L-Msa-OH by using an Asymmetric Hydrogenation reaction to introduce chirality.

Rosario's syntheses provided straightforward access to the final products, thus we envisaged the acquisition of our non-natural amino acids taking her experimental conditions as a starting point. Several advantages of the asymmetric hydrogenation route prompted us to consider this pathway as a priority for the synthesis of our new products. Furthermore, an ongoing project devoted to the synthesis of new catalysts for asymmetric hydrogenation was being carried out in our research group at that time. Therefore, the collection of new substrates (dehydroamino acid derivatives) susceptible to hydrogenation by means of these new ligands was considered of great interest. With the key dehydroamino acid derivatives in hand, a Rhodium-Catalyzed Asymmetric Hydrogenation reaction would provide a variety of enantioenriched α -

5 a) R. Ramón, M. Alonso, A. Riera, *Tetrahedron: Asymmetry* **2007**, *18*, 2797-2802; b) Rosario Ramón, PhD Thesis, University of Barcelona, 2008.

amino acid derivatives (Scheme 2.3). Subsequent hydrolysis and opportune protection of the amino group would lead to the desired Fmoc-amino acids conveniently protected for their use in SPPS. During her graduate research, Rosario described that the syntheses of the key dehydroamino acid Msa resulted in poor reproducibility and low yields. In this regard, the first objective was to further optimize the syntheses of all these key intermediate derivatives.

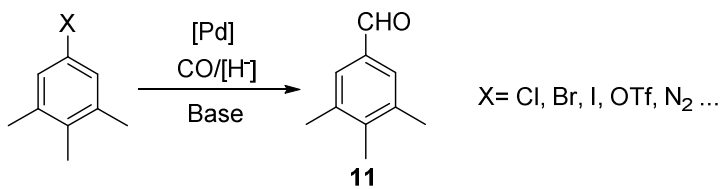


Scheme 2.3. Proposed route to non-natural derivatives by Asymmetric Hydrogenation.

2.2. Syntheses of dehydroamino acids

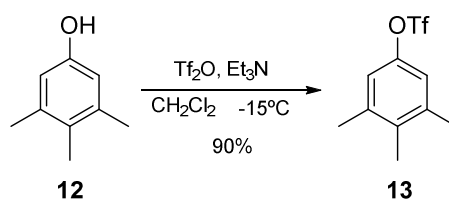
Since the aromatic groups of the amino acids vary, and therefore, also their properties do, we planned different pathways to gain access to them. Four routes were proposed and examined: the Horner-Wadsworth-Emmons olefination (HWE), the Heck reaction, the azlactone route, and the classic but economically attractive Perkin reaction.

The correspondent aryl aldehydes or aryl halides were used as starting materials in all the routes. The 3,4,5-trimethylbenzaldehyde was not commercially accessible, so we planned to synthesize the aldehyde **11** starting from the available 3,4,5-trimethylphenol **12** via a Palladium-Catalyzed Carbonylation Reaction (Schemes 2.4 and 2.5).



Scheme 2.4. General conditions for the Palladium-Catalyzed Reductive Carbonylation (formylation) reaction.

Although only a few examples in the literature report the use of aryl triflates as substrates for this reaction,⁶ we considered that the 3,4,5-trimethylphenol would offer a convenient access to the triflate derivative **13**, suitable for the proposed carbonylation reaction that would allow us to achieve the 3,4,5-trimethylbenzaldehyde **11** in a satisfactory manner. Aryl triflate **13** was prepared from the corresponding phenol by treatment with triflic anhydride in the presence of triethylamine (Scheme 2.5).



Scheme 2.5. Synthesis of the 3,4,5-trimethylphenyl trifluoromethanesulfonate.

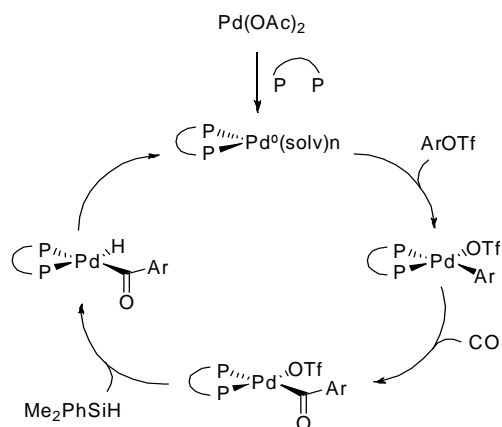
In general (Scheme 2.4), aryl iodides, benzylic halides, vinyl iodides and some triflates, and a few allylic halides are successfully carbonylated in 2.5–3.5 h under mild conditions (50°C , 1-3 bar CO) by using tributyltin hydride (Bu_3SnH).⁷ In our particular case, with the triflate **13** in hand, a range of conditions utilizing $[\text{PdCl}_2(\text{Ph}_3\text{P})_2]$ or $[\text{Pd}(\text{Ph}_3\text{P})_4]$ as catalyst, Et_3N , CO (bar), Bu_3SnH and THF at different temperatures failed to give the desired aryl aldehyde.

An alternative approach for this reaction is based on the use of organosilanes in conjunction with carbon monoxide (thus avoiding the toxicity and waste generation that comes from the use of tin hydrides). Ashfield and Barnard⁸ tested the practicability of several R_3SiH systems for various known palladium catalysts. Many optimization experiments were required to find the appropriate parameters (catalyst, base, solvent, temperature, pressure, concentration) for the transformation of (hetero)aryl bromides and iodides. The mechanism of this transformation is shown in Scheme 2.6.

6 C. F. J. Barnard, *Organometallics* **2008** 27, 5402-5422.

7 A. Brennfürer, H. Neumann, M. Beller, *Angew. Chem. Int. Ed.*, **2009** 48, 4114-4133.

8 L. Ashfield, C. F. J. Barnard, *Org. Process Res. Dev.* **2007**, 11, 39-43.



Scheme 2.6. Simplified mechanism for the Palladium-Catalyzed formylation by using aryltriflates as substrate and Me_2PhSiH as reducing agent.

Their catalyst system failed with aryl chlorides, suggesting that aryl triflates may undergo this reaction with difficulties. Nevertheless, in our hands, the use of the $[\text{Pd}(\text{OAc})_2(\text{dppe})]/\text{DMF}/\text{Et}_3\text{N}$ system under CO pressure (1 bar) by using Me_2PhSiH at 70°C afforded our desired aldehyde **11** in 48% yield. This process was optimized by modifying the phosphine ligand, temperature, and CO (source and bar) and by testing the effect after LiCl addition (Table 2.1).

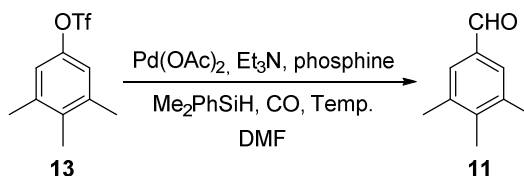


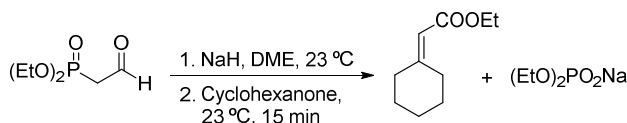
Table 2.1. Optimization for the synthesis of the 3,4,5-trimethylphenylaldehyde.

Entry	Ligand	CO	T ^a	Time	Conversion	Yield
1	Ph_3P	1 bar	70°C	12h	n.m	<10%
2	dppe	1 bar	90°C	8h	86%	44%
3	dppe	1 bar	70°C	14h	78%	48%
4	dppe	3 bar	70°C	14h	76%	73%
5	dppf	3 bar	70°C	14h	78%	70%
6	dppe	3 bar	70°C	54h	77%	45%
7	dppe	5 bar	70°C	14h	54%	18%
8	dppe	Bubbled	65°C	12h	27%	12%
9	dppe	Bubbled (LiCl)	65°C	12h	25%	10%

n.m. not measured. dppe: Ethylenebis(diphenylphosphine) dppf: 1,1'-Bis(diphenylphosphino)ferrocene

The use of the bidentate ligands dramatically increased the yield of the reaction in comparison to PPh_3 (entry 2 vs. 1), probably both by a more effective coordination of Pd and by accelerating the reductive elimination step. The best reaction conditions were found using dppe, CO (3 bar) at 70 °C for 14 h (entry 4). Higher conversions were achieved by increasing the temperature or the reaction times; however diminished yields were obtained, probably as a result of aldehyde decomposition (entries 2 and 6). The use of a different bidentate ligand as dppf did not appear to improve the yield or the conversion (entry 5). On the other hand, either lower or higher CO pressure caused a significant drop in yield, presumably due to poor CO insertion at 1 bar and an excessive competition at 5 bar. Bubbled CO proved to be ineffective. We also examined the effect of LiCl addition. A more stable reaction intermediate $\text{Ar}[\text{Pd}]\text{Cl}$ (with LiOTf formation) would be formed, thus favoring CO insertion in this complex, in comparison to that of $\text{Ar}[\text{Pd}]\text{OTf}$. Although attempts to enhance yields by using this additive were unsuccessful, LiCl addition played a fundamental role in increasing the reproducibility of this reaction. Multigram amounts of 3,4,5-trimethylbenzaldehyde were obtained via this Palladium-Catalyzed formylation reaction.

2.2.1 Horner-Wadsworth-Emmons olefination: Since Georg Wittig pioneered the first olefination of a carbonyl compound back in 1953⁹ the synthesis of alkenes has become an indispensable strategic tool for the construction of complex molecules. In 1958, Horner¹⁰ disclosed a modified reaction employing phosphonate-stabilized carbanions (Scheme 2.7). The scope of the reaction was further defined by Wadsworth and Emmons.¹¹



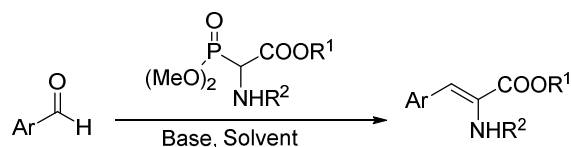
Scheme 2.7. First Horner-type olefination reaction.

9 G. Wittig, G. Geissler, *Liebigs Ann.* **1953**, 580, 44-57.

10 L. Horner, H. M. R. Hoffmann, H. G. Wippel, *Chem. Ber.* **1958**, 91, 61-63.

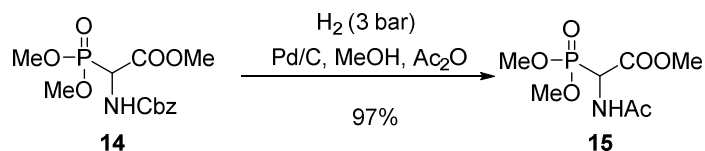
11 W. S. Wadsworth, W. D. Emmons, *J. Org. Chem.* **1961**, 83, 1733-1738.

In contrast to the phosphonium ylides used in the Wittig reaction, phosphonate-stabilized carbanions are more nucleophilic but less basic, so they readily react with practically all aldehydes and ketones under mild reaction conditions. The α -carbon of the phosphonate anions can be further functionalized with various electrophiles prior to the olefination. Furthermore, water-soluble phosphates are formed as byproduct, thereby facilitating the purification of the products. Double bond selectivity is strongly substrate-dependent. Several examples in the literature have demonstrated the efficient use of this reaction for (*Z*)-selective dehydroamino acid synthesis.¹² The use of a conveniently protected phosphonate derivative provides the appropriate (*Z*)-double bond configuration of the final dehydroamino acid (Scheme 2.8).



Scheme 2.8. General conditions for the synthesis of dehydroamino acid derivatives using a HWE olefination.

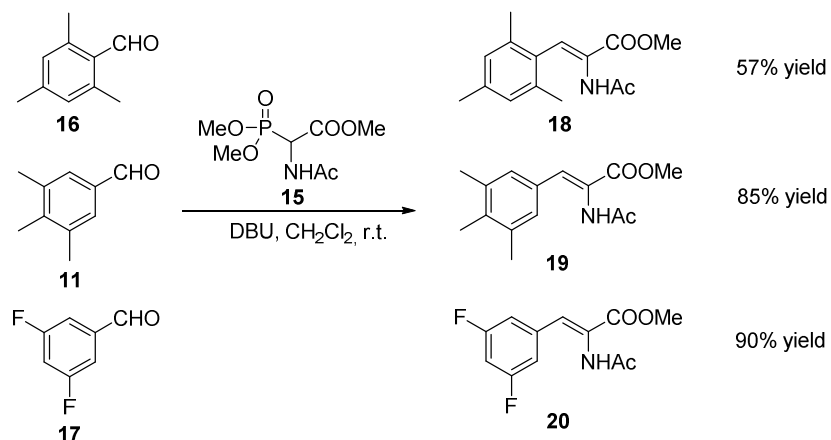
Previous studies in our research group showed that the most convenient amino protecting group for the hydrogenation reaction was the Ac-group. Both Cbz- and Bz-amino protected dehydroamino acid derivatives offered lower enantiomeric excesses upon asymmetric hydrogenation or after hydrolysis, in comparison to those of the N-acetamido derivatives. We therefore changed the amino protecting group in the commercially available phosphonoglycine derivative **14** (Scheme 2.9).



Scheme 2.9. Synthesis of the conveniently protected HWE reagent.

12 S. T. Marino, D. Stachurska-Buczek, D. A. Huggins, B. M. Krywult, C. S. Sheehan, T. Nguyen, N. Choi, J. G. Parsons, P. G. Griffiths, I. W. James, A. M. Bray, J. M. White, R. S. Boyce, *Molecules* **2004**, 9, 405-426.

With the N-acetyl phosphonate derivative **15** in hand and using the experimental conditions optimized by Rosario Ramón as a starting point, we tested the Horner-Wadsworth-Emmons reactions with the corresponding aryl aldehydes (Scheme 2.10).



Scheme 2.10. Synthesis of the key dehydroamino acids by an HWE olefination reaction.

Although the mesityl-derivative was obtained in moderate yield, all α,β -dehydro acetamido esters were satisfactorily achieved by using this reaction. In comparison to the first results obtained, yields were increased by ~20% using both the minimum amount of dichloromethane and meticulously dried phosphonate. We assumed that the olefination proceeded with very high (*Z*)-double bond selectivity, since no signal corresponding to the (*E*)-enantiomer was detected by ¹H-NMR.

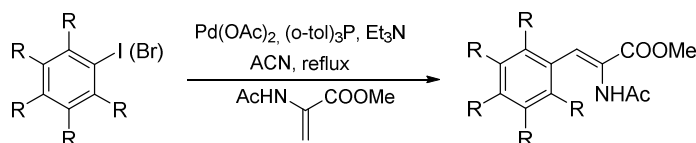
2.2.2. Heck and Suzuki cross-coupling reactions: Palladium-Catalyzed arylation or vinylation of olefins by aryl or vinyl halides (or pseudo-halides), that is, the Heck reaction, is one of the most useful tools for constructing C-C bonds in synthetic chemistry. To date, most of the reported Heck reactions deal with olefins bearing electron-withdrawing substituents, such as -COOR and -CN, which selectively lead to products resulting from arylation or vinylation at the less-substituted (β) position of the olefin double bond.¹³ Recent developments in the

¹³ N. J. Whitcombe, K. K. Hii, S. E. Gibson, *Tetrahedron* **2001**, 57, 7449-7476.

catalysts and reaction conditions have resulted in a much broader range of donors and acceptors being amenable to this transformation.

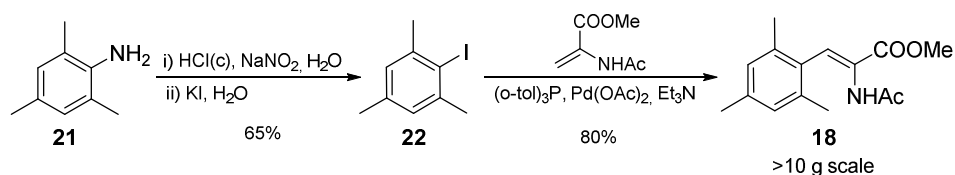
Several α,β -dehydroamino acid derivatives have been synthesized by using a Heck reaction (Scheme 2.11).¹⁴ Most of them involved a Palladium-Catalyzed C-C bond formation between an aryl iodide or bromide and methyl 2-acetamidoacrylate, conditions appropriate for our substrates. At this point, our research in somatostatin analogs mainly demanded the Msa and Tmp amino acids. Consequently, only the syntheses of these two methylated phenyl alanine analogs were carried out by using this route.

The Msa derivative: Okada and co-workers¹⁵ described the enantioselective synthesis the 2,4,6-trimethylphenyl dehydroamino acid derivative **18** in nearly 50% total yield.



Scheme 2.11. Okada's synthesis of phenylalanine derivatives

By following this procedure, the commercially available mesitylaniline **21** provided rapid access to the 2,4,6-trimethyliodobenzene **22**, by diazotization and subsequent replacement with iodide (Scheme 2.12). Then, a Heck reaction provided the (*Z*)-dehydroamino acid derivative **18**, achieving a 52% overall yield.



Scheme 2.12. Synthesis of the (*Z*)-methyl 2-acetamido-3-(mesityl)acrylate via Okada's chemistry

14 M. Suhartono, M. Weidlich, T. Stein, M. Karas, G. Dürner, M. W. Göbel, *Eur. J. Org. Chem.* **2008**, 2008, 1608-1614.

15 T. Li, Y. Tsuda, K. Minoura, Y. In, T. Ishida, L. H. Lazarus, Y. Okada, *Chem. Pharm. Bull.* **2006**, 54, 873-877.

It should be emphasized here that Okada and co-workers confirmed the expected (*Z*)-configuration of the double bond both by NMR and X-ray studies. In all our dehydroamino acid syntheses, the (*Z*)-product was consistently obtained and identified by NMR by analogy either with the literature data or with the previous studies carried out by Rosario Ramón.

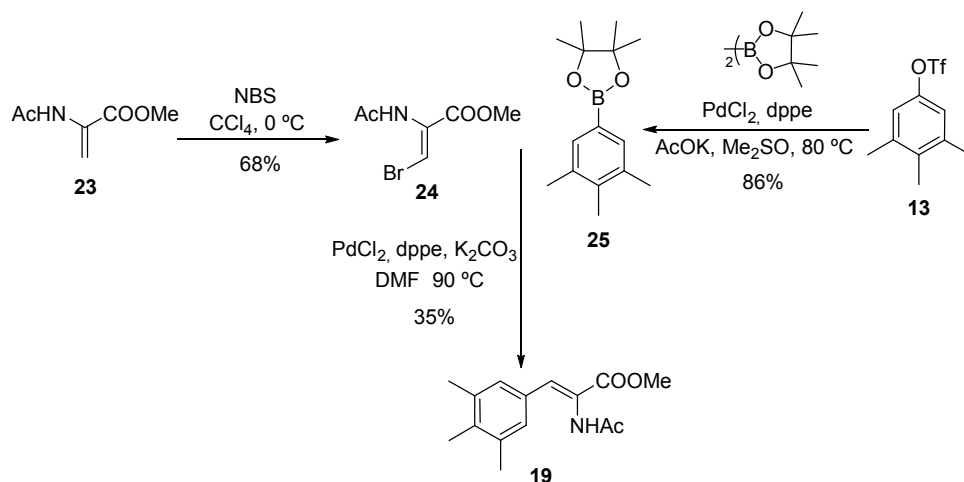
The “Heck pathway” offers a noteworthy improvement for the synthesis of the Msa derivative, in comparison to the HWE route that we previously presented. The low-cost starting materials and reagents (since only catalytic amounts of Pd(OAc)₂ and (*o*-tol)₃P are used), the reasonable yields and the fact that the final product is efficiently purified by recrystallization point to this route as the preferred approach for the synthesis of the (*Z*)-methyl 2-acetamido-3-mesitylacrylate.

The Tmp amino acid: Okada’s coupling conditions failed when using 3,4,5-trimethylphenyl trifluoromethanesulfonate **13** as substrate, since the dehydroamino acid derivative was not detected by TLC or ¹H-NMR. We did not find any improvement by modifying the order of addition of the reagents, the solvent (DMF and THF were studied) or the type of phosphine (bidentate phosphines such as dppe and dppf were also ineffective). Appreciably, the addition of LiCl (1-3 eq) led to the trimethylphenyl acrylate **19** in 15% yield. Although the replacement of the triflate by iodine would most likely have improved the yield of this transformation, we considered that further refinement of this reaction was not worthwhile, since more accessible pathways leading to our product were still readily available and the phenol is the only commercially available substrate.

We went one step further and addressed a different cross-coupling reaction in order to obtain the Tmp derivative. The Suzuki reaction involves the coupling of an aryl- or vinyl-boronic acid with an aryl- or vinyl-halide or pseudohalide catalyzed by a palladium(0) complex.¹⁶ Potassium trifluoroborates and organoboranes or boronate

16 A. Suzuki, *J. Organomet. Chem.* **1999** 576, 147-168.

esters may be used instead of boronic acids. Bromination of **23** with NBS resulted in the predominant formation of (*Z*)-methyl 2-acetamido-3-bromoacrylate (**24**), suitable for the proposed cross-coupling with the corresponding boronic acid pinacol ester **25**. The commercially available 3,4,5-trimethylphenol offered convenient access to the boronic acid derivative **25**. The phenol was first converted to its triflate (**13**) using the general reaction described in this chapter (Scheme 2.5). The resulting triflate was subjected to a Pd-Catalyzed reaction with bis(pinacolato)diboron which furnished the 4,4,5,5-tetramethyl-2-(3',4',5'-trimethylphenyl)-1,3,2-dioxaborolane **25** in 86% yield.



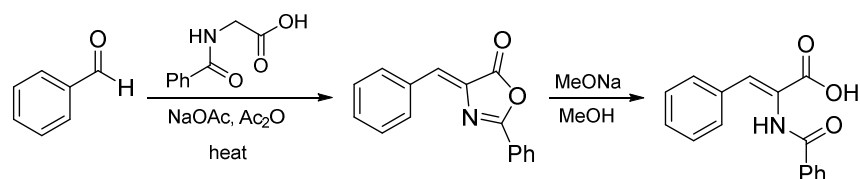
Scheme 2.13. Synthesis of the (*Z*)-methyl 2-acetamido-3-(3',4',5'-trimethylphenyl)acrylate via Suzuki cross-coupling.

Boronate **25** underwent a Suzuki cross-coupling reaction with the acetamido bromoacrylate **24** using PdCl₂, ethylenebis(diphenylphosphine) and K₂CO₃ as base, which afforded the dehydroamino acid derivative **19** in 35% yield. Unfortunately, variation of temperature (90-120 °C), solvent (DMF + 5% H₂O or Tol/EtOH/H₂O) or the catalytic system ([dppf]PdCl₂·CH₂Cl₂) did not produce any substantial improvement.

2.2.3. The azlactone route: Azlactones are key synthons for the synthesis of several biologically active compounds.¹⁷ The most well-known route to azlactones is

17 M. González-Esguevillas, J. Adrio, J. C. Carretero, *Chem. Commun.* **2013**, 49, 4649-4651.

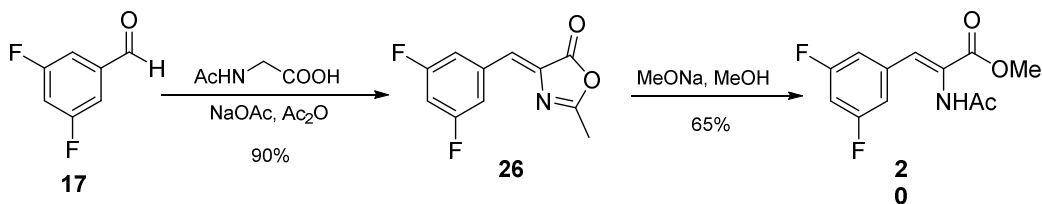
the Erlenmeyer method,¹⁸ which involves the direct condensation of aldehydes with hippuric acid in the presence of stoichiometric amounts of fused anhydrous sodium acetate as a basic catalyst in acetic anhydride. In the well-known Erlenmeyer synthesis of amino acids, the ring of the intermediate azlactone is subsequently opened to give the corresponding dehydroamino acid (Scheme 2.14).



Scheme 2.14. Dehydroamino acid formation via Erlenmeyer synthesis.

Rosario Ramón first tried to adapt the Erlenmeyer synthesis to achieve multigram quantities of the Msa amino acid. The use of N-acetylglycine (instead of hippuric acid) yielded the correspondent azlactone in modest yield. However, ring opening failed under a number of reaction conditions.

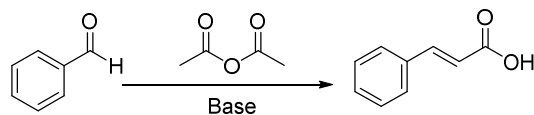
Since the Heck route provided the Tmp dehydroamino acid in a very effective manner, only the 3,5-difluorobenzaldehyde **17** was selected as substrate to test the Erlenmeyer conditions (Scheme 2.15). N-Acetylglycine was used for azlactone formation. Subsequent ring opening (MeONa/MeOH) produced the (Z)-methyl-2-acetamido-3-(3,5-difluorophenyl)acrylate **20** in 58% total yield (>10 g scale). The (E)-isomer was not detected by TLC or by NMR. In this case, the success in the dehydroamino acid synthesis coupled with the low-cost reagents used here reveals the azlactone route as a highly competent pathway towards the synthesis of the Dfp amino acid.



Scheme 2.15. Synthesis of the fluorinated dehydroamino acid derivative via the azlactone route.

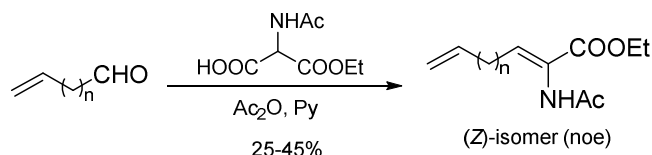
18 a) E. E. Jun, *Justus Liebigs Ann. Chem.*, **1893** 275,1-8; b) J. Lamb, W. Robson, *Biochem J.* **1931** 25, 1231-1236.

2.4. The Perkin reaction: The condensation of aromatic aldehydes with anhydrides of aliphatic carboxylic acids in the presence of a weak base to afford α,β -unsaturated carboxylic acids is known as the Perkin reaction (Scheme 2.16).¹⁹



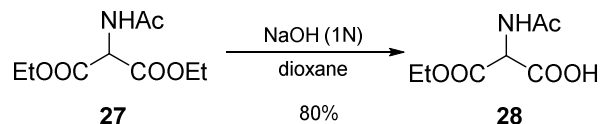
Scheme 2.16. “The Perkin Reaction”.

Several modifications of this transformation have been done in recent decades (in fact, the Erlenmeyer azlactone synthesis could be considered a Perkin-type reaction), and some of these variations led to the so-called “Perkin route” for the selective synthesis of (Z)-amino acids.²⁰ Several examples of this transformation involving linear aldehydes are found in the literature (Scheme 2.17).²¹



Scheme 2.17. Synthesis of linear ethyl-2-acetamidoacrylate derivatives via the Perkin route.

It is widely known that the classic Perkin reaction usually works better with aromatic aldehydes.²⁰ In fact, the reaction is more facile and gives higher yield of the product when the aromatic aldehyde has one or more electron-withdrawing substituents. It was thus mandatory to examine the synthesis of the dehydrodifluorophenyl derivative via the Perkin route. For this purpose, commercial diethyl 2-acetamidomalonate **27** was first monohydrolyzed to **28** using 1 eq of sodium hydroxide (Scheme 2.18).



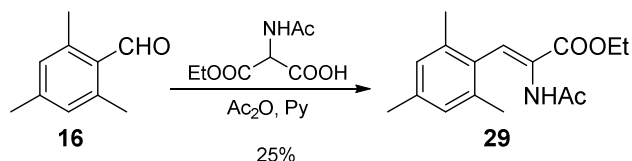
19 a) W. H. Perkin, *J. Chem. Soc.* **1868**, 21, 181-186; b) J. F. J. Dippy, R. M. Evans, *J. Org. Chem.* **1950**, 15, 451-456.

20 H. Hoshina, H. Tsuru, K. Kubo, T. Igarashi, T. Sakura, *Heterocycles* **2000**, 53, 2261-2274.

21 F. Velázquez, S. Venkatraman, W. Wu, M. Blackman, A. Prongay, V. Girijavallabhan, N. Shih, F. G. Njoroge, *Org. Lett.* **2007**, 9, 3061-3064.

Scheme 2.18. Synthesis of the monoethyl N-acetamide malonate, the “Perkin reagent” for the synthesis α -amino acid derivatives.

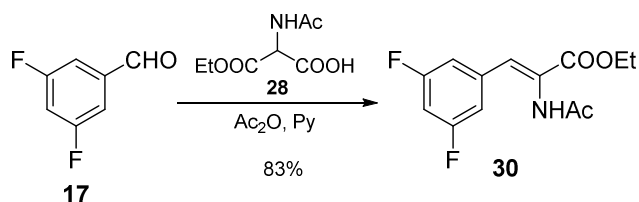
We first subjected the mesitylaldehyde **16** to Perkin conditions. The corresponding dehydroamino acid **30** derivative was obtained in only 25% yield (Scheme 2.19). Once again, the steric hindrance of the *ortho*-methyl groups in the mesityl moiety probably accounts for the poor yield.



Scheme 2.19. Synthesis of the mesityl dehydroamino acid derivative by the Perkin route.

Since the Tmp derivative was efficiently synthesized by the Heck route, we did not assay the synthesis of the Tmp dehydroamino acid by this route.

A Perkin type reaction between the 3,5-difluorobenzaldehyde **17** and the monoethyl N-acetamide malonate **28** in acetic anhydride and pyridine afforded the correspondent (*Z*)-dehydroamino acid **30** in 80% yield (Scheme 2.20). Despite the unclean crude mixtures that this reaction offered (meticulous column chromatography is necessary for product purification) we considered that the Perkin route would be able to compete with the other pathways presented previously for the synthesis of this dehydroamino acid derivative. Both the reduced price of all the reagents involved and the satisfactory yields are the major advantages of this particular synthetic strategy.



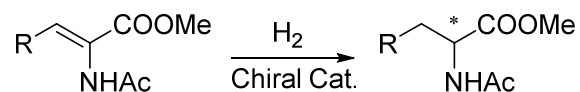
Scheme 2.20. Synthesis of the fluorinated dehydroamino acid derivative by the Perkin route.

With gram amounts of the dehydroamino acids in hand, achieved by these different routes, an Asymmetric Hydrogenation reaction allowed as to obtain the enantiomerically enriched conveniently protected amino acid derivatives.

2.3. Rhodium-Catalyzed Asymmetric Hydrogenation

The increasing demand for enantiomerically pure pharmaceuticals, agrochemicals, and fine chemicals has driven the development of asymmetric catalytic technologies. Asymmetric Hydrogenation, using molecular hydrogen to reduce prochiral olefins, ketones, and imines, has become one of the most efficient, practical, and atom-economical methods for the construction of chiral compounds.²²

During the last few decades of the 20th century, significant attention was devoted to the discovery of new asymmetric catalysts, in which transition metals bound to chiral phosphorous ligands emerged as preferential catalysts for asymmetric hydrogenation. Dozens of efficient chiral phosphorous ligands with diverse structures have been developed and their application to asymmetric hydrogenation established.²³ Indeed, many represent the key step in industrial processes for the preparation of enantiomerically pure compounds. The immense significance of asymmetric hydrogenation was recognized when the 2001 Nobel Prize in Chemistry was awarded to Knowles and Noyori (shared with Sharpless) "for their work on chirally catalysed hydrogenation reactions".



Scheme 2.21. Asymmetric-Hydrogenation reaction involving dehydroamino acid derivatives as substrates.

The invention of efficient chiral phosphorous ligands has played a critical role in the development of asymmetric hydrogenation. To a certain extent, the development of chiral phosphorous ligands parallels that of asymmetric hydrogenation. Several chiral phosphorous ligands with great structural diversity are effective for the asymmetric hydrogenation of α -dehydroamino acid derivatives. In particular, the Rhodium-Catalyzed Enantioselective Hydrogenation of N-acylated dehydroamino acids or their esters is a standard tool for the synthesis of natural and

22 P. Etayo, A. Vidal-Ferran, *Chem. Soc. Rev.*, **2013**,42, 728-754.

23 S. Lühr, J. Holz, A. Börner, *ChemCatChem* **2011**, 3, 1708-1730.

unnatural amino acids of high enantiomeric purity (Scheme 2.21).²⁴ In these cases, in contrast to the high enantioselectivity achieved for the *Z*-isomeric substrates, hydrogenation of the *E*-isomers usually proceeds with lower rates and affords products with diminished enantioselectivities.²⁵ Although not fully understood, this result is particularly important, since dehydroamino acid derivatives may be difficult to prepare in a geometrically pure form. All the different routes that we have previously described for the synthesis of dehydroamino acid intermediates proceeded with very high (*Z*)-double bond selectivity, since no signal corresponding to the (*E*)-enantiomer was detected by ¹H-NMR.

2.3.2. The use of DuPHOS and DIPAMP as ligands: During her doctoral thesis, Rosario Ramón succeeded in synthesizing the Msa amino acid derivative via asymmetric hydrogenation using commercially available Rh(I) chiral catalysts (Figure 2.1), so we took her reaction conditions as starting point for our experiments.

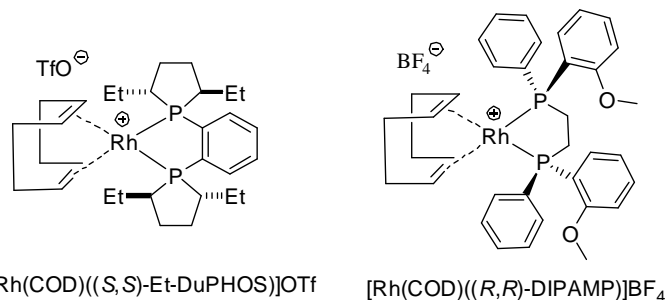


Figure 2.1. Commercial Rh(I) catalysts used in Asymmetric-Hydrogenation reactions.

Since only the natural (*S*)-enantiomer of our derivatives was considered of interest at that point, (*S,S*)-DuPHOS²⁶ and (*R,R*)-DIPAMP²⁷ were tested as ligands. A Rhodium-Catalyzed Asymmetric Hydrogenation using these ligands allowed us to

24 P. Etayo, J. L. Núñez-Rico, H. Fernández-Pérez, A. Vidal-Ferran, *Chem. Eur. J.*, **2011**, 17, 13978-13982.

25 I. D. Gridnev, T. Imamoto, *Chem. Commun.* **2009**, 7447-7464.

26 a) Burk, M. J.; Calabrese, J. C.; Davidson, F.; Harlow, R. L.; Roe, D. C. *J. Am. Chem. Soc.* **1991**, 113, 2209-2222. b) Burk, M. J.; Feaster, J. E.; Nugent, W. A.; Harlow, R. L. *J. Am. Chem. Soc.* **1993**, 115, 10125-10138.

c) Burk, M. J.; Bienewald, F.; Challenger, S.; Derrick, A.; Ramsden, J. A. *J. Org. Chem.* **1999**, 64, 32903293.

27 Knowles, W. S.; Sabacky, M. J.; Vineyard, B. D.; Weinkauff, D. J. *J. Am. Chem. Soc.* **1975**, 97, 2567-2568.

obtain the enantioenriched Msa, Tmp and Dfp acetamidoesters in excellent yields and e.e.'s (Table 2.2).

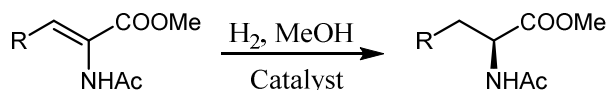
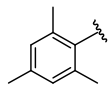
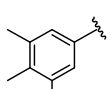
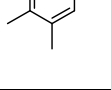
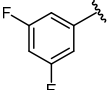


Table 2.2. Synthesis of the enantioenriched Msa, Tmp and Dfp derivatives by Rh-Catalyzed Asymmetric Hydrogenation using commercially available ligands.^a

Entry	R	Cat.	T ^a	P (bar)	Yield	e.e.
1		[(COD) (R,R)-DIPAMP] Rh(I)BF ₄	25 °C	40 bar	99 %	94% ^b
2		[(COD) (R,R)-DIPAMP] Rh(I)BF ₄	25 °C	2 bar	99 %	77%
3		[(COD) (S,S)-Et-DuPHOS] Rh(I)OTf	25 °C	2 bar	99 %	99%
4		[(COD) (S,S)-Et-DuPHOS] Rh(I)OTf	25 °C	5 bar	99 %	99%

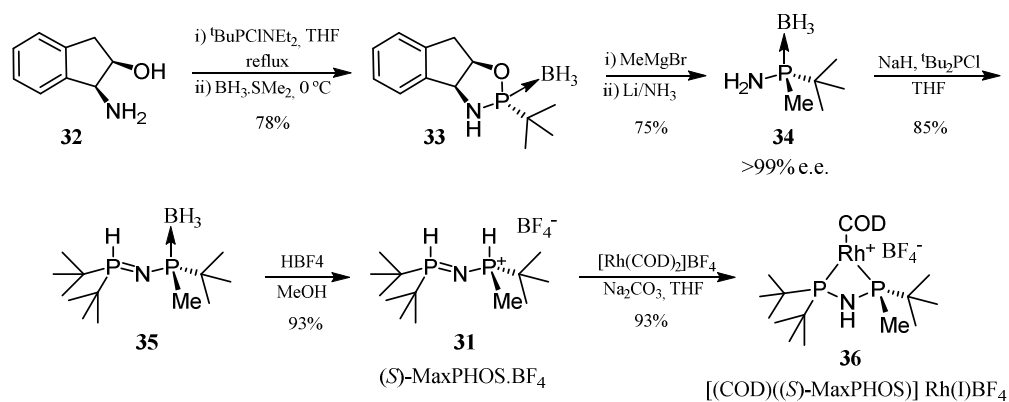
a: All reaction times were 24 h. 3% cat. was used in all cases. b: 99% e.e. after recrystallization.

2.3.3. The Rh(I)-MaxPHOS system: While we were optimizing the asymmetric hydrogenation conditions for the synthesis of these products, a project focused on the development of new chiral phosphine ligands was running simultaneously in our research group.

One of the most interesting compounds they found was the air-stable phosphonium salt **31**, so-called MaxPHOS. The synthesis of this ligand is summarized in Scheme 2.22. This compound is a nitrogen-containing analog of the trichickenfootPHOS (TCFP) ligand reported by Hoge *et al.*,²⁸ one of the most efficient ligands ever developed for Asymmetric Hydrogenation reactions.

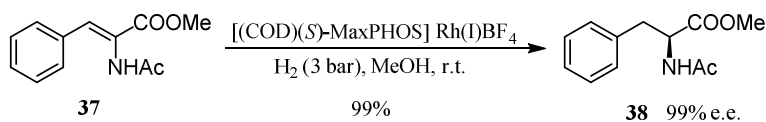
²⁸ Hoge, G.; Wu, H. P.; Kissel, W. S.; Pflum, D. A.; Greene, D. J.; Bao, J. *J. Am. Chem. Soc.* **2004**, *126*, 5966-5967.

2. Enantioselective syntheses of non-natural aromatic amino acids



Scheme 2.22. Optimized synthesis of Rh(I)-MaxPHOS catalyst.

Preliminary studies of the performance of the Rh-MaxPHOS catalytic system in asymmetric hydrogenation reactions showed that (*Z*)- α -acetamidocinnamate (the correspondent methylacetamido acrylate derivative from the natural phenylalanine amino acid) was reduced with complete selectivity (>99 % e.e.) in less than 4 hours using only 0.3 mol% of **36** as catalyst (Scheme 2.23).²⁹



Scheme 2.23. [Rh(I)-MaxPHOS]-Catalyzed Asymmetric Hydrogenation of (*Z*)-MAC

This encouraging result prompted us to study the Asymmetric Hydrogenation reaction of our substrates by using this catalyst. The *N*-acetyl-protected Msa, Tmp and Dfp dehydroamino acid derivatives were subjected to a Rh(I)-Catalyzed Asymmetric Hydrogenation reaction using [(COD) (*S*)-MaxPHOS] Rh(I)BF₄ (Table 2.3).

Using the (*S*)-MaxPHOS containing catalyst, (*S*)-methyl 2-acetamido-3-mesitylpropanoate (entry 2) was obtained in 96% e.e. working at 60 bar of hydrogen. The enantiomeric hydrogenation of this highly sterically hindered substrate is particularly challenging. This result implies a small but solid enhancement in e.e. in comparison to that achieved when using the commercially available [(COD)(*R,R*)-DIPAMP] Rh(I)BF₄ catalyst.

29 M. Reves, C. Ferrer, T. Leon, S. Doran, P. Etayo, A. Vidal-Ferran, A. Riera, X. Verdaguier, *Angew. Chem., Int. Ed.* **2010**, *49*, 9452-9455.

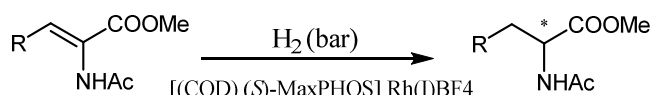


Table 2.3. Synthesis of the enantioenriched Msa, Tmp and Dfp derivatives by Rh-Catalyzed Asymmetric Hydrogenation using the Rh(I)-MaxPHOS system.^a

Entry	R	Solvent	T ^a	Pressure	Yield	e.e.
1		MeOH	25 °C	40 bar	78 %	n.m.
2		MeOH	25 °C	60 bar	99 %	96 % ^b (S)
3		MeOH	25 °C	5 bar	99 %	98 % (S)
4		MeOH	25 °C	2 bar	99 %	99 % (S)
5		MeOH	25 °C	20 bar	99 %	95 % (S)
6		MeOH	25 °C	15 bar	99 %	96 % (S)
7		MeOH	25 °C	2 bar	< 5%	-
8		MeOH	25 °C	5 bar	99 %	97 % (S)

a: All reaction times were 24h. 3% cat. was used in all cases. n.m.: not measured. b: 99% e.e. after recrystallization. Only the relevant reaction conditions tested are shown.

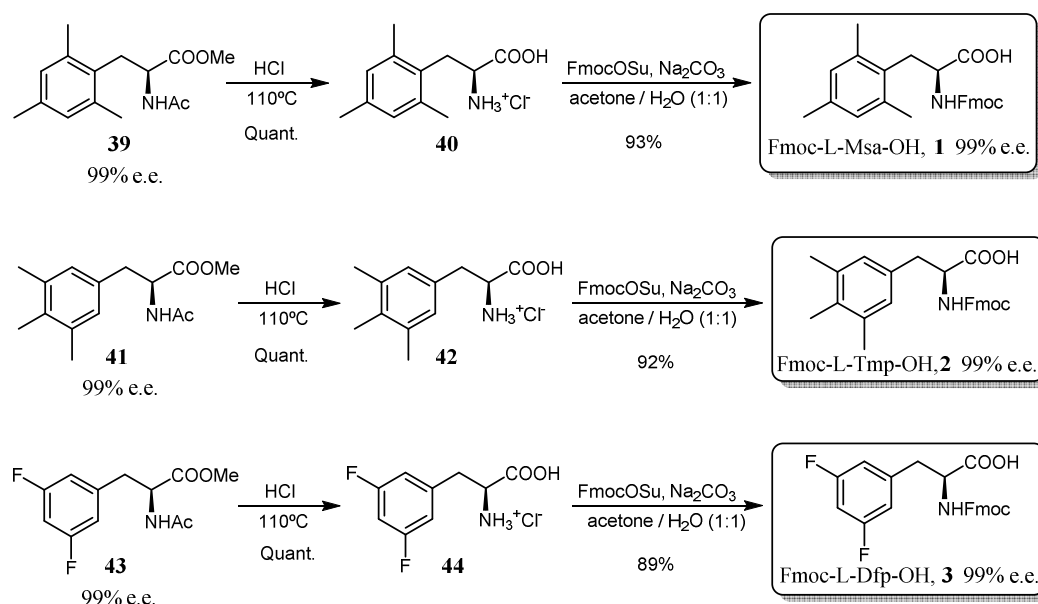
Asymmetric hydrogenation of the 3,4,5-trimethyl dehydroamino acid derivative proceeded with total enantioselectivity to afford the (S)-methyl 2-acetamido-3-(3',4',5'-trimethylphenyl)-propanoate in 99% e.e. (entry 4). On the other hand, after exploration of several reaction conditions (entries 5-8), the electron-poor difluorophenyl derivative was quantitatively reduced with 97% e.e. The Asymmetric Hydrogenation reaction of dehydroamino acids containing electron-poor aromatic rings have been proved to be difficult to achieve using the Rh(I)-MaxPHOS.BF₄ catalytic system in numerous cases.²⁴ When the hydrogenation of the difluorinated residue was carried out using (S)-MaxPHOS as ligand, the final recrystallization of the Fmoc-L-Dfp-OH amino acid derivative allowed us to obtain this product in 99% e.e.

In summary, by using Rh(I) containing commercially available (DuPHOS or DIPAMP) or “home-made” (MaxPHOS) chiral phosphine ligands, we obtained the three different enantioenriched acetamidoesters in 99% e.e. Subsequent hydrolysis

of these products and N-Fmoc protection would produce the corresponding amino acid derivatives for their use in SPPS.

2.4. Hydrolysis and Fmoc-protection

Rosario Ramon described that strong acidic conditions (occasionally required for the hydrolysis of the acetyl and ester moieties) may led to racemization at the α -carbon of these types of substrates. In all our cases, these two final steps towards the acquisition of the conveniently protected amino acid derivatives proceeded without inconveniences, since final e.e.'s of all products were found to be identical to those of the precursors. All Fmoc-derivatives were obtained in excellent yield under standard protection conditions (Scheme 2.24).



Scheme 2.24. Hydrolysis and Fmoc-protection of the three aromatic non-natural amino acids.

At this time, we had more than enough of all the amino acids to address our objectives. Thus, with gram quantities of these enantiomerically pure Fmoc-amino acids in hand, we started the synthesis of 14-residue SRIF analogs containing site-directed modifications.

3

Somatostatin analogs containing the Msa amino acid

Chapter 3. Somatostatin analogs containing the Msa amino acid	
3.1. Introduction: Aromatic interactions in peptides and proteins	35
3.2. Somatostatin analogs containing Msa residues	39
3.2.1. Synthesis	39
3.2.2. Serum stability studies	41
3.2.3. Receptor-subtype selectivity assays	42
3.2.4. Structure.....	44
3.3. Conclusions	54

3.1. Introduction:

Aromatic interactions in peptides and proteins

Noncovalent inter- and intra-molecular interactions involving aromatic rings are ubiquitous in chemical and biological processes. The understanding of these interactions is essential in medicinal chemistry and lead optimization for drug design. The diversity of environments and multitude of functions in which they participate reflects their relevance; for example, vertical stacking interactions provide stability to duplex DNA.¹ Other important phenomena include the spike–nucleocapsid interaction in viruses,² molecular self-assembly in supramolecular systems,³ and host–guest molecular recognition events.⁴ In addition, aromatic residues have been found to stabilize protein structures through clusters and tertiary contacts.⁵ Isolated motifs of secondary structure have also been shown to benefit from the presence of aromatic residues.⁶ Although many theoretical and experimental studies have focused on the investigation of aromatic interactions in recent decades, a clear and consistent picture has not yet emerged.

The potential significance of aromatic interactions in protein folding and structure was first appreciated by Burley and Petsko.^{5a} About 60% of the aromatic side-chains of proteins are involved in aromatic pairs, and 80% of these interactions contributes to stabilize the tertiary structure by linking various elements of the secondary structure. It has been proposed that a typical aromatic-aromatic interaction has an energy of between -1 and -2 kcal/mol and contributes between -0.6 and -1.3 kcal/mol to protein stability.⁷

1 W. Saenger, *Principal of Nucleic Acid Structure*, Springer, New York, 1984.

2 U. Skoging, M. Vihinen, L. Nilsson, P. Liljeström, *Structure* **1996**, 4, 519–529.

3 M. Ma, Y. Kuang, Y. Gao, Y. Zhang, P. Gao, B. Xu, *J. Am. Chem. Soc.* **2010**, 132, 2719–2728.

4 C. A. Hunter, *J. Chem. Soc. Chem. Commun.* **1991**, 749–751.

5 a) S. K. Burley, G. A. Petsko, *Science* **1985**, 229, 23–28; b) Blundell, J. Singh, J. Thornton, S. K. Burley, G. A. Petsko, *Science* **1986**, 234, 1005–1005; c) J. Singh, J. M. Thornton, *FEBS Lett.* 1985, 191, 1–6.

6 R. Mahalakshmi, S. Raghothama, P. Balaram, *J. Am. Chem. Soc.* **2006**, 128, 1125–1138.

7 L. Serrano, M. Bycroft, A. R. Fersht, *J. Mol. Biol.* **1991**, 218, 465–475.

The observation that aromatics are found in networks rather than as isolated units suggests that there is a unique interaction that is not purely hydrophobic and that aromatic groups interact in a distinct manner from aliphatic side-chains, providing specificity in protein folding as a result of their aromatic nature. Aromatic interactions have been proposed to consist of a combination of forces including electrostatic, hydrophobic, and van der Waals interactions.⁴ This combination of factors makes the aromatic interactions favorable and strong in water –because of the hydrophobic component– yet at the same time selective –when the electrostatic component is significant–. The relative contribution and magnitude of each of these components depends on many factors, and is still under investigation.

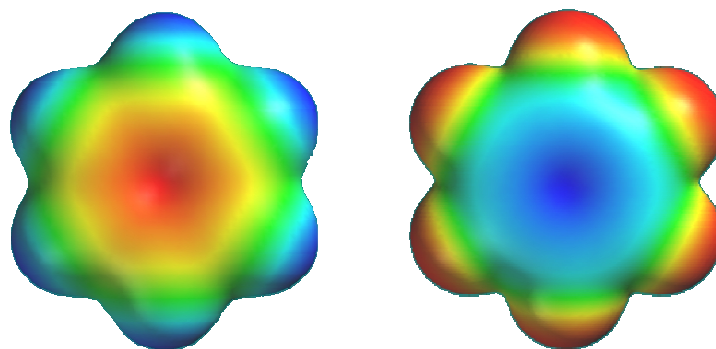


Figure 3.1. Aromatic moieties of Phe (benzene) and F5Phe (hexafluorobenzene). Electrostatic potential maps (blue=positive, red=negative) were generated with Spartan (PM3 semi-empirical).

The possible geometries that aromatic rings adopt in aromatic interactions are limited. It has been proposed that favorable quadrupole-quadrupole interactions promote association and give rise to the orientational preferences for the interactions of two aromatic rings.⁸ The simplest aromatic structure benzene, exhibits an uneven electron distribution even though it does not have a net dipole. Since a sp^2 carbon is more electronegative than hydrogen, benzene displays a negative potential on the π face and a positive potential around the periphery, which gives rise to the quadrupole moment (Figures 3.1 and 3.2). Benzene molecules pack in an *edge-to-face* fashion in the solid state (Figure 3.2, b)). This geometry, which can

⁸ C. A. Hunter, J. K. M. Sanders, *J. Am. Chem. Soc.* **1990**, *112*, 5525-5534.

be considered as a type of CH- π interaction, is usually found between aromatic residues in proteins. The offset-stacked orientation is also commonly found in proteins and is the geometry of base-stacking in DNA. In this geometry, more surface area is buried and the van der Waals and hydrophobic interactions are increased. The *face-to-face* stacked geometry (Figure 3.2, c)) is commonly observed with donor-acceptor pairs and compounds that have opposite quadrupole moments, such that the interaction between the faces of the rings is attractive.

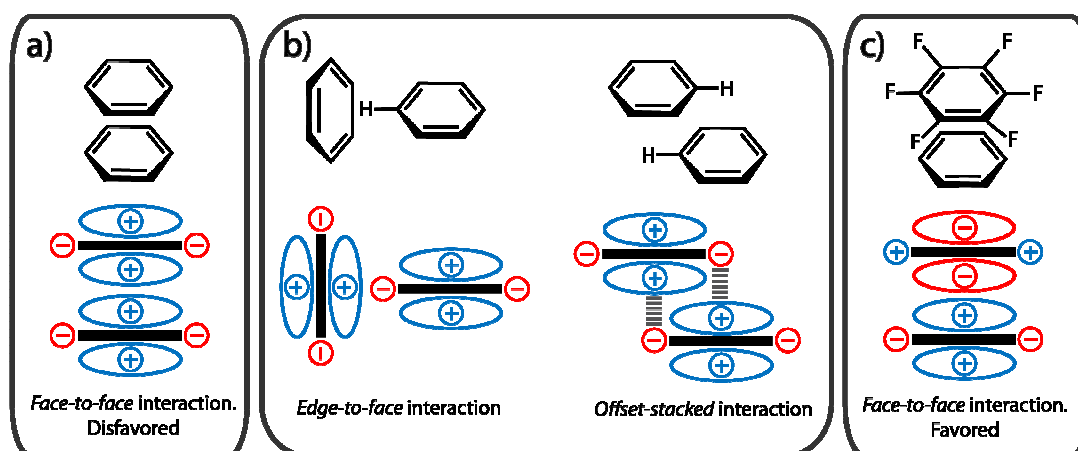


Figure 3.2. Schematic representations of different aromatic interaction geometries. Cartoons are presented to qualitatively describe aromatic quadrupole moments in electron-rich or electron-poor aromatic rings (benzene and perfluorobenzene, respectively). a) *Face-centered* stacking is disfavored between two electron-rich aromatics by electronic repulsion. b) *Edge-to-face* (T-shaped) and *offset-stacked* geometries for two electron-rich aromatics. c) The benzene-perfluorobenzene *face-to-face* aromatic interaction.

A wide range of theoretical and experimental studies have addressed the importance of polar- π interactions, and recent lines of research have provided new insight into the driving force, stability, selectivity, strength and geometrical preferences of these interactions.⁹ Nonetheless, many critical questions regarding their nature and directionality remain to be answered. Despite the lack of their complete understanding, aromatic interactions have been exploited to improve

⁹ These studies have been recently reviewed by Diederich: a) E. A. Meyer, R. K. Castellano, F. Diederich, *Angew. Chem. Int. Ed.* **2003**, *42*, 1210-1250; b) L. M. Salonen, M. Ellermann, F. Diederich, *Angew. Chem. Int. Ed.* **2011**, *50*, 4808-4842.

various parameters in the context of material science,¹⁰ biological systems,¹¹ asymmetric catalysis¹² and supramolecular chemistry.¹³ The strengthening of this type of noncovalent interaction has also been used to increase peptide¹⁴ and protein¹⁵ stability and selectivity. We considered that research into the existence, nature and significance of the presumed aromatic interactions that stabilize some bioactive conformations in SRIF¹⁶ would further facilitate our understanding of these interaction energies, the application of which would be useful in peptide design and structure prediction. In particular, the conformational flexibility of these somatostatin analogs will decrease if we are able to intensify some key non-covalent interactions. Thus, the 3D structure of the major conformations of these tetradecapeptides will be captured by NMR techniques, allowing us for the first time to study and characterize the corresponding aromatic interactions in detail. Ideally, these more structured analogs will be more stable and receptor-selective than the natural counterpart –offering highly valuable therapeutic peptides–, and their main conformations in solution may shed light on the particular conformations SRIF adopts when it binds to its five receptors subtypes.

10 G. W. Coates, A. R. Dunn, L. M. Henling, D. A. Dougherty, R. H. Grubbs, *Angew. Chem. Int. Ed.* **1997**, *36*, 248-251.

11 R. Faraoni, R. K. Castellano, V. Gramlich, F. Diederich, *Chem. Commun.* **2004**, *0*, 370-371.

12 a) H. C. Kolb, P. G. Andersson, K. B. Sharpless, *J. Am. Chem. Soc.* **1994**, *116*, 1278-1291; b) M. Yamakawa, I. Yamada, R. Noyori, *Angew. Chem. Int. Ed.* **2001**, *40*, 2818-2821.

13 R. A. Bissell, E. Cordova, A. E. Kaifer, J. F. Stoddart, *Nature* **1994**, *369*, 133-137.

14 S. M. Butterfield, P. R. Patel, M. L. Waters, *J. Am. Chem. Soc.* **2002**, *124*, 9751-9755.

15 J. Georis, F. D. L. Esteves, J. Lamotte-Brasseur, V. Bougnet, F. Giannotta, J. Frère, B. Devreese, B. Granier, *Protein Sci.* **2000**, *9*, 466-475.

16 a) J. E. Rivier, M. R. Brown, W. W. Vale *J. Med. Chem.* **1976**, *19*, 1010-1013; b) D. F. Veber, F. W. Holly, W. J. Paleveda, R. F. Nutt, S. J. Bergstrand, M. Torchiana, M. S. Glitzer, R. Saperstein, R. Hirschmann, *Proc. Natl. Acad. Sci. U. S. A.* **1978**, *75*, 2636-2640.

3.2. Somatostatin analogs containing Msa residues

We first prepared various analogs by replacing the aromatic ring of the phenylalanine with a mesityl group (2,4,6-trimethylphenyl), that is, by substituting each Phe with the 3-mesityl alanine amino acid (Msa; see Figure 3.2). We chose the Msa residue on the basis of the higher hydrophobicity and electronic density that the methyl groups confer upon the aromatic moiety, and of the reduced conformational mobility of the mesityl ring relative to Phe.¹⁷ Hence, we expected that the polar- π interactions between the Msa and the remaining Phe residues would be stronger than those between the Phe groups of the parent compound, and envisaged that the intrinsic rigidity of the Msa amino acid could be extended to the whole peptidic architecture.

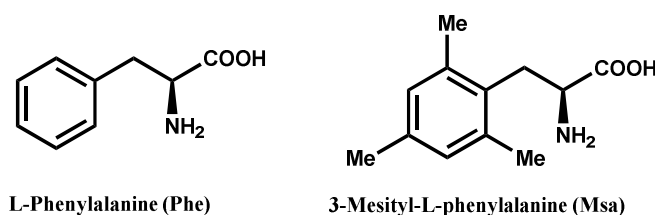


Figure 3.2. The Phe and the Msa amino acids.

3.2.1. Synthesis: We studied three groups of SRIF analogs containing specific site-directed modifications (Table 3.1). The single residue substitution in position 6, 7 or 11 led to the first group of peptides (**45-47**). Since it is known that the exchange of the L-Trp8 by its enantiomer increases the stability of the molecule while not significantly affecting the activity profile, a second group of analogs containing a D-Trp in position 8 was also prepared (**48-50**). Replacement of the natural phenylalanine in two or three positions with Msa residues led to the third group of peptides (**51-54**).

17 E. Medina, A. Moyano, M. A. Pericas, A. Riera, *Helv. Chim. Acta* **2000**, 83, 972-988.

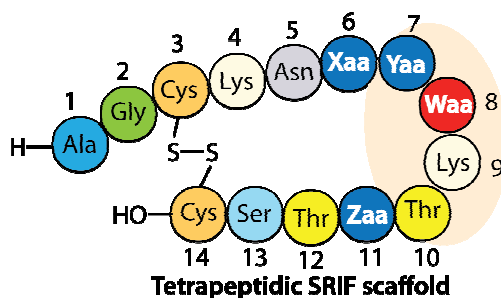
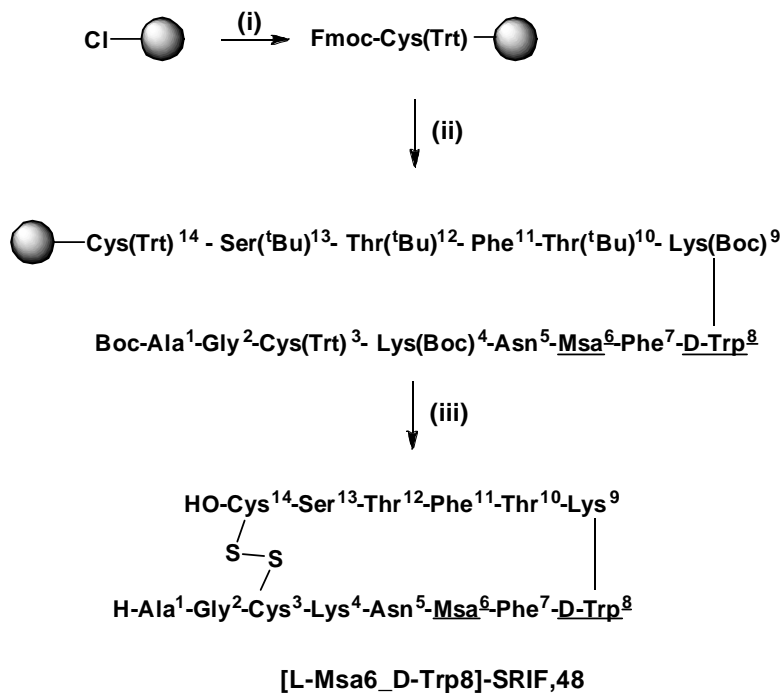


Table 3.1. Somatostatin analogs obtained by replacement of the Phe in positions 6, 7 and 11 by mesityl alanine (Msa).

6 th	7 th	8 th	11 th	Peptidic analog
Msa	Phe	L-Trp	Phe	[L-Msa6]-SRIF, 45
Phe	Msa	L-Trp	Phe	[L-Msa7]-SRIF, 46
Phe	Phe	L-Trp	Msa	[L-Msa11]-SRIF, 47
Msa	Phe	D-Trp	Phe	[L-Msa6_D-Trp8]-SRIF, 48
Phe	Msa	D-Trp	Phe	[L-Msa7_D-Trp8]-SRIF, 49
Phe	Phe	D-Trp	Msa	[L-Msa11_D-Trp8]-SRIF, 50
Msa	Msa	L-Trp	Phe	[L-Msa6,7]-SRIF, 51
Msa	Phe	L-Trp	Msa	[L-Msa6,11]-SRIF, 52
Phe	Msa	L-Trp	Msa	[L-Msa7,11]-SRIF, 53
Msa	Msa	L-Trp	Msa	[L-Msa6,7,11]-SRIF, 54

SRIF analogs **45-54** were prepared by solid-phase peptide synthesis (SPPS) on 2-chlorotrityl chloride resin, using the Fmoc/^tBu strategy (Scheme 3.1, SPPS of peptide **48** is shown as a general example; see the experimental section for a more detailed description). The coupling of the first amino acid Fmoc-Cys(Trt)-OH was performed in dichloromethane (DCM) in the presence of *N*-ethyl-diisopropylamine (DIPEA). After the coupling was finished, the remaining free chlorides were capped with methanol. The next Fmoc-protected amino acids (and the last Boc-Ala-OH) were added using *N,N'*-diisopropylcarbodiimide (DIPCDI) and 1-hydroxybenzotriazole (HOBt) in DMF. 20% piperidine in DMF was used to remove the Fmoc protecting group. When the non-natural amino acid was introduced, only 1.5 eq were used in the coupling. The formation of the disulfide bridge was achieved in solution at room temperature with iodine (I₂), after cleavage (DCM/TFE/AcOH) of the fully protected linear peptide from the resin. Finally, side chain deprotection using a mixture of

TFA/DCM/Anisole/H₂O for 4 h afforded SRIF-14 analogs in modest yields (20-50%) and moderate purities that were improved up to 99% by HPLC chromatography.



Scheme 3.1. SPPS of peptide [L-Msa6_D-Trp8]-SRIF, **4**. (i) (a) Fmoc-L-Cys(Trt)-OH (3 eq), DIEA (3 eq) (b) MeOH; (ii) (a) Piperidine 20% DMF, (b) Fmoc-AA-OH (1.5-3 eq), DIPCDI (3 eq), HOBt (3 eq), DMF; (iii) (a) DCM/TFE/AcOH, (b) I₂, (c) TFA/DCM/anisole/H₂O

3.2.2. Serum stability: The low stability of natural SRIF (with a half-life of 2-3 minutes *in vivo* in human plasma) is one of the main drawbacks of its pharmaceutical use. Thus, we were interested in determining whether our new analogs had longer lifetimes than the wild-type SRIF molecule. To this end, the half-life of the newly designed molecules in human serum was determined and compared them with the values obtained for SRIF, [D-Trp]-SRIF and octreotide. These experiments were carried out by BCN Peptides, S.A. The results of these experiments are shown in Table 3.2. Peptidic analogs **45-47**, containing only one Msa residue, showed low serum stability. Among these, only analog **46** was more stable than SRIF. However, those peptides containing the double modification of one Msa residue and D-Trp8 (**48-50**) showed a remarkable increase in stability (7 to 20-fold larger than SRIF).

Peptides with two Msa residues (**51-53**) also showed higher stability than SRIF, with peptide **51** having a half-life of 43.9 h (versus 2.75 h for the parent compound). Analog **54**, with three Msa residues in its sequence, showed the highest serum stability (34 times more stable than the natural hormone); however, as we discuss below, this peptide has no affinity toward any of the somatostatin receptors. In summary, the incorporation of non-natural amino acids resulted in enhanced serum stability for the majority of analogs. The effect of only one residue was relatively small but replacing two or three residues with non-natural amino acids in the somatostatin scaffold increased the overall stability up to 30-fold. Although this value is still far from the stability of octreotide (200 h in serum), the increase from hours to days constitutes a significant improvement.

3.2.3. Receptor-subtype selectivity: The SSTR-selectivity was measured using competition-binding assays in CHO (*Chinese hamster ovary*) cell lines. For comparative purposes, the same test was applied to SRIF, [D-Trp8]-SRIF and octreotide. The biological studies of the ten Msa containing analogs were carried out by Dr. Maria Alicia Cortés in the University of Alcalá de Henares, under the supervision of Prof. Begoña Colás and Prof. Pilar López-Ruiz. We, however, performed the rest of the SSTR-selectivity studies. First, a short-research stay in the University of Alcalá de Henares allowed us to determine the SSTR3 and SSTR5 affinities. Second, we carried out the SSTR2-affinity studies in the Radioactivity Unit located at the Barcelona Science Park.¹⁸ In short, stable CHO cell lines that specifically express each of the five SSTR receptors were cultured and their membranes were extracted. Inhibitor selectivity was determined with a competitive assay using ¹²⁵I-labeled SRIF-14 and unlabeled ligand in all five receptors. All binding

¹⁸ Please note that the K_i values of the control peptides slightly fluctuate from the experiments that were first achieved in the University of Alcalá and the experiments that we carried out four years later. Thus, K_i values of Msa containing analogs should not be directly compared with the rest of analogs. However, comparison between Msa analogs and their controls vs. the rest of analogs and their controls provides a clear relative estimation of their affinity values. To improve the accuracy, peptide [L-Msa7_D-Trp8]-SRIF (**49**) was included in the SSTR2-selectivity studies that were carried out by us, as control compound.

data of these SRIF analogs containing Msa residues are shown in Table 3.2. As can be readily seen, the new peptides show a wide scope of biological activity, ranging from moderately active in all receptors (**45**), to remarkably selective (**48-49**) or even completely inactive (**54**). These affinity values will be discussed below in more detail, together with their structures.

Table 3.2. Human serum half-life and K_i values (nM) of SRIF, [D-Trp8]-SRIF, octreotide and SRIF analogs to receptors SSTR1-5. ^a K_i values are mean \pm SEM.						
	SSTR1	SSTR2	SSTR3	SSTR4	SSTR5	$t_{1/2}$ (h) ^b
Somatostatin, SRIF	0.43 \pm 0.08	0.0016 \pm 0.0005	0.53 \pm 0.21	0.74 \pm 0.07	0.23 \pm 0.04	2.75
[D-Trp8]-SRIF	0.32 \pm 0.11	0.0010 \pm 0.0007	0.61 \pm 0.02	5.8 \pm 0.4	0.46 \pm 0.24	19.7
Octreotide	300 \pm 85	0.053 \pm 0.011	15 \pm 6	>10 ³	11 \pm 1	200
[L-Msa6]-SRIF, 45	8.5 \pm 1.4	1.5 \pm 1.4	1.4 \pm 1.3	3.6 \pm 1.5	0.91 \pm 1.45	2.1
[L-Msa7]-SRIF, 46	4.2 \pm 1.5	0.019 \pm 0.009	>10 ³	28 \pm 6	>10 ³	5.2
[L-Msa11]-SRIF, 47	20 \pm 5	0.024 \pm 0.004	2.8 \pm 0.2	6.5 \pm 2.2	2.1 \pm 0.7	1.7
[L-Msa6_D-Trp8], 48	3.1 \pm 0.9	4.6 \pm 0.7	0.78 \pm 0.12	4.7 \pm 0.9	0.36 \pm 0.03	26
[L-Msa7_D-Trp8], 49	0.33 \pm 0.09	0.0024 \pm 0.0011	7.5 \pm 0.6	>10 ³	>10 ³	25
[L-Msa11_D-Trp8], 50	3.4 \pm 1.3	0.14 \pm 0.06	1.3 \pm 0.2	>10 ³	0.73 \pm 0.19	41
[L-Msa6,7]-SRIF, 51	>10 ³	14 \pm 1	>10 ³	>10 ³	>10 ³	43.9
[L-Msa6,11]-SRIF, 52	>10 ³	>10 ³	13 \pm 2	>10 ³	9.1 \pm 0.6	nm ^c
[L-Msa7,11]-SRIF, 53	105 \pm 30	1.4 \pm 0.3	>10 ³	>10 ³	>10 ³	10
[L-Msa6,7,11]-SRIF, 54	>10 ³	>10 ³	>10 ³	>10 ³	>10 ³	93.3

a: Shaded cells represent data in close proximity to the SRIF values. b: Human serum half-life (see Experimental Section for details). c: Not measured.

3.2.4. Structure:

Compounds with one Msa residue (45-47): The SRIF analogs containing only one Msa insertion (in position 6, 7 or 11, analogs **45**, **46** and **47**) were analyzed by NMR. Unlike somatostatin, which populates several conformations in aqueous solution, the two dimensional TOCSY and NOESY homonuclear experiments¹⁹ of the new analogs showed a major set of NOE peaks. The well-defined 2D spectra of compounds **45-47** enabled us to characterize their main conformation in solution using the software Crystallography & NMR System (CNS)²⁰ and StructCalc (StructCalc program was used by courtesy of its recent developers (unpublished data), Pau Martín-Malpartida and Maria J. Macias). It is necessary to mention that all the structural studies of all the SRIF analogs were carried out under the supervision of Prof. Maria Macias, from the Protein NMR Spectroscopy laboratory at the IRB Barcelona. To generate the list of experimental restraints required for the calculation, the volume of all assigned peaks was integrated, and then converted into distances. Three calculations (120 structures each) were run until the best match between the NMR assignments and final structures was obtained. On the basis of these results we concluded that under the experimental conditions used, compounds **45-47** were sufficiently structured to obtain defined families of the 3D structures of their main conformers that are in good agreement with the experimental data (Figures 3.3-3.5).

The 3D structure of the main conformation of peptide [L-Msa6]-SRIF (**45**) in solution showed a singular aromatic ring cluster among Msa6, Phe7 and Phe11 as well as a hairpin (Figure 3.3). This arrangement of aromatic rings was defined by a number of NOEs among the aromatic protons of these three residues. However, the absence of an additional stabilizing effect in the hairpin area increased the conformational mobility of this peptide. Thus, our NMR data suggested that other minor conformations were present in solution. As shown in Table 3.2, compound **45**

19 K. Wuethrich, G. Wider, G. Wagner, W. Braun, *J. Mol. Biol.* **1982**, *155*, 311-319;

20 A. T. Brunger, P. D. Adams, G. M. Clore, W. L. DeLano, P. Gros, R. W. Grosse-Kunstleve, J. S. Jiang, J. Kuszewski, M. Nilges, N. S. Pannu, R. J. Read, L. M. Rice, T. Simonson, G. L. Warren, *Acta Crystallogr. D Biol. Crystallogr.* **1998**, *54*, 905-921.

presents a considerably universal profile, although it binds SSTR1-5 with weaker affinity than that of somatostatin. Furthermore, the presence of only one unnatural residue in its sequence did not increase its stability in serum; its half-life is slightly lower than that of the natural hormone.

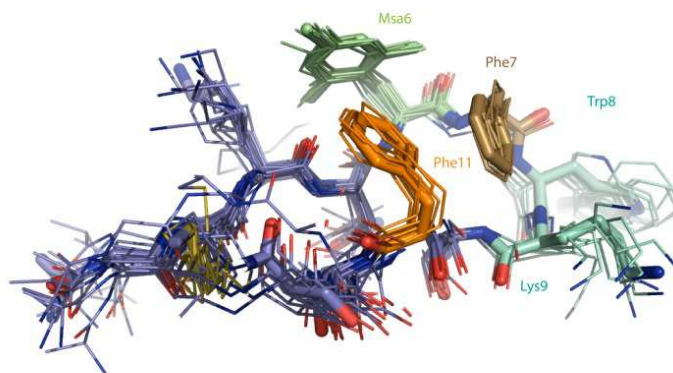


Figure 3.3. Superimposition of the lower energy conformers of [L-Msa6]-SRIF (**45**) that fit the NMR data.

The NMR data of [L-Msa7]-SRIF (**46**) clearly showed that this compound was conformationally more rigid than SRIF in solution. The 3D structure of the lower energy conformers showed a highly structured region from residues 6 to 11, with a clear aromatic interaction between Phe6 and Phe11 (Figure 3.4) which presents a clear *edge-to-face* geometry. The Msa residue in the seventh position does not participate in the aromatic interaction, lying flat at the opposite face of the molecule. However, it probably plays an essential role in conformer stabilization, helping the aromatic rings of Phe6 and Phe11 to attain optimal geometry.

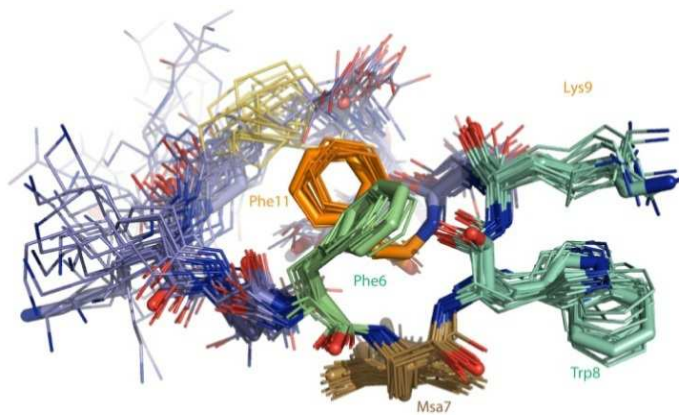


Figure 3.4. Superimposition of the 24 lower energy conformers of [L-Msa7]-SRIF (**46**) that fit the NMR data.

The NOE cross-peaks of the Lys9-Trp8 interaction were weak and difficult to identify. Peptide **46** displays high selectivity towards receptor SSTR2, with a K_i of 0.019 nM. Interestingly, and perhaps due to its conformational rigidity, the stability of peptide **46** in serum (5.2 h) is almost double to that of SRIF. This compound has the highest stability of the three analogs with only one residue modification (**45-47**).

The set of low energy conformers calculated for peptide [L-Msa11]-SRIF (**47**) showed a remarkable level of convergence in most geometrical parameters as a result of the high number of experimental restraints generated and the intrinsically high conformational rigidity in the molecule (Figure 3.5). In this analog, the Msa amino acid at position 11 participates in a π -aromatic interaction, with the phenyl ring of Phe6 oriented in an *offset-tilted* arrangement on one side of the molecular plane. Moreover, the Phe7 ring lies on the other side of the plane as it occurs in the structure of molecule **46**, but in **47** the orientation is almost perpendicular to the plane.

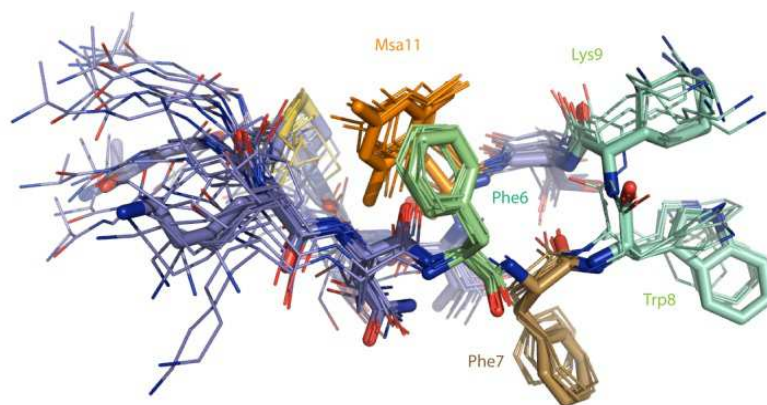


Figure 3.5. Superimposition of the lower energy conformers of [L-Msa11]-SRIF (**47**) as calculated on the basis of the experimental NMR data.

As observed in peptide **46**, the interaction between the side chains of Lys9 and Trp8 is instrumental in defining the formation of the hairpin. However, in this group of peptides these interactions are not strong enough to maintain the L-Trp8 in fixed conformation, and some structures of peptide **47** bring the L-Trp8 indole side-chain in close proximity to the benzyl side-chain of Phe7, which is reflected by some NOE contacts between these two aromatic moieties. Remarkably, the binding profile

of this compound reflects that it is moderately selective toward SSTR2, despite having a dissociation constant larger than that of compound **46**. However, its stability in serum is poor, displaying a shorter half-life than that of natural SRIF.

Msa and D-Trp8 containing analogs (48-50). The discovery of a main populated conformation in peptides **45-47**, which allowed us to determine their 3D structures by NMR in aqueous solution, prompted us to concentrate our efforts on increasing the stability of these analogs while maintaining their binding properties. Pioneering work by Rivier and co-workers in 1975,²¹ showed that [D-Trp8]-SRIF exhibits an excellent binding profile toward all receptors but greater stability than its [L-Trp8]-SRIF natural counterpart. Indeed, several studies²² have demonstrated that the Lys9 side-chain is more effectively shielded by D-Trp8 because its D-configuration favors an orientation where the indole ring is in close proximity to the aliphatic side-chain of Lys9. These hydrophobic contacts maintain the Lys9 side-chain in a defined orientation stabilizing the hairpin centered at Trp8-Lys9.

Our aim was to study whether the introduction of the D-Trp8 residue would increase the stability of the peptides containing a Msa residue while maintaining the conformational structure and the receptor-selectivity profile. For this purpose, we used SPPS to prepare three new analogs (**48**, **49** and **50**) carrying Msa and D-Trp8 residues and determined whether these substitutions affected the structure or stability of the peptides. In addition, we also prepared the [D-Trp8]-SRIF analog and compared its NMR properties with those of the natural [L-Trp8]-SRIF. A section of the 2D NOESY spectra of the natural hormone, [D-Trp8]-SRIF, [L-Msa7]-SRIF (**46**) and [L-Msa7_D-Trp8]-SRIF (**49**), is shown to illustrate the improvement in the NMR data (Figure 3.6). As can be seen, [D-Trp8]-SRIF maintains the intrinsic flexibility of the natural hormone whereas **46** and **49** show an increasing number of NOE signals.

21 J. Rivier, M. Brown, W. Vale, *Biochem. Biophys. Res. Commun.* **1975**, 65, 746-75.

22 a) B. H. Arison, R. Hirschmann, D. F. Veber, *Bioorg. Chem.* **1978**, 7, 447-451; b) O. Ovadia, S. Greenberg, B. Laufer, C. Gilon, A. Hoffman, H. Kessler, *Expert Opin. Drug Discov.* **2010**, 5, 655-671.

3. Somatostatin Analogs Containing the Msa Amino Acid

The conformational flexibility of both SRIF and [D-Trp8]-SRIF accounts perfectly for their functional versatility against all receptors (SSTR1-5) (Table 3.2). In both cases, the coexistence of several different conformations prevented us from carrying out definitive structural studies. In contrast, the 2D spectra of compounds **48-50** were extremely well-defined, enabling us to characterize their main conformation in solution using the CNS software.

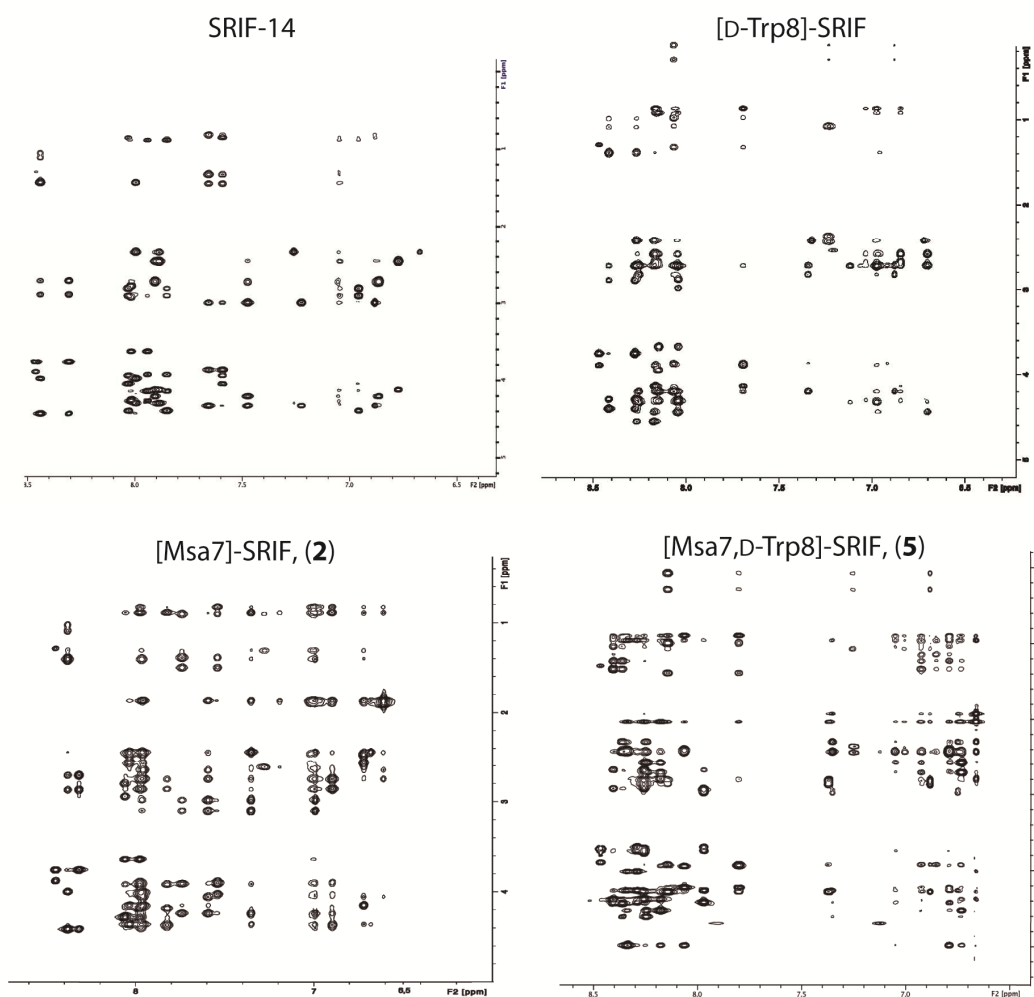


Figure 3.6. NOESY (600 MHz, D₂O, 200 ms) of the aromatic ring-long range interaction region (upper left quadrant) of the natural hormone, [D-Trp8]-SRIF, [L-Msa7]-SRIF (**46**) and [L-Msa7,D-Trp8]-SRIF (**49**). NMR data were acquired at 285 K, using trifluoroacetate as a counter-ion at pH 1.5.

As before, the volume of all assigned peaks was integrated, transformed into distances and used to generate the list of experimental restraints for calculation. Three sets of calculations (120 structures each) were run until the best match

between assignments and final structures was obtained. As expected, the generated structures (from the experimental NMR data) of these new peptides showed a clear increase in convergence not only with respect to SRIF and [D-Trp8]-SRIF, but also with respect to monosubstituted analogs **45-47**.

Peptide [L-Msa6_D-Trp8]-SRIF (**48**) gave a well-defined conformation in solution (Figure 3.7) in which the two aromatic rings of Msa6 and Phe11 are markedly proximal as a result of an enhanced polar- π interaction, while Phe7 also participates in the aromatic cluster. This cluster of three aromatic rings is similar to that found in [L-Msa6]-SRIF (**45**).

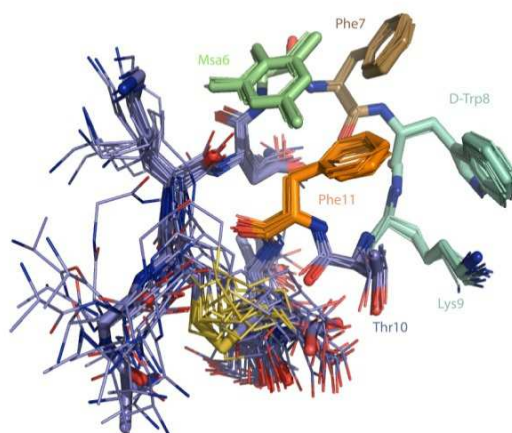


Figure 3.7. Superimposition of the lowest energy conformers of [L-Msa6_D-Trp8]-SRIF (**48**) that best fit the NMR data.

It is apparent that the region containing residues 6-11 (the pharmacophore part of SRIF) is much more structured than the rest of the molecule. The binding profile of peptide **48** is also similar to peptide **45**, although its affinity towards receptors SSTR3 and SSTR5 is comparable to that of the natural hormone, with an affinity 20-30 times more potent than octreotide (Table 3.2). The lack of affinity of peptides **45** and **48** (which both have an Msa residue in the sixth position) towards receptor SSTR2 does not support Hirschmann's hypothesis that residue 6 interacts with an amino acid side chain in SSTR2 *via* a π -donation.²³

23 S. Neelamkavil, B. Arison, E. Birzin, J. Feng, K. Chen, A. Lin, F. Cheng, L. Taylor, E. R. Thornton, A. B. Smith III, R. Hirschmann *J. Med. Chem.* **2005**, *48*, 4025-4030.

Peptide [L-Msa7_D-Trp8]-SRIF (**49**) also showed a strong interaction between Phe6-Phe11 and a well-defined hairpin at the pharmacophore region (Figure 3.8). Again, the calculated structures display a good degree of convergence, being the pharmacophore region (residues 6-11) more structured than the remaining part of the molecule. In contrast to peptide **46**, a large set of interactions between Trp8 and Lys9 can be clearly observed in compound **49**.

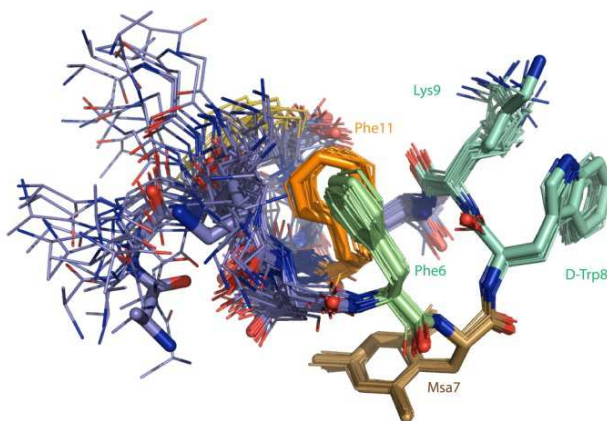


Figure 3.8. Superimposition of the lowest energy conformers of [L-Msa7_D-Trp8]-SRIF (**49**) that fit the NMR data.

In this case, the D-Trp8Lys9 interaction is reflected in the upfield shift γ protons of Lys9 (see Experimental Section for chemical shifts) which are shielded by the aromatic indole ring. Not only is the side-chain disposition in peptides **46** and **49** quite similar but also the aromatic interaction geometry between residues Phe6 and Phe11 are quite similar (Figure 3.9; the backbone is shown as a cartoon representation and the Phe6 and Phe11 residues as sticks).

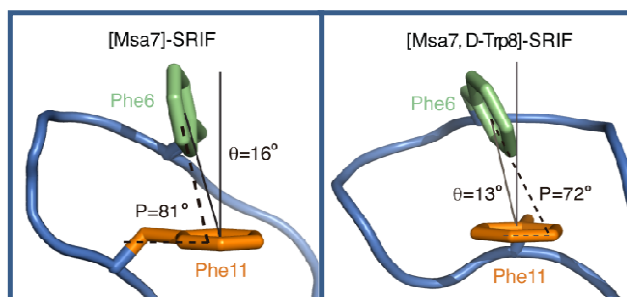


Figure 3.9. Schematic representation of the aromatic interactions in peptides **46** and **49**. The molecules were rotated with respect to previous figures to provide a close view of these interactions.

The aromatic pair association can be classified as an *edge-to-face* geometry.²⁴ The shortest inter-residue carbon-carbon distances (SICD) are 3.3 and 2.7 Å respectively. The angle formed between the ring centroid to centroid segment and the z-axis of an axial system centered on the centroid of the reference ring (θ) is very small (16° and 13° for **46** and **49** respectively). The ring planes are almost perpendicular with interplanar angles (P) of 81° and 72° respectively. The mesityl ring in peptide **49**, as in peptide **46**, is not involved in any aromatic interactions. The aromatic ring lies flat at the other side of the molecule, probably facilitating the interaction between Phe6 and Phe11 by steric repulsion. The lowest energy conformation is fairly similar to **46**, but the synergistic stabilizing effect caused by the presence of the D-Trp8 leads to one of the least flexible 14-residue SRIF analog described to date. Its outstanding affinity for SSTR2 probably correlates with having a well-defined structure close to the conformation that fits best in the structure of the SSTR2 receptor, which is so far uncharacterized. Its inhibition constant was 22-fold lower than that of octreotide and similar to that of SRIF. Unlike octreotide, peptide **49** exhibited a markedly high affinity toward SSTR1, at the same level than SRIF. To the best of our knowledge, peptide **5** is the first SRIF analog with such an impressive affinity and selectivity both to SSTR1 and SSTR2. We hypothesized that the significant activity of **49** against SSTR1 is derived from a reinforced π -interaction between Msa7 and the Phe¹⁹⁵ present in SSTR1, according to the pharmacophore proposed by Kaupmann *et al.*²⁵ Thus, in line with the suggested induced-fit mechanism for SSTR1,²⁶ the enhanced aromatic–aromatic interactions between Msa7 and Phe¹⁹⁵ would be essential for the affinity of **49** (which is much more rigid than peptide **46**) to receptor SSTR1.

24 Useful geometrical parameters of the aromatic interactions are described in: U. Samanta, D. Pal, P. Chakrabarti *Acta Crystallogr. , Sect. D: Biol. Crystallogr.* **1999**, *D55*, 1421-1427; b) R. Bhattacharyya, U. Samanta, P. Chakrabarti *Protein Eng.* **2002**, *15*, 91-100.

25 K. Kaupmann, C. Bruns, F. Raulf, H. P. Weber, H. Mattes, H. Lubbert, *EMBO J.* **1995**, *14*, 727–735.

26 J. Erchegyi, R. Cescato, C. R. R. Grace, B. Waser, V. Piccand, D. Hoyer, R. Riek, J. E. Rivier, J. C. Reubi, *J. Med. Chem.* **2009**, *52*, 2733–2746.

The analog [L-Msa11_D-Trp8]-SRIF (**50**) also had a remarkable conformational rigidity. The most stable conformers showed a strong π -aromatic interaction between the Phe6 and Msa11 residues (Figure 3.10). It was also apparent that peptides **47** and **50** showed a remarkable similarity to one another. The geometric values of the aromatic interaction in peptides **47** and **50** (Figure 3.11; only the backbone and the two aromatic rings of the most stable conformer are shown) allowed us to classify the position of the two aromatic rings as an *offset-tilted* interaction,²⁷ with the θ angles wider than in previous analogs (30° and 34° for **47** and **50** respectively). In this case, the interplanar angles (P) are 53° and 61° .

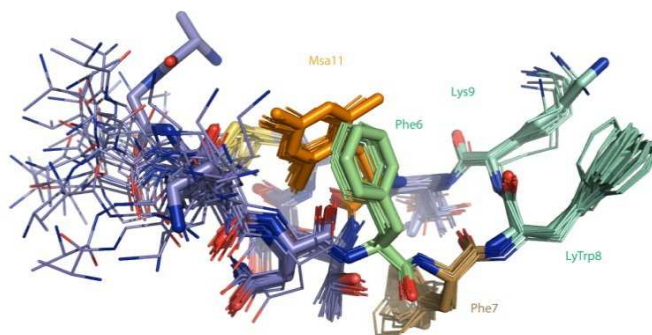


Figure 3.10. Superimposition of the lowest energy conformers of [L-Msa11_D-Trp8]-SRIF (**50**) that fit the NMR data.

Peptide **6** displayed high affinity towards the SST5 receptor, although it displayed a lower level of selectivity, since it also binds to SSTR1, SSTR2 and SSTR3 with comparable affinities. Its stability in serum is very high (41 h), which is higher than any of the analogs prepared carrying one Msa and the D-Trp8 residues.

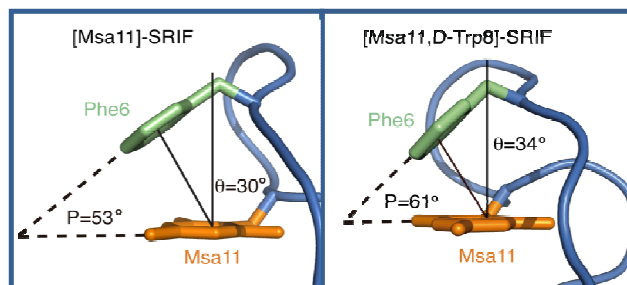


Figure 3.11. Schematic representation of the aromatic interactions in peptides **47** and **50**.

²⁷ A referee suggested that, since the topology of the mesityl moiety precludes the mesityl alanine playing the “edge” role in an *edge-to-face* interaction, it favors offset related geometries.

Overall, the structures of the major conformations of peptides with L-Trp8 (**45-47**) are remarkably similar to those with D-Trp8 (**48-50**). Nearly all of the observed proton-proton NOEs for compounds **45-47** were also present in the spectra of compounds **48-50**, indicating that the D-Trp8 residue additionally shifts the conformational equilibrium toward bioactive conformations that are already populated in a considerable manner in peptides **45-47**.

Compounds with multiple incorporations of Msa residues (51-54). Since a simple substitution of Phe by Msa in the natural sequence remarkably increased the conformational rigidity of the corresponding analogs, we went a step further and studied whether the addition of multiple Msa residues could have an impact on their structure and/or their interaction with the receptors. To obtain this information, we prepared peptides **51-54** (Table 3.1) using general SPPS methods. Analogs **51-54** showed a minimal number of NOE signals (only sequential NOE's could be assigned), proving that the presence of more than one Msa in the 14-amino acid sequence does not improve the conformational stability of these SRIF derivatives in solution. A probable explanation for this negative effect on the fold of the peptide can be rationalized based on the large steric hindrance imposed by the *ortho*-methyls of Msa residues, preventing the aromatic interaction between Msa residues. In addition, the high electron density of these aromatic moieties may increase the π -electron repulsions between Msa residues. These explanations are supported by the lack of NOEs between the aromatic mesityl protons. It appears that the tetrapeptidic scaffold of somatostatin would accommodate more than one Msa in positions 6, 7 and/or 11 but this is at the expense of reduced stability in the peptide. Most importantly, the presence of several Msa residues reduces the affinity of the peptides towards the five SSTR receptors. In particular, compound **54**, containing 3 Msa residues, was completely inactive towards all of the SSTR receptors (Table 3.2).

3.3. Conclusions

We have synthesized and studied ten new somatostatin analogs (Table 3.1). These can be grouped as follows: a) introduction of one Msa residue in positions 6, 7 or 11 of the natural 14 amino acid sequence (peptides **45-47**); b) the same but replacing natural L-Trp with D-Trp at position 8 (peptides **48-50**); and c) multiple incorporations of Msa in positions 6, 7 and 11 (peptides **51-54**). All analogs were tested for their capacity to bind to the SST receptors and for their stability in serum (Table 3.2) and were studied in detail by NMR.

The presence of favorable defined conformations in peptides **45-47** allowed us to characterize their structures in detail by NMR and computational techniques. Analogs containing one Msa and D-Trp are more structured than those with the natural amino acids although the most stable set of conformers did not appear to change significantly with the replacement of L-Trp by D-Trp (comparing compounds **45 to 48**, **46 to 49** and **47 to 50**). The increase in conformational rigidity stems from the reinforcement of aromatic interaction between certain residues when Msa is present, and the preferential interaction of the indole ring with the lysine side chain when the Trp8 residue has a D-configuration. The upfield shifting of the γ -protons of Lys9 in peptides **48-50** allowed us to further corroborate the greater conformational stability in the pharmacophoric part of these analogs relative to that of SRIF or peptides **45-47**. The single modification of introducing one Msa residue combined with the presence of D-Trp8 enhanced the non-covalent interactions among the specific side-chains in SRIF, leading to analogs with greater stability and higher affinity and selectivity towards SSTR.

It is worth noting that most of the contacts present in the NOESY spectra of these peptides were also detected in the parent compound, indicating that these Msa containing analogs preferentially populate a dominant conformation already present in solution in somatostatin. Furthermore, we found that the D-Trp8 incorporation additionally shifts the conformational equilibrium towards specific conformations. As indicated by the increased in number and intensity of the NOE peaks in peptides **48-50**, in solution they spend more time in the particular

conformations depicted above that peptides **45-47**, and far more time that the highly flexible wild-type SRIF, thus displaying an appropriate selectivity to SSTR1-5. In all cases (**45-50**) we have found that non-covalent aromatic interactions occur between residues in sixth and eleventh position. Therefore our results are consistent with the hypothesis described by Veber and co-workers^{16b} that an aromatic interaction between Phe6 and Phe11 stabilizes some bioactive conformations to a certain degree in SRIF. Analogs **46** and **49** satisfy both high conformational rigidity and excellent SSTR2 selectivity; consequently, the 3D structure of these 14-aa SRIF analogs should be close to that of SRIF binding receptor SSTR2.

The structures of peptides with L-Trp8 (**45-47**) are remarkably similar to those with D-Trp8 (**48-50**). It appears that the configuration of this amino acid does not play a fundamental role in the architecture of the peptide. However, the presence of D-Trp8 proved to be important not only in hairpin stabilization, but also in increasing serum stability. This could be due to the unnatural configuration of the residue and also to the increased conformational stability of the peptide. The synergistic effect that arises from the combined presence of Msa and D-Trp8 explains the higher serum stability of peptides **48-50** than [D-Trp8]-SRIF or compounds **45-47**. The enrichment of non-covalent interactions (stabilization of the hairpin area caused by the presence of D-Trp8 and intensification of the aromatic-aromatic interactions due to the Msa) perfectly explains their higher serum stability in comparison to SRIF. However, peptides **51-54** with two or three Msa residues, although having a longer half-life in serum, do not show any defined structure in solution (their 3D structure could not be determined) and have poor affinity towards most of the SSTR receptors.

The potential therapeutic utility of SSTR-selective ligands has been extensively reported.²⁸ In the past decade, the somatostatin-based receptor-targeted anti-cancer therapy has emerged as a promising tool in order to improve the

28 a) G. Garcia-Tsao, A. J. Sanyal, N. D. Grace, W. Carey *Hepatology* **2007**, *46*, 922-938. b) Ayuk, M. C. Sheppard *Postgrad. Med. J.* **2006**, *82*, 24-30; c) M. Pawlikowski, G. Melen-Mucha *Curr. Opin. Pharmacol.* **2004**, *4*, 608-613; d) W. W. de Herder, L. J. Hofland, A. J. van der Lely, S. W. J. Lamberts *Endocr.-Relat. Cancer* **2003**, *10*, 451-458.

traditional chemotherapy.²⁹ In this regard, in tumor cells SSTR2 is expressed at remarkably higher levels than in healthy tissues. The coupling of potent chemotherapeutic agents to SSTR2-selective somatostatin analogs has provided new cytotoxic SRIF-conjugates that selectively target SSTR2-specific sites, displaying significant anti-tumor capacity in many types of tumors.^{29a} Given the short half-life of full length somatostatin analogs, only octreotide derivatives are currently used in SSTR-targeted chemotherapy. In this regard, an array of additional studies on the use of peptide **49** (10 times more stable in serum than SRIF and 10-fold more active against SSTR2 than octreotide) in receptor-targeted anti-cancer therapy is currently underway in our laboratory.

In summary, the replacement of Phe residues by Msa in the original somatostatin sequence has allowed us to fine-tune the structural and biological properties of the corresponding peptide analogs, thus facilitating deeper insights to the main factors that control the conformation and receptor selectivity of this important hormone.

Portions of this chapter have appeared in the publication:

P. Martin-Gago, M. Gomez-Caminals, R. Ramon, X. Verdaguer, P. Martin-Malpartida, E. Aragon, J. Fernandez-Carneado, B. Ponsati, P. Lopez-Ruiz, M. A. Cortes, B. Colas, M. J. Macias, A. Riera *Angew. Chem., Int. Ed.* **2012**, *51*, 1820-1825.

²⁹ a) G. Mezo, M. Manea, *Expert Opin. Drug Delivery* **2010**, *7*, 79-96. b) L. Sun, D. H. Coy, *Curr. Drug Delivery* **2011**, *8*, 2-10.

4

SRIF analogs containing the Tnp residue

Chapter 4. SRIF analogs containing the Tnp residue

4.1. Introduction: The Msa versus the Tnp amino acid	59
4.2. SRIF analogs containing the Tnp residue	60
4.2.1. Receptor-subtype selectivity	60
4.2.2. Structure.....	62
4.3. Msa and Tnp in position 7 and SSTR2-selectivity.....	66
4.4. Conclusions.....	69

4.1. Introduction:

The Msa versus the Tmp amino acid

In order to gain insights into the effects that arise from the introduction of conformationally constrained amino acids in peptides, Riera and co-workers¹ compared the conformational restriction of the phenylglycine and the mesitylglycine amino acid side-chains (Phe and Msa counterpart residues, respectively) with variable-temperature ¹H-NMR experiments. This showed that the activation free energy for the rotation around the χ_1 dihedral (see Figure 4.1, a)) of a mesitylglycine derivative was almost 5 times higher than that of the correspondent phenylglycine derivative ($\Delta G^\ddagger = -9.7$ vs. -2.0 Kcal mol⁻¹). The increase of the rotational barrier resulted from an effect of the two *ortho*-Me groups, thus the conformational restriction of the Msa amino acid side-chain should be markedly higher than that of the Phe or the Tmp residues (see Figure 4.1, b)).

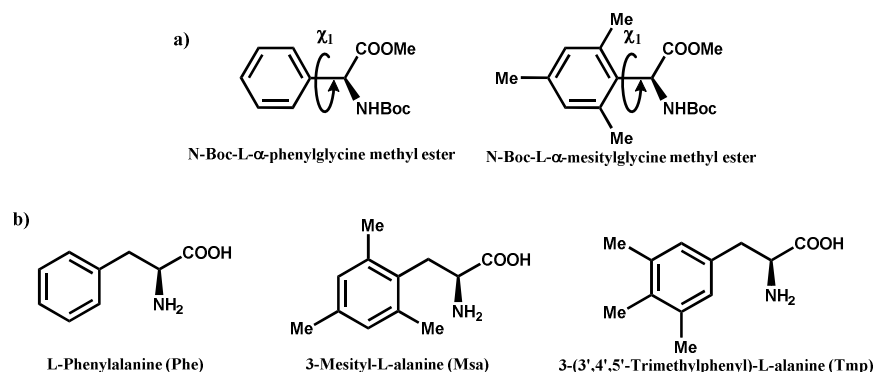


Figure 4.1. The phenylglycine and the mesitylglycine derivatives, and the Phe, the Msa and the Tmp residues. The dihedral angle χ_1 is labeled. The energy barrier associated with the rotation around this dihedral has proved to be directly related to the conformational restriction of these aromatic amino acids side-chains.

In the previous chapter, we showed how the replacement of certain Phe residues by Msa in the somatostatin sequence provided more conformationally restricted analogs which displayed significant affinity and selectivity for different somatostatin receptors. We considered that the Msa amino acid causes this impact as a result of the higher hydrophobicity and electron density that the methyl groups

¹ E. Medina, A. Moyano, M. A. Pericas, A. Riera, *Helv. Chim. Acta* **2000**, 83, 972-988.

confer to the aromatic moiety (intensifying certain aromatic interactions), and/or the intrinsic side-chain rigidity provided by the *ortho*-methyl substitution (which has been proved to limit the mobility of its side-chain, an effect that may be extended to the whole peptidic architecture).

However, we did not know whether steric or electronic factors contribute most to the enhanced conformational rigidity of peptides **45-50**. To investigate the role of the methyl substitution, we introduced the L-3-(3',4',5'-trimethylphenyl) alanine (Tmp amino acid, Figure 4.1, b)) in positions 6, 7 or 11 of the natural sequence of SRIF. Despite the shape difference, this non-natural amino acid displays similar hydrophobic and electronic properties to those of Msa, but the three methyl groups barely restrict the mobility of its aromatic side-chain.

4.2. SRIF analogs containing the Tmp amino acid

We used standard SPPS to prepare three [D-Trp8]-SRIF analogs containing the Tmp amino acid in position 6, 7 and 11 (Table 4.1).

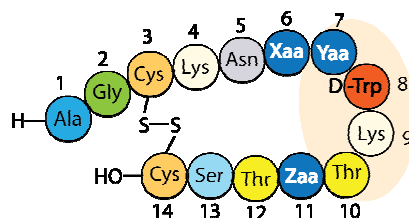


Table 4.1. Somatostatin analogs obtained by replacement of the Phe in positions 6, 7 and 11 by L-3-(3',4',5'-trimethylphenyl) alanine (Tmp).

6 th	7 th	8 th	11 th	Peptidic analog
Tmp	Phe	D-Trp	Phe	[L-Tmp6_D-Trp8]-SRIF, 55
Phe	Tmp	D-Trp	Phe	[L-Tmp7_D-Trp8]-SRIF, 56
Phe	Phe	D-Trp	Tmp	[L-Tmp11_D-Trp8]-SRIF, 57

4.2.1. Receptor-subtype selectivity: We measured the affinity and selectivity of these peptides for the SSTR2, SSTR3 and SSTR5 receptors by binding assays using extracted membranes of cultured stable CHO cell lines that overexpressed one specific somatostatin subtype receptor. Unless otherwise noted, K_i values for the SSSTR2 receptor were determined by us at the Radioactivity Unit located in the

Barcelona Science Park. We included in our experiments the peptide [L-Msa7_D-Trp8]-SRIF as control. The K_i values of the control compounds and the Msa containing analogs in receptors SSTR1, SSTR3, SSTR4 and SSTR5 were determined by Dr. M. A. Cortes. On the other hand, the affinities of **55-57** for the SSTR3 and SSTR5 receptors were determined by me during a short-research stay in the University of Alcalá de Henares, so normalized K_i values (with respect to the K_i values of SRIF) are shown. Experiments devoted to determine the affinity of these compounds to SSTR1 and SSTR5 are currently underway. In short, the efficacy of the interaction was assessed in competitive radioligand binding assays using 125 I-labeled somatostatin in the presence or absence of various concentrations of unlabeled peptides. Somatostatin, [D-Trp8]-SRIF and octreotide were used as controls. The receptor-subtype selectivity of peptides containing Tmp residues proved to be very similar to that of the Msa counterparts (Table 4.2).

Table 4.2. K_i values (nM) and human serum half-life of SRIF, [D-Trp8]-SRIF, octreotide and SRIF analogs containing either the Msa or the Tmp residue. ^a K_i values are mean \pm SEM.

	SSTR1	SSTR2	SSTR3	SSTR4	SSTR5	$t_{1/2}$ (h) ^b
Somatostatin, SRIF	0.43 ± 0.08	0.0034 ± 0.0006	0.53 ± 0.21	0.74 ± 0.07	0.23 ± 0.04	2.75
[D-Trp8]-SRIF	0.32 ± 0.11	0.0027 ± 0.0020	0.61 ± 0.02	5.8 \pm 0.4	0.46 ± 0.24	19.7
Octreotide	300 ± 85	0.029 ± 0.012	15 ± 6	$>10^3$	11 ± 2	200
[L-Msa6_D-Trp8]-SRIF 48	3.1 ± 0.9	4.6 $\pm 0.7^c$	0.78 ± 0.10	4.7 \pm 0.9	0.36 ± 0.03	26
[L-Msa7_D-Trp8]-SRIF 49	0.33 ± 0.09	0.0063 ± 0.0011	7.5 ± 0.6	$>10^3$	$>10^3$	25
[L-Msa11_D-Trp8]-SRIF 50	3.4 ± 1.3	0.14 $\pm 0.06^c$	1.3 ± 0.2	$>10^3$	0.73 ± 0.19	41
[L-Tmp6_D-Trp8]-SRIF 55	t.b.d.	2.8 ± 1.12	0.64 $\pm 0.18^d$	t.b.d.	0.32 $\pm 0.07^d$	t.b.d.
[L-Tmp7_D-Trp8]-SRIF 56	t.b.d.	0.0086 ± 0.0008	5.6 $\pm 0.5^d$	t.b.d.	49 $\pm 6^d$	t.b.d.
[L-Tmp11_D-Trp8]-SRIF 57	t.b.d.	0.74 ± 0.32	9.7 $\pm 2.6^d$	t.b.d.	2.5 $\pm 0.8^d$	43

a: Shaded cells represent data in close proximity to the SRIF values. b: Human serum half-life (see Experimental Section for details). c: These values were determined by Dr. M. A. Cortes at the University of Alcalá de Henares. d: Normalized value. t.b.d.: To be determined.

SRIF analog **56**, containing the synthetic amino acid in position 7, displayed impressive affinity and selectivity to SSTR2 (similar to that of **49**, which is shown in Table 4.2 for comparison). This finding indicates that the introduction of highly hydrophobic and electron-rich trimethylated aromatic amino acids in the scaffold of SRIF shifts the conformational equilibrium towards a major conformation in solution that should be very similar to that of the natural hormone when it binds to SSTR2. The Tmp modification in position 6 provides an analog (**55**) that is highly active and modestly selective against SSTR3 and SSTR5 (similar to that of peptide **48**, containing an Msa residue in the same position). In this regard, peptide containing the Tmp amino acid in position 11 (compound **57**) presents a more universal binding profile, displaying moderately higher K_i values than those of the wild-type hormone in SSTR1-5. The serum stability of peptide **57** was measured and compared to that of peptide **50**. The stability of these peptides containing an Msa or Tmp residue in position 11 is very similar, since both compounds proved to have the same half-life time in serum under our experimental conditions (Table 4.2).

4.2.2. Structure: The three [D-Trp8]-SRIF analogs containing one Tmp amino acid were analyzed by NMR techniques. Spin system and sequential assignments for each sample were obtained from 2D TOCSY and NOESY homonuclear experiments. As in the case of Msa-containing analogs, these peptides showed a major set of NOE peaks, suggesting the presence of one dominant conformation in solution. Most of the key proton-proton NOEs observed in peptides **48**, **49** and **50** were also identified in the spectra of compounds **55**, **56** and **57**, respectively (Figure 4.2). In addition, the shared proton-proton interactions were found to show a similar intensity. This finding suggested that SRIF-analogs containing either Msa or Tmp at equivalent positions adopt similar major conformations in solution. Hence, we used the software Crystallography & NMR System (CNS) to characterize their 3D structures. To generate the list of experimental restraints required for the calculation, the volume of all assigned peaks was integrated, and then converted into distances (this means, the larger the volume of a NOE signal originated from a specific proton-proton

interaction is, the closer the computational program will attempt to situate these protons in the space). Three calculations (120 structures each) were run until the best match between the NMR assignments and final structures was obtained. The remarkable similarity of the binding profiles between these two groups of peptides (containing either Msa or Tmp residues) prompted us to predict that they adopt similar major conformations. Indeed, the 3D structures of the major conformations in solution of peptides containing the Tmp residue were quite similar to those of the Msa analogs (**48-50**), which perfectly matches the similarities between their receptor selectivity profiles.

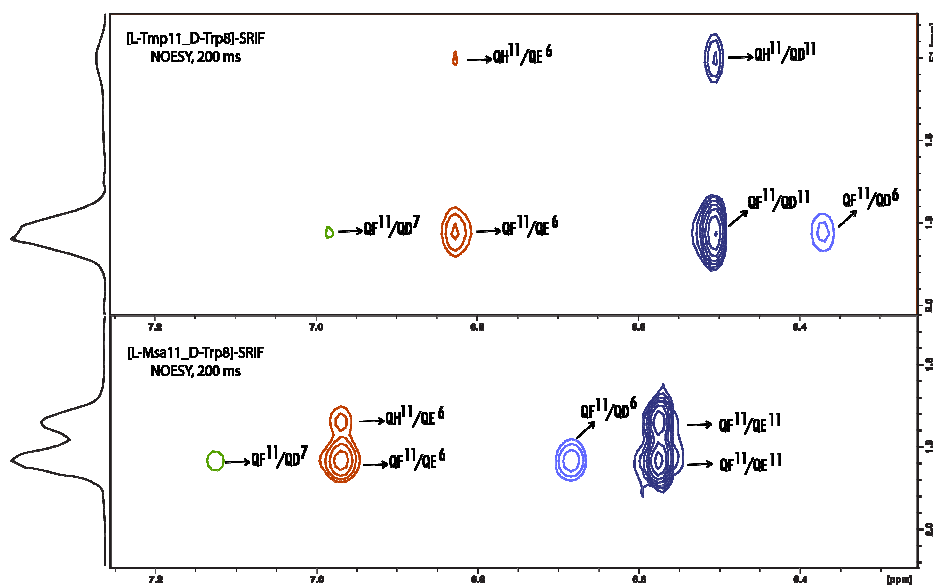


Figure 4.2. NOESY (600 MHz, D₂O) of [D-Trp8]-SRIF analogs containing Tmp11 and Msa11. Relevant methyl protons-aromatic protons contacts are shown for residue 11 (top Tmp, bottom Msa). Same color code means same interaction.

Peptide [L-Tmp6_D-Trp8]-SRIF (**55**) exhibits the same type of aromatic cluster as the Msa6 analog (Figure 4.3). The structure is further stabilized by the close proximity of D-Trp8 and Lys9 side-chains. Despite the fact that the ring orientations of the aromatic side-chains that participate in the cluster are not exactly the same, the 3D structures in solution of peptides containing L-Tmp6 and L-Msa6 are remarkably similar. This observation suggests that the presence of a highly hydrophobic and electron-rich aromatic amino acid in position 6 —regardless of

whether the aromatic substituents constrain the mobility of its side-chain—, induces the formation of this type of aromatic cluster in 14-residue SRIF analogs, thereby shifting the conformational equilibrium in the direction of this major conformation that proved to be highly active and modestly selective against SSTR3 and SSTR5.

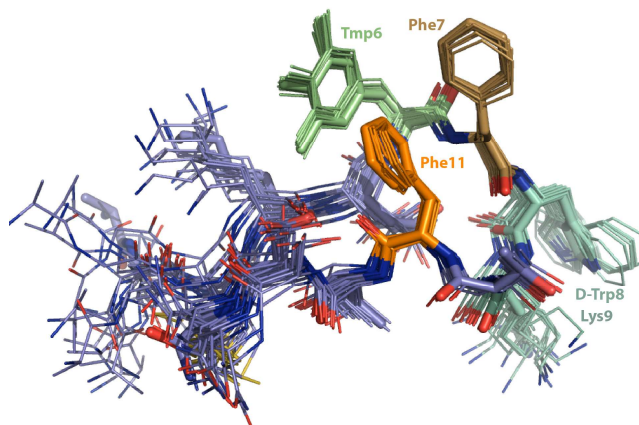


Figure 4.3. Superimposition of the lower energy conformers of [L-Tmp6_D-Trp8]-SRIF (**55**) as calculated on the basis of NMR data.

The NMR data suggest that peptide [L-Tmp7_D-Trp8]-SRIF, **56**, is the least flexible Tmp-containing analog. The 3D structure of the set of low-energy conformers (Figure 4.4) showed a clear Phe6-Phe11 association, as a consequence of the contacts detected in the NOESY spectrum. The side-chain orientations in this analog are quite related to those of peptide [L-Msa7_D-Trp8]-SRIF, as reflected by the NOE pattern similarity.

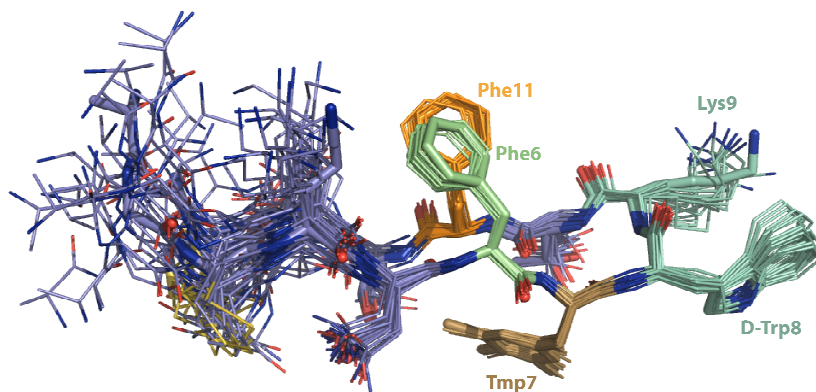


Figure 4.4. Superimposition of the lowest energy conformers of [L-Tmp7_D-Trp8]-SRIF (**56**) that fit the NMR data.

The two natural Phe6 and Phe11 residues are engaged in an aromatic interaction that displays an *edge-to-face* geometry, which provides conformational stability to the whole molecule. The Tmp residue is not involved in any aromatic interaction *per se*. However, as in the case of Msa7 derivatives, the Tmp residue most probably plays a fundamental role in promoting the interaction between Phe6 and Phe11 by steric (due to its bulky side-chain) or/and electronic repulsion (due to the enriched negative π -cloud on the trimethyl-substituted benzene moiety). NOE cross-peaks between D-Trp8-Lys9 were abundant, intense and well-defined, thus indicating the close proximity of the aliphatic Lys9 side-chain and the indole ring. This hydrophobic interaction, evidenced also by the upfield shift γ -protons of Lys9, further stabilizes the main conformation of this peptide by providing rigidity to the pharmacophoric part of the molecule, which, indeed, appeared to be far more structured than the rest of the peptide (Figure 4.4).

The 3D structure derived from the experimental NMR data of the dominant conformer of [L-Tmp11_D-Trp8]-SRIF (Figure 4.5) displays an *offset-stacked* type of aromatic interaction between the Tmp11-Phe6 residues. This non-covalent interaction probably accounts for the main conformation of this tetradecapeptide in solution. Not only is the geometry of the aromatic interaction of this peptide analogous to that of the [L-Msa11_D-Trp8]-SRIF analog, but also its overall structure is very similar.

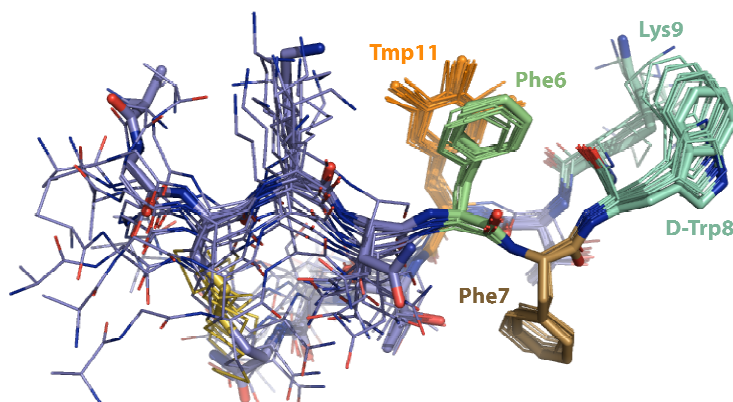


Figure 4.5. Superimposition of the minimum-energy conformers of [L-Tmp11_D-Trp8]-SRIF (57) calculated on the basis of NMR data.

The NMR data show that the aromatic side-chain of Phe7 is not fixed, rather alternating between a populated conformation in which the phenyl ring is located below the molecule –numerous NOE contacts of the aromatic protons with Thr10 and Asn5 were identified– and a conformation in which this residue is positioned closer to the indole ring of D-Trp8. This promiscuity was easily identified by the presence of NOE signals associated with these two arrangements. The half-life time of this peptide ([L-Tmp11_D-Trp8]-SRIF, (**57**)) in serum was remarkably similar to that of [L-Msa11_D-Trp8]-SRIF (**50**) (43 and 41 hours, respectively). The presence of highly hydrophobic and electron-rich aromatic residues in this position contribute equally to serum stability, regardless of whether the aromatic substituents constrain the mobility of its aromatic side-chain.

4.3. Msa and Tmp in position 7 and SSTR2-selectivity

The introduction of either an Msa or a Tmp residue in particular positions of the tetrapeptidic SRIF scaffold shifts the conformational equilibrium toward very similar conformations. Analogs bearing an Msa or Tmp residue in position 7 proved to be among the least flexible tetrapeptidic SRIF analogs synthesized to date. Their highly related structures (Figure 4.6) and striking affinity and selectivity to SSTR2 (Table 4.2) prompted us to stand by our assumption that the 3D structure of their major conformations should be quite similar to the structure that SRIF adopts when it binds to the SSTR2 receptor. This particular receptor is currently considered as the main target of SRIF analogs. Its pharmacological relevance is reflected in the large number of SSTR2-selective SRIF analogs that have been synthesized and explored in recent years.²

2 a) G. Weckbecker, I. Lewis, R. Albert, H. A. Schmid, D. Hoyer, C. Bruns, *Nat Rev Drug Discov* **2003**, 2, 999-1017; b) A. Janecka, M. Zubrzycka, T. Janecki, *J. Pept. Res.* **2001**, 58, 91-107.

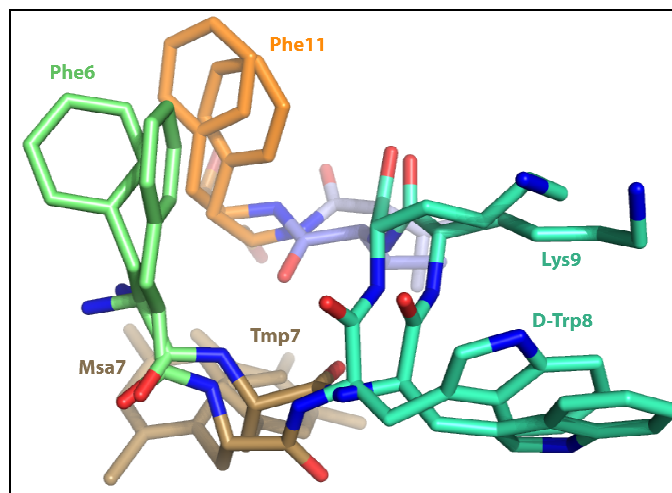


Figure 4.6. Superposition of the pharmacophoric part of the main conformers of peptides [L-Msa7_D-Trp8]-SRIF (**49**) and [L-Tmp7_D-Trp8]-SRIF (**56**). Only residues from Phe6 to Phe11 are shown for simplicity.

Several studies using receptor-subtype selective SRIF analogs in both in vivo and in vitro experiments demonstrated that SSTR2 mediates the inhibition of growth hormone release from pituitary somatotrophes, glucagon release from the pancreas, and gastrin and acid secretion.³ In addition, SSTR2 is the functionally dominant somatostatin receptor in human pancreatic β - and α -cells⁴ and it is expressed in tumor cells at markedly higher concentrations than other somatostatin receptors.⁵ These data clarified the usefulness of SSTR2-selective analogs in the treatment of acromegaly, pituitary tumors, retinopathy, and diabetes and in receptor-targeted anti-cancer therapy.²⁻⁴ Indeed, all of the commercially available and clinically used SRIF-analogs (octreotide, vapreotide and lanreotide) are preferential ligands of the SSTR2 receptor subtype.⁶ The structural similarities between octreotide, [L-Msa7_D-Trp8]-SRIF (**49**) and [L-Tmp7_D-Trp8]-SRIF (**56**) are shown in Figure 4.7 (only [L-Tmp7_D-Trp8]-SRIF and octreotide are shown for simplicity, since the similarities

3 L. Yang, L. Guo, A. Pasternak, R. Mosley, S. Rohrer, E. Birzin, F. Foor, K. Cheng, J. Schaeffer, A. A. Patchett, *J. Med. Chem.* **1998**, *41*, 2175-2179.

4 B. Kailey, M. van de Bunt, S. Cheley, P. R. Johnson, P. E. MacDonald, A. L. Gloyn, P. Rorsman, M. Braun, *Am. J. of Physiol. Endocrinol. Metab.* **2012**, *303*, E1107-E1116.

5 L. Sun, D. H. Coy, *Curr. Drug Delivery* **2011**, *8*, 2-10.

6 SOM230 (Signifor®), recently approved for the treatment of Cushing's disease, inhibits ACTH secretion, an effect that depends mainly on the activation of SSTR5: see ref. 3.

between **49** and **56** can be observed in Figure 4.6). Although octreotide is an octapeptide containing a shorter-ring than that of our tetradecapeptidic analogs, there is a similarity between the pharmacophoric parts of these molecules, which perfectly accounts for their similar receptor-selectivity profiles.

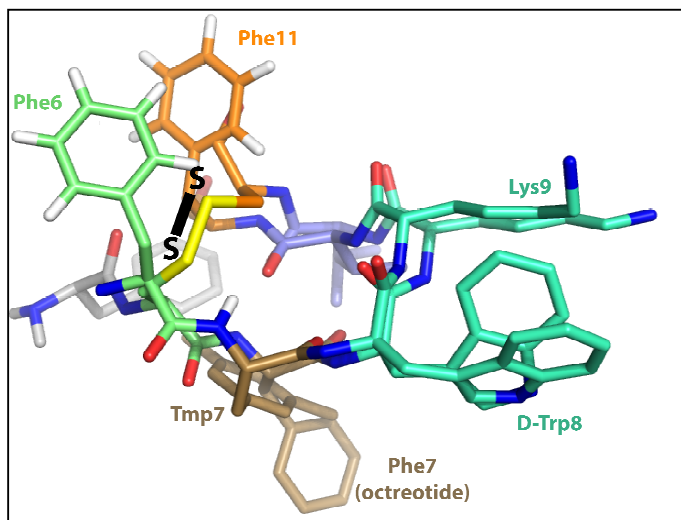


Figure 4.7. Superposition of octreotide (RCSB PDB1SOC) and the pharmacophoric part of the main conformers of peptide [L-Tmp7_D-Trp8]-SRIF (**56**). Only residues from Phe6 to Phe11 (in sticks) are shown for simplicity.

The disulfide bond that provides the high rigidity to octreotide accurately mimics the noncovalent interaction between the aromatic Phe6 and Phe11. This polar- π interaction is intensified in our analogs by the presence of an Msa or Tmp residue in position 7, which forces a close proximity between Phe6-Phe11 by steric or electronic factors, thus inducing a higher conformational stability. We consider that this type of peptidic architecture is crucial for conferring SSTR2-activity to SRIF analogs. Furthermore, the high affinity to SSTR1 of the [L-Msa7_D-Trp8]-SRIF peptide (and presumably, of [L-Tmp7_D-Trp8]-SRIF as well) can be attributed to the direct interaction of the residue in position 7 with the receptor via an aromatic interaction driven by hydrophobic and/or electronic factors. The high affinity to SSTR1 is not

necessarily associated with these 3D structures, since an induced-fit mechanism has been postulated for the binding of SRIF and SRIF analogs to this receptor.⁷

4.4. Conclusions

The structures of peptides containing a Tmp residue (**55-57**) greatly resemble those bearing Msa (**48-50**) in the same positions; moreover, they displayed quite similar receptor-subtype selectivity profiles. We considered that the intrinsic rigidity imposed by the *ortho*-methyl substitution in the aromatic the side-chain of the Msa residue does not play the main role in controlling the architecture of these tetradecapeptides.

In addition, the geometries of the aromatic interactions in the Tmp series are quite similar to those found in the Msa-containing analogs. SRIF analogs containing either an Msa or a Tmp residue in position 7 (peptides **49** and **56**) display a clear *edge-to-face* aromatic interaction between the two natural Phe6-Phe11. The fact that these two aromatic rings interact in an *edge-to-face* geometry even though they are solvent-exposed may indicate that the interaction is not driven by the hydrophobic effect, which would favor the maximum burial of surface area.⁸ In peptide **57**, an *offset-stacked* geometry was found for the interaction between Tmp11-Phe6. The three methyl substituents increase the negative charge of the Tmp aromatic moiety, leading to a more favorable electrostatic interaction between its π -cloud and the partial positive charged ϵ^- or/and δ^- -protons of Phe6, which are pointing down at it. In addition, this geometry may be favored by the fact that the Tmp residue is not able to play the “*edge*” role in an *edge-to-face* geometry.

We postulate that the origin of the conformational stability in these peptides depends on the enhanced hydrophobicity and electron density of these trimethyl-substituted aromatic amino acids relative to the natural Phe, that shift the

7 J. Erchegyi, R. Cescato, C. R. R. Grace, B. Waser, V. Piccand, D. Hoyer, R. Riek, J. E. Rivier, J. C. Reubi, *J. Med. Chem.* **2009**, *52*, 2733-2746.

8 C. D. Tatko, M. L. Waters, *J. Am. Chem. Soc.* **2002**, *124*, 9372-9373.

4. SRIF Analogs Containing the Tmp residue

conformational equilibrium to a major peptidic conformation that is stabilized by the enhancement of specific non-covalent interactions.

5

Linear 14-residue SRIF analogs containing the L-Msa7_D-Trp8 motif

Chapter 5. Linear 14-residue SRIF analogs containing the L-Msa7_D-Trp8 motif

5.1. Introduction: Searching for SSTR2-selective analogs	73
5.2. Linear [D-Trp8]-SRIF analogs bearing Msa7	74
5.2.1. Structure.....	74
5.2.2. Binding affinity to SSTR1-5.....	77
5.3. Conclusions.....	79

5.1. Introduction:

Searching for SSTR2-selective analogs

In the previous chapters, we developed the L-Msa7_D-Trp8 and the L-Tmp7_D-Trp8 fragments as key structural motifs for 14-residue SRIF analogs to display high SSTR2-activity and -selectivity.

In order to test the relevance of this motif for both conformational stability and SSTR2-affinity and -selectivity even in the absence of the disulfide bond, we synthesized a linear peptide containing an Ala residue in positions 3 and 14 (instead of the natural Cys) while maintaining the L-Msa7-DTrp8 motif in the sequence (Figure 5.1, peptide **58**). In addition, since we proved that a non-covalent Phe6-Phe11 interaction has a similar effect than the disulfide covalent union of octapeptides in the context of receptor-selectivity,¹ we synthesized another SRIF analog (Figure 5.1, **59**) containing a Phe residue in positions 3 and 14, while maintaining the L-Msa7-D-Trp8 motif. Thus, if the molecule is able to conserve the β -hairpin, a Phe3-Phe14 aromatic interaction would further stabilize the peptidic architecture in comparison to that of the analog containing Ala3,14. In both cases, the preservation of the postulated SSTR2-bioactive conformation in the pharmacophoric part of both peptides (Figure 5.1) was examined both by NMR and receptor-subtype selectivity studies.

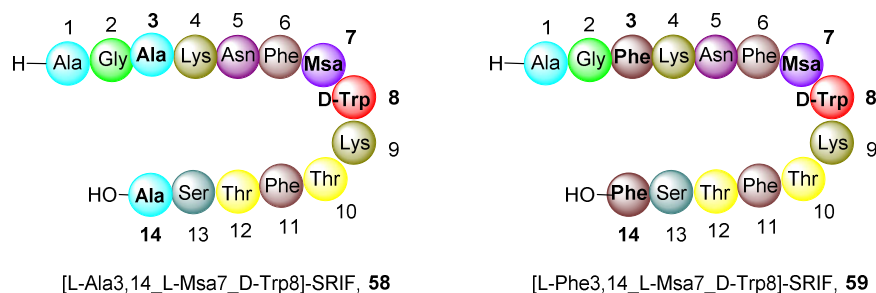


Figure 5.1. Peptidic sequence of [L-Ala3,14_Msa7_D-Trp8]-SRIF (**58**) and [L-Phe3,14_Msa7_D-Trp8]-SRIF (**59**).

1 P. Martin-Gago, M. Gomez-Caminals, R. Ramon, X. Verdaguer, P. Martin-Malpartida, E. Aragon, J. Fernandez-Carneado, B. Ponsati, P. Lopez-Ruiz, M. A. Cortes, B. Colas, M. J. Macias, A. Riera, *Angew. Chem., Int. Ed.* **2012**, *51*, 1820-1825.

5.2. Linear [D-Trp8]-SRIF analogs bearing Msa7

The syntheses of **58** and **59** (Figure 5.1) were performed by SPPS on a 2-chlorotrityl chloride resin by using the standard Fmoc/^tBu strategy.

5.2.1. Structure: The NOE patterns of the two linear SRIF analogs were analyzed in aqueous solution. Spin systems and sequential assignments for the two compounds were obtained from 2D TOCSY and NOESY homonuclear experiments. The NMR data showed that these peptides displayed a high conformational flexibility in comparison to that of the natural somatostatin. Although useful structural information can be extracted from the NMR studies, the 3D structures of their major conformers in solution cannot be obtained due to the presence of a number of different conformations in equilibrium.

In both peptides, several cross-strand NOE signals were present, indicating the preservation of the β -turn. Like other β -hairpins, these linear peptides interconvert between folded and unfolded conformations rapidly on the NMR time scale. Thus, the chemical shifts represent an average of folded and unfolded states. In this regard, the H α proton downfield shifting of the β -sheet has been shown to correlate well with the extent of β -hairpin folding, since H α resonances are shifted downfield relative to the random coil chemical shifts due to the proximity of the to amide carbonyls in an extended sheet conformation.^{2,3} In the fully folded peptide [L-Msa7_D-Trp8]-SRIF (**49**), the downfield chemical shift of the H α resonances relative to the linear peptide [L-Phe3,14_Msa7_D-Trp8]-SRIF (**59**) reflects the differences in folded fraction of both compounds (Figure 5.2; Ala1, Gly2, D-Trp8 and Lys9 are shifted upfield, as expected for terminal and turn residues). The lack of random coil control compounds did not allow us to accurately quantify the folded fraction of our peptides. However, the differences in H α resonances between the fully folded state and the linear peptides were only moderate, suggesting that the non-cyclized SRIF

2 G. J. Sharman, S. Griffiths-Jones, M. Jourdan, M. S. Searle, *J. Am. Chem. Soc.* **2001**, *123*, 12318-12324.

3 Shifting of ≥ 0.1 ppm for three residues provides enough evidence for significant β -sheet population: D. S. Wishart, B. D. Sykes, F. M. Richards, *J. Mol. Biol.* **1991**, *222*, 311-333.

analogs present a significant extent of folding (average $\Delta\delta$ differences of 0.2 ppm between the peptide and the correspondent fully folded derivative have been shown to correlate well with 40% to 70% extent of folding in β -hairpin peptides).⁴

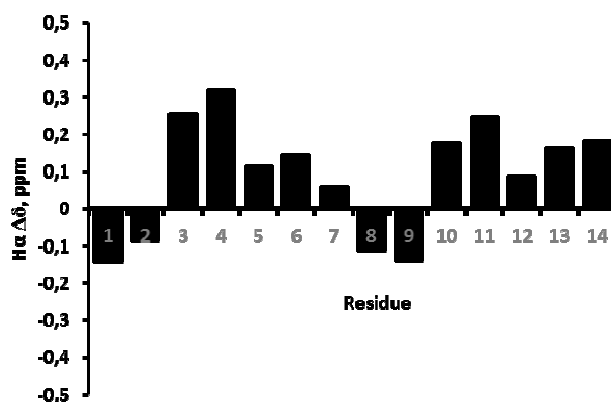


Figure 5.2. Downfield shifting of the cyclic fully folded peptide [L-Msa7_D-Trp8]-SRIF (**49**) relative to [L-Phe3,14_Msa7_D-Trp8]-SRIF (**59**). DSS was used as internal chemical shift reference in 2D TOCSY homonuclear experiments.

Only marginal shift differences among the H α resonances were found between the two linear peptides containing either a cross-strand PhePhe or AlaAla pair in positions 3 and 14. However, a higher population of β -sheet conformation in peptide **59** (Phe3,14) relative to **58** (Ala3,14) can be deduced on the basis of the chemical shift perturbation of the aliphatic side-chain of Lys9. The upfield shifting of the Lys9 H γ resonances has been shown to correlate well with the conformational stability of the β -hairpin in SRIF analogs.⁵ Therefore, the higher upfield shift of the side-chain resonances of Lys9 in peptide **59** (containing two Phe residues in positions 3 and 14) indicates that the β -turn population is markedly higher than the peptide containing Ala3,14 (Figure 5.3). This study also corroborated that, based on the upfield shifting of Lys9 and its NOE resonances, the aliphatic side-chain of this residue directs the γ -methylene at the aromatic indole ring of D-Trp8. This orientation reflects that the D-

4 a) C. D. Tatko, M. L. Waters, *J. Am. Chem. Soc.* **2002**, *124*, 9372-9373; b) S. E. Kiehna, M. L. Waters, *Prot. Sci.* **2003**, *12*, 2657-2667; c) C. D. Tatko, M. L. Waters, *Prot. Sci.* **2003**, *12*, 2443-2452.

5 G. Weckbecker, I. Lewis, R. Albert, H. A. Schmid, D. Hoyer, C. Bruns, *Nat Rev Drug Discov* **2003**, *2*, 999-1017

Trp8-Lys9 interaction is hydrophobic rather than electrostatic in nature.⁶ The large amount of upfield shifting of the γ -protons of Lys9 in the fully folded peptide ([L-Msa7_D-Trp8]-SRIF (**49**), which was indeed one the most conformationally rigid tetradecapeptidic SRIF analog synthesized at that point) further confirms that Lys9 HY resonances provide valuable information with regard to the β -hairpin stability in 14-residue SRIF analogs. The greater population of β -sheet conformations in peptide **59** (Phe3,14) relative to **58** (Ala3,14) may be associated with the higher β -sheet propensity of Phe relative to that of Ala,⁷ or/and a cross-strand aromatic interaction between Phe3-Phe14, which cannot take place in peptide **58**.

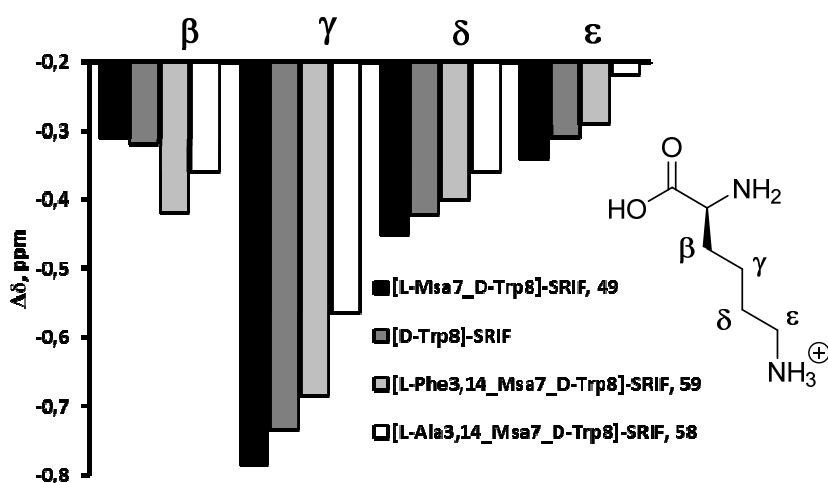


Figure 5.3. The upfield shifting of the Lys9 side-chain resonances relative to the natural hormone. [L-Msa7_D-Trp8]-SRIF (**49**) and [D-Trp8]-SRIF are shown for the sake of comparison. DSS was used as internal chemical shift reference.

The NMR data allowed us to confirm that, in the [L-Phe3,14_L-Msa7_D-Trp8]-SRIF analog **59**, several NOE interactions were found throughout the length of the

6 It has been proved that the favored geometry for a Lys-Trp cation- π interaction directs the ϵ -methylene of Lys at the aromatic ring, since this orientation allows the protonated amine to remain solvated by water while packing against the indole. The interaction of Lys via C ϵ reflects a combined hydrophobic and electrostatic effect, because the methylene is highly polarized by the neighboring ammonium cation, yet poorly solvated by water. See: a) J. P. Gallivan, D. A. Dougherty, *Proc. Natl. Acad. Sci. USA* **1999**, *96*, 9459-9464; b) J. P. Gallivan, D. A. Dougherty, *J. Am. Chem. Soc.* **2000**, *122*, 870-874.; c) C. D. Tatko, M. L. Waters, *Protein Sci.* **2003**, *12*, 2443-2452.

7 a) S. J. Russell, A. G. Cochran, *J. Am. Chem. Soc.* **2000**, *122*, 12600-12601; b) C. M. Santiveri, M. Rico, M. A. Jiménez, *Prot. Sci.* **2000**, *9*, 2151-2160.

strands between residues that are linearly up to 8 residues apart: e.g. Phe6-Phe11, Phe7-Thr10, Asn5-Thr12, Lys4-Phe11, etc.⁸ Most of the long-distance NOEs observed in this peptide were difficult to identify in the Ala3,14 analog. However, although some contacts between cross-strand residues were missing (e.g. Asn5-Thr12 and Lys4-Phe11), proton-proton interactions among *face-to-face* residues in the proximity of the hairpin were still present and well-defined (e.g. Phe6-Phe11). This finding suggests that the presence of the L-Msa7-D-Trp8 motif stabilizes the hairpin area (by positioning the Msa7 below the upheld Phe6-Phe11 aromatic interaction) and that the presence of an extra side-chain-side-chain interaction between the Phe residues at the N- and C-terminal positions modestly contributes to the β -sheet stability in tetradecapeptidic SRIF analogs.

5.2.2. Binding affinity to SSTR1-5: The receptor-subtype selectivity of these linear peptides was measured by means of radioligand binding assays on membranes prepared from CHO cells that stably expressed individually cloned SRIF receptors. The compounds, which were tested at different concentrations, competed for the binding of ¹²⁵I-labeled SRIF to SSTR2, SSTR3 and SSTR5. Binding studies demonstrated that these L-Msa7-D-Trp8 containing peptides displayed satisfactory affinities and outstanding selectivity to SSTR2 (Table 5.1).

The two synthetic linear peptides exhibited negligible activity to SSTR3 and SSTR5, while proving to be highly selective for SSTR2, having slightly higher K_i values than octreotide. This is significant because only a few linear active agonists have been developed,⁹ as linearization of native SRIF results in a loss of binding and functional activity.¹⁰ Reisine and co-workers reported for the first time the binding

8 Few NOEs between Phe3 and Phe14 aromatic rings were suspected, but difficult to identify due to overlapping between them and other aromatic residues.

9 a) K. Gademann, T. Kimmerlin, D. Hoyer, D. Seebach, *J. Med. Chem.* **2001**, *44*, 2460-2468; b) A. Miyazaki, Y. Tsuda, S. Fukushima, T. Yokoi, T. Vántus, G. Bökönyi, E. Szabó, A. Horváth, G. Kéri, Y. Okada, *J. Med. Chem.* **2008**, *51*, 5121-5124.

10 W. Vale, J. Rivier, N. Ling, M. Brown, *Metab., Clin. Exp.* **1978**, *27*, 1391-1401 and references therein.

affinities of active linear SRIF analogs.¹¹ Some of these octapeptidic linear SRIF derivatives displayed high affinity binding for SSTR2 and SSTR3, while others were exclusively selective for SSTR3 (SSTR4 and SSTR5 receptors were not included in their binding studies). To the best of our knowledge, peptides **58** and **59** are the first linear tetradecapeptidic SRIF analogs that possess such a potency and selectivity for SSTR2.

Table 5.1. K_i values (nM) and human serum half-life of SRIF, [D-Trp8]-SRIF, octreotide and SRIF analogs to receptors SSTR2, SSTR3 and SSTR5.^a K_i values are mean \pm SEM.

	SSTR2	SSTR3	SSTR5
Somatostatin	0.0034 \pm 0.0006	0.14 \pm 0.03	0.072 \pm 0.018
[D-Trp8]-SRIF	0.0027 \pm 0.0020	0.24 \pm 0.03	0.046 \pm 0.018
Octreotide	0.029 \pm 0.012	8.4 \pm 1.1	4.2 \pm 0.6
[L-Phe3,14_Msa7_D-Trp8]-SRIF, 59	0.069 \pm 0.013	> 10 ³	> 10 ³
[L-Ala3,14_Msa7_D-Trp8]-SRIF, 58	0.093 \pm 0.017	> 10 ³	> 10 ³

a: Shaded cells represent data in close proximity to the SRIF values.

Rivier and co-workers¹² reported that a synthetic [L-Ala3,14]-SRIF analog inhibits the secretion of growth-hormone with a potency of 0.6% relative to that of the wild-type SRIF. This result proved the lack of affinity of this linear SRIF analog to SSTR2 –which is the somatostatin receptor that plays the main role in repressing growth hormone secretion¹³– and provided the first insights into the observation that conformationally rigid ligands bind more effectively to this particular receptor. The finding that our linear analogs are active and selective to SSTR2 indicates that the Msa7 amino acid plays a crucial role in the stabilization of the postulated SSTR2-bioactive conformation. Even in the absence of a covalent bond that closes up the peptide terminus, this non-natural aromatic residue located at position 7 sufficiently fixes the bioactive conformation of these peptides to bind SSTR2 with high affinity

11 K. Raynor, W. A. Murphy, D. H. Coy, J. E. Taylor, J. P. Moreau, K. Yasuda, G. I. Bell, T. Reisine, *Mol. Pharmacol.* **1993**, *43*, 838-844.

12 J. Rivier, P. Brazeau, W. Vale, R. Guillemin, *J. Med. Chem.* **1975**, *18*, 123-126.

13 G. I. Bell, T. Reisine, *Trends Neurosci.* **1993**, *16*, 34-38.

and selectivity. We also consider the possibility that the Msa7 may be involved in a direct interaction with this receptor via its π -donor capability.¹⁴

5.3. Conclusions

We have developed the first highly SSTR2-active and -selective linear 14-residue SRIF analogs. Their inhibition constants are only one order of magnitude higher than that of the natural hormone and the cyclic parent compound [L-Msa7_D-Trp8]-SRIF (**49**), and are at the same order of magnitude as octreotide.

Taking into account the dramatic differences in biological activity between [L-Ala3,14]-SRIF and the natural hormone,¹⁰ the effect of the Msa7 incorporation in the receptor-subtype selectivity of linear [D-Trp8]-SRIF analogs is remarkable.¹⁵ We consider that the Msa residue in this position induces a remarkable synergistic effect, yet noticeable in the absence of the disulfide union.

Rivier and co-workers¹⁶ reported that the aromatic ring at position 7 (Phe7) is not critical for SSTR2-binding in cyclic octapeptidic SRIF analogs, since the substitution of Phe7 either by Ala or 4-aminophenylalanine (Aph) had no effect on SSTR2 activity or selectivity. Our studies further confirmed that the 3D conformations that somatostatin adopts to bind its receptors are not necessarily similar to those adopted by octapeptides.¹⁷

On the basis of the cross-strand NOE signals and the chemical shift perturbation of the Lys9 side-chain, we have determined that peptide **59**, [L-

14 The assumption that the residue in position 7 may be involved in a direct interaction with some receptors has been reported here: S. Neelamkavil, B. Arison, E. Birzin, J. Feng, K. Chen, A. Lin, F. Cheng, L. Taylor, E. R. Thornton, A. B. Smith III, R. Hirschmann, *J. Med. Chem.* **2005**, *48*, 4025-4030.

15 There are no literature precedents regarding the study of the biological activity of [L-Ala3,14_D-Trp8]-SRIF.

16 C. R. R. Grace, J. Erchegyi, S. C. Koerber, J. C. Reubi, J. Rivier, R. Riek, *J. Med. Chem.* **2006**, *49*, 4487-4496.

17 That Phe7 is essential for SSTR2-affinity in SRIF-14 has been also demonstrated by the fact that the K_i value of [L-Ala7]-SRIF analog is three orders of magnitude higher than that of the wild-type SRIF. See: I. Lewis, W. Bauer, R. Albert, N. Chandramouli, J. Pless, G. Weckbecker, C. Bruns, *J. Med. Chem.* **2003**, *46*, 2334-2344.

Phe3,14_L-Msa7_D-Trp8]-SRIF, has a β -sheet population that is modestly higher than that of [L-Ala3,14_L-Msa7_D-Trp8]-SRIF (**58**). Therefore, an additive Phe-Phe aromatic interaction at the terminus, where the residues have significantly more conformational freedom, moderately contributes to the conformational stability of this linear 14-residue SRIF analog.¹⁸ This small effect could be the cause of the slightly higher affinity of the Phe3,14 peptide to the SSTR2 receptor.

Although these SSTR2-active and -selective peptides are postulated to have low metabolic stability¹⁹ and therefore their clinical development is a long term goal, they have provided significant insights into the SAR that arises from Msa7 incorporation. Advances in our understanding of these compounds should prove useful for their application in *de novo* design of future somatostatin analogs.

¹⁸ That a hydrophobic cluster near the turn provides greater stability to a hairpin than when it is at the terminus has been reported here: J. F. Espinosa, V. Muñoz, S. H. Gellman, *J. Mol. Biol.* **2001**, *306*, 397-402.

¹⁹ Experiments devoted to determine the serum stability of these compounds are currently underway.

6

Tetradecapeptidic SRIF analogs bearing the Dfp residue

Chapter 6. Tetradecapeptidic SRIF analogs bearing Dfp residues

6.1. Introduction: The role of fluorine substituents in aromatic interactions	83
6.2. 14-Residue SRIF analogs containing Dfp residues	88
6.2.1. Receptor-subtype selectivity	88
6.2.2. Structure.....	89
6.3. Conclusions.....	95

6.1. Introduction:

The role of fluorine atoms in aromatic interactions

Site-directed incorporation of fluorinated amino acids has become an increasingly attractive approach in protein engineering for basic research and biomedical applications.¹ This strategy has been successful in so many cases that fluorine substitutions are now considered a standard method for modulating the properties of chemical leads.² While fluorinated aliphatic residues have been demonstrated to be effective in stabilizing protein structures³ and functioning as recognition motifs,⁴ amino acids containing fluorinated aromatic side-chains are only beginning to be investigated and their energetic contribution to protein structural stability remains unclear.⁵

As we discussed in previous chapters, the simplest aromatic structure, benzene, exhibits an uneven electron distribution even though it does not have a net dipole. Since a sp² carbon is more electronegative than hydrogen, benzene displays a negative potential on the π face and positive around the periphery. It is widely accepted that this electron distribution, referred to as a quadrupole, prompts aromatic moieties to associate in electrostatic interactions with a charge (e.g., cation- π interaction), a partial charge, a dipole, or another quadrupole. Benzene and perfluorobenzene exhibit quadrupole moments of the same magnitude but opposite signs (-29.0×10^{-40} Cm⁻² and 31.7×10^{-40} Cm⁻² respectively).⁶ Such polar- π interactions explain why benzene molecules pack in the *edge-to-face* (T-shaped) or *offset-stacked* geometries in crystal structures, but benzene and perfluorobenzene mix readily to

-
- 1 M. Salwiczek, E. K. Nyakatura, U. I. M. Gerling, S. Ye, B. Koksich, *Chem. Soc. Rev.* **2012**, *41*, 2135-2171.
 - 2 S. Purser, P. R. Moore, S. Swallow, V. Gouverneur, *Chem. Soc. Rev.* **2008**, *37*, 320-330.
 - 3 a) J. Horng, D. P. Raleigh, *J. Am. Chem. Soc.* **2003**, *125*, 9286-9287; b) C. Jäckel, M. Salwiczek, B. Koksich, *Angew. Chem., Int. Ed.* **2006**, *45*, 4198-4203.
 - 4 B. Bilgiçer, K. Kumar, *Proc. Natl. Acad. Sci. U.S.A.* **2004**, *101*, 15324-15329.
 - 5 a) J. S. Thorson, E. Chapman, E. C. Murphy, P. G. Schultz, J. K. Judice, *J. Am. Chem. Soc.* **1995**, *117*, 1157-1158; b) H. Chiu, Y. Suzuki, D. Gullickson, R. Ahmad, B. Kokona, R. Fairman, R. P. Cheng, *J. Am. Chem. Soc.* **2006**, *128*, 15556-15557.
 - 6 E. A. Meyer, R. K. Castellano, F. Diederich, *Angew. Chem., Int. Ed.* **2003**, *42*, 1210-1250.

give a solid with an alternating, stacked geometry with the aromatic faces parallel to each other.⁷

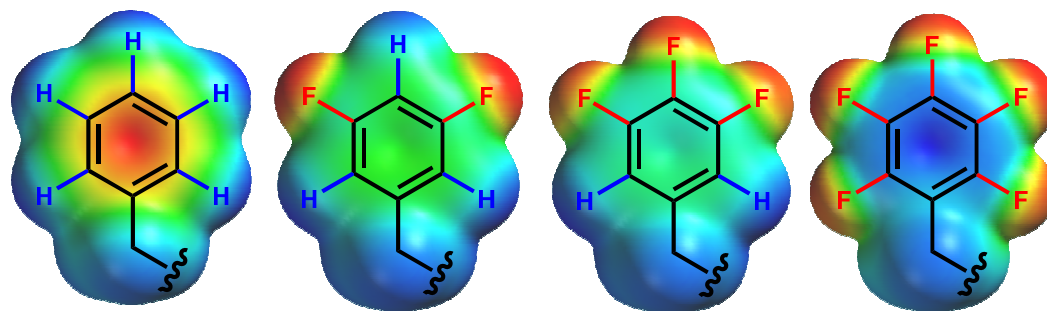


Figure 6.1. Side chains of relevant fluorinated phenylalanine derivatives. Electrostatic potential maps (blue=positive, red=negative) were generated for the toluene derivatives with Spartan (PM3 semi-empiric).

In this regard, the electrostatic potential (ESP) maps of the implicated aromatic molecules have been extensively used in the analyses of non-covalent interactions (Figure 6.1).⁸ However, the traditional view of the substituent effect in aromatic interactions, which depends on the polarization of the aryl π -system by the substituent (*i.e.* the molecular quadrupole moments or the sign of the ESP above the aromatic ring), has been demonstrated to expose several flaws.^{9,10} As a clear example, in the solid state 1,2,3-trifluorobenzene (which has a negligible quadrupole moment) exhibits stacking interactions analogous to those observed in benzene-perfluorobenzene (Figure 6.2),¹¹ which is contrary to expectations based solely on molecular quadrupole moments.¹² Different studies also showed that 1,3,5-

7 M. L. Waters, *Curr. Opin. Chem. Biol.* **2002**, *6*, 736-741.

8 a) F. Cozzi, M. Cinquini, R. Annuziata, J. S. Siegel, *J. Am. Chem. Soc.* **1993**, *115*, 5330-5331; b) S. L. McKay, B. Haptonstall, S. H. Gellman, *J. Am. Chem. Soc.* **2001**, *123*, 1244-1245; c) S. L. Cockroft, C. A. Hunter, K. R. Lawson, J. Perkins, C. J. Urch, *J. Am. Chem. Soc.* **2005**, *127*, 8594-8595.

9 S. E. Wheeler, K. N. Houk, *J. Chem. Theory Comput.* **2009**, *5*, 2301-2312.

10 a) K. Müller-Dethlefs, P. Hobza, *Chem. Rev.* **2000**, *100*, 143-168; b) S. Grimme, *Angew. Chem., Int. Ed.* **2008**, *47*, 3430-3434; c) S. E. Wheeler, K. N. Houk, *J. Am. Chem. Soc.* **2008**, *130*, 10854-10855; d) A. L. Ringer, C. D. Sherrill, *J. Am. Chem. Soc.* **2009**, *131*, 4574-4575.

11 M.T. Kirchner, D. Bläser, R. Boese, T. S. Thakur, G. R. Desiraju, *Acta Crystallogr.* **2009**, E65, 2670.

12 J. D. Dunitz, *ChemBioChem* **2004**, *5*, 614-621.

trifluorobenzene exhibits similar stacking interactions,¹³ even though both fluorinated aromatic moieties display very different molecular dipole moments and both have negligible quadrupole moments. Interestingly, in both systems the rings are oriented so that each C-H bond is positioned above and parallel to a C-F bond. Thus, substituent effects can be understood in terms of local, direct interactions¹⁴ between the substituent and the closest vertex of the other ring, since these stacking arrangements maximize favorable direct interactions between the local C-F and C-H dipoles; *i. e.*, favorable interactions between the partially positively charged hydrogens and the partially negative fluorines.¹¹

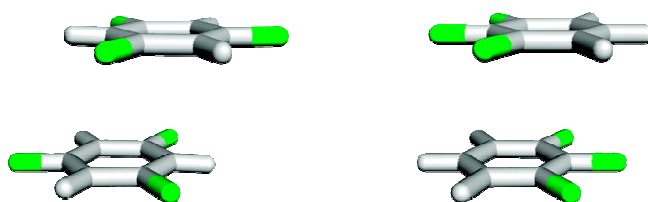


Figure 6.2. 1,3,5-trifluorobenzene and 1,2,3-trifluorobenzene in the solid state (Ref. 11).

The stabilizing effect of fluorinated phenylalanine derivatives in peptides and small proteins has been recently investigated. By introducing aromatic amino acids into a host Ala-Lys peptide, Waters and co-workers¹⁵ studied the contribution of aromatic interactions to α -helix stability. They showed that a Phe-Phe pair stabilized the helix at the C-terminus by $-0.80 \text{ kcal mol}^{-1}$, while a phenylalanine-perfluorophenylalanine pair (Phe-F5Phe) stabilized it by lesser extent, $-0.55 \text{ kcal mol}^{-1}$. Molecular modeling studies suggested that a Phe-Phe pair associated either in *edge-to-face* or *offset-stacked* geometries contributes to a higher stabilization because a *face-to-face* interaction geometry (Phe-F5Phe) is not preferred at the *i* and *i+4* positions of an α -helix. In addition, since the side-chain of F5Phe is more

13 V. R. Thalladi, H. Weiss, D. Bläser, R. Boese, A. Nangia, G. R. Desiraju, *J. Am. Chem. Soc.* **1998**, *120*, 8702-8710.

14 S. E. Wheeler, *J. Am. Chem. Soc.* **2011**, *133*, 10262-10274.

15 S. M. Butterfield, P. R. Patel, M. L. Waters, *J. Am. Chem. Soc.* **2002**, *124*, 9751-9755.

hydrophobic than that of Phe, the fact that a Phe-Phe pair is more stabilizing may indicate that the interaction is not hydrophobic but mainly electrostatic.

In a different context, the Gellman group¹⁶ examined F5Phe substitutions in the chicken villin headpiece subdomain (cVHP), a 35-residue small folded protein containing a nonpolar core which features a cluster of three Phe side-chains. Six of the seven perfluorophenylalanine-containing mutants proved to be less stably folded than the parent compound. They proposed that the destabilizing effect could be explained by disruption of *edge-to-face* interactions between aromatic residues due to side-chain perfluorination.

Gao and co-workers¹⁷ tested this hypothesis by using a set of tetrafluorinated phenylalanine derivatives, named as F4Phe_x, where x indicates the relative position of the remaining hydrogen. Their results showed that, in contrast to the use of fully fluorinated F5Phe, the introduction of F4Phe_{ortho} and F4Phe_{para} in key positions afforded a substantial improvement in the stability of cVHP subdomain because these amino acids retained favorable *edge-to-face* interactions in the aromatic cluster. This type of interaction is expected to be promoted by the particularly high acidity of the remaining protons of these tetrafluorinated phenylalanine derivatives. Nevertheless, it has been found that aromatic stacking involving fluorinated aromatic amino acids are mechanistically complicated, involving a combination of hydrophobic and van der Waals forces, as well as quadrupole, dipole-dipole, and dipole-induced dipole interactions, with no single factor explaining the majority of the observations.¹⁸

Although our understanding of the effects of fluorination on the interaction between aromatic residues remains incomplete, we considered that fluorinated aromatic residues represented an ideal way to further prove and study polar- π

16 M. G. Woll, E. B. Hadley, S. Mecozzi, S. H. Gellman, *J. Am. Chem. Soc.* **2006**, *128*, 15932-15933.

17 H. Zheng, K. Comeforo, J. Gao, *J. Am. Chem. Soc.* **2009**, *131*, 18-19.

18 a) H. Adams, J. Jimenez Blanco, G. Chessari, C. A. Hunter, C. M. R. Low, J. M. Sanderson, J. G. Vinter, *Chem. Eur. J.* **2001**, *7*, 3494-3503; b) L. M. Salonen, M. Ellermann, F. Diederich, *Angew. Chem., Int. Ed.* **2011**, *50*, 4808-4842.

interactions in SRIF analogs, due to the small steric yet large electronic impact that they imply.¹⁹ From among the eleven possible fluorinated derivatives of phenyl alanine (from one fluorine atom in different positions of the phenyl ring to the completely fluorinated F5Phe) we considered that the 3-(3',5'-difluorophenyl)-alanine amino acid, Dfp (See Table 6.1), partially meets all of the important requirements:

1. This non-natural amino acid is markedly more hydrophobic ($\log P = 2.84$) than the natural Phe ($\log P = 2.54$).¹⁷
2. The fluorine atom may be considered isosteric with hydrogen, since the van der Waals radius of fluorine (1.35 Å) is only slightly larger than that of hydrogen (1.20 Å).²⁰ Thus, the Dfp aromatic moiety is only slightly bigger than that of the natural Phe (surface areas are 146.5 Å² vs. 134.7 Å²).²⁰
3. The particular fluorine atom distribution in the aromatic moiety would allow this residue to retain (presumably) ArH- π interactions.¹⁷
4. The three remaining hydrogen atoms will provide acceptable structural information (via NOEs signals), which is required to study the peptidic architecture of SRIF-analogs containing the Dfp amino acid.
5. Although a C-F bond (1.34 Å for a sp² carbon) is ~20% longer than a C-H bond (1.09 Å), we predicted difluorination to cause minimal perturbation in the parent structures of SRIF.¹
6. The electron-poor difluorinated aromatic side-chain should promote aromatic ring association with the native electron-rich Phe residues present in the SRIF sequence.

19 B. C. Buer, E. N. G. Marsh, *Prot. Sci.* **2012**, *21*, 453-462.

20 C. J. Pace, J. Gao, *Acc. Chem. Res.* **2013**, *46*, 907-915.

6.2. 14-Residue SRIF analogs containing a Dfp residue

With gram quantities of 3-(3',5'-difluorophenyl)-alanine (Chapter 2), we proceeded to substitute the Phe6, Phe7 and Phe11 residues with this fluorinated amino acid in the sequence of the [D-Trp8]-SRIF analog (Table 6.1).

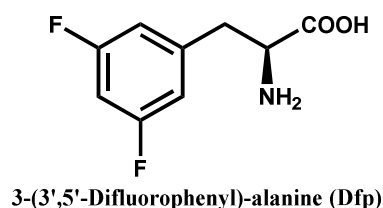
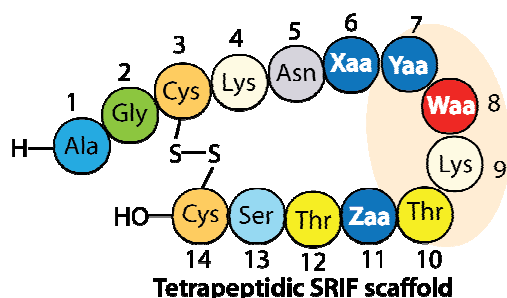


Table 6.1. Somatostatin analogs obtained by replacement of the Phe in positions 6, 7 and 11 by 3-(3',5'-difluorophenyl)-alanine (Dfp) residues.

6 th	7 th	8 th	11 th	Peptide analog
Dfp	Phe	D-Trp	Phe	[L-Dfp6_D-Trp8]-SRIF, 60
Phe	Dfp	D-Trp	Phe	[L-Dfp7_D-Trp8]-SRIF, 61
Phe	Phe	D-Trp	Dfp	[L-Dfp11_D-Trp8]-SRIF, 62

6.2.1. Receptor-subtype selectivity: The affinity and selectivity for receptor 2, 3 and 5 was measured by a competitive binding assay using ¹²⁵I-labeled SRIF-14 and different concentrations of unlabeled ligand. These studies were carried out by us either in the University of Alcalá or in the Barcelona Science Park facilities. For comparative purposes, the same test was applied to SRIF, [D-Trp8]-SRIF and octreotide. The receptor-subtype selectivity profiles of these analogs (Table 6.2) will be discussed in detail in parallel with their structural studies. Experiments devoted to determine the half-life time of these peptides in human serum are currently underway.

Table 6.2. K_i values (nM) of SRIF, [D-Trp8]-SRIF, octreotide and SRIF analogs to receptors SSTR2, SSTR3 and SSTR-5.^a K_i values are mean \pm SEM.

	SSTR2	SSTR3	SSTR5
Somatostatin	0.0034 \pm 0.0006	0.14 \pm 0.03	0.072 \pm 0.018
[D-Trp8]-SRIF	0.0027 \pm 0.0020	0.24 \pm 0.03	0.046 \pm 0.018
Octreotide	0.029 \pm 0.012	8.4 \pm 1.1	4.2 \pm 0.6
[L-Dfp6_D-Trp8]-SRIF, 60	0.040 \pm 0.010	1.2 \pm 0.3	0.060 \pm 0.008
[L-Dfp7_D-Trp8]-SRIF, 61	0.18 \pm 0.07	0.58 \pm 0.12	0.18 \pm 0.05
[L-Dfp11_D-Trp8]-SRIF, 62	0.025 \pm 0.006	3.7 \pm 1.7	0.36 \pm 0.09

a: Shaded cells represent data in close proximity to the SRIF values.

6.2.2. Structure: The SRIF analogs containing both the Dfp and the D-Trp8 variations were analyzed by NMR. The well-dispersed two dimensional NOESY homonuclear experiments clearly showed a major set of NOE peaks, which enabled us to characterize their main conformations in solution using the software Crystallography & NMR System (CNS).²¹

The high conformational stability of the [L-Dfp6_D-Trp8]-SRIF analog (**60**) was confirmed by the large number of NOE signals that were found among side-chains of cross-strand residues. The well-dispersed 2D spectra allowed us to characterize the main conformation in solution for this peptide, which exhibited a high similarity to the bioactive conformation we postulated that SRIF adopts when it binds to the SSTR2 receptor.

It is not surprising that this peptide displayed high activity towards SSTR2 and SSTR5. Numerous key proton-proton interactions were found between D-Trp8 and Lys9, which are involved in a hydrophobic interaction that further stabilizes the hairpin area. It is clear that the pharmacophoric part of the molecule is more

21 A. T. Brunger, P. D. Adams, G. M. Clore, W. L. DeLano, P. Gros, R. W. Grosse-Kunstleve, J. S. Jiang, J. Kuszewski, M. Nilges, N. S. Pannu, R. J. Read, L. M. Rice, T. Simonson, G. L. Warren, *Acta Crystallogr. D Biol. Crystallogr.* **1998**, 54, 905-921.

structured than the terminus. Particularly under our experimental conditions, almost all of the NOE contacts that the side-chains of Dfp6 and Phe11 display are between them, thus this peptide presents a 3D structure that exposes a Dfp6-Phe11 aromatic interaction (Figure 6.3).

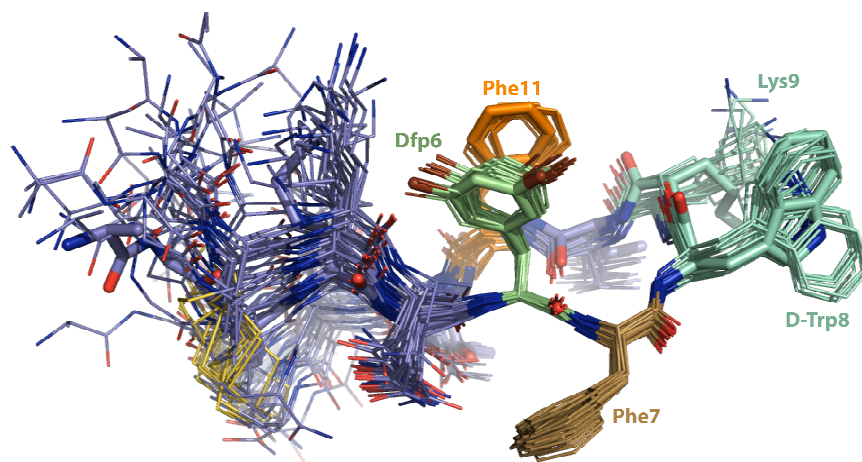


Figure 6.3. Superimposition of the lowest energy conformers of [L-Dfp6_D-Trp8]-SRIF (**60**) that fit the NMR data.

As previously mentioned, substituent effects in aromatic interactions have been described primarily in terms of the electrostatic model reported by Hunter and Sanders²² or the polar- π model supported by Cozzi and Siegel.^{8a,23} Both models consider that electron-withdrawing substituents enhance the π -stacking interactions because they reduce the aryl π -electron density, thus relieving the electrostatic repulsion with the π -electron cloud of the other ring (Figure 6.4). These models would explain why these two aromatic residues engage in a stacking type of interaction: difluorination enhances stacking interactions because it decreases the Ar6 π -electron density, which minimizes the unfavorable electrostatic interactions with the π -cloud of the natural Phe11 aromatic ring.

22 a) C. A. Hunter, K. R. Lawson, J. Perkins, C. J. Urch, *J. Chem. Soc., Perkin Trans. 2* **2001**, 0, 651-669; b) S. L. Cockroft, J. Perkins, C. Zonta, H. Adams, S. E. Spey, C. M. R. Low, J. G. Vinter, K. R. Lawson, C. J. Urch, C. A. Hunter, *Org. Biomol. Chem.* **2007**, 5, 1062-1080.

23 F. Cozzi, F. Ponzini, R. Annunziata, M. Cinquini, J. S. Siegel, *Angew. Chem., Int. Ed.* **1995**, 34, 1019-1020.

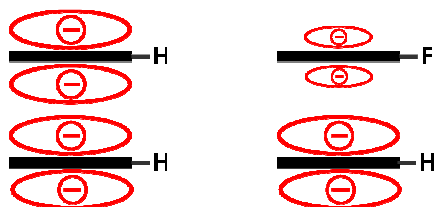


Figure 6.4. Schematic view of substituent effects in stacking interactions.

The local, direct interaction model outlined by Wheeler¹⁴ explains the ring orientations that were found in solution for this peptide (Figure 6.5): in this slightly *offset-stacked* aromatic interaction, two of the Phe11 partially positively charged hydrogens are pointing directly to the partially negative fluorinated part of the Dfp6, thus maximizing favorable direct interactions.

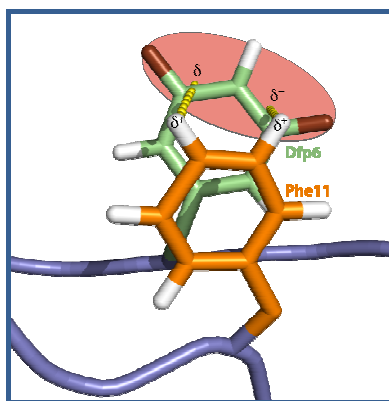


Figure 6.5. Close-up view of the Dfp6-Phe11 aromatic interaction in peptide **60**. The distances between C_Z11-C_E16 and C_E11-C_E26 are 4.4 and 4.0 Å respectively.

Peptide [L-Dfp7_D-Trp8]-SRIF (**61**) displayed very low affinity to the SSTR2 receptor. According to the NMR data, the main conformation of **61** displayed a 3D structure in which the three aromatic residues are located on the other face of the molecule than in peptide **60**. The Dfp7 residue showed several NOE contacts with the Phe6 and Phe11 side-chains, which are in close proximity presenting an *edge-to-face* aromatic interaction (Figure 6.6). The NMR data indicated that the aromatic side-chain of the Dfp7 fluctuates to a position nearby the D-Trp8 residue. In addition, the indole ring of this residue displays numerous NOE signals with the aliphatic side-chain of Lys9, indicating a D-Trp8-Lys9 hydrophobic interaction.

This analog proved to be moderately active and selective towards the SSTR3 receptor. [D-Trp8]-SRIF analogs containing either an Msa or Tmp in position 6, displayed a similar major conformation in solution and a high potency and selectivity for SSTR3. These observations indicate that this type of peptidic architecture might be similar to the conformation of the natural hormone when it binds to SSTR3.

The NMR data suggested that, under our experimental conditions, this peptide also populates a minor conformation quite similar to the postulated bioactive conformation for SSTR2. This conformation is defined by several key proton-proton interactions characteristic of the analogs that preferentially populate this bioactive conformation. In this case, however, the contacts observed for the residue in position 7 are not enough to define a unique structure for this peptide. This mixture of conformations probably reduces the efficiency of the interaction with SSTR2, thus its K_i value for this receptor is two orders of magnitude higher than that of the natural hormone.

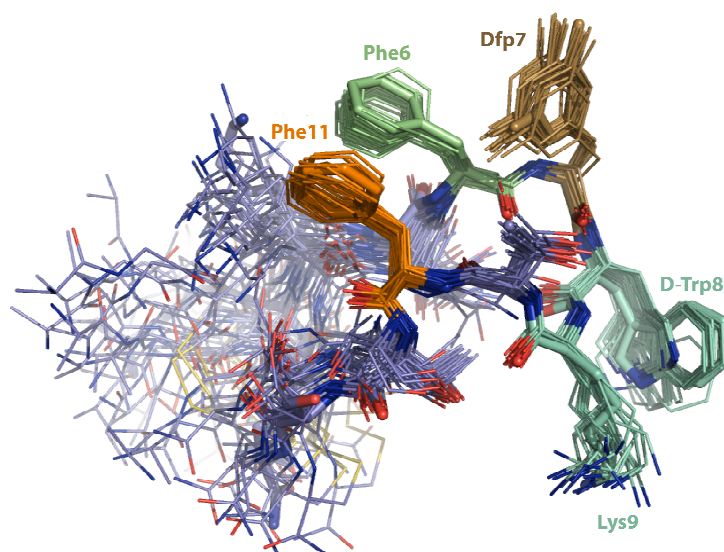


Figure 6.6. Superimposition of the lowest energy conformers of [L-Dfp7_D-Trp8]-SRIF (**61**) that were calculated on the basis of the experimental NMR data.

According to the NMR data, peptide [L-Dfp11_D-Trp8]-SRIF (**62**) displayed a highly populated conformation in solution. As a result of this, its 3D structure is well-defined by an abundant number of NMR restraints (Figure 6.7). This analog displayed

high affinity and selectivity to SSTR2, presenting K_i values at the same level than octreotide. This result was unexpected, since the Dfp11 lacks the necessary π -electron density to shield Phe6, an effect that has been assumed to provide conformational stability to the tetradecapeptidic architecture.²⁴ NOE contacts between these residues were both abundant and intense, which indicates a close proximity between their side-chains. The Phe6-Dfp11 aromatic moieties are engaged in a parallel displaced aromatic interaction in which the most negatively charged part of the Dfp11 ring points away of the π -cloud of the natural Phe. This ring orientation, defined by several NOE contacts between Dfp11 and Lys4, Phe6, Thr12 and Ser13 side-chains, is remarkably similar to that of the aromatic interaction between Dfp6-Phe11 in peptide [L-Dfp6_D-Trp8]-SRIF (**60**).

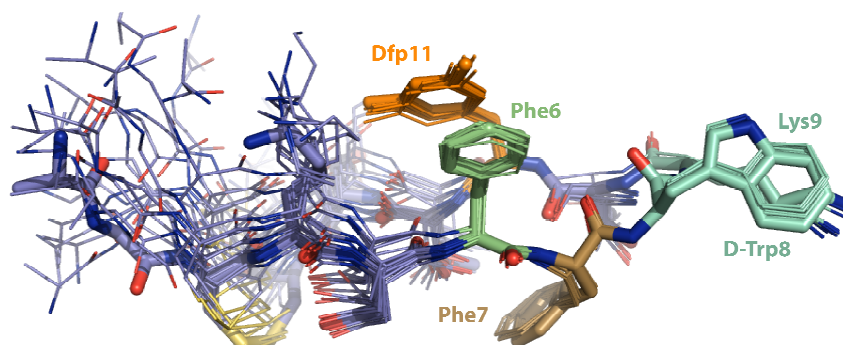


Figure 6.7. Lowest energy conformers of [L-Dfp11_D-Trp8]-SRIF (**62**) that best fit the NMR data.

Our findings in SRIF analogs bearing Dfp residues agree with Hirschmann studies of somatostatin analogs containing the L-pyrazinylalanine (Pyz) amino acid.²⁴ These authors investigated the replacement of the natural phenylalanine residues by Pyz in the tetradecapeptidic SRIF scaffold. The [L-Pyz6_D-Trp8] and [L-Pyz11_D-Trp8]-SRIF analogs were shown to retain significant SSTR2-potency, displaying quite similar K_i values that were only one order of magnitude higher than that of the [D-Trp8]-SRIF (Table 6.3). On the other hand, [L-Pyz7_D-Trp8]-SRIF showed no binding

²⁴ This article constitutes one of the few reports regarding full-length SRIF analogs: S. Neelamkavil, B. Arison, E. Birzin, J. Feng, K. Chen, A. Lin, F. Cheng, L. Taylor, E. R. Thornton, A. B. Smith III, R. Hirschmann, *J. Med. Chem.* **2005**, *48*, 4025-4030.

to this receptor.²⁵ The observation that the introduction of either Pyz or Dfp amino acids results in identical SSTR2 receptor-subtype selectivity values may indicate that the aromatic interaction between residues 6 and 11 that stabilize the SSTR2 bioactive conformation is more electrostatic in nature than hydrophobic.

Table 6.3. Normalized (to [D-Trp8]-SRIF) K_i values of octreotide and SRIF analogs to receptor SSTR2.

Peptidic nalog	Dfp	Pyz
[D-Trp8]-SRIF	1	
Octreotide	10	
[L-Xaa6_D-Trp8]-SRIF	14	14 ^a
[L-Xaa7_D-Trp8]-SRIF	67	> 100 ^a
[L-Xaa11_D-Trp8]-SRIF	10	14 ^a

a: Normalized values from Ref. 21.

The somatostatin “Ala-scan” carried out by Lewis *et. al.*²⁶ indicated that replacement of Phe6 by Ala6 results in a decrease of affinity larger than that of the corresponding Ala11 modification. This observation, together with the Pyz receptor-subtype selectivity values, led Hirschmann and co-workers to suggest that Phe6 interacts with the receptor via its π -donor mechanism.²⁴ On the basis of our recent investigations on tetradecapeptidic SRIF analogs, we propose a more precise hypothesis: since the [L-Msa6_D-Trp8] and [L-Tmp6_D-Trp8]-SRIF analogs showed no affinity to SSTR2 and its main conformation in solution is different to the SSTR2-bioactive structure, we propose that the putative direct interaction of Xaa6 with the receptor is only important when the peptidic architecture is close to that bioactive conformation. These results suggest that SSTR2 recognition is highly favored by the presence of an optimal peptidic conformation prior binding, rather than by an induced-fit mechanism.

25 Only SSTR2 and SSTR4 were investigated. The three analogs containing the Pyz amino acid showed negligible affinity to SSTR4. The authors did not consider the fact that, even lacking a π -donor capability, the aromatic moiety of the Pyz residue is able to be involved in aromatic interactions.

26 I. Lewis, W. Bauer, R. Albert, N. Chandramouli, J. Pless, G. Weckbecker, C. Bruns, *J. Med. Chem.* **2003**, *46*, 2334-2344.

6.3. Conclusions

The incorporation of 3-(3',5'-difluorophenyl)-alanine in positions 6 or 11 (peptides [L-Dfp6_D-Trp8] (**60**) and [L-Dfp11_D-Trp8]-SRIF (**62**)) shifts the conformational equilibrium of these peptides toward similar conformations, which contain an aromatic interaction between residues 6 and 11. The geometries of the polar- π interactions in peptides **60** and **62** are quite similar, and have been explained on the basis of the traditional polar- π model and in terms of the local interaction viewpoint. In addition, as expected by the 3D structures of their main conformations, these analogs display a high potency to the SSTR2 receptor.

When the electron-poor aromatic side-chain is situated in the position 7, the resulted main conformation in solution was different. The high affinity and selectivity of the [Dfp7_D-Trp8]-SRIF analog **61** to SSTR3 may arise from the formation of an aromatic cluster on that specific face of the molecule.

It has been previously postulated that electron-deficient aromatic residues in position 11 destabilize the peptidic architecture due to their inefficient role shielding the natural Phe6. Interestingly, we have found that a Phe6-Dfp11 aromatic interaction plays a key role in stabilizing the bioactive conformation that is necessary to bind SSTR2, developing a moderately active and selective [D-Trp8]-SRIF analog that display a markedly higher conformational rigidity than the parent compound.

7

Somatostatin derivatives containing Cha residues

Chapter 7. Somatostatin derivatives containing Cha residues

7.1. Introduction: The Cha amino acid	99
7.2. Structural data and radioligand binding assays.....	102
7.3. Conclusions	107

7.1. Introduction:

The Cha amino acid

So far we have shown that the presence of aromatic amino acids containing specific electronic properties in the SRIF sequence modulates its peptidic architecture by altering some non-covalent interactions. The enhancement of these aromatic interactions increases the conformational stability of SRIF analogs, but the origin of this conformational stability, which may be dependent on hydrophobicity, electrostatic interactions, and van der Waals forces, is still a matter of debate.

In order to investigate separately the relative contributions of hydrophobic and electronic factors to this stabilization, we have examined different 14-residue SRIF analogs containing the commercially available 3-cyclohexylalanine amino acid (Figure 7.1). Although slightly larger (10%) than the planar phenylalanine, the unnatural Cha amino acid has a similar hydrophobicity and polarity, but it lacks the ability to participate in aromatic interactions driven by electronic factors. In this regard, if the aromatic interactions that stabilize some bioactive conformations in SRIF are more electrostatic in nature than hydrophobic, substitution of one or more natural Phe by the Cha residue would entail a total or partial loss of structure that would be reflected in lower affinity to SSTR1-5.

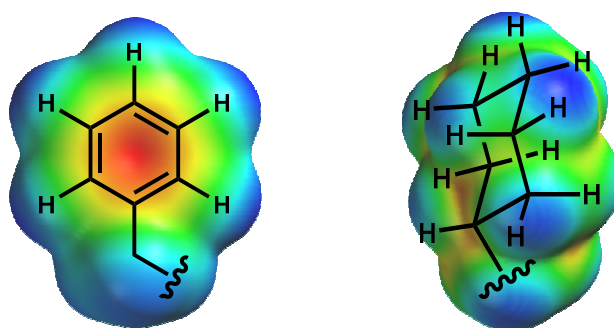


Figure 7.1. Electrostatic potential maps for Phe and Cha side-chains that highlight the distinct differences in electronics despite their similar size. Electron-rich region is highlighted in red. PM3 semiempirical model in Spartan'10 (Wavefunction, Inc.)

The Cha amino acid has been recently used to test the contribution of the hydrophobic and electronic components to aromatic and aliphatic interactions in

aromatic clusters. Tatko and Waters¹ investigated the interaction of two Phe residues located cross-strand from each other in the context of a β -hairpin (Figure 7.2). This was compared to a cross-strand pair of Cha residues as well as the two peptides containing the mixed Phe-Cha pairs. The β -sheet propensity of a Cha amino acid was proved to be higher than Phe². Thus, in the absence of a side-chain - side-chain interaction, the ChaCha peptide was predicted to be more stable than the PhePhe counterpart. Nevertheless, the two hairpins were found to be equally stable, which suggests that the ring association in the PhePhe derivative compensates for the difference in the propensity of hairpin formation as well as any hydrophobic interaction between the two Cha residues. NMR studies showed that the Phe-Phe residues engage an *edge-to-face* aromatic interaction.

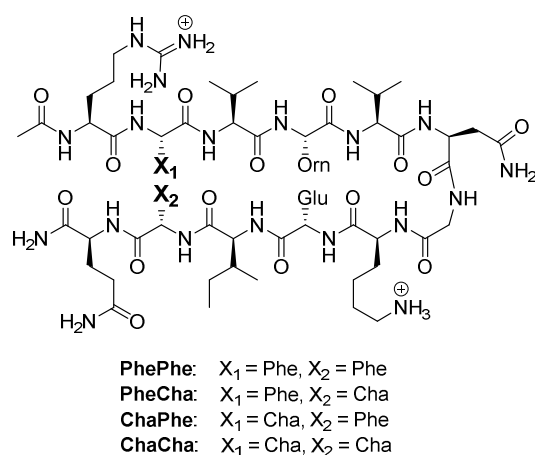


Figure 7.2. β -Hairpin peptides studied by Tatko and Waters.

The fact that the two aromatic rings interact in an *edge-to-face* geometry even though they are solvent-exposed provides another evidence of the interaction not being driven by the hydrophobic effect, which would favor the maximum burial of surface area. The authors also found a preference for self-association between aromatic and aliphatic side-chains, by being PhePhe and ChaCha markedly more stable than PheCha and ChaPhe. Thermal denaturation studies indicated that

1 C. D. Tatko, M. L. Waters, *J. Am. Chem. Soc.* **2002**, *124*, 9372-9373.

2 When Cha is cross-strand from Ala, the correspondent peptide is about 7% more folded at 283K than the Phe-Ala containing derivative.

PhePhe has a greater enthalpic driving force and a concomitant greater entropic cost than any other peptide, suggesting a greater dispersive or electrostatic component to the interaction than a classical hydrophobic interaction.

Sakaguchi and co-workers³ investigated the substitution of three key Phe residues at positions 328, 338 and 341 in the hydrophobic core of the p53 tetrameric structure (Figure 7.3) using thermal denaturation experiments. It is known that Phe328 and Phe338 interact with each other through polar- π interactions, whereas Phe341 is buried in the surrounding alkyl side-chains of the hydrophobic core of the p53 tetramerization domain.⁴ Substitution of Phe328 or Phe338 by a Cha residue significantly reduced stability by 6 Kcal mol⁻¹, probably by invalidating the electronic contribution to the aromatic interaction. In contrast, the substitution of Phe341 in the hydrophobic core with a Cha residue enhanced the stability of the tetrameric structure by 3.6 Kcal mol⁻¹, since the more flexible, hydrophobic and slightly bigger Cha residue fills the cavity in the hydrophobic core better than a Phe residue.

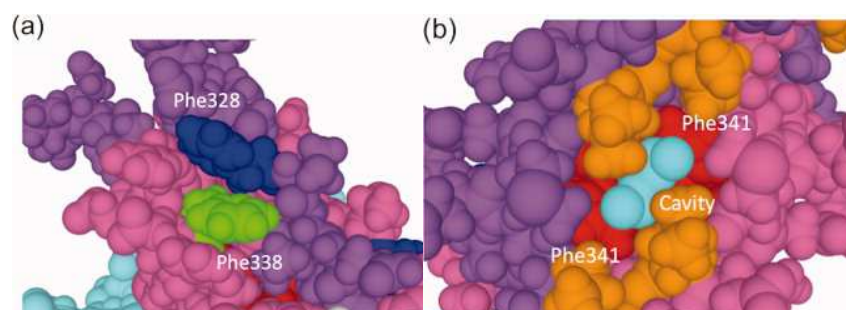


Figure 7.3. The position of each Phe residue within the hydrophobic core, (a) Phe328 and Phe338 and (b) Phe341. (a) Phe328 (blue) in one peptide chain is facing Phe338 (green) in the neighboring chain. (b) Phe341 (red) is buried in the p53 hydrophobic core composed of Ile, Leu and Met (orange). The internal structure at the interface between the primary dimers is shown.

In order to gain insights into the relative effect of electronic and hydrophobic interactions in the conformational stabilization of somatostatin, we substituted

3 T. Nomura, R. Kamada, I. Ito, K. Sakamoto, Y. Chuman, K. Ishimori, Y. Shimohigashi, K. Sakaguchi, *Biopolymers* **2011**, *95*, 410-419.

4 B. S. Frank, D. Vardar, D. A. Buckley, C. J. McKnight, *Prot. Sci.* **2002**, *11*, 680-687.

natural Phe residues with the L-3-cyclohexylalanine amino acid (Table 7.1). We prepared three [D-Trp8]-SRIF analogs containing the Cha residue in positions 6, 7 or 11 (peptides **63**, **64** and **65**, respectively). In order to investigate Water's observation, namely the preference for self-association between aromatic and aliphatic side-chains,¹ we also synthesized a peptide containing two cross-strand Cha (in positions 6 and 11, **66**).

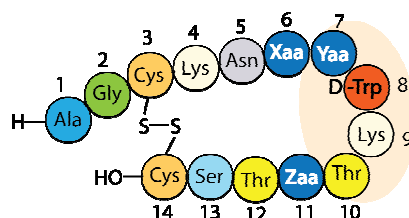


Table 7.1. Somatostatin analogs obtained by replacement of the Phe in positions 6, 7 and 11 by cyclohexyl alanine (Cha).

6 th	7 th	8 th	11 th	Peptidic analog
Cha	Phe	D-Trp	Phe	[L-Cha6_D-Trp8]-SRIF, 63
Phe	Cha	D-Trp	Phe	[L-Cha7_D-Trp8]-SRIF, 64
Phe	Phe	D-Trp	Cha	[L-Cha11_D-Trp8]-SRIF, 65
Cha	Phe	D-Trp	Cha	[L-Cha6,11_D-Trp8]-SRIF, 66

7.2. Structural data and radio-ligand binding assays

To examine the functional effects of the Cha mutations at the structural level, we analyzed the NOE pattern of these new peptides in aqueous solution. Spin systems and sequential assignments for the four peptides were obtained from 2D TOCSY and NOESY homonuclear experiments. As reflected in the number and intensities of most of the medium- and long-range contacts, Cha containing analogs displayed a comparable or slightly higher conformational flexibility to that of the parent compound (Figure 7.4).

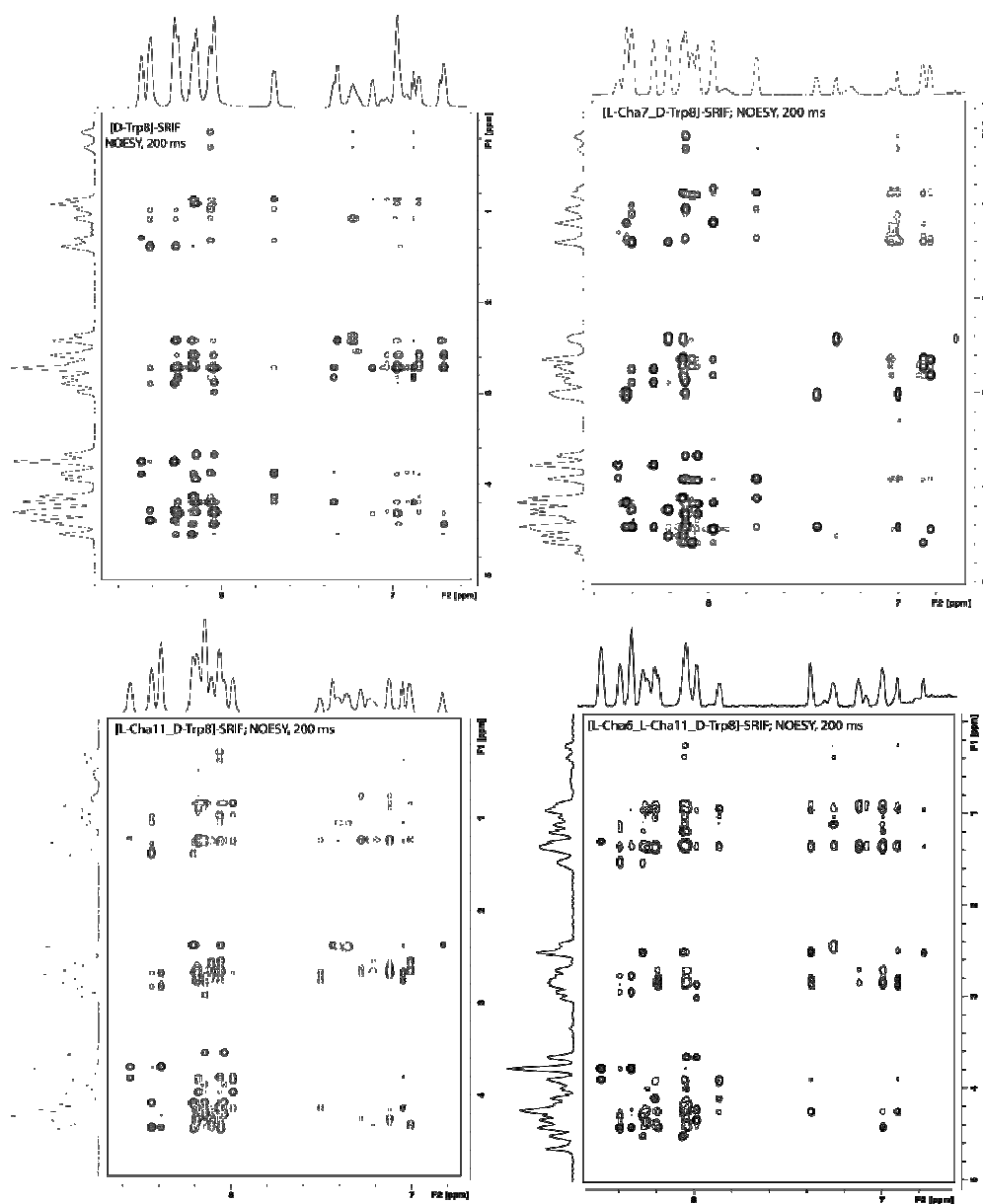


Figure 7.4. NOESY (200 ms) of the aromatic ring-long range interaction region of [D-Trp8]-SRIF, [L-Cha7_D-Trp8]-SRIF (**64**), [L-Cha6,11_D-Trp8]-SRIF (**66**) and [L-Cha11_D-Trp8]-SRIF (**65**).

Some NOE signals arising from proton-proton interactions between *face-to-face* residues were still present, which indicates the preservation of the β -turn. The hairpin is stabilized by a D-Trp8-Lys9 hydrophobic interaction. This is confirmed by the upfield shift γ -protons of Lys9, which are shielded by the aromatic indole ring of the D-Trp8. The upfield shifting of the Lys9 H_γ resonances has been shown to

correlate well with the conformational stability of the pharmacophoric region in SRIF analogs⁵. In this regard, substitution of natural Phe with Cha residues provides peptides in which the Lys9 H_γ protons resonances are not shifted as upfield as they are in the parent compound (Figure 7.5; [L-Msa7,D-Trp8]-SRIF (**49**), a well-known conformationally stable analog, is included for the sake of comparison). These observations indicate that Cha containing SRIF analogs, in which only a Xaa6-Yaa11 hydrophobic interaction is possible, present higher conformational flexibility than the parent compound. Specifically, γ-protons of Lys9 in peptide **63** (containing a Cha in the 6th position) are significantly less downfielded than in the rest of the analogs. This observation is in agreement with the assumption that the electronic properties of the amino acid in position 6 do not play a key role in the conformational stability of SRIF.⁶

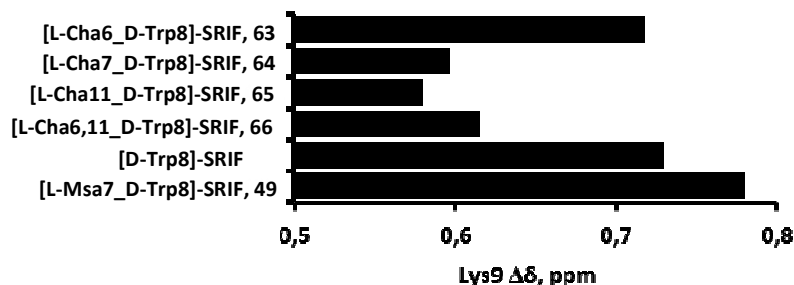


Figure 7.5. Upfield shifting of γ-hydrogens of Lys9 in peptides (**63-66**), in the parent compound and in peptide **49**, relative to that in SRIF. DSS was used as NMR (TOCSY) internal standard.

Many of the NOE contacts that were found between cross-strand residues in peptides **63-66** were associated to the presence of different conformers. In all of the Cha analogs, only few NOEs between the side-chains of residues in positions 6 and 11 (and those residues with 7) were found. These few NOEs account for the high flexibility of the peptidic structure (which lacks a stabilization driven by electronic factors) and also for the mobility of the saturated side-chain of the Cha amino acid.

5 G. Weckbecker, I. Lewis, R. Albert, H. A. Schmid, D. Hoyer, C. Bruns, *Nat Rev Drug Discov* **2003**, 2, 999-1017.

6 B. H. Arison, R. Hirschmann, W. J. Paleveda, S. F. Brady, D. F. Veber, *Biochem. Biophys. Res. Commun.* **1981**, 100, 1148-1153.

Peptides **63-66** do not display a defined main conformation in solution under our NMR experimental conditions. Hence, no attempt was made by us to obtain the 3D structures of these new analogs.

The receptor-subtype selectivity of these new tetradecapeptidic SRIF analogs containing Cha residues was assessed by binding assays. We cultured stable CHO cell lines, each of which expressed one of the five somatostatin subtype receptors. Membrane preparations from these cultures were used to evaluate the efficacy of the interaction with each receptor by competitive binding assays with the ¹²⁵I-labeled SRIF in the presence or absence of various concentrations of unlabeled peptides (Table 7.2).

Table 7.2. Human serum half-life and K_i values (nM) of SRIF, [D-Trp8]-SRIF, octreotide and SRIF analogs to receptors SSTR2, SSTR3 and SSTR5.^a K_i values are mean \pm SEM.

	SSTR2	SSTR3	SSTR5	$t_{1/2}$ (h) ^b
Somatostatin	0.0034 \pm 0.0006	0.14 \pm 0.03	0.072 \pm 0.018	2.75
[D-Trp8]-SRIF	0.0027 \pm 0.0020	0.24 \pm 0.03	0.046 \pm 0.018	19.7
Octreotide	0.029 \pm 0.012	8.4 \pm 1.1	4.2 \pm 0.6	200
[L-Cha6_D-Trp8]-SRIF, 63	0.096 \pm 0.004	4.6 \pm 1.5	6.0 \pm 1.4	10
[L-Cha7_D-Trp8]-SRIF, 64	0.61 \pm 0.09	3.3 \pm 0.5	0.39 \pm 0.02	73
[Cha11_D-Trp8]-SRIF, 65	3.3 \pm 0.3	6.7 \pm 1.6	4.4 \pm 1.3	40
[Cha6,11_D-Trp8]-SRIF, 66	0.71 \pm 0.18	5.4 \pm 1.0	3.3 \pm 0.5	t.b.d.

a: Shaded cells represent data in close proximity to the SRIF values. b: Human serum half-life (see Experimental Section for details). t.b.d.: To be determined.

Binding studies demonstrated that peptides **63-66** displayed no receptor-subtype selectivity, having a universal activity profile similar to those of SRIF and [D-Trp8]-SRIF. However, these peptides were significantly less potent, with K_i values that fluctuate from one or two orders of magnitude (in SSTR3 and SSTR5) to four orders of magnitude higher (in SSTR2). We consider that, even though the hydrophobic factors are relevant –some affinity to the receptors is retained– a simple stabilization through hydrophobic factors is not sufficient to stabilize the bioactive conformations of these analogs, at least not at the same level than the two natural Phe's do it in the parent compound.

Several studies have postulated that analogs with a high conformational rigidity are necessary to be potent against SSTR2.⁵ The low activity of Cha analogs is in agreement with this hypothesis, since they do not have a defined conformation in solution. Interestingly, the introduction of a Cha residue in position 6 led to an analog (**63**) that maintains a modest hairpin stability and displays the highest affinity for SSTR2 (see Figure 7.5 and Table 7.2).⁷ This finding supports the hypothesis that is Phe11 that shields Phe6 in the SSTR2-bioactive conformation.⁶ Our binding data indicate that this particular conformation is more populated in the parent compound (and far more populated in derivatives in which an Ar6-Ar11 interaction is enhanced)⁸ than in the Cha containing analogs. The unique nature of the aromatic interactions between aromatic residues appears to be the source of this selectivity.

The effect of this hydrophobic substitution in peptide **64**, containing a Cha residue in the 7th position, is worthy to be discussed. The NMR data suggest that the conformational flexibility of this peptide is slightly higher than that of [D-Trp8]-SRIF. We have shown that the replacement of Phe7 with highly hydrophobic and electron-rich aromatic amino acids⁸ shifts the conformational equilibrium towards a stable conformation in which its aromatic side-chain lies below the molecule, promoting an interaction between Phe6-Phe11. This observation could explain why the [L-Cha7_D-Trp8]-SRIF analog (**64**) displays a lower affinity for most of the somatostatin receptors, as a highly flexible saturated cyclohexyl side-chain may not be able to fix this singular conformation at the same level than planar aromatic residues do. Interestingly, this peptide retained some affinity to SSTR5 and showed the higher serum stability of this series of compounds.⁷

We did not observe a preference for self-association between aromatic and aliphatic side-chains, since either by NMR or receptor-subtype selectivity studies we cannot conclude that [L-Cha7_D-Trp8] (**64**) or [L-Cha6,11_D-Trp8]-SRIF (**66**) analogs are conformationally more stable than [L-Cha6_D-Trp8]-SRIF (**63**) or [L-Cha11_D-

7 The comparison between the half-life time in human serum of peptide **63** (which is only 10 h) and peptide **64** (70 h) reflects, once again, that conformational and serum stability are not necessarily correlated.

8 See Chapters 3 and 4 (Msa7 and Tmp7 derivatives) and Chapter 8.

Trp8]-SRIF (**65**). These findings would appear to contradict Tatko and Waters' observations.¹ An explanation for this discrepancy is the type of system used: their non-cyclic model peptide contains a highly flexible β -hairpin that locates the two key residues in an isolated site for the study of cross-strand interactions, which allows the quantification of small differences in stability. In our particular case, the presence of a disulfide bond highly contributes to the folding of our analogs, imposing a cross-strand proximity –which minimizes the effect that arises from Cha having a larger β -sheet propensity than Phe–.⁹ In addition, the interaction point is not isolated at all, since it is adjacent both to the β -hairpin and to a remaining aromatic residue (e.g. Phe7), two structural factors that surely interfere in the interaction between residues in the position 6 and 11.

7.3. Conclusions

To give insight into the relative effect of hydrophobic and electronic factors in SRIF, we have studied four analogs in which Phe residues have been replaced by the Cha amino acid.

The NMR data first suggested that peptides containing the Cha residue present a slightly lower conformational rigidity than that of the parent compound. In addition, the greater magnitude of the anisotropic effect for the γ -methylene of Lys9 in [D-Trp8]-SRIF relative to those in the Cha containing analogs indicated that the aliphatic side-chain of Lys9 spends more time in close proximity to the indole ring in [D-Trp8]-SRIF than in peptides **63-66**. This reasoning indicates that the Phe-Phe cross-strand interaction in the parent compound –in which both hydrophobic and electronic factors may contribute– is more favorable than interactions between Cha-Phe, Phe-Cha and Cha-Cha – which may be exclusively driven by a hydrophobic collapse–.

9 D. L. Minor, P. S. Kim, *Nature* **1994**, 367, 660-663.

Whereas the NMR studies gave a picture of the local interactions of the side-chains, we used receptor-subtype selectivity data to obtain a more global perspective. Peptides **63-66** having a reduced affinity to SRIF receptors provides evidence of the less effective stabilization of their bioactive conformations, which are less populated in these analogs than in the rest of compounds that we have studied. Thus, our observations are not consistent with simple burial of surface area between specific side-chains as the main contributor to the conformational stability, since the surface area of residues 6, 7 and 11 are similar in all peptides, concluding that the Ar6-Ar11 residues engage in a specific interaction that is unique to aromatic moieties.

8

[L-Msa7_D-Trp8]- SRIF analogs containing Tmp and Dfp residues

Chapter 8. [L-Msa7_D-Trp8]- SRIF analogs containing Tmp and Dfp residues

8.1. Introduction: Multiple residue substitutions for SSTR2-selectivity	111
8.2. [L-Msa7_D-Trp8]-SRIF analogs containing Tmp and Dfp residues	111
8.2.1. Receptor-subtype selectivity	112
8.2.2. Structure.....	113
8.3. Conclusions.....	118

8.1. Introduction:

Multiple residue substitutions for SSTR2-selectivity

Our previous results suggested that the optimal sequence for a specific biological response may contain a combination of non-natural amino acids in positions 6, 7, 8 and 11. This assumption led us to explore the additive effect of non-natural aromatic amino acids substitutions in SRIF.

In our search for SSTR2-selective analogs, the peptide [L-Msa7_D-Trp8]-SRIF (**49**) was chosen as template. We considered this system as peptide model to gain final insight into the aromatic interactions in SRIF, since the “Msa7 effect” promotes ring association between Ar6-Ar11 residues (see Chapter 3). Our previous results demonstrate that Tmp/Dfp-Phe aromatic interactions adopt preferentially *face-to-face* related geometries. While the electrostatic model maintains that electron-donor substituents weaken stacking interactions, many recent studies showed that both electron-donating and electron-withdrawing substituents stabilize the benzene sandwich dimer.¹ Thus, in order to intensify the Phe6-Phe11 non-covalent interaction, we substituted these cross-strand amino acids by Tmp and/or Dfp residues.

8.2. [L-Msa7_D-Trp8]-SRIF analogs containing Tmp and Dfp residues

We used standard SPPS to obtain three analogs bearing the L-Msa7-D-Trp8 fragment (Table 8.1).² We first synthesized two peptides including a double modification,

1 a) M. O. Sinnokrot, C. D. Sherrill, *J. Phys. Chem. A* **2003**, 107, 8377-8379; b) M. O. Sinnokrot, C. D. Sherrill, *J. Am. Chem. Soc.* **2004**, 126, 7690-7697; c) A. L. Ringer, M. O. Sinnokrot, R. P. Lively, C. D. Sherrill, *Chem.-Eur. J.* **2006**, 12, 3821-3828; d) M. O. Sinnokrot, C. D. Sherrill, *J. Phys. Chem. A* **2006**, 110, 10656-10668; e) S. A. Arnstein, C. D. Sherrill, *Phys. Chem. Chem. Phys.* **2008**, 10, 2646-2655; f) S. E. Wheeler, K. N. Houk, *J. Am. Chem. Soc.* **2008**, 130, 10854-10855; g) A. L. Ringer, C. D. Sherrill, *J. Am. Chem. Soc.* **2009**, 131, 4574-4575; h) M. Watt, L. K. E. Hardebeck, C. C. Kirkpatrick, M. Lewis, *J. Am. Chem. Soc.* **2011**, 133, 3854-3862.

2 Although we also investigated the substitution of Phe6 and Phe11, at the same time, by Dfp and Msa residues while maintaining the natural Phe7 in the sequence, we will not include this group of peptides in the present report.

namely the substitution of Phe6 and Phe11 by Tmp and Dfp residues (peptides **67** and **68**). In a second approach, we replaced both Phe's by Dfp amino acids (compound **69**). The Msa residue was not included in position 6 or 11, since more than one Msa in the SRIF sequence has proved to be unfavorable (see Chapter 3).

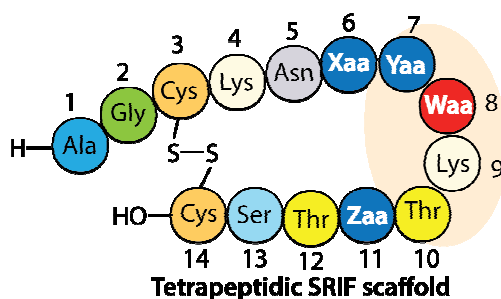


Table 8.1. [L-Msa7_D-Trp8]-somatostatin analogs obtained by replacement of the Phe's in positions 6 and/or 11 by Dfp and Tmp residues.

6 th	7 th	8 th	11 th	Peptidic analog
Dfp	Msa	D-Trp	Tmp	[L-Dfp6_Msa7_Tmp11_D-Trp8]-SRIF, 67
Tmp	Msa	D-Trp	Dfp	[L-Tmp6_Msa7_Dfp11_D-Trp8]-SRIF, 68
Dfp	Msa	D-Trp	Dfp	[L-Dfp6,11_Msa7_D-Trp8]-SRIF, 69

8.2.1. Receptor-subtype selectivity: The SSTR-affinity and selectivity of the new synthetic analogs was measured by competitive radioligand binding assays in CHO (*Chinese hamster ovary*) cell lines. Inhibitor selectivity was determined by means of a competitive assay using ¹²⁵I-labeled SRIF and unlabeled ligands in the SSTR2, SSTR3 and SSTR5 receptors (Table 8.2). Peptides **67** and **69** displayed outstanding potency and selectivity for SSTR2. On the other hand, peptide **68**, the [L-Msa7_D-Trp8]-SRIF analog containing Tmp6 and Dfp11 residues, did not show a high affinity for any of the tested subtype receptors. These affinity values will be discussed below in more detail in parallel with their structures.

Table 8.2. K_i values (nM) of SRIF, [D-Trp8]-SRIF, octreotide and SRIF analogs to receptors SSTR2, 3 and 5. ^a K_i values are mean \pm SEM.			
	SSTR2	SSTR3	SSTR5
Somatostatin	0.0034 \pm 0.0006	0.14 \pm 0.03	0.072 \pm 0.018
[D-Trp8]-SRIF	0.0027 \pm 0.0020	0.24 \pm 0.03	0.046 \pm 0.018
Octreotide	0.029 \pm 0.012	8.4 \pm 1.1	4.2 \pm 0.6
[L-Msa7_D-Trp8]-SRIF, 49	0.0063 \pm 0.0029	7.5 \pm 0.6 ^b	>10 ³ ^b
[L-Dfp6_Msa7_Tmp11_D-Trp8]-SRIF, 67	0.0037 \pm 0.0015	19 \pm 5	11 \pm 2
[L-Tmp6_Msa7_Dfp11_D-Trp8]-SRIF, 68	2.8 \pm 0.9	23 \pm 3	2.5 \pm 1.3
[L-Dfp6,11_Msa7_D-Trp8]-SRIF, 69	0.0021 \pm 0.0006	>10 ²	>10 ²

a: Shaded cells represent data in close proximity to the SRIF values. b: These values were determined by Dr. M. A. Cortes at the University of Alcalá de Henares.

8.2.2. Structure: The NOE patterns of these highly modified SRIF analogs were analyzed in aqueous solution. Spin systems and sequential assignments were obtained from 2D TOCSY and NOESY homonuclear experiments. These peptides displayed a striking conformational rigidity in solution. Clear major sets of NOE peaks were detected, which evidenced the presence of unique major conformations in solution. Most of the key proton-proton interactions that we found in peptides **67-69** were also detected in peptides that highly populate the SSTR2-bioactive conformation. This observation perfectly correlates with the 3D structures of the major conformations of peptides **67-69** (Figures 8.1 to 8.3), which were obtained and characterized using the software Crystallography & NMR System (CNS).

On the basis of the experimental NMR data, the structure of the main conformation in solution of peptide [L-Dfp6_Msa7_Tmp11_D-Trp8]-SRIF (**67**) displayed conformation that we have postulated to be active for SSTR2. The mesityl moiety lies below the molecule, promoting a parallel-displaced Dfp6-Tmp11 aromatic interaction that should greatly contribute to stabilize this specific conformation. The close proximity of the Dfp6 and Tmp11 rings arises from the large number and intense NOE signals among their aromatic protons. The same circumstance is observed for the D-Trp8 and Lys9 residues. The hydrophobic

interaction between their side-chains provides an extra stabilization to this molecule, which proved to be one of the least flexible 14-residue SRIF analogs synthesized to date.

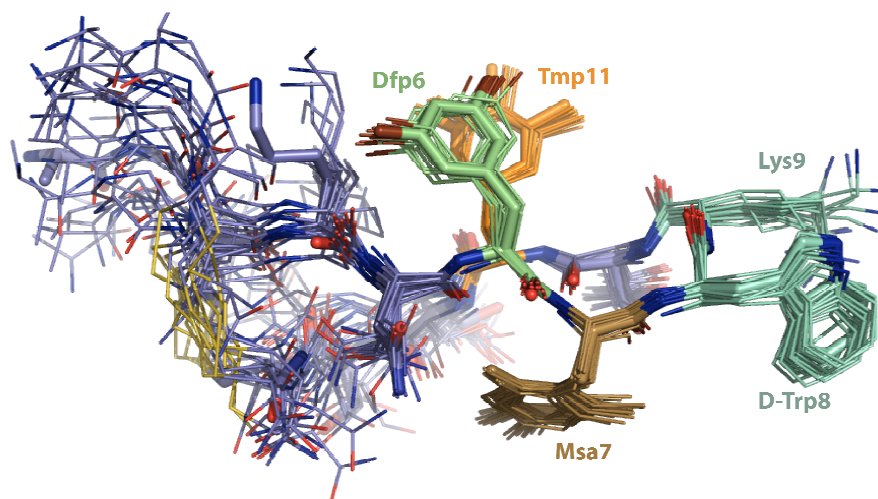


Figure 8.1. Superimposition of the lowest energy conformers of [L-Dfp6_Msa7_Tmp11_D-Trp8]-SRIF (**67**) that best fit the NMR data.

This analog displays a huge SSTR2-potency, with a K_i value similar to that of the natural hormone for this receptor (Table 8.2). Its high rigidity perfectly accounts for its low affinity to SSTR3 and SSTR5, since we have demonstrated that this particular conformation should not be the same than the one that binds to these receptors. Although the NMR data suggest that this peptide is fairly more structured than the parent compound [L-Msa7_D-Trp8]-SRIF (**49**), their K_i values for SSTR2 are quite similar within the error. Thus we consider that, in this specific context, an aromatic interaction between the acceptor aromatic moiety of the Dfp6 and the electron-rich trimethyl-substituted ring of the Tmp11 residue (both of them more hydrophobic than the Phe ring) provides a slightly higher stabilization to the molecule than a Phe6-Phe11 aromatic interaction. However, this mild effect barely affects the SSTR-affinity and -selectivity.

NMR studies proved that peptide [L-Tmp6_Msa7_Dfp11_D-Trp8]-SRIF (**68**) also displayed a high conformational rigidity in solution. However, the 3D structure of its dominant conformer, relatively similar to the postulated SSTR2-active conformation,

does not account for its lack of affinity to this receptor (see Figure 8.2 and Table 8.1, respectively). It is noteworthy that the Msa7 is somehow not able to fix its aromatic ring below the molecule, since the mesityl moiety was found to point away the backbone, probably because of a high steric and/or electronic repulsion with the sequential Tmp6 residue. Despite this fact, on the basis of the NMR data the Tmp6 and Dfp11 side-chains were found to be engaged in a *face-to-face* aromatic interaction. Apart from sequential proton-proton interactions, this arrangement arises from a large number of NOE contacts between the Tmp6 and Dfp11 side-chains, as well as contacts between them with the aliphatic side-chain of Lys4. Some NOEs between Tmp6 and Dfp11 with the Msa7 were also detected. These proton-proton interactions were attributed to secondary scarcely populated conformations different to the defined 3D structure that Msa6 and Tmp6 derivatives adopt. The fact that this analog does not populate that specific conformation is reflected in its lack of affinity for the SSTR3 receptor.

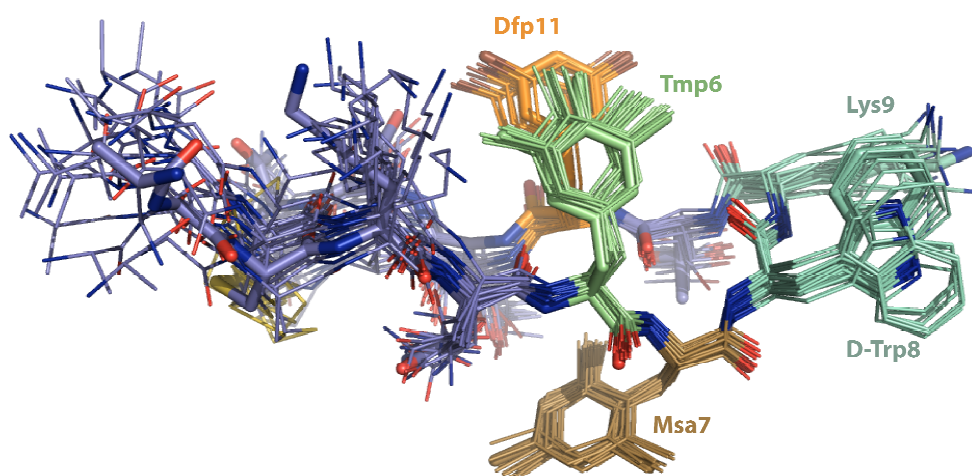


Figure 8.2. The 3D structure of the most stable conformers of [L-Tmp6_Msa7_Dfp11_D-Trp8]-SRIF (**68**) as deduced on the basis of NMR data.

We have reported here several 14-residue SRIF analogs containing bulky and electron-rich aromatic amino acids in position 6 (analogs **45**, **48**, **51**, **52** and **55**). All of these peptides displayed K_i values at least three times higher than that of the natural hormone to the SSTR2 receptor. In these cases, the major conformations in solution

of these peptides proved to be different to the SSTR2-bioactive conformation, and their lack of SSTR2-affinity had been so far associated to these structural differences.

The finding that this highly structured analog (**68**) does not bind to SSTR2 may be explained in terms of direct interaction with the receptor. We already suggested that the mesityl moiety may not only play the structural role of bringing the Ar6-Ar11 aromatic rings close, but it may be actively involved in the binding to the SSTR2 when it is lying below the molecular plane.³ The assumption that the Msa7 (or Tmp7) is actively involved in the binding to the receptor⁴ would explain the high SSTR2-affinity of the linear [Ala3,14_Msa7_D-Trp8] (**58**) and [Phe3,14_Msa7_D-Trp8]-SRIF (**59**) analogs. Although these peptides display a high conformational flexibility, the Msa7 seemed to be able to locate its aromatic moiety in that particular disposition to interact with the receptor, which would result in a high SSTR2-potency. The finding that the [L-Dfp7_D-Trp8]-SRIF analog (**61**, Chapter 6) does not bind to SSTR2 suggests that Ar7 is involved in a direct interaction with this receptor via its π -donor capability. In the context of the [L-Tmp6_Msa7_Dfp11_D-Trp8]-SRIF analog (**68**), the Msa7 is thrown away from the center of the molecule by repulsions with the adjacent Tmp6 residue (which is strongly fixed because of the stable Tmp6-Dfp11 aromatic interaction). Thus, the mesityl moiety is not able to be located below the molecule and consequently does not interact efficiently with the SSTR2 receptor.

We determined the half-life time of this highly modified analog in human serum. Peptide [L-Tmp6_Msa7_Dfp11_D-Trp8]-SRIF (**68**) displayed impressive serum stability (86 h), which is far higher than that of the natural hormone (2.75 h). This compound has the highest half-life of all our synthetic 14-residue SRIF analogs.⁵ This extraordinary serum stability probably arises both from the four non-natural residues that are included in the sequence and from the high conformational rigidity displayed by this peptide.

3 See Chapter 5.

4 The Msa or Tmp residues in position 7 may interact better with the receptor than the natural Phe in different SRIF-analogs via their improved π -donor capability and/or their higher size and hydrophobicity.

5 The half-life time of the rest of analogs is currently being determined.

At this point we considered that Tmp-Dfp aromatic interactions provide an efficient stabilization the peptidic architecture of 14-residue SRIF analogs: The [L-Dfp6_Msa7_Tmp11_D-Trp8]-SRIF analog (**67**), containing Dfp6 and Tmp11, proved to be modestly more structured than the parent compound, and in the [L-Tmp6_Msa7_Dfp11_D-Trp8]-SRIF analog (**68**) the Tmp6-Dfp11 aromatic interaction seemed to overwhelm the Msa7 effect.

Moving one step further, we substituted the two natural Phe6 and Phe11 by Dfp residues in the [L-Msa7_D-Trp8]-SRIF scaffold.⁶ As usually, spin system and sequential assignments for the [L-Dfp6,11_Msa7 _D-Trp8]-SRIF analog (**69**) were obtained from 2D TOCSY and NOESY homonuclear experiments. On the basis of the NMR data, this peptide showed a remarkable conformational rigidity, with most of the side-chains displaying no promiscuity whatsoever. With such a well-defined NOESY spectrum in hand, we used the software Crystallography & NMR System (CNS) to characterize the 3D structure of this analog, which proved to be similar to the postulated SSTR2-bioactive conformation of SRIF. Receptor-subtype selectivity assays demonstrated that this highly rigid analog displayed the best SSTR2-directed biological profile that we have ever found (Table 8.2).

In this analog, the two “small” Dfp residues in position 6 and 11 are associated in a *face-to-face* aromatic interaction that allows the Msa7 to locate its aromatic side-chain below the molecule, strongly fixing this particular conformation. We were unable to accurately refine the arrangement of the Dfp6-Dfp11 aromatic rings, due to the missing structural NMR information that arises from the substitution of four hydrogens by fluorine atoms. However, we found that a *face-to-face* aromatic interaction in which the fluorine region of the Dfp6 points away of the fluorine region of the Dfp11 best matched the NMR data.⁷ That the interaction between these more hydrophobic and electron-poor aromatic rings provides more

⁶ Double Tmp substitution was not considered because of the expected steric or electronic congestion

⁷ It appears that in this specific arrangement, both side-chains are located in such a way that the C-F bonds of one ring overlap a C-H bond of the other. This disposition would be in a perfect agreement with the local, direct interaction model reported by Wheeler. See: S. E. Wheeler, *J. Am. Chem. Soc.* **2011**, *133*, 10262-10274.

stabilization than the Phe6-Phe11 interaction that is present in the parent compound is in agreement with the electrostatic⁸ and the polar/ π model⁹: electron-withdrawing substituents enhance the π -stacking interactions because they decrease the aryl π -electron density, thus making minimum the repulsion between two electron-poor rings.

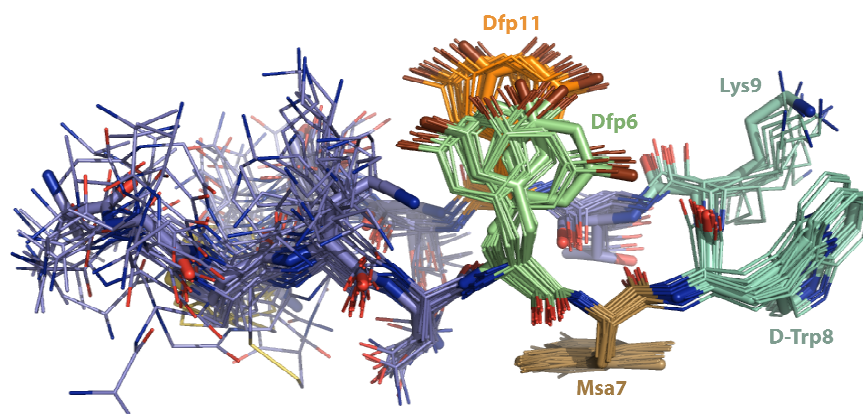


Figure 8.3. Superimposition of the minimum-energy conformers of [L-Dfp6,11_Msa7_D-Trp8]-SRIF (**69**) as calculated on the basis of the NMR data.

8.3. Conclusions

The syntheses, structural studies and receptor-subtype selectivity of a battery of [L-Msa7_D-Trp8]-SRIF analogs allowed us to further demonstrate the applicability of the L-Msa7-DTrp8 motif to obtain SSTR2-active and selective SRIF analogs.

In particular, the incorporation of Dfp residues in position 6 and 11, allowed us to obtain the peptide [L-Dfp6,11_Msa7_D-Trp8]-SRIF (**69**), a SRIF analog with remarkably high affinity and selectivity to the SSTR2 receptor.

Although less selective than peptide **69**, the [L-Dfp6_Msa7_Tmp11_D-Trp8]-SRIF (**67**) analog proved to have a similar 3D conformation and SSTR2-affinity. On the

8 a) C. A. Hunter, K. R. Lawson, J. Perkins, C. J. Urch, *J. Chem. Soc., Perkin Trans. 2* **2001**, 0, 651-669; b) S. L. Cockroft, J. Perkins, C. Zonta, H. Adams, S. E. Spey, C. M. R. Low, J. G. Vinter, K. R. Lawson, C. J. Urch, C. A. Hunter, *Org. Biomol. Chem.* **2007**, 5, 1062-1080.

9 a) F. Cozzi, M. Cinquini, R. Annunziata, J. S. Siegel, *J. Am. Chem. Soc.* **1993**, 115, 5330-5331; b) F. Cozzi, F. Ponzini, R. Annunziata, M. Cinquini, J. S. Siegel, *Angew. Chem., Int. Ed.* **1995**, 34, 1019-1020.

other hand, peptide [L-Tmp6_Msa7_Dfp11_D-Trp8]-SRIF, (**68**), displayed a K_i value three orders of magnitude higher than **67** and **69** for SSTR2. This observation allowed us to further demonstrate that 14-residue SRIF analogs bearing bulky and electron-rich aromatic residues in position 6 do not bind to the SSTR2 receptor, regardless of whether additional non-natural residues are present in the sequence or not. When the electron-poor Dfp and the π -cloud free Cha amino acids were included in position 6, the correspondent SRIF analogs did retain the SSTR2 affinity.¹⁰ The very low SSTR2-affinity of **68**, together with some structural features, led us to consider that the amino acid in position 7 plays a role by direct union to the SSTR2 receptor when it is located lying below the molecule.

In addition, the finding that the [L-Tmp6_Msa7_Dfp11_D-Trp8]-SRIF (**68**) analog is 30 times more stable in serum than the natural hormone is very encouraging. Although the half-life times of the rest of analogs remains to be determined, we expect that analogs **67** and **69** will show similar serum stability. In this case, the potential therapeutic utility of these peptides could compete with the SSTR2-selective marketed drugs, since **67** and **69** are more active and selective to SSTR2 than octreotide.

¹⁰ The K_i value (SSTR2) of peptides containing non-natural residues in position 6 are summarized here: [L-Msa6] (**45**) $K_i = 1.5$ nM, [L-Msa6_D-Trp8] (**48**) $K_i = 4.6$ nM; [L-Tmp6_D-Trp8] (**55**) $K_i = 1.3$ nM; [L-Tmp6_Msa7_Dfp11_D-Trp8]-SRIF, (**68**) $K_i = 2.8$ nM; [L-Msa6_Dfp11_D-Trp8] ($K_i = 283$ nM; this compound has not been included in this report); [L-Dfp6_D-Trp8] (**60**) $K_i = 0.040$ nM; [L-Cha6_D-Trp8] (**63**) $K_i = 0.096$ nM.

9

Global conclusions

We have synthesized and studied 24 SRIF-analogs containing aromatic non-natural amino acids as site-directed modifications. The gram-scale syntheses of these amino acids (3-mesitylalanine (Msa), 3-(3',4',5'-trimethylphenyl)-alanine (Tmp) and 3-(3',5'-difluorophenyl)-alanine (Dfp)) were achieved by different routes, using a Rhodium-Catalyzed Asymmetric Hydrogenation reaction as source of enantioselectivity. These non-natural residues displayed specific hydrophobic, electronic and steric properties. The introduction of Msa, Tmp and Dfp residues in the tetradecapeptidic SRIF scaffold allowed us to prove and modulate the non-covalent interactions between the aromatic residues in the natural hormone somatostatin.

Several of these SRIF-analogs showed a high conformational rigidity relative to that of SRIF, which allowed us to characterize the 3D structures of their major conformations in solution using NMR and computational techniques. These investigations allowed us to prove that bulky, hydrophobic and electron-rich residues (*i.e.* Msa or Tmp) in position 7 shifts the conformational equilibrium in solution toward a major conformation that should be very similar to that of SRIF when it binds to the SST2 receptor. We considered that an aromatic interaction between the Ar6-Ar11 residues is the factor that contributes the most to stabilize this particular conformation. In this regard, we have used the L-Msa7_D-Trp8 fragment to fine-tune the Ar6-Ar11 interaction, thus developing several highly SSTR2-active and -selective 14-residue SRIF analogs. The introduction of Dfp residues allowed us to prove that this electron-poor aromatic amino acid in position 11 engage an aromatic interaction with the cross-strand Phe6 (peptide **62**). Our studies involving SRIF analogs containing the Cha amino acid indicated that the specific interaction between aromatic residues that contributes to the conformational stabilization in SRIF is unique to aromatic moieties, and is not exclusively driven by a hydrophobic collapse.

Our studies, initially devoted to prove the postulated Phe6-Phe11 interaction in somatostatin, have led us to gain invaluable and unprecedented insight into structure-activity relationships of somatostatin and SRIF analogs. Looking ahead, despite we have been able to exploit specific aromatic interactions to obtain directed SSTR-selectivity, there is still much that we do not yet understand regarding

the nature of these non-covalent interactions. Our combination of NMR and computational techniques in the study of 14-residue SRIF analogs has provided a powerful tool to fill this gap. Taking into account the wide distribution of SSTR2 and its role in SRIF-regulated processes, the therapeutic potential of SRIF analogs that bind exclusively to this receptor continue to be of high importance. Our highly potent and selective peptides **67** and **69**, which presumably show an appropriate persistence (half-life) in blood, would certainly present a potential alternative to the currently marketed drugs. The success in future design of 14-residue SRIF analogs will rely on the right modifications of its sequence based on the structural information obtained from our studies.

10

Experimental section

Chapter 10. Experimental section

10.1. Experimental section for the synthesis of amino acids	
10.1.1. General methods and instrumentation	127
10.1.2. Compounds from the HWE olefination	128
10.1.3. Compounds from the Heck reaction	132
10.1.4. Compounds from the azlactone route	133
10.1.5. Compounds from the Perkin reaction	134
10.1.6. Rh-Catalyzed Asymmetric Hydrogenations	135
10.1.7. Compounds obtained after hydrolysis	139
10.1.8. Compounds subjected to Fmoc-protection	140
10.2. Experimental section for the synthesis of SRIF analogs	
10.2.1. General methods and instrumentation	143
10.2.2. General considerations for the SPPS	145
10.2.3. General methods for the synthesis of SRIF analogs	146
10.2.4. 14-Residue SRIF analogs (in order of appearance)	147
10.3. Computational methods	153
10.4. Receptor-subtype selectivity assays	153
10.5. Serum stability assays	155

The attached CD contains:

Appendix I: ¹H-NMR Spectra of the final Fmoc-protected amino acids.

Appendix II: Full characterization of SRIF analogs.

TOCSY and NOESY spectra of SRIF, [D-Trp8]-SRIF and SRIF analogs.

Structural statistics from the computational calculations.

9.1. Experimental section for the synthesis of amino acids

9.1.1. General methods and instrumentation:

All reactions were carried out under nitrogen atmosphere unless otherwise specified. When dry solvents were necessary (dichloromethane, diethyl ether and tetrahydrofuran), the Innovative Technology Inc. Puresolv purification system Solvent Purification System (SPS) were used. Other dry solvents were purchased from Sigma-Aldrich and used without further purification.

All experiments were monitored by analytical thin layer chromatography (TLC) performed on silica gel TLC-aluminum sheets (Merck 60 F₂₅₄). Chromatographic purifications were carried out using a Combiflash® (Teledyne Isco) automated chromatography system unless otherwise stated. Silica gel RediHep® columns were used. The elution was carried out using hexanes/EtOAc gradients.

NMR spectra were recorded at room temperature on a Varian Mercury 400, Varian Unity 300 or Bruker 250 apparatus. ¹H NMR and ¹³C NMR spectra were referenced to residual solvent peaks. ¹⁹F NMR spectra were referenced by the spectrometer without external reference. Signal multiplicities in the ¹³C spectra have been assigned by DEPT (Direct Enhancement by Polarization Transfer) and HSQC (Hetero-nuclear Single Quantum Correlation) experiments and are described as C (quaternary), CH (tertiary), CH₂ (secondary) and CH₃ (primary). The following abbreviations were used to define the multiplicities: s, singlet; d, doublet; t, triplet; q, quartet; m, multiplet; br, broad. The coupling constants (*J*) are measured in hertz (Hz).

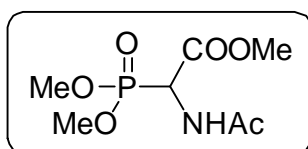
Melting points were measured using DSC 822e Mettler-Toledo apparatus. HRMS experiments were carried out in The Mass Spectrometry Core Facility located in the Institute for Research in Biomedicine of the using NanoESI techniques. CHNS elemental analyses have all been determined by the *Unitat de Tècnics Separatives i Síntesi de Pèptids* (The Separation Techniques and Peptide Synthesis Unit) located at the Barcelona Science Park. All IR spectrums have been obtained using a Thermo Nicolet Nexus FT-IR Fourier transform spectrometer. The samples were prepared by

either dissolution in solvent and subsequent formation of a film on a NaCl disc by evaporation of the prepared solution or by the preparation of a KBr disc.

The values of optical rotation ($[\alpha]_D$) have been determined using a Perkin-Elmer polarimeter 241 at 25 °C. A cell with a length of 1 dm and a volume of 1 mL has been used. The concentration is expressed in the form g/100 mL. A sodium lamp with a wavelength of 589 nm has been employed.

9.1.2. Compounds from the Horner-Wadsworth-Emmons olefination:

Methyl 2-acetamido-2-(dimethoxyphosphoryl)acetate, 15

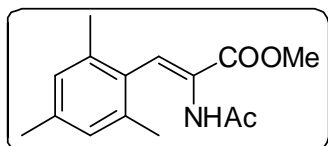


In a 500 mL hydrogenation reactor, 33.46 g (101.1 mmol) of methyl-2-(benzyloxycarbonylamino)-2-(dimethoxyphosphoryl) acetate were dissolved in MeOH (286 mL). Then, 1.67 g of Pd/C (5%) and 25.8 mL of acetic anhydride were added. The reactor was purged with N₂ and H₂ and finally charged with 3 bar of hydrogen. After 4 h, the mixture was filtered over Celite® and concentrated in vacuum to afford 23.60 g of a white solid (97% yield) that showed spectroscopic data identical with the literature.¹

¹H-NMR (400 MHz, CDCl₃): δ 6.71 (s, 1H), 5.23 (dd, 1H, J= 10 and 22 Hz), 3.81 (t, 9H, J= 10 and 12 Hz), 2.06 (s, 3H) ppm.

¹³C-NMR (100 MHz, CDCl₃): δ 170.0 (CO), 167.4 (CO), 54.5 (CH), 53.5 (CH₃), 50.9 (CH₃), 49.5 (CH₃), 23.0 (CH₃) ppm.

(Z)-Methyl 2-acetamido-3-mesitylacrylate, 18



DBU (4.8 mL, 31.5 mmol) was added dropwise to a solution of methyl 2-acetamido-2-(dimethoxyphosphoryl) acetate (7.4 g, 31.0 mmol) in DCM (8 mL). After 30 min of stirring at room temperature, a solution of mesitylaldehyde (2.6 g, 17.6 mmol) in DCM (4 mL) was added. After 3 h of stirring at

¹ U. Schmidt, A. Lieberknecht, J. Wild, *Synthesis* **1984**, 53-60.

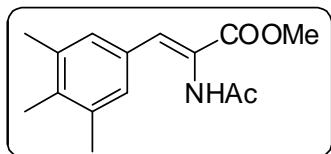
room temperature, the reaction was complete. The solvent was removed at reduced pressure and the residue was diluted with AcOEt (50 mL). The organic layer was washed with 1 M HCl and brine, and then dried and evaporated. The crude product was purified by chromatography with hexanes/AcOEt mixtures to afford 2.6 g of **18** (57% yield) as a white solid. The spectroscopic data of this product was identical to data previously reported in the literature.²

Mp: 165-166 °C.

¹H-NMR (400 MHz, CDCl₃): δ 7.13 (s, 1H), 6.89 (s, 2H), 6.57 (s, 1H), 3.87 (s, 3H), 2.28 (s, 3H), 2.17 (s, 6H), 1.95 (s, 3H) ppm.

¹³C-NMR (100 MHz, CDCl₃): δ 168.2 (NHCO), 164.9 (-CO), 137.7 (C, Ar), 135.9 (2 C, Ar), 129.2 (C, Ar), 128.6 (CH, CHβ), 128.4 (2 CH, Ar), 128.2 (C, Cα), 52.5 (CH₃, OCH₃), 22.8 (CH₃, C(O)CH₃), 20.9 (CH₃, CH₃(Ar)), 20.0 (2CH₃, CH₃(Ar)) ppm.

(Z)-Methyl 2-acetamido-3-(3',4',5'-trimethylphenyl)acrylate, 19



DBU (6.6 mL, 43.2 mmol) was added drop-wise to a solution of methyl 2-acetamido-2-(dimethoxyphosphoryl) acetate (10.1 g, 42.3 mmol) in DCM (8 mL). After 30 min of stirring at room temperature, a solution of 3,4,5-trimethylbenzaldehyde (3.5 g, 23.6 mmol) in DCM (4 mL) was added. After 3 h of stirring at room temperature, the reaction was complete. The solvent was removed at reduced pressure and the residue was diluted with AcOEt (50 mL). The organic layer was washed with 1 M HCl and brine, and then dried and evaporated. The crude product was purified by chromatography with hexanes/AcOEt mixtures to afford 5.24 g of **19** (85% yield) as a white solid.

Mp: 176-178 °C.

IR (KBr): ν_{\max} 3217(b), 2977, 1713, 1657 cm⁻¹.

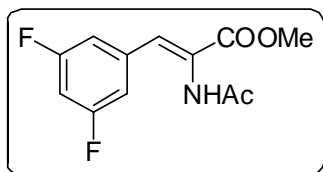
2 T. Li, Y. Tsuda, K. Minoura, Y. In, T. Ishida, L. H. Lazarus, Y. Okada, *Chem. Pharm. Bull. (Tokyo)* **2006**, *54*, 873-877.

¹H-NMR (400 MHz, CDCl₃): δ 7.33 (s, 1H, CHβ), 7.12 (s, 2H, 2 CH Ar), 6.9 (s, 1H, NH) 3.84 (s, 3H, OCH₃), 2.27 (s, 6H, 2CH₃), 2.18 (s, 3H, CH₃), 2.15 (s, 3H, C(O)CH₃).

¹³C-NMR (100 MHz, CDCl₃): δ 168.9 (C, NHCO), 166.1 (C, -CO), 137.6 (C, Ar), 136.9 (C, Ar), 133.3 (CH, Cβ), 130.8 (C, Ar), 129.2 (2 CH, Ar), 123.5 (C, Cα), 52.8 (CH₃, -OCH₃), 23.6 (CH₃, C(O)-CH₃), 20.9 (2 CH₃, Ar), 15.8 (CH₃, Ar).

HRMS: calcd. for C₁₅H₁₉NO₃: 261.136; (M+H)⁺ found, 262.143.

(Z)-Methyl 2-acetamido-3-(3',5'-difluorophenyl)acrylate, **20**



DBU (6.6 mL, 43.2 mmol) was added drop-wise to a solution of methyl 2-acetamido-2-(dimethoxyphosphoryl) acetate (10.1 g, 42.3 mmol) in DCM (8 mL). After 30 min stirring at room temperature, a solution of 3,4,5-trimethylbenzaldehyde (3.5 g, 23.6 mmol) in DCM (4 mL) was added. The reaction was complete after 3 h of stirring at room temperature. The solvent was removed at reduced pressure and the residue was diluted with AcOEt (50 mL). The organic layer was washed with 1 M HCl and brine, and then dried and evaporated. The crude product was purified by chromatography with hexanes/AcOEt mixtures to afford 5.24 g of **20** (85% yield) as a white solid.

Mp: 176-178 °C.

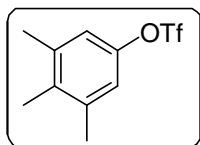
IR (KBr): ν_{\max} 3261(b), 1719, 1663, 1284 cm⁻¹.

¹H-NMR (400 MHz, CDCl₃): δ 7.28 (s, 1H, CHβ), 7.09 (s, 1H, NH), 6.96 (d, J = 5 Hz, 2H, Ar), 6.77 (t, J = 9 Hz, 1H, Ar), 3.87 (s, 3H, -OCH₃), 2.15 (s, 3H, -C(O)CH₃) ppm.

¹³C-NMR (100 MHz, CDCl₃): δ 168.4 (C, CO), 165.2 (C, CO), 162.8 ((dd, J_F = 248, 13 Hz) 2 CH, CHε Ar), 137.1 ((t, J_F = 9 Hz), C, Ar), 128.9 (CH, Cβ), 125.5 (C, Cα), 110.1 (m, 2 CH, Cδ Ar), 104.5 ((t, J_F = 25 Hz), CH, Cz Ar), 53.0 (CH₃, MeO), 23.5 (CH₃, Ac) ppm.

¹⁹F-NMR (376 MHz, CDCl₃): δ -110.6 (t, J = 8, 2F).

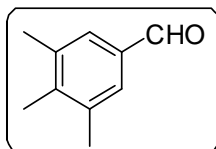
HRMS: calcd. for C₁₂H₁₁F₂NO₃: 255.071; (M+H)⁺ found, 256.078.

3,4,5-Trimethylphenyl trifluoromethanesulfonate, 13

To a mixture of 3,4,5-trimethylphenol (4,0 g, mmol) and Et₃N (9.1 mL, 90 mmol) in CH₂Cl₂ (50 mL) at -15 °C is added a solution of triflic anhydride (12,7 mL, 45 mmol) in CH₂Cl₂ (20 mL) in a dry single-neck round-bottom flask under a nitrogen atmosphere. After the reaction is complete, the mixture is diluted with CH₂Cl₂ and washed with sat. NHCO₃ and brine. The organic layer is dried and the solvent is evaporated. The residue is purified by column chromatography on a short column to provide 7.2 g (90% yield) of the aryl triflate as a colorless oil. The spectroscopic data of this product was identical to data previously reported in the literature.³

¹H-NMR (400 MHz, CDCl₃): δ 6.90 (s, 2H, Ar), 2.30 (s, 6H, CH₃), 2.16 (s, 3H, CH₃).

¹⁹F-NMR (376 MHz, CDCl₃): δ -73.8 (s, 3F).

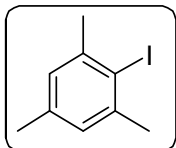
3,4,5-Trimethylbenzaldehyde, 11

In a high-pressure reactor vessel, a mixture of the triflate (1 mmol), Pd(OAc)₂ (4% mmol), dppe (6% mmol) and LiCl (1 mmol) in DMF (5 mL) was purged with nitrogen, charged with CO (3 bar) and heated to 65 °C over 20-25 min. At this time, Et₃N (2,5 mmol) is added drop-wise via pressure syringe followed by addition of silane (2.0 mmol) during 20 minutes. Stirring continued overnight at the same temperature. After dilution with water, the mixture was extracted with Et₂O. The combined extracts were washed with H₂O, sat. NaHCO₃ and brine. The mixture was dried with Na₂SO₄, and evaporated. The crude product was purified by column chromatography to give the desired aldehyde, whit spectroscopic data was identical to previously reported values in the literature.⁴

¹H-NMR (400 MHz, CDCl₃): δ 9.90 (s, 1H, CHO), 7.51 (s, 2H, Ar), 2.36 (s, 6H, 2 CH₃), 2.25 (s, 3H, CH₃).

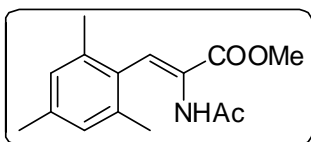
3 T. F. Walsh, R. B. Toupence, F. Ujjainwalla, J. R. Young, M. T. Goulet, *Tetrahedron* **2001**, *57*, 5233-5241.

4 A. Fischer, D. R. A. Leonard, *Can. J. Chem.* **1976**, *54*, 1795-806.

9.1.3. Compounds from the Heck reaction:**2,4,6-trimethyliodobenzene, 22**

To a suspension of 2,4,6-trimethylaniline (14.9 g, 110 mmol), in conc. HCl (50 mL) and 30 g of ice, a solution of NaNO₂ (7.95 g, 115 mmol) in H₂O (35 mL) was added dropwise over 30 min at 0 to 5 °C. The solution was stirred for another 30 min at the same temperature. Then, a solution of KI (24.9 g, 150 mmol) in H₂O (35 mL) was added dropwise over 20 min at 0 to 5 °C. The reaction mixture was allowed to warm to room temperature and the red colored solution was stirred for 18 h. The mixture was extracted with ethyl acetate (AcOEt, 3 x 100 mL). The combined extracts were washed with 15% sodium thiosulfate solution (2 x 80 mL), brine solution and dried over MgSO₄. After removal of MgSO₄, the solvent was removed under vacuum. The colored residue was purified by silica gel flash chromatography to give pure 17.6 g of 2,4,6-trimethyliodobenzene (65% yield) as a colorless oil. The spectroscopic data of this product was identical to data previously reported in the literature.²

¹H-NMR (400 MHz, CDCl₃): δ 6.88 (s, 2H, Ar), 2.43 (s, 6H, 2 CH₃), 2.23 (s, 3H, CH₃).

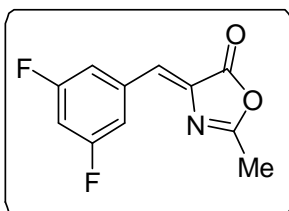
(Z)-Methyl 2-acetamido-3-mesitylacrylate, 18

A mixture of 2,4,6-trimethyliodobenzene (8.6 g, 34.9 mmol), methyl-2-acetamidoacrylate (5.0 g, 34.9 mmol), tri-*o*-tolylphosphine (0.56 g, 1.85 mmol), triethylamine (10.0 mL, 69.9 mmol) and Pd(OAc)₂ (0.15 g, 0.65 mmol) in CH₃CN (50 mL) was subjected to reflux conditions for 10 h. The mixture was cooled to room temperature and filtered. The solvent was removed *in vacuo* and the residue was diluted with water (50 mL). The aqueous phase was extracted with AcOEt (3 x 100 mL). The combined organic phase was washed with saturated NaCl solution (3 x 50 mL) and dried (Na₂SO₄). The mixture was concentrated to about 60 mL. To this solution, hexane (50 mL) was added. The crystals appeared were collected by filtration and dried *in vacuo* to yield 4.83 g (53%) of the titled compound. Extra product (2.5 g, 27% yield) was obtained by purification of the filtrate by flash chromatography (SiO₂,

hexanes/AcOEt (2:1)). The spectroscopic data of this product has been shown previously in this chapter.

9.1.4. Compounds from the Azlactone route:

(Z)-4-(3',5'-Difluorobenzylidene)-2-methyloxazol-5(4H)-one, 26



To a two-neck 100-mL round-bottom flask fitted with a mechanical stirrer and a condenser, under N₂ atmosphere, was added N-acetylglycine (8.2 g, 70 mmol), Ac₂O (18 mL, 175 mmol), NaOAc (5.8 g, 70 mmol) and 3,5-difluorobenzaldehyde (10 g, 70 mmol). The mixture was stirred for 2 h at 100 °C to provide a light brown solution. The crude was allowed to cool to room temperature and a stirrable paste was formed. Then, it was cooled to 0 °C and cold water (60 mL) was added. The mixture was stirred 10 min. Filtration, washing the collected solid with cold water (3 x 15 mL) and drying at 50 °C in vacuo provided 14.1 g (90% yield) of the titled compound as a light brown powder, which was used in the next reaction without further purification.

Mp: 155-158 °C.

IR (KBr): ν_{\max} 3051, 1800, 1665 cm⁻¹.

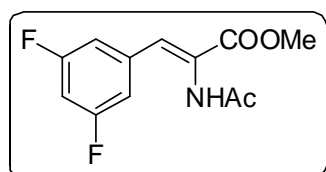
¹H-NMR (400 MHz, CDCl₃): δ 7.6 (m, 2H, Ar), 7.0 (s, 1H, CH), 6.9 ((tt, J = 9 and 2 Hz, 1H), 1H, Ar), 2.4 (s, 3H, CH₃) ppm.

¹³C-RMN (100 MHz, CDCl₃): δ 167.6 (C, CO), 167.0 (C, Az), 162.9 (dd, J_F = 249, 13 Hz, 2 C, C ϵ Ar), 135.8 (t, J_F = 10 Hz, C, Ar), 134.6 (C, Az), 128.1 (t, J_F = 3 Hz, CH, C β), 114.5 (m, 2 CH, C δ Ar), 106.7 (t, J_F = 26 Hz, CH, C ζ Ar), 15.7 (CH₃) ppm.

¹⁹F-NMR (376 MHz, CDCl₃): δ -108.4 (t, J = 7, 2F).

HRMS: calcd. for C₁₁H₇F₂NO₂: 223.0445; (M+H)⁺ found, 224.0519.

(Z)-Methyl 2-acetamido-3-(3',5'-difluorophenyl)acrylate, 20

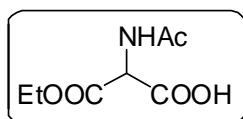


(Z)-4-(3',5'-Difluorobenzylidene)-2-methyloxazol-5(4H)-one (10 g, 45 mmol, 1 eq) was dissolved in anhydrous MeOH (133 mL) in a two-neck 250-mL round-bottom

flask fitted with a mechanical stirrer and a condenser, and under N₂ atmosphere. MeONa (3.8 g, 49 mmol, 1.1 eq) was added dropwise, and the reaction mixture was stirred for 2 h at 70 °C. The crude was allowed to cool to room temperature and the solvent was evaporated under reduced pressure. The crude mixture was redissolved, neutralized with HCl and extracted with AcOEt. The combined extracts were washed with brine solution and dried over MgSO₄. After filtration of MgSO₄, the solvent was removed under vacuum and the brown colored residue was purified by silica gel flash chromatography to give pure 6.9 g (27 mmol, 65 % yield) of the titled product as a white solid. The spectroscopic data of this product has been shown previously in this chapter.

9.1.5. Compounds from the Perkin reaction:

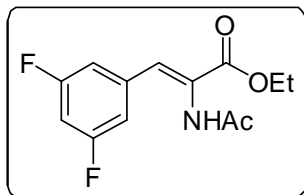
2-Acetamido-3-ethoxy-3-oxopropanoic acid, 28



To a stirred solution of diethyl 2-acetamidomalonate (10 g, 46 mmol) in dioxane (60 mL) was added aqueous sodium hydroxide (1 M, 46.5 mL, 1.01 eq.) dropwise over 2 h. The resulting mixture was stirred at room temperature for 15 h, then dioxane was evaporated under reduced pressure, the aqueous solution was washed with three portions of 300 mL of EtOAc and filtered. The filtrate was cooled down to 0 °C and acidified to pH 1 with concentrated HCl. After the appearance of a few crystals, the mixture was sonicated and an abundant precipitate appeared. Filtration and drying under reduced pressure afforded the titled compound **28**, (6.9 g, 80% yield) as a white solid. The spectroscopic data of this product was identical to data previously reported in the literature.⁵

¹H-NMR (400 MHz, DMSO): δ: 8.63 (d, J = 7 Hz, 1H, NH), 4.95 (d, J = 7 Hz, 1H, CH α), 4.13 (q, J = 7 Hz, 2H, CH₂), 2.43 (s, 3H, CH₃), 1.89 (s, 3H, Ac), 1.18 (t, J = 7 Hz, 3H, CH₃) ppm.

5 A. Faucher, M. D. Bailey, P. L. Beaulieu, C. Brochu, J. Duceppe, J. Ferland, E. Ghiron, V. Gorys, T. Halmos, S. H. Kawai, M. Poirier, B. Simoneau, Y. S. Tsantrizos, M. Llinàs-Brunet, *Org. Lett.* **2004**, *6*, 2901-2904.

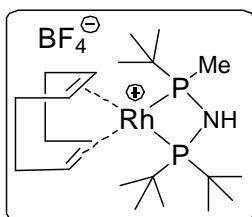
(Z)-Ethyl 2-acetamido-3-(3',5'-difluorophenyl)acrylate, 30

To solid ethyl 2-acetamido-3-ethoxy-3-oxopropanoic acid (378 mg, 2 mmol.) was added 3,5-difluorobenzaldehyde **6** (224 mg, 1.58 mmol) in solution in pyridine (2 mL) The resulting solution was cooled in a 15 °C bath and acetic anhydride (0.6 mL) was added over 12 min. The resulting orange solution was stirred for 3 h at RT and another portion of ethyl 2-acetamido-3-ethoxy-3-oxopropanoic acid (189 mg) was added. The resulting mixture was stirred at room temperature for an extra 15 h. Ice (8 mL) was then added and the solution was stirred for 1.5 h, then the mixture was diluted with 18 mL of water and extracted with two portions (10 mL) of ether. The ethereal solution was washed with 1N HCl, sat. NaHCO₃ and brine, dried with Na₂SO₄, concentrated to afford an orange oil that was purified by flash chromatography (hexanes/EtOAc) to give pure **30** (353 mg, 83% yield) as a white solid.

Mp: 174-178 °C.

IR (KBr): ν_{\max} 3246(b), 1719, 1662 cm⁻¹.

¹H-NMR (400 MHz, CDCl₃): δ 7.27 (s, 1H, CH), 6.96 (d, J = 6 Hz, 2H, CH Ar), 6.76 (t, J = 9 Hz, 1H, CH Ar), 4.32 (q, J = 7 Hz, 2H, CH₂), 2.13 (s, 3H, -C(O)CH₃), 1.36 (t, J = 7 Hz, 3H, CH₃) ppm.

10.1.6. Compounds from the Rhodium-Catalyzed Asymmetric Hydrogenation reaction:**[(COD) (S)-MaxPHOS]Rh(I)BF₄, 36**

[Rh(acac)(cod) (3.45 g, 11.14 mmol), (S)-MaxPHOS·HBF₄ (3.95 g, 11.25 mmol) and anhydrous MeOH (80 mL) were stirred in a round bottomed flask under N₂ atmosphere overnight. The MeOH was removed under vacuum and solved again with CH₂Cl₂ (14 mL). The solution was filtered through a cannula to another flask and crystallization was then induced with the addition of anhydrous Et₂O (50 mL) to yield **36** as an orange crystalline solid (5.93 g, 95%).

Mp: 155-158 °C.

IR (KBr): ν_{\max} 3277, 2946, 1475, 1056 cm^{-1} .

$^1\text{H-NMR}$ (400 MHz, CDCl_3): δ 1.21 (d, $J = 16$ Hz, 9H), 1.38 (d, 9H, $J = 15$ Hz), 1.40 (d, 9H, $J = 14$ Hz), 1.77 (dd, 3H, $J = 8$ and 1 Hz), 2.10-2.30 (m, 4H), 2.36-2.57 (m, 4H), 5.11 (br, 2H), 5.39 (br, 1H), 5.54 (m, 2H) ppm.

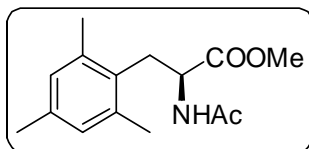
$^{13}\text{C-RMN}$ (100 MHz, CDCl_3): δ 13.6 (d, $J_p = 20$ Hz, CH_3), 26.4 (d, $J_p = 5$ Hz, 3CH_3), 28.8 (CH_2), 28.9 (CH_2), 29.0 (d, $J_p = 6$ Hz, 3CH_3), 29.1 (d, $J_p = 6$ Hz, 3CH_3), 31.3 (CH_2), 31.9 (CH_2), 35.8 (d, $J_p = 26$ Hz, C), 38.8 (d, $J_p = 12$ Hz, 2C), 91.1 (dd, $J_p = 10$ and 7 Hz, CH), 91.7 (t, $J_p = 8$ Hz, CH), 95.5 (dd, $J_p = 9$ and 6 Hz, CH), 98.1 (dd, $J_p = 9$ and 7 Hz, CH) ppm.

$^{31}\text{P NMR}$ (121 MHz, CDCl_3): δ 47.8 (dd, $J = 128$ and 48 Hz), 70.1 (dd, $J = 128$ and 49 Hz) ppm.

$^{19}\text{F NMR}$ (376 MHz, CDCl_3): δ -151.3 ppm.

HRMS: calcd. for $\text{C}_{21}\text{H}_{43}\text{NP}_2\text{Rh}$ [$\text{M} - \text{BF}_4$] $^+$: 474.1920; found: 474.1919.

(S)-Methyl 2-acetamido-3-mesitylpropanoate, **39**



A high pressure reaction vessel was charged with a mixture of (Z)-methyl 2-acetamido-3-mesitylacrylate (6.3 g, 24.0 mmol), [(COD) (S)-MaxPHOS] Rh(I)BF₄ cat (3%) and degassed MeOH (60 mL). The reactor was purged with nitrogen-vacuum cycles and subsequently, with hydrogen. Finally, the reaction vessel was pressurized to 60bar with H₂ and stirred at room temperature for 20 h. The mixture was vented with nitrogen and the solvent was removed at reduced pressure. The resulted mixture was redissolved in AcOEt and the catalyst was removed by filtration of the crude in a silica column. After elimination of the solvent at reduced pressure, the (S)-methyl 2-acetamido-3-mesitylpropanoate was obtained as a white pure solid in 99% yield and 96% of enantiomeric excess. Recrystallization of the product in toluene allowed us to obtain the product with more than 99% e.e. The spectroscopic data of this product was identical to data previously reported in the literature.²

$[\alpha]_D^{25} = +15.0$ (c 0.60, CH₃OH); [lit.² $[\alpha]_D = +12.2$ (c 0.55, CH₃OH)]

Mp: 141-142 °C.

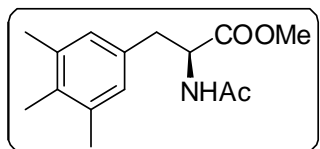
$^1\text{H-RMN}$ (400 MHz, CDCl_3): δ 6.83 (s, 2H, CH), 5.95 (d, 1H, $J=8\text{Hz}$, NH), 4.78 (q, 1H, $J=8\text{Hz}$, CH), 3.63 (s, 3H, CH_3), 3.00-3.12 (m, 2H, CH_2), 2.30 (s, 6H, CH_3), 2.24 (s, 3H, CH_3), 1.96 (s, 3H, CH_3) ppm.

$^{13}\text{C-RMN}$ (100 MHz, CDCl_3): δ 173.4 (CO), 169.7 (CO), 137.0 (C), 136.5 (C), 130.0 (CH), 129.4 (CH), 51.9 (CH), 32.8 (CH_3), 31.1 (CH_2), 23.3 (CH_3), 21.1 (CH_3), 20.3 (CH_3) ppm.

HRMS: calcd. for $\text{C}_{15}\text{H}_{21}\text{NO}_3$: 263.1600; $(\text{M}+\text{H})^+$ found, 264.1594.

HPLC (CHIRALPAK-IA, heptane/IPA 90:10, 0.5 mL/min, $\lambda=254\text{ nm}$, $t_{\text{R}}(\text{R})=12\text{ min}$, $t_{\text{R}}(\text{S})=17\text{ min}$).

(S)-Methyl 2-acetamido-3-(3',4',5'-trimethylphenyl)propanoate, 41



A high pressure reaction vessel was charged with a mixture of (Z)-methyl 2-acetamido-3-(3',4',5'-trimethylphenyl)acrylate (86 mg, 0.33 mmol), $[\text{Rh}(\text{COD})(\text{S-MaxPHOS})]\text{BF}_4$ cat (3%) and degassed MeOH (1 mL). The reactor was purged with nitrogen-vacuum cycles and subsequently, with hydrogen. Finally, the reaction vessel was pressurized to 2 bar with H_2 and stirred at room temperature for 20h. The mixture was vented with nitrogen and the solvent was removed at reduced pressure. The resulted mixture was redissolved in AcOEt and the catalyst was removed by filtration of the crude in a silica column. After elimination of the solvent at reduced pressure, the (S)-methyl 2-acetamido-3-mesitylpropanoate was obtained as a white pure solid in 99% yield and 99% enantiomeric excess.

$[\alpha]_{\text{D}}^{25} = +103.7$ (c 0.50, CDCl_3)

Mp: 88-91 °C.

IR (KBr): ν_{max} 3267(b), 2936, 1759, 1637 cm^{-1} .

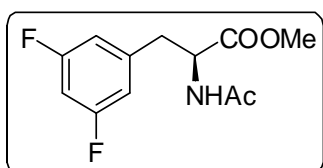
$^1\text{H-NMR}$ (400 MHz, CDCl_3): δ 6.72 (s, 2H, 2 CH Ar), 5.88 (d, $J=7\text{Hz}$, NH), 4.82 (dt, $J=6, 6$ and 8 Hz , $\text{CH}\alpha$), 3.74 (s, 3H, OCH_3), 3.01 (qd, $J=6, 14, 14$ and 14 Hz , 2H, $\text{CH}_2\beta$), 2.24 (s, 6H, 2 CH_3), 2.13 (s, 3H, CH_3), 1.98 (s, 3H, $\text{C}(\text{O})\text{CH}_3$) ppm.

$^{13}\text{C-RMN}$ (100 MHz, CDCl_3): δ 172.6 (C, NHCO), 170.0 (C, CO), 136.8 (2 C, Ar), 134.0 (C, Ar), 132.7 (C, Ar), 128.6 (2 CH, Ar), 53.5 (CH, $\text{CH}\alpha$), 52.4 (CH_3 , $-\text{OCH}_3$), 37.5 (CH_2 , $\text{CH}_2\beta$), 23.3 (CH_3 , $\text{C}(\text{O})-\text{CH}_3$), 20.8 (2 CH_3 , Ar), 15.3 (CH_3 , Ar) ppm.

HRMS: calcd. for $C_{15}H_{21}NO_3$: 263.1521; $(M+H)^+$ found, 264.1601.

HPLC (CHIRALPAK-IA, heptane/IPA 95:5, 1 mL/min, $\lambda=254$ nm, $t_R(S)=10$ min, $t_R(R)=12$ min).

(S)-Methyl 2-acetamido-3-(3',5'-difluorophenyl)propanoate, 43



A high pressure reaction vessel was charged with a mixture of (Z)-methyl 2-acetamido-3-(3',5'-difluorophenyl)acrylate (7.35 g, 32.7 mmol), [(COD) (S,S)-Et-DuPHOS] Rh(I)OTf cat (3%) and degassed MeOH (70 mL). The reactor was purged with nitrogen-vacuum cycles and subsequently, with hydrogen. Finally, the reaction vessel was pressurized to 5 bar with H_2 and stirred at room temperature for 20 h. The mixture was vented with nitrogen and the solvent was removed at reduced pressure. The resulted mixture was redissolved in AcOEt and the catalyst was removed by filtration of the crude in a silica column. After elimination of the solvent at reduced pressure, the (S)-methyl 2-acetamido-3-mesitylpropanoate was obtained as a white pure solid in 99% yield and 99% enantiomeric excess.

$[\alpha]_D^{25} +156.2$ (c 0.50, $CDCl_3$)

Mp: 113-117 °C.

IR (KBr): ν_{max} 3246(b), 2994, 1719, 1661 cm^{-1} .

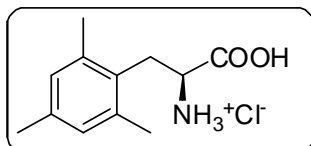
1H -NMR (400 MHz, $CDCl_3$): δ 6.71 (m, 1H, CH Ar), 6.63 (m, 2H, CH Ar), 5.96 (d, $J = 6$ Hz, 1H, NH), 4.87 (dt, $J = 6$ and 8 Hz, 1H, $CH\alpha$), 3.76 (s, 3H, $-OCH_3$), 3.12 (ddd, $J = 6, 14$ and 35 Hz, 2H, $CH_2\beta$), 2.02 (s, 3H, $-C(O)CH_3$) ppm.

^{13}C -RMN (100 MHz, $CDCl_3$): δ 171.5 (C, CO), 169.6 (C, CO), 162.9 ((dd, $J_F = 249, 13$ Hz) 2 C, $C\epsilon$ Ar), 139.9 ((t, $J_F = 9$ Hz) C, Ar), 112.1 (m, 2 CH, $C\delta$ Ar), 102.9 ((t, $J_F = 25$ Hz) CH, Cz Ar), 52.9 (CH, $C\alpha$), 52.5 (CH_3, MeO), 37.6 ($CH_2, C\beta$), 23.1 (CH_3, Ac) ppm

^{19}F NMR (376 MHz, $CDCl_3$) $\delta = -110.1$ (t, $J = 8$ Hz, 2F) ppm.

HRMS: calcd. for $C_{12}H_{13}F_2NO_3$: 257.0863; $(M+H)^+$ found, 258.0937

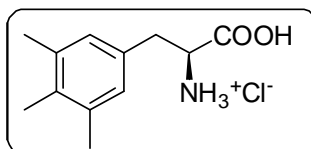
HPLC (CHIRALPAK-IA, heptane/IPA 90:10, 1 mL/min, $\lambda=254$ nm, $t_R(R)=9$ min, $t_R(S)=11$ min).

9.1.7. Compounds obtained after the hydrolysis:**L-3-mesitylalanine hydrochloride, 40**

A mixture of (S)-methyl 2-acetamido-3-mesitylpropanoate (6.1 g, 23.2 mmol) and concentrated HCl (31 mL) was subjected to reflux conditions for 30 min. Then, 62 mL of HCl (6M) was added, and the reaction was stirred for 6 h at the same temperature. After the reaction vessel spontaneously get the room temperature, the solvent is evaporated at reduced pressure and the white solid obtained was filtrated, washed and dried to quantitatively afford the hydrochloric salt of the L-3-mesitylalanine. The spectroscopic data of this product was identical to data previously reported in the literature.²

Mp: 267-270 °C.

¹H-RMN (400 MHz, D₂O): δ 13.45 (s, 1H), 8.68 (s, 3H), 6.81 (s, 2H, CH Ar), 3.79 (t, J = 8 Hz, 1H, CH_α), 3.04-3.16 (m, 2H, CH₂β), 2.26 (s, 6H, CH₃), 2.21 (s, 3H, CH₃) ppm.

L-3-(3',4',5'-trimethylphenyl)-alanine hydrochloride, 42

A mixture of (S)-methyl 2-acetamido-3-(3',4',5'-trimethylphenyl) propanoate (2.2 g, 8.37 mmol) and concentrated HCl (12 mL) was subjected to reflux conditions for 30 min. Then, 24 mL of HCl (6 M) was added, and the reaction was stirred for 6 h at the same temperature. After the reaction vessel spontaneously get the room temperature, the solvent is evaporated at reduced pressure and the white solid obtained was filtrated, washed and dried to quantitatively afford the hydrochloric salt of the L-3-(3',4',5'-trimethylphenyl)alanine.

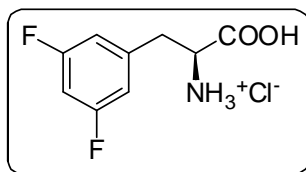
[α]_D = +24.8 (c 0.50, D₂O).

Mp: 238-242 °C.

¹H-NMR (400 MHz, CD₃OD): δ 6.90 (s, 2H, CH Ar), 4.18 (dd, J = 5 and 7 Hz, 1H, CH_α), 3.10 (ddd, J = 7, 14 and 22 Hz, 2H, CH₂β), 2.26 (s, 6H, CH₃), 2.16 (s, 3H, CH₃).

¹³C-RMN (100 MHz, CD₃OD): δ 172.1 (C, CO), 134.6 (2C, C ϵ Ar), 126.3 (C, C γ Ar), 117.4 (2C, C δ Ar), 101.1 (C, C ζ Ar), 49.8 (C, C α), 37.5 (C, C β) ppm.

L-3-(3',5'-difluorophenyl)-alanine hydrochloride, 44



A mixture of (S)-methyl 2-acetamido-3-(3',5'-difluorophenyl) propanoate (7.0 g, 27.2 mmol) and concentrated HCl (36 mL) was subjected to reflux conditions for 30 minutes. Then, 77 mL of HCl (6M) was added, and the reaction was stirred for 6 h at the same temperature. After the reaction vessel spontaneously get the room temperature, the solvent is evaporated at reduced pressure and the white solid obtained was filtrated, washed and dried to quantitatively afford the hydrochloric salt of the L-3-(3',5'-difluorophenyl)alanine.

$[\alpha]_D^{25} = +11.3$ (c 0.50, D₂O).

Mp: 215-219 °C.

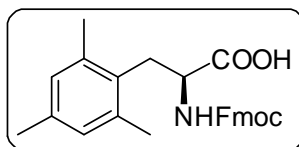
¹H-NMR (400 MHz, CD₃OD) δ 7.06 – 6.79 (m, 3H, CH Ar), 4.29 (dd, J = 8 and 6 Hz, 1H CH α), 3.33 (m, 1H, CH₂ β), 3.16 (dd, J = 8 and 15 Hz, 1H, CH₂ β) ppm.

¹³C-RMN (100 MHz, CD₃OD): δ 169.3 (C, CO), 164.5 (d, $J_F = 13$ Hz, C, C ϵ Ar), 162.1 (d, $J_F = 13$ Hz, C, C ϵ Ar), 138.6 (C, C γ Ar), 112.2 (m, 2C, C δ Ar), 102.7 (t, $J_F = 26$ Hz, C, C ζ Ar), 53.2 (C, C α), 35.3 (C, C β) ppm.

¹⁹F NMR (376 MHz, CDCl₃) δ -111.5 (t, J = 8 Hz) ppm.

9.1.8. Compounds subjected to Fmoc-protection:

N-Fmoc-L-3-mesitylalanine, 1



The L-mesitylalanine hydrochloride (6.1 g, 25.1 mmol) was suspended in 66 mL of an aqueous solution of Na₂CO₃ (7.6 g, 72 mmol). The mixture was cooled to 0 °C and a solution of FmocOSu (12.1 g, 36 mmol) in acetone (66 mL) was slowly added. The resulting mixture was allowed to warm to room temperature and stirred for 20h. Then, 20mL of water was added and the reaction mixture was extracted with ethyl acetate. The organic layer was back extracted with water, and the combined

aqueous layers were washed with AcOEt, acidified to a pH of 1 with aqueous HCl and extracted with AcOEt. The combined organic layers were dried and concentrated *in vacuo* to give 10.1 g of N-Fmoc-L-mesitylalanine as a white solid (93% yield, 99% e.e.). The resulting product can be purified by flash chromatography if necessary using mixtures AcOEt/Hexanes (1% AcOH). The spectroscopic data of this product was identical to data previously reported in the literature.²

[α]_D = - 26.0 (c 1.00, CHCl₃).

MP: 187-188 °C.

IR (film): ν_{\max} 3321, 2962, 1713, 1450, 1265 cm⁻¹.

¹H-RMN (400 MHz, CDCl₃): δ 7.74 (d, 2H, J= 8 Hz), 7.51 (t, 2H, J= 8 Hz), 7.40 (t, 2H, J= 8 Hz), 7.30 (t, 2H, J= 8 Hz), 6.83 (s, 2H), 5.25 (d, 1H, J= 8 Hz), 4.60 (dd, 1H, J= 8.0 and 8.4 Hz), 4.30 (m, 1H), 4.14 (m, 1H), 3.18 (m, 2H), 2.32 (s, 6H), 2.21 (s, 6H) ppm.

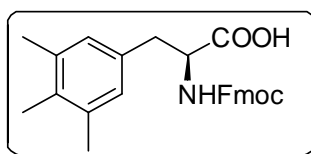
¹³C-RMN (100 MHz, CDCl₃): δ 176.7 (CO), 156.1 (CO), 144.0 (C), 141.5 (C), 137.2 (C), 136.6 (C), 130.0 (C), 129.6 (C), 129.5 (CH), 127.9 (CH), 127.3 (CH), 125.3 (CH), 120.2 (CH), 67.4 (CH₂), 53.7 (CH₂), 47.3 (CH), 32.5 (CH₂), 21.3 (CH₃), 20.4 (CH₃) ppm.

HRMS: Calcd. for C₂₇H₂₇NO₄: 429.2029; (M+H)⁺ found 430.2018.

Anal.: 74.94 % C, 6.21 % H, 3.41 % N (calc. C₂₇H₂₇NO₄, 75.50 % C, 6.34 % H, 3.26 % N).

HPLC CHIRALPAK-IA. Heptane/EtOH-0.1% DEA 70:30, 0.5 mL/min, λ =254 nm, $t_R(D)$ =19 min, $t_R(L)$ =15 min.

N-Fmoc-L-3-(3',4',5'-trimethylphenyl)-alanine, 2



The L-3-(3',4',5'-trimethylphenyl)-alanine hydrochloride (1.7 g, 6.8 mmol) was suspended in 20 mL of an aqueous solution of Na₂CO₃ (2.1 g, 20 mmol). The mixture was cooled to 0 °C and a solution of FmocOSu (3.4 g, 10.1 mmol) in acetone (20 mL) was slowly added. The resulting mixture was allowed to warm to room temperature and stirred for 20 h. Then, 20 mL of water was added and the reaction mixture was extracted with ethyl acetate. The organic layer was back extracted with water, and

the combined aqueous layers were washed with AcOEt, acidified to a pH of 1 with aqueous HCl and extracted with AcOEt. The combined organic layers were dried and concentrated *in vacuo* to give 2.7 g of N-Fmoc-L-3-(3',4',5'-trimethylphenyl)-alanine as a white solid (92% yield, 99% e.e.). The resulting product can be purified by flash chromatography if necessary using mixtures Hexanes/AcOEt (1% AcOH).

$[\alpha]_D = -122.4$ (c 0.50, CDCl_3)

Mp: 165-168 °C.

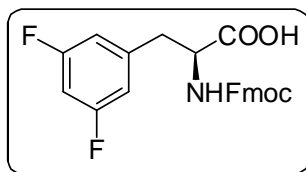
IR (film): ν_{max} 3420, 3216, 1723, 1518 cm^{-1}

$^1\text{H-NMR}$ (400 MHz, CDCl_3): δ : 7.76 (d, $J = 8$ Hz, 2H, CH), 7.54 (dd, $J = 8$ and 11 Hz, 2H, CH), 7.40 (t, $J = 7$ Hz, 2H, CH), 7.29 (t, $J = 8$ Hz, 2H, CH), 6.82 (s, 2H, Ar), 5.20 (d, $J = 8$ Hz, 1H, NH), 4.66 (m, 1H, CH_α), 4.38 (dt, $J = 10$ and 17 Hz, 2H, CH_2 (Fmoc)), 4.21 (t, $J = 7$ Hz, 1H, CH (Fmoc)), 3.07 (ddd, $J = 7, 15$ and 38 Hz, 2H, $\text{CH}_2\beta$), 2.24 (s, 6H, CH_3), 2.13 (s, 3H, CH_3) ppm.

$^{13}\text{C-RMN}$ (100 MHz, CDCl_3): δ 176.1 (CO), 155.9 (CO), 143.7 (2C, Fmoc), 141.3 (2C, Fmoc), 136.8 (2C, Ar), 134.1 (C, Ar), 132.0 (C, Ar), 128.4 (2CH, Ar), 127.7 (2CH, Fmoc), 127.0 (2CH, Fmoc), 125.0 (2CH, Fmoc), 120.0 (2CH, Fmoc), 67.2 (CH_2 , Fmoc), 54.4 (CH, C_α), 47.1 (CH, Fmoc), 37.2 (CH_2 , C_β), 20.6 (2 CH_3 , Ar), 15.1 (CH_3 , Ar) ppm.

HPLC CHIRALPAK-IA. Heptane/EtOH-0.1% DEA 70:30, 0.5 mL/min, $\lambda=254$ nm, $t_R(D)=15$ min, $t_R(L)=14$ min.

N-Fmoc-L-3-(3',5'-difluorophenyl)-alanine, 3



The L-3-(3',5'-difluorophenyl)-alanine hydrochloride (6.2 g, 26.2 mmol) was suspended in 66 mL of an aqueous solution of Na_2CO_3 (7.6 g, 72 mmol). The mixture was cooled to 0 °C and a solution of FmocOSu (12.1 g, 36 mmol) in acetone (66 mL) was slowly added. The resulting mixture was allowed to warm to room temperature and stirred for 20h. Then, 20mL of water was added and the reaction mixture was extracted with ethyl acetate. The organic layer was back extracted with water, and the combined aqueous layers were washed with AcOEt,

acidified to a pH of 1 with aqueous HCl and extracted with AcOEt. The combined organic layers were dried and concentrated *in vacuo* to give 9.9 g of N-Fmoc-L-3-(3',5'-difluorophenyl)-alanine as a white solid (89% yield, 99% e.e.). The resulting product can be purified by flash chromatography if necessary using mixtures AcOEt/Hexanes (1% AcOH).

$[\alpha]_D = -139.1$ (c 0.50, CDCl_3)

Mp: 151-155 °C.

IR (film): ν_{max} 3320, 3072, 1734, 1652 cm^{-1}

$^1\text{H-NMR}$ (400 MHz, CDCl_3) δ 7.77 (d, $J = 8$ Hz, 2H, CH (Fmoc)), 7.56 (t, $J = 7$ Hz, 2H, CH (Fmoc)), 7.40 (t, $J = 7$ Hz, 2H, CH (Fmoc)), 7.35 – 7.28 (m, 2H, CH (Fmoc)), 6.70 (m, 3H, Ar), 5.26 (d, $J = 8$ Hz, 1H, NH), 4.69 (dd, $J = 6$ and 13 Hz, 1H, $\text{CH}\alpha$), 4.44 (dt, $J = 10$ and 17 Hz, 2H, CH_2 (Fmoc)), 4.22 (t, $J = 7$ Hz, 1H, CH (Fmoc)), 3.14 (ddd, $J = 6, 14$ and 39 Hz, 2H, $\text{CH}_2\beta$).

$^{13}\text{C-RMN}$ (100 MHz, CDCl_3): δ 174.7 (C, CO), 155.9 (C, CO), 143.7 (2C, Fmoc), 141.6 (2C, Fmoc), 139.6 (m, C, Ar), 128.0 (2CH, Fmoc), 127.3 (2CH Fmoc), 127.2 (2CH Fmoc), 125.2 (d, $J_F = 8$ Hz, 2C, Ar), 120.3 (2 CH, Fmoc), 115.5 (m, 2C, Ar), 103.1 (t, $J_F = 25$ Hz, CH, Ar), 67.4 (CH_2 , Fmoc), 54.4 (CH, $\text{C}\alpha$), 47.4 (CH, Fmoc), 37.8 (CH_2 , $\text{C}\beta$) ppm.

$^{19}\text{F-NMR}$ (376 MHz, CDCl_3) δ -109.86 (t, $J = 7$ Hz, 2F) ppm.

HPLC CHIRALPAK-IA. Heptane/IPA-0.1% TFA 90:10, 0.5 mL/min, $\lambda=254$ nm, $t_R(D)=12$ min, $t_R(L)=13$ min.

9.2. Experimental section for the synthesis of SRIF analogs

9.2.1. General methods and instrumentation:

All commercial amino acid were purchased from Chem-Impex International, Inc. or obtained from BCN Peptides, S.A. HOBt and DIPCDI were purchased from SDS and SAF respectively. SRIF and octreotide were obtained from BCN Peptides S.A. 2-Chlorotriyl chloride resin was purchased from Iris Biotech GmbH or Novabiochem. Piperidine was purchased from SDS. All other reagents were purchased from Sigma-

Aldrich unless otherwise noted and used without further purification. All the solvents have been purchased to Panreac, SDS and Sigma-Aldrich.

2D TOCSY (50 ms) and NOESY (200 and 350 ms) homonuclear experiments were acquired in a Bruker Avance III spectrometer (600 MHz) at 285 K unless otherwise noted. When necessary, DSS was used as internal chemical shift reference. Chemical shifts are recorded in ppm.

Experiments were monitored by analytical HPLC or HPLC-MS. Analytical HPLC was carried out on a Waters instrument comprising a Sunfire™ C18 reversed-phase analytical column (3.5 μ m, 4.6 x 100 mm), a separation module (Waters 2695), automatic injector, and photodiode array detector (Waters 2298). Data were managed with Empower 2 software (Waters). UV detection was performed at 220 nm, and linear gradients of ACN (0.036% TFA) into H₂O (0.045% TFA) were run at a flow rate of 1.0 mL/min over 8 min. HPLC-MS analyses of samples were carried out on a Waters instrument comprising a Sunfire™ C18 reversed-phase analytical column (3.5 μ m, 4.6 x 100 mm), a separation module (Waters 2695), automatic injector, photodiode array detector (Waters 2298), and a Waters micromass ZQ unit. Data were managed with MassLynx V4.1 software (Waters). UV detection was performed at 220 nm, and linear gradients of ACN (0.07% formic acid) into H₂O (0.1% formic acid) were run at a flow rate of 0.3 mL/min over 8 min.

SRIF analogs were purified by RP-HPLC using a C8 Kromasil column and gradients of solvent A (0.1% TFA in H₂O) and solvent B (0.07% TFA in ACN). Purity was determined by analytical HPLC using C18 Luna (COL-HP-42) H₂O (0.1% TFA)/ACN (0.07%) (70:30), λ =254 nm, 1mL/min, and stop time: 30 min. Yields of peptides are based in re-calculated loading of the resin.

HRMS determinations were carried out in the Mass Spectrometry Core Facility (IRB Barcelona). Samples were reconstituted in 1000 μ L of H₂O/ACN (1% formic acid) for MS analysis and introduced by automated nanoelectrospray in a LTQ-FT Ultra (Thermo Scientific) Mass Spectrometer. The NanoMate (Advion BioSciences) aspirated the samples from a 384-well plate (protein Lobind) with disposable,

conductive pipette tips, and infused the samples through the ESI Chip, which consists of 400 nozzles in a 20 x 20 array. Spray voltage was 1.80 kV and delivery pressure was 0.80 psi. MS conditions: NanoESI, positive ionization. Capillary temperature: 200 °C. Tube lens: 100 V. Range of m/z: 200-2000 a.m.u. Samples were acquired with Xcalibur software (vs. 2.0SR2). Ion deconvolution to zero charged monoisotopic masses was performed with Xtract algorithm in Xcalibur software. Elemental compositions from experimental exact mass monoisotopic values are obtained with Xcalibur software (vs. 2.0SR2).

9.2.2. General considerations for solid-phase peptide synthesis:

All peptides were synthesized by SPPS using the Fmoc/^tBu strategy. Solid-phase peptide syntheses were performed in polypropylene syringes provided with a porous polyethylene filter and attached to a vacuum manifold. The syringes volumes used were 5, 10 or 20 mL, depending on the scale of the synthesis. Reagents and solvents were added to the syringe containing the resin and the mixture was stirred in an orbital shaker. After each treatment, the solvent and the excess of reagents were removed by filtration through the vacuum system. After each synthetic step, the resin was washed with DCM (3 x 1 min), DMF (3 x 1 min) and DCM (3 x 1 min) unless otherwise specified.

Conventional couplings during the elongation of the peptide in solid phase were monitored by the “ninhydrin test”. This colorimetric test allows the detection of primary amine groups on the resin. To perform the Kaiser or ninhydrin test⁶, the peptidyl-resin was washed with appropriate solvents and dried. A small amount of peptidyl-resin (0.5-2 mg) was transferred to a small glass tube. To this tube were added 6 drops of the reagent solution A and 3 drops of the reagent solution B. The mixture was heated at 100 °C for 3 min. The formation of a blue color on the beads or the supernatant is indicative of the presence of free primary amines (positive test) and thus of an uncompleted coupling. Conversely, a yellow coloration indicates the

6 Kaiser, E.; Colescott, R. L.; Bossinger, C. D.; Cook, P. I. *Anal. Biochem.* **1970**, *34*, 595-598.

absence of free primary amines (negative test). The method is highly sensitive and a negative test ensures amino acid incorporation higher than 99.5%.

– Preparation of reagent solution A: Phenol (40 g) was dissolved in EtOH (10 mL) and the mixture was heated until complete dissolution of the phenol. An aqueous solution (20 mL, 10 mM) of KCN (65 mg in 100 mL of H₂O) was added to freshly distilled pyridine (100 mL). Both solutions were stirred for 45 min with 40 g of Amberlite MB-3 ion exchange resin, filtered and combined.

– Preparation of reagent solution B: Ninhydrin (2.5 g) was dissolved in EtOH (50 mL). The resulting solution was kept in a flask protected from light.

9.2.3. General method for the syntheses of SRIF analogs:

The syntheses were performed by SPPS on a 2-Cl-Trt resin using the Fmoc/^tBu strategy. In most cases, decreasing of the loading of commercial resin (from 1.60 to 0.80 mmol/g) was carried out to avoid aggregation problems when growing the peptidic chains. In these cases, only 0.5 eq of the first amino acid was used. The 2-Cl-Trt resin was first swelled in DCM (15 min). Then, the resin was washed with DCM (3 x 1 min), DMF (3 x 1 min) and DCM (3 x 1 min). Incorporation of the first amino acid into a 2-chlorotriyl chloride resin is achieved through a nucleophilic attack of the carboxylate from the corresponding Fmoc-protected amino acid to form an ester bond. Thus initially, the first amino acid Fmoc-L-Xaa-OH (0.5 eq) was coupled in the presence of DIPEA (4 eq) in DCM as solvent for 40 min. Remaining reactive positions were end-capped with methanol (0.8 mL·g⁻¹). Then, the solvents are removed by suction, and the resin washed with DCM (3 x 1 min), DMF (3 x 1 min), and DCM (3 x 1 min). Fmoc removal was performed by treating the peptidyl resin with 20% piperidine in DMF (1 x min and 1 x min). The second amino acid Fmoc-L-Yaa-OH (2.5 eq) was coupled using DIPCDI (2.5 eq) and HOBT (2.5 eq), as activating reagents, in DMF for 40-60 min. Kaiser test was used to check coupling completions. This procedure was repeated for the following Fmoc-protected amino acids and for the

last Boc-L-Zaa-OH. When non-natural amino acids were coupled, only 1.5 eq were used.

The cleavage of the fully protected linear peptide from the resin was carried out using a cleavage cocktail (DCM/TFE/AcOH, 70:20:10 (v/v)) for 2 h. The formation of the disulfide bridge in all the analogs was achieved using iodine (10 eq) in solution at room temperature for 15 min and then quenched with an aqueous solution of sodium thiosulphate 1N. The aqueous layer was extracted with DCM (3 x 4 mL), the combined organic layer were washed with a mixture of aqueous 5% citric acid/sodium chloride (1:1) solution and evaporated under reduced pressure. Finally, total deprotection of the side-chains was performed using an acidic mixture (TFA/DCM/Anisole/H₂O, 12:6:2:1 (v/v)) for 4h. Then, the remaining solution was washed with heptane (8 mL) and the aqueous layer was precipitated in Et₂O (-10 °C). Filtration of this mixture allowed us to obtain the synthetic somatostatin analogs that were subsequently subjected to purification.

Resin loading was determined by quantification of the UV-absorbance of dibenzofulvene-piperidine adduct measured at 290 nm. Yields of peptides are based in this re-calculated loading of the resin. After incorporating the first amino acid, the Fmoc- group was removed and the washes of all treatments were collected in a volumetric flask. The piperidine washes were diluted with DMF and the absorbance of the resulting solution was measured at 290 nm. The resin loading was calculated using the following formula: $Z = (A \cdot V) / (\epsilon \cdot Y \cdot l)$; where: Z: resin loading (mmol/g resin), A: absorbance, V: volume of solvent (mL), ϵ : molar extinction coefficient ($\epsilon = 5800 \text{ L} \cdot \text{mol}^{-1} \cdot \text{cm}^{-1}$), Y: weight of resin (g), l: path length (cm).

9.2.5. 14-Residue synthetic SRIF analogs (in order of appearance):

Analog containing the Msa amino acid:

[L-Msa6]-SRIF, **45**: Somatostatin analog **45** was synthesized following the general procedure from 0.136g of 2-Cl-Trt resin (1.60 mmol/g) and using Fmoc-L-Msa-OH, affording 0.20 g in 60% yield (95% purity after purification). HPLC: $t_R = 14.3$ [Gradient

25-60% B in 20 min, flux: 1 mL.min⁻¹, λ=220 nm]. HRMS: calcd. for C₇₉H₁₁₀N₁₈O₁₉S₂: 1678.8; found, 1680.2.

[L-Msa7]-SRIF, 46: Somatostatin analog **46** was synthesized following the general procedure from 0.136 g of 2-Cl-Trt resin (1.60 mmol/g) and using Fmoc-L-Msa-OH, affording 0.24 g in 22% yield and 73.8% of purity (97% purity after purification). HPLC: t_R = 14.8 [Gradient 25-60% B in 20 min, flux: 1 mL.min⁻¹, λ=220 nm]. HRMS: calcd. for C₇₉H₁₁₀N₁₈O₁₉S₂: 1678.8; found, 1679.8.

[L-Msa11]-SRIF, 47: Somatostatin analog **47** was synthesized following the general procedure from 0.136 g of 2-Cl-Trt resin (1.60 mmol/g) and using Fmoc-L-Msa-OH, affording 0.28 g in 44% yield (99% purity after purification). HPLC: t_R = 14.1 [Gradient 25-60% B in 20 min, flux: 1 mL.min⁻¹, λ=220 nm]. HRMS: calcd. for C₇₉H₁₁₀N₁₈O₁₉S₂: 1678.8; found, 1680.0.

[L-Msa6_D-Trp8]-SRIF, 48: Somatostatin analog **48** was synthesized following the general procedure from 2.0 g of 2-Cl-Trt resin (1.60 mmol/g) and using Fmoc-L-Msa-OH, affording 1.93 g in 45% yield and 90% of purity (99% after purification). HPLC: t_R = 13.4 [Gradient 25-60% B in 20 min, flux: 1 mL.min⁻¹, λ=220 nm]. HRMS: calcd. for C₇₉H₁₁₀N₁₈O₁₉S₂: 1678.8; found, 1680.4.

[L-Msa7_D-Trp8]-SRIF, 49: Somatostatin analog **49** was synthesized following the general procedure from 2 g of 2-Cl-Trt resin (1.60 mmol/g) and using Fmoc-L-Msa-OH, affording 2.15 g in 48% yield and 88% of purity (98% after purification). HPLC: t_R = 13.4 [Gradient 25-60% B in 20 min, flux: 1 mL.min⁻¹, λ=220 nm]. HRMS: calcd. for C₇₉H₁₁₀N₁₈O₁₉S₂: 1678.8; found, 1680.4.

[L-Msa11_D-Trp8]-SRIF, 50: Somatostatin analog **50** was synthesized following the general procedure from 2 g of 2-Cl-Trt resin (1.60 mmol/g) and using Fmoc-L-Msa-OH, affording 1.59 g in 35% yield and 88% of purity (98% after purification). HPLC: t_R = 12.8 [Gradient 25-60% B in 20 min, flux: 1 mL.min⁻¹, λ=220 nm]. HRMS: calcd. for C₇₉H₁₁₀N₁₈O₁₉S₂: 1678.8; found, 1680.6.

[L-Msa6,7]-SRIF, 51: Somatostatin analog **51** was synthesized following the general procedure from 0.10 g of 2-Cl-Trt resin (1.60 mmol/g) and using Fmoc-L-Msa-OH, affording 0.12 g of **10** in 20% yield (98% purity after purification). HPLC: $t_R = 16.5$ [Gradient 25-60% B in 20 min, flux: 1 mL.min⁻¹, $\lambda = 220$ nm]. HRMS: calcd. for C₈₂H₁₁₆N₁₈O₁₉S₂: 1721.1; found, 1721.0.

[L-Msa6,11]-SRIF, 52: Somatostatin analog **52** was synthesized following the general procedure from 0.136 g of 2-Cl-Trt resin (1.60 mmol/g) and using Fmoc-L-Msa-OH, affording 0.28 g in 44% yield (99% purity after purification). HPLC: $t_R = 15.4$ [Gradient 25-60% B in 20 min, flux: 1 mL.min⁻¹, $\lambda = 220$ nm]. HRMS: calcd. for C₈₂H₁₁₆N₁₈O₁₉S₂: 1721.1; found, 1720.8.

[L-Msa7,11]-SRIF, 53: Somatostatin analog **53** was synthesized following the general procedure from 0.10 g of 2-Cl-Trt resin (1.60 mmol/g) and using Fmoc-L-Msa-OH, affording 0.13 g in 44% yield (99% purity after purification). HPLC: $t_R = 16.4$ [Gradient 25-60%B in 20min, flux: 1 mL.min⁻¹, $\lambda = 220$ nm]. HRMS: calcd. for C₈₂H₁₁₆N₁₈O₁₉S₂: 1721.1; found, 1721.0.

[L-Msa6,7,11]-SRIF, 54: Somatostatin analog was synthesized following the general procedure from 0.10 g of 2-Cl-Trt resin (1.60 mmol/g) and using Fmoc-L-Msa-OH, affording 0.10 g in 44% yield (95% purity after purification). HPLC: $t_R = 18.4$ [Gradient 25-60% B in 20 min, flux: 1 mL.min⁻¹, $\lambda = 220$ nm]. HRMS: calcd. for C₈₅H₁₂₂N₁₈O₁₉S₂: 1762.9; found, 1763.2.

Analogs containing the Tmp amino acid:

[L-Tmp6_D-Trp8]-SRIF, 55: Somatostatin analog **55** was synthesized following the general procedure from 0.20 g of 2-Cl-Trt resin (0.8 mmol/g) and using Fmoc-L-Tmp-OH, affording 0.18 g in 63% yield (98% purity after purification). HPLC: $t_R = 14.2$ [Gradient 25-60% B in 20 min, flux: 1 mL.min⁻¹, $\lambda = 220$ nm]. HRMS: calcd for C₇₉H₁₁₀N₁₈O₁₉S₂: 1678.7636; found, 1678.7638.

[L-Tmp7_D-Trp8]-SRIF, 56: Somatostatin analog **56** was synthesized following the general procedure from 0.20 g of 2-Cl-Trt resin (0.8 mmol/g) and using Fmoc-L-Tmp-OH, affording 0.16 g in 59% yield (99% purity after purification). HPLC: $t_R = 13.8$ [Gradient 25-60%B in 20min, flux: 1 mL.min⁻¹, $\lambda = 220$ nm]. HRMS: calcd. for C₇₉H₁₁₀N₁₈O₁₉S₂: 1678.7636; found, 1678.7656.

[L-Tmp11_D-Trp8]-SRIF, 57: Somatostatin analog **57** was synthesized following the general procedure from 0.20 g of 2-Cl-Trt resin (0.8 mmol/g) and using Fmoc-L-Tmp-OH, affording 0.15 g in 42% yield (99% purity after purification). HPLC: $t_R = 14.3$ [Gradient 25-60% B in 20 min, flux: 1 mL.min⁻¹, $\lambda = 220$ nm]. HRMS: calcd. for C₇₉H₁₁₀N₁₈O₁₉S₂: 1678.7636; found, 1678.7644.

Linear Derivatives:

[Ala(3,14)_L-Msa7_D-Trp8]-SRIF, 58: Somatostatin analog **58** was synthesized following the general procedure from 0.10 g of 2-Cl-Trt resin (0.8 mmol/g) and using Fmoc-L-Msa-OH, affording 0.12 g in 86% yield (99% purity after purification). HPLC: $t_R = 10.7$ [Gradient 25-60% B in 20 min, flux: 1 mL.min⁻¹, $\lambda = 220$ nm]. HRMS: calcd for C₇₉H₁₁₂N₁₈O₁₉: 1616.8351; found, 1616.8337.

[Phe(3,14)_L-Msa7_D-Trp8]-SRIF, 59: Somatostatin analog **59** was synthesized following the general procedure from 0.10 g of 2-Cl-Trt resin (0.8 mmol/g) and using Fmoc-L-Msa-OH, affording 0.14 g in 81% yield (99% purity after purification). HPLC: $t_R = 12.2$ [Gradient 25-60% B in 20 min, flux: 1 mL.min⁻¹, $\lambda = 220$ nm]. HRMS: calcd for C₉₁H₁₂₀N₁₈O₁₉: 1768.8977; found, 1768.8969.

Analogs containing the Dfp amino acid:

[L-Dfp6_D-Trp8]-SRIF, 60: Somatostatin analog **60** was synthesized following the general procedure from 0.20 g of 2-Cl-Trt resin (0.8 mmol/g) and using Fmoc-L-Dfp-OH, affording 0.08 g in 43% yield (99% purity after purification). HPLC: $t_R = 16.5$ [Gradient 25-60% B in 20 min, flux: 1 mL.min⁻¹, $\lambda = 220$ nm]. HRMS: calcd. for C₇₆H₁₀₂F₂N₁₈O₁₉S₂: 1672.6978; found, 1672.6981.

[L-Dfp7_D-Trp8]-SRIF, 61: Somatostatin analog **61** was synthesized following the general procedure from 0.20 g of 2-Cl-Trt resin (0.8 mmol/g) and using Fmoc-L-Dfp-OH, affording 0.11 g in 53% yield (99% purity after purification). HPLC: $t_R = 15.6$ [Gradient 25-60%B in 20min, flux: 1 mL.min⁻¹, $\lambda=220$ nm]. HRMS: calcd for C₇₆H₁₀₂F₂N₁₈O₁₉S₂: 1672.6978; found, 1672.6964.

[L-Dfp11_D-Trp8]-SRIF, 62: Somatostatin analog **62** was synthesized following the general procedure from 0.20 g of 2-Cl-Trt resin (0.8 mmol/g) and using Fmoc-L-Dfp-OH, affording 0.14 g in 67% yield (99% purity after purification). HPLC: $t_R = 17.2$ [Gradient 25-60% B in 20 min, flux: 1 mL.min⁻¹, $\lambda=220$ nm]. HRMS: calcd. for C₇₆H₁₀₂F₂N₁₈O₁₉S₂: 1672.6978; found, 1672.6894.

Analogs containing the Cha amino acid:

[L-Cha6_D-Trp8]-SRIF, 63: Somatostatin analog **63** was synthesized following the general procedure from 0.4 g of 2-Cl-Trt resin (0.8 mmol/g) and using Fmoc-L-Cha-OH, affording 0.38 g in 66% yield (99% purity after purification). HPLC: $t_R = 12.3$ [Gradient 25-60% B in 20 min, flux: 1 mL.min⁻¹, $\lambda=220$ nm]. HRMS: calcd. for C₇₆H₁₁₀N₁₈O₁₉S₂: 1642.7631; found, 1642.7630.

[L-Cha7_D-Trp8]-SRIF, 64: Somatostatin analog **64** was synthesized following the general procedure from 0.4 g of 2-Cl-Trt resin (0.8 mmol/g) and using Fmoc-L-Cha-OH, affording 0.34 g in 59% yield (98% purity after purification). HPLC: $t_R = 16.4$ [Gradient 25-60% B in 20 min, flux: 1 mL.min⁻¹, $\lambda=220$ nm]. HRMS: calcd. for C₇₆H₁₁₀N₁₈O₁₉S₂: 1642.7631; found, 1642.7632.

[L-Cha11_D-Trp8]-SRIF, 65: Somatostatin analog **65** was synthesized following the general procedure from 0.4 g of 2-Cl-Trt resin (0.8 mmol/g) and using Fmoc-L-Cha-OH, affording 0.35 g in 61% yield (98% purity after purification). HPLC: $t_R = 16.3$ [Gradient 25-60% B in 20 min, flux: 1 mL.min⁻¹, $\lambda=220$ nm]. HRMS: calcd. for C₇₆H₁₁₀N₁₈O₁₉S₂: 1642.7631; found, 1642.7632.

[L-Cha6,11_D-Trp8]-SRIF, 66: Somatostatin analog **66** was synthesized following the general procedure from 0.2 g of 2-Cl-Trt resin (0.8 mmol/g) and using Fmoc-L-Cha-OH, affording 0.11 g in 48% yield (98% purity after purification). HPLC: $t_R = 17.6$ [Gradient 25-60% B in 20 min, flux: $1 \text{ mL}\cdot\text{min}^{-1}$, $\lambda=220 \text{ nm}$]. HRMS: calcd. for $\text{C}_{76}\text{H}_{116}\text{N}_{18}\text{O}_{19}\text{S}_2$: 1648.8100; found, 1648.8114.

Highly modified analogs:

[L-Dfp6_L-Msa7_L-Tmp11_D-Trp8]-SRIF, 67: Somatostatin analog **67** was synthesized following the general procedure from 0.05 g of 2-Cl-Trt resin (0.8 mmol/g) and using Fmoc-L-Tmp-OH, Fmoc-L-Dfp_OH and Fmoc-L-Msa-OH, affording 0.06 g in 73% yield (99% purity after purification). HPLC: $t_R = 17.4$ [Gradient 25-60% B in 20 min, flux: $1 \text{ mL}\cdot\text{min}^{-1}$, $\lambda = 220 \text{ nm}$]. HRMS: calcd. for 1756.7917; found, 1756.7923.

[L-Tmp6_L-Msa7_L-Dfp11_D-Trp8]-SRIF, 68: Somatostatin analog **68** was synthesized following the general procedure from 0.05 g of 2-Cl-Trt resin (0.8 mmol/g) and using Fmoc-L-Tmp-OH, Fmoc-L-Dfp_OH and Fmoc-L-Msa-OH, affording 0.03 g of **68** in 42% yield (99% purity after purification). HPLC: $t_R = 17.9$ [Gradient 25-60% B in 20 min, flux: $1 \text{ mL}\cdot\text{min}^{-1}$, $\lambda=220 \text{ nm}$]. HRMS: calcd. for 1756.7917; found, 1756.7929.

[L-Dfp6,11_L-Msa7_D-Trp8]-SRIF, 69: Somatostatin analog **69** was synthesized following the general procedure from 0.05 g of 2-Cl-Trt resin (0.8 mmol/g) and using Fmoc-L-Dfp-OH and Fmoc-L-Msa-OH, affording 0.05 g in 61% yield (99% purity after purification). HPLC: $t_R = 16.1$ [Gradient 25-60% B in 20 min, flux: $1 \text{ mL}\cdot\text{min}^{-1}$, $\lambda=220 \text{ nm}$]. HRMS: calcd. for 1756.7917; found, 1756.7923.

9.3. Computational methods

All NMR data was processed with NMRPipe.⁷ Cara⁸ was used to assign the spectra. Distance restraints derived from fully assigned peaks in NOESY experiments were used for structure calculation. The structures were calculated under the supervision of Prof. Maria J. Macias with the programs CNS⁹ and StructCalc (StructCalc program was used by courtesy of its recent developers (unpublished data), Pau Martín-Malpartida and Maria J. Macias). PyMOL was used to visualize the structures and generate the figures. Statistics from the analysis are shown in the tables of the attached CD.

9.4. Receptor-subtype selectivity assays:

All peptides were subjected to anion exchange ($F_3C(O)O^- \rightarrow AcO^-$) by using DOWEX resin (Dowex Monosphere 550A (OH)). Biological tests were carried out with previously purified peptides containing acetate counter-ion.

Preparation of cells stably expressing the SRIF-14 receptor: CHO-K1 cells (American Type Culture Collection, Rockville, MD) were maintained in Kaighn's modification of Ham's F12 medium (F12K) supplemented with 10% fetal bovine serum. pcDNA3 vectors encoding each of the SSTR receptors were obtained from UMR cDNA Resource Center (University of Missouri, MO, USA). CHO-K1 cells were stably transfected with these vectors by using Lipofectamine (Invitrogen). Stable clones were selected in F12K containing G418 (700 $\mu\text{g}/\text{ml}$) and were screened for SRIF-14 receptor expression and then maintained in a G418 (400 $\mu\text{g}/\text{ml}$)-containing medium. Expression was detected by RT-PCR and Western-blot and confirmed by radioligand binding assays.

7 F. Delaglio, S. Grzesiek, G. Vuister, G. Zhu, J. Pfeifer, A. Bax *J. Biomol. NMR* **1995**, *6*, 277-293.

8 R. Keller, *The Computer Aided Resonance Assignment Tutorial*, 1st ed. CANTINA Verlag, 2004.

9 A. T. Brunger, P. D. Adams, G. M. Clore, W. L. DeLano, P. Gros, R. W. Grosse-Kunstleve, J. S. Jiang, J. Kuszewski, M. Nilges, N. S. Pannu, R. J. Read, L. M. Rice, T. Simonson, G. L. Warren *Acta Crystallogr. D Biol. Crystallogr.* **1998**, *54*, 905-921.

Receptor Ligand-Binding Assay: All receptor-binding assays were performed with membranes isolated from CHO-K1 cells expressing the cloned human SRIF-14 receptor, as reported previously.¹⁰ The assay buffer consisted of 50 mM Tris (pH 7.5) with 1 nM EGTA, 5 mM MgCl₂, leupeptin (10 µg/ml), pepstatin (10 µg/ml), bacitracin (200 µg/ml), aprotinin (0.5 µg/ml) and 0.2% BSA. CHO-K1 cell membranes, radiolabeled SRIF-14 and unlabelled test compounds were diluted in this assay buffer. All assays were performed in 96-well polypropylene plates. Ten micrograms of membrane proteins were incubated with 0.1nM of ¹²⁵I-Tyr¹¹-SRIF (specific activity-2000 Ci/mmol) in the presence or absence of various concentrations of unlabeled peptides (1pM-1000 nM) in a total volume of 200 µl, for 1 h at 30 °C. The binding reaction was terminated by vacuum filtration over Whatman GF/F glass fibre filters previously pre-soaked in 0.5% (w/v) polyethyleneimine and 0.2% bovine serum albumin, using a 98-well harvester (Tomtec). The filters were washed with ice-cold 50 mM Tris-HCl (pH 7.5) and dried, after which scintillator sheets were melted onto the filter and the bound radioactivity was analyzed in a liquid scintillation counter (microβ plus, Wallac). Specific binding was defined as the total ¹²⁵I-Tyr¹¹-SRIF binding minus the amount bound in the presence of 1000 nM SRIF (non-specific binding). Inhibition curves were analyzed and IC₅₀ values were calculated using a curve-fitting program (GraphPad Prism, La Jolla, Ca). The K_i values for the compounds were determined as described by Cheng and Prusoff.¹¹ Data are the mean ± S.E.M. of, at least, three separate experiments, each performed in triplicate. K_d values for [¹²⁵I]-Tyr¹¹-somatostatin-14 with each of the five receptors were determined from isotope saturation experiments. The apparent dissociation constants were 0.68, 0.09, 0.41, 0.96, and 0.27 nM for somatostatin receptors 1 through sst5, respectively.

9.5. Serum selectivity assays

Half-life time determinations were carried out by BCN peptides. A peptide solution of 6 mg/mL in water (1.8 mg in 300 µL) was sterilized by filtration (0.22 µm filter).

10 S. Rens-Domiano, S. F. Law, Y. Yamada, S. Seino, G. I. Bell, T. Reisine *Mol. Pharmacol.* **1992**, *42*, 28-34.

11 Y. Cheng, W. H. Prusoff *Biochem. Pharmacol.* **1973**, *22*, 3099-3108.

Aliquots from this solution (10 μL) were added to 90 μL of serum (from human male AB plasma, sterile filtered; SIGMA). These solutions were incubated at 37 $^{\circ}\text{C}$ and samples were taken at 5 min, 30 min, 1 h, 2 h, 3 h, 5 h, 8 h, 15 h, 20 h, 24 h, 30 h and 48 h. Each sample was treated with acetonitrile (200 μL) and cooled to 0 $^{\circ}\text{C}$ for 30 min to precipitate the proteins. The suspensions were centrifuged at 10000 rpm, during 10 min at 4 $^{\circ}\text{C}$. The process was repeated twice. The solution was filtered through 0.45 μm PVDF filters (Millipore). The samples were analyzed by RP-HPLC; eluent: 20-80% B (B=0.07%TFA in acetonitrile); 20 min gradient; flow: 1 mL/min. For each peptide the experiment was repeated twice. Cleavage of the Ala1-Gly2 moiety was not considered as peptide deterioration.

The half-life of the peptide in serum was calculated from the analysis of the degradation data. Analysis of the kinetics of degradation was carried out using a linear fit (least squares) of the natural logarithm of the percentage of peak area integration with respect to time. The determination of the slope, the experimental constant, allowed the calculation of the half-life:

$$\ln[A] = \ln[A_0] - K_e \cdot t$$

$$t_{1/2} = \ln 2 / K_e$$

Appendix I

Summary in Spanish

Capítulo 1. Introducción, antecedentes y objetivos.

La hormona peptídica somatostatina (SRIF) fue descubierta por primera vez en extractos de hipotálamo en 1973, como una forma activa de 14 aminoácidos (Figura S.1).¹ Esta hormona está implicada en un gran número de funciones biológicas, mediadas por la interacción directa del péptido con una familia de cinco GPCRs, que contienen ciertas similitudes estructurales.² Estos receptores son comúnmente denominados SSTR1-5, y se diferencian tanto en sus propiedades farmacológicas como en su distribución en tejidos. Uniéndose a estos receptores en ciertas células, la somatostatina actúa como neuromodulador y neurotransmisor, y también como un potente inhibidor de ciertos procesos de secreción y proliferación celular.³

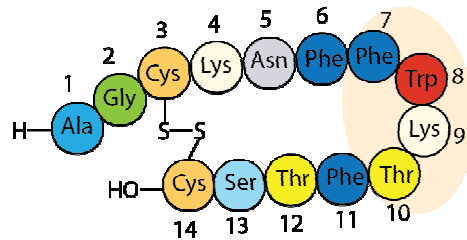


Figura S.1. Secuencia de aminoácidos de la somatostatina, con su fármaco marcado.

La somatostatina es capaz de promover efectos de inhibición únicos tanto en secreción endocrina —de la hormona del crecimiento, insulina, glucagón, gastrina, etc.—como secreción exocrina —de ácido gástrico, fluido intestinal y enzimas pancreáticas—.⁴ Este amplio perfil biológico ha llevado a la somatostatina natural a ser explotada en experimentos clínicos para el tratamiento de un amplio rango de dolencias, incluyendo la diabetes de tipo I y II, la hipersecreción tumoral, adenomas y gastrinomas pituitarios o afecciones gastrointestinales como úlceras gástricas o pancreatitis.⁵ Sin embargo, no ha sido posible maximizar el potencial

1 a) P. Brazeau, W. Vale, R. Burgus, N. Ling, M. Butcher, J. Rivier, R. Guillemin, *Science* **1973**, *179*, 77-79; b) R. Burgus, N. Ling, M. Butcher, R. Guillemin, *Proc. Natl. Acad. Sci. U S A* **1973**, *70*, 684-688.

2 D. Hoyer, G. I. Bell, M. Berelowitz, J. Epelbaum, W. Feniuk, P. P. A. Humphrey, A. O'Carroll, Y. C. Patel, A. Schonbrunn, et al *Trends Pharmacol. Sci.* **1995**, *16*, 86-88.

3 a) G. Weckbecker, F. Raulf, B. Stolz, C. Bruns, *Pharmacol. Ther.* **1993**, *60*, 245-264; b) G. Gillies, *Trends Pharmacol. Sci.* **1997**, *18*, 87-95.

4 a) S. Reichlin, *N. Engl. J. Med.* **1983**, *309*, 1495-1501; b) S. Reichlin, *N. Engl. J. Med.* **1983**, *309*, 1556-1563.

terapéutico de la somatostatina debido a su bajo tiempo de vida media en plasma (que, en vivo, es menor de 3 min) y su falta de selectividad por sus receptores. El hecho de que se degrade tan rápidamente hace necesaria una constante infusión del medicamento, y su amplio espectro de actividad biológica conlleva a tratamientos poco óptimos con numerosos efectos secundarios.

Con el objetivo de superar esas limitaciones, en los últimos veinte años se han sintetizado un gran número de análogos de somatostatina. Las investigaciones pioneras de Brazeau, Coy, Rivier, Schally y Vale, entre otros, contribuyeron al descubrimiento de los primeros análogos de somatostatina.^{1a,5} Bauer y colaboradores, en Novartis, sintetizaron el octreótido, un derivado ciclooctapeptídico de SRIF con mayor estabilidad metabólica y que inhibe la secreción de un gran número de hormonas.⁶ Octreótido (Sandostatin®), lanreótido (Somatuline®),⁷ vapreotide (Sanvar®)⁸ y pasireotide (Signifor®)⁹ son los cuatro análogos sintéticos que, hasta la fecha, han llegado al mercado (Figura S.2). Tres de ellos son octapéptidos, mientras que el pasireotide es un hexapéptido, conteniendo un anillo más pequeño y rígido que el que tiene SRIF. Por ello, son análogos cuyo efecto es más duradero y su selectividad frente a los cinco receptores distintos es mayor. Estructuralmente comparten un fragmento similar que forma un β -turn e incluye los residuos Phe/Thr7-D-Trp8-Lys9-Thr/Val10. Este fragmento constituye el farmacóforo de la hormona.^{5a}

El descubrimiento de los cinco receptores (SSTR1-5)^{4,10} reveló que los análogos comerciales octreótido y lanreótido se unen preferencialmente al receptor SSTR2.

5 a) J. Rivier, M. Brown, C. Rivier, N. Ling, W. Vale, *Pept., Proc. Eur. Pept. Symp., 14th* **1976**, 427-51; b) D. H. Coy, E. J. Coy, A. Arimura, A. V. Schally, *Biochem. Biophys. Res. Commun.* **1973**, *54*, 1267-1273.

6 a) W. Bauer, U. Briner, W. Doepfner, R. Haller, R. Huguenin, P. Marbach, T. J. Petcher, J. Pless *Life Sci.* **1982**, *31*, 1133-1140.

7 J. Marek, V. Hána, M. Kršek, V. Justová, F. Catus, F. Thomas, *Eur. J. Endocrinol.* **1994**, *131*, 20-26.

8 P. M. Girard, E. Goldschmidt, D. Vittecoq, P. Massip, J. Gastiaburu, M. C. Meyohas, J. P. Coulaud, A. V. Schally, *AIDS* **1992**, *6*, 715-718.

9 En relación a SOM230 (Signifor, aprobado recientemente para el tratamiento de Cushing) see: C. Bruns, I. Lewis, U. Briner, G. Meno-Tetang, G. Weckbecker, *Eur. J. Endocrinol.* **2002**, *146*, 707-716.

10 Y. C. Patel, C. B. Srikant, *Endocrinology* **1994**, *135*, 2814-2817.

Esto condujo a numerosas aproximaciones racionales con el objetivo de descubrir análogos peptídicos (o no peptídicos) de somatostatina que se unieran selectivamente a ciertos receptores. La mayor parte de la investigación se centró en la síntesis y el estudio de derivados de octreótido, que es considerado como un importante precursor en el descubrimiento de fármacos. De esta manera, mientras muy pocos análogos reales (de catorce aminoácidos) de somatostatina fueron sintetizados, se publicaron los estudios de gran número de octapéptidos que contenían ciertas modificaciones clave: intercambio de aminoácidos, ajustes del tamaño del anillo, modificaciones del enlace disulfuro, múltiples *N*-metilaciones o introducción de cadenas de polietilenglicol.¹¹ Muchos de estos análogos mejoraban las propiedades de la hormona natural como fármaco.

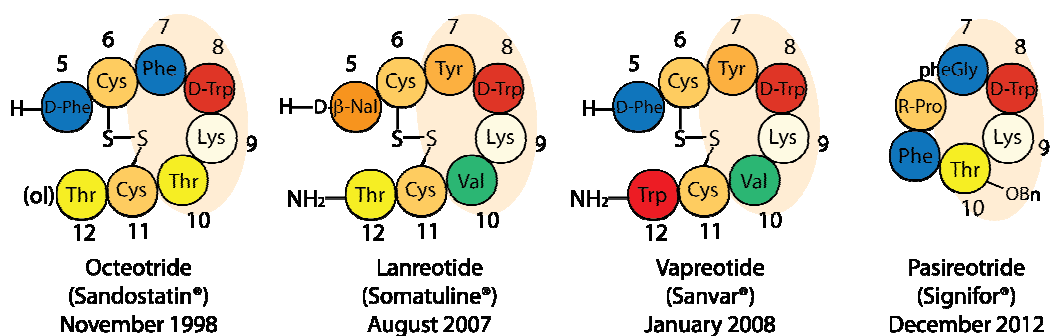


Figura S.2. Secuencia de aminoácidos de los análogos comerciales, con sus respectivos farmacóforos marcados. R-Pro = [(2-aminoetil)aminocarbonilo]-L-prolina.

Los recientes avances en la síntesis de péptidos en fase sólida nos llevaron a reconsiderar la estructura completa de la somatostatina (es decir, los catorce residuos) como molde para sintetizar nuevos análogos que tuvieran mayor estabilidad y selectividad. Además, trabajando con tetradecapéptidos estaríamos estructuralmente mucho más cerca de la hormona natural de lo que lo están los octapéptidos. Pensamos que, si conseguimos obtener análogos

11 a) C. R. R. Grace, J. Erchegy, S. C. Koerber, J. C. Reubi, J. Rivier, R. Riek, *J. Med. Chem.* **2006**, *49*, 4487-4496. b) A. Di Cianni, A. Carotenuto, D. Brancaccio, E. Novellino, J. C. Reubi, K. Beetschen, A. M. Papini, M. Ginanneschi, *J. Med. Chem.* **2010**, *53*, 6188-6197. c) J. Chatterjee, B. Laufer, J. G. Beck, Z. Helyes, E. Pintér, J. Szolcsányi, A. Horvath, J. Mandl, J. C. Reubi, G. Kéri, H. Kessler, *ACS Med. Chem. Lett.* **2011**, *2*, 509-514. d) M. Morpurgo, C. Monfardini, L. J. Hofland, M. Sergi, P. Orsolini, J. M. Dumont, F. M. Veronese, *Bioconjugate Chem.* **2002**, *13*, 1238-1243.

conformacionalmente rígidos de catorce residuos con alta selectividad frente a ciertos receptores, podríamos llegar a caracterizar la principal conformación de SRIF cuando se une a éstos.

La estructura de la somatostatina ha sido objeto de debate durante las tres últimas décadas, y numerosos estudios han probado la flexibilidad innata de esta hormona en disolución.¹² Todos los intentos de caracterizar su estructura en detalle han fallado, y actualmente la estructura nativa de la somatostatina se considera como un conjunto de varias conformaciones en equilibrio, algunas de las cuales son parcialmente estructuradas.¹³

Varios estudios revelaron la posibilidad de que una interacción aromática entre las Phe7, Phe7 ó Phe11 jugara un papel fundamental en la estabilización estructural de esta hormona.¹⁴ El intercambio los aminoácidos Phe6 y Phe11 por alanina daba lugar a un análogo un 98% menos activo.^{15,16} Sin embargo, cuando estos dos residuos eran unidos por una cistina, el péptido correspondiente retenía la actividad biológica,¹⁴ sugiriendo una cercanía espacial entre estos dos residuos en algunas de las conformaciones bioactivas de SRIF (Figura S.3).^{12a} Esta hipótesis fue respaldada por estudios de RMN llevados a cabo por Arison y colaboradores.¹⁷ Estos experimentos de RMN probaron que los desplazamientos químicos de los protones de Phe6 eran dependientes de la temperatura, que sugería que éstos se encuentran

12 a) M. Knappenberg, A. Michel, A. Scarso, J. Brison, J. Zanen, K. Hallenga, P. Deschrijver, G. Van Binst, *Biochim.Biophys.Acta, Protein Struct. Mol. Enzymol.* **1982**, 700, 229-246; b) K. Hallenga, G. Van Binst, A. Scarso, A. Michel, M. Knappenberg, C. Dremier, J. Brison, J. Dirx, *FEBS Lett.* **1980**, 119, 47-52; c) L. A. Buffington, V. Garsky, J. Rivier, W. A. Gibbons *Biophys. J.* **1983**, 41, 299-304; d) L. A. Buffington, V. Garsky, J. Rivier, W. A. Gibbons, *Int. J. Pept. Protein Res.* **1983**, 21, 231-241.

13 A. Kaerner, K. H. Weaver, D. L. Rabenstein, *Magn. Reson. Chem.* **1996**, 34, 587-594.

14 a) J. E. Rivier, M. R. Brown, W. W. Vale, *J. Med. Chem.* **1976**, 19, 1010-1013; b) D. F. Veber, F. W. Holly, W. J. Paleveda, R. F. Nutt, S. J. Bergstrand, M. Torchiana, M. S. Glitzer, R. Saperstein, R. Hirschmann, *Proc. Natl. Acad. Sci. U. S. A.* **1978**, 75, 2636-2640.

15 W. W. Vale, C. Rivier, M. R. Brown, J. E. Rivier *Hypothalamic Peptide Hormones and Pituitary Regulation, Advances in Experimental Medicine and Biology.* Plenum Press **1977**, pp 123-156.

16 Los análogos fueron comparados con SRIF en su habilidad para disminuir los niveles de insulina y glucagón en la vena porta de ratas anestesiadas.

17 B. H. Arison, R. Hirschmann, W. J. Paleveda, S. F. Brady, D. F. Veber, *Biochem. Biophys. Res. Commun.* **1981**, 100, 1148-115

apantallados por un anillo aromático. Cutnell y colaboradores realizaron varios estudios de RMN de SRIF y un análogo más corto, y ofrecieron información acerca de la geometría de esta supuesta interacción no covalente.¹⁸ El efecto de la temperatura en el desplazamiento de los protones de la Phe6 no era consistente con un *stacking* paralelo, por lo que se propuso una interacción perpendicular (con los protones *orto*- y *meta*- de la Phe6 apuntando cerca del anillo del segundo ciclo aromático). Los autores también observaron que la sustitución de la Phe7 por alanina en este análogo retenía el desplazamiento a campos altos de los protones *orto*- de (presumiblemente) la Phe6, mientras que cuando era la Phe11 la que se sustituía por alanina, este desplazamiento desaparecía. Estas observaciones apoyaban la idea de que la Phe11 apantalla la Phe6 en esta supuesta interacción aromática “perpendicular”, estabilizando así ciertas conformaciones bioactivas en la hormona natural.

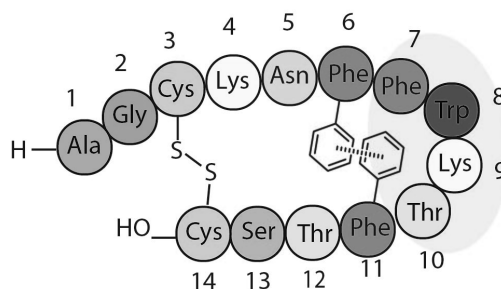


Figura S.3. Interacción aromática propuesta entre Phe6-Phe11.

Por otro lado, este mismo tema fue tratado de nuevo por Van Binst y colaboradores cuatro años más tarde.¹⁹ Tras llevar a cabo experimentos bidimensionales de RMN (NOESY), no se observaron NOEs entre la Phe11 y ninguno de los demás residuos aromáticos. Estos autores concluyeron que la interacción Phe6-Phe11 no está presente significativamente en la principal conformación que

18 J. D. Cutnell, G. N. La Mar, J. L. Dallas, P. Hug, H. Ring, G. Rist, *Biochim.Biophys.Acta, Protein Struct.Mol.Enzymol.* **1982**, 700, 59-66.

19 a) A. W. H. Jans, K. Hallenga, G. Van Binst, A. Michel, A. Scarso, J. Zanen, *Biochim.Biophys.Acta, Protein Struct.Mol.Enzymol.* **1985**, 827, 447-452. b) E. M. M. Van den Berg, A. W. H. Jans, G. Van Binst, *Biopolymers* **1986**, 25, 1895-1908.

SRIF adopta en solución acuosa, y propusieron una orientación de la Phe7 hacia los protones aromáticos de la Phe6. En este sentido, Rivier y colaboradores llevaron a cabo un *scan* de tirosina en la secuencia de SRIF.²⁰ Estos estudios sugerían que la Phe6 estaría involucrada en el proceso de activación del receptor, mientras que la Phe7 se involucraría más en la estabilización interna de la estructura secundaria de SRIF por asociándose vía *stacking* con otros residuos aromáticos. Estas hipótesis no han podido ser nunca probadas o rechazadas hasta ahora, pues no ha sido posible obtener estructuras detalladas por RMN o rayos-X de la estructura de este péptido. En los años 90, el “boom” de los octapéptidos hizo que este tema fuera pasado por alto y toda la atención se centró en la síntesis de análogos de somatostatina de ocho aminoácidos que, de hecho, contienen un enlace disulfuro como sustituto de la presunta interacción aromática entre Phe6 y Phe11 (Figuras S.2 y S.3).

Nosotros consideramos que el estudio de las presuntas interacciones aromáticas que estabilizan ciertas conformaciones bioactivas en SRIF podría funcionar como un método único para obtener análogos con mayor estabilidad y rigidez conformacional, así como una actividad biológica mejorada. Para ello, decidimos incorporar puntualmente ciertos aminoácidos aromáticos no naturales en el molde de 14 residuos de la somatostatina natural. Si algunas interacciones no covalentes se intensificaran, la flexibilidad conformacional disminuiría, y las estructuras 3D de estos tetradecapéptidos podrán ser susceptibles de ser caracterizadas por técnicas de RMN por primera vez. Idealmente, si estos análogos altamente estructurados son más estables y más selectivos frente a ciertos receptores que SRIF, sus conformaciones en disolución podrían aclarar qué particulares conformaciones adopta la hormona natural cuando se une a sus distintos receptores. Además, estos análogos de somatostatina altamente estables y selectivos podrían tener un importante potencial terapéutico.

En esta tesis doctoral estudiaremos la sustitución de las Phe6, Phe7 y Phe11 naturales por tres aminoácidos aromáticos no naturales (Figura S.4): 3-mesitilalanina

20 J. E. Rivier, M. R. Brown, W. W. Vale, *J. Med. Chem.* **1976**, *19*, 1010-1013.

(Msa), 3-(3',4',5'-trimetilfenil)-alanina (Tmp) y 3-(3',5'-difluorofenil)-alanina (Dfp). Seleccionamos estos tres residuos teniendo en cuenta su alta hidrofobicidad y sus peculiares propiedades electrónicas y estéricas.

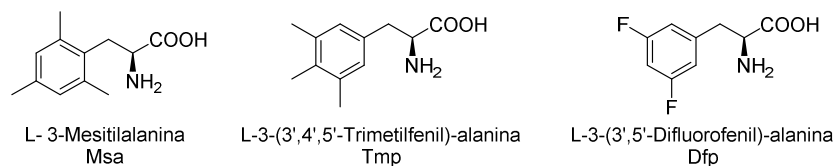


Figura S.4. Aminoácidos aromáticos no naturales seleccionados para su introducción en la secuencia de la somatostatina.

La presente tesis doctoral ha sido organizada de la siguiente manera:

Las síntesis asimétricas de los aminoácidos aromáticos no naturales han sido descritas en el **Capítulo 2**.

En el **Capítulo 3**, describimos nuestra primera aproximación enfocada al estudio de las interacciones aromáticas en la somatostatina. En esta parte de la tesis, estudiamos diez análogos que contenían el aminoácido Msa. La introducción de un residuo de Msa en posición 6, 7 u 11 nos permitió obtener análogos con una alta rigidez conformacional, puesto que las interacciones entre ciertos residuos aromáticos se incrementaban.

En el **Capítulo 4**, discutimos sobre si el impacto estructural causado por la Msa es un resultado derivado de su alta densidad electrónica o de la rigidez intrínseca de su cadena lateral (debido a la rigidez conformacional que ocasiona la sustitución en *orto*-).

En este punto, observamos que se obtenían resultados excelentes cuando la Phe7 era sustituida por residuos de Msa o de Tmp. En el **Capítulo 5**, investigamos el alcance de esta modificación en ausencia del enlace disulfuro.

El **Capítulo 6** engloba el estudio de análogos de somatostatina que contienen el aminoácido Dfp. Consideramos que este residuo, que contiene un ciclo aromático difluorado y pobre en electrones, sería clave para continuar estudiando las

interacciones aromáticas en somatostatina, debido al pequeño efecto estérico pero gran efecto electrónico que implica.

Los resultados obtenidos en estos capítulos previos nos llevaron a investigar, por separado, las contribuciones relativas de la hidrofobicidad y de los factores electrónicos a las interacciones aromáticas en SRIF. En el **Capítulo 7**, estudiamos cuatro análogos en los que las fenilalaninas naturales han sido sustituidas por ciclohexilalaninas.

Finalmente, describimos cuatro análogos tetradecapeptídicos que contenían, al mismo tiempo, más de dos aminoácidos aromáticos no naturales (*i.e.* Msa, Tmp y Dfp). El efecto combinado de estos residuos en la estructura, estabilidad y selectividad de estos análogos es comentado en el **Capítulo 9**.

Desde el punto de vista metodológico, los principales objetivos durante el PhD se enumeran aquí:

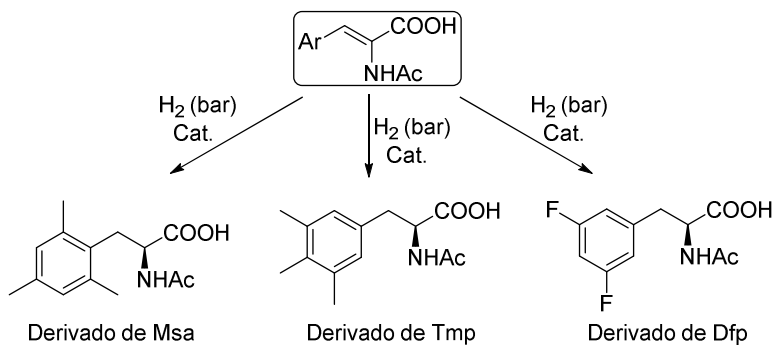
1. Escalar la síntesis asimétrica de aminoácidos aromáticos no naturales que posean determinadas propiedades electrónicas y/o estéricas.
2. Sintetizar nuevos análogos de somatostatina de 14 residuos que contengan, como modificaciones puntuales, alguno de estos aminoácidos no naturales en su secuencia.
3. Estudiar las estructuras de los análogos sintéticos por técnicas computacionales y de RMN. En el caso de obtener péptidos altamente estructurados, sus conformaciones mayoritarias deberán ser caracterizadas y discutidas en detalle.
4. Determinar si existe alguna interacción aromática que estabiliza ciertas conformaciones bioactivas en SRIF, y si la hay, identificar los residuos implicados.
5. Obtener los valores de K_i de los nuevos análogos por ensayos de *binding* para los receptores de somatostatina.

6. Determinar los tiempos de vida media de los análogos sintéticos en suero humano y relacionar dicha estabilidad con las modificaciones estructurales.
7. Ganar conocimientos sobre las relaciones estructura-actividad de la somatostatina natural y de sus análogos: identificar, por analogía, las conformaciones activas de la hormona natural cuando se une a un receptor específico y determinar factores estructurales o propiedades clave que sean necesarias para la unión de SRIF o sus análogos a los receptores SSTR1-5.

Capítulo 2. Síntesis enantioselectiva de aminoácidos aromáticos no naturales.

Dado nuestro interés en introducir este tipo de compuestos en la secuencia de la somatostatina, necesitábamos plantear síntesis asimétricas eficientes para obtener estos aminoácidos convenientemente protegidos a escala de multigramo. Teniendo en cuenta resultados previos que Rosario Ramón obtuvo durante su tesis, propusimos introducir la quiralidad en estos compuestos por una reacción de hidrogenación asimétrica (Esquema S.1).²¹ Además, un proyecto destinado al descubrimiento de ligandos efectivos para este tipo de catálisis se estaba llevando a cabo en nuestro grupo de investigación durante esa época. Por lo tanto, estábamos animados a recopilar nuevos sustratos (derivados de deshidroaminoácidos) susceptibles de ser hidrogenados usando estos nuevos ligandos.

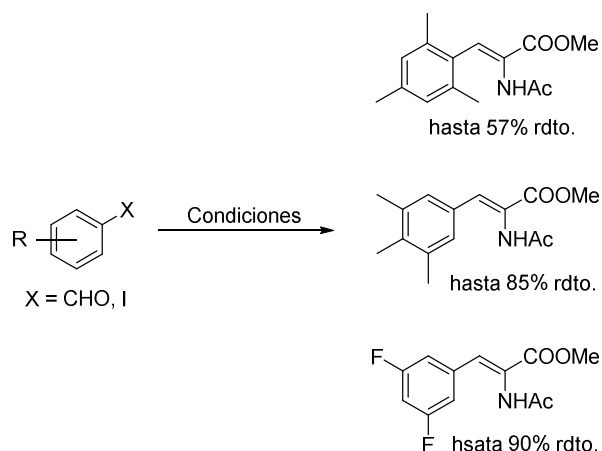
²¹ P. Etayo, A. Vidal-Ferran, *Chem. Soc. Rev.*, **2013**,42, 728-754.



Esquema S.1. Ruta propuesta para la síntesis de los derivados de aminoácidos por hidrogenación asimétrica.

Síntesis de los derivados de deshidroaminoácidos:

Puesto que los ciclos aromáticos de estos aminoácidos son distintos, los son también sus propiedades. Por ello, propusimos y probamos cuatro rutas distintas para llegar a estos intermedios clave: olefinación de Horner-Wadsworth-Emmons,²² reacción de Heck,²³ vía azalactona²⁴ y la reacción de Perkin.²⁵ Distintas condiciones de reacción nos permitieron obtener los deshidroaminoácidos correspondientes con rendimientos de hasta el 90% (Esquema S.2).



Esquema S.2. Síntesis de los distintos derivados de deshidroaminoácidos.

22 W. S. Wadsworth, W. D. Emmons, *J. Org. Chem.* **1961**, *83*, 1733-1738.

23 M. Suhartono, M. Weidlich, T. Stein, M. Karas, G. Dürner, M. W. Göbel, *Eur. J. Org. Chem.* **2008**, *2008*, 1608-1614.

24 a) E. E. Jun, *Justus Liebigs Ann. Chem.*, **1893** 275,1-8; b) J. Lamb, W. Robson, *Biochem J.* **1931** *25*, 1231-1236.

25 a) W. H. Perkin, *J. Chem. Soc.* **1868**, *21*, 181-186; b) J. F. J. Dippy, R. M. Evans, *J. Org. Chem.* **1950**, *15*, 451-456.

Hidrogenación asimétrica catalizada por complejos de rodio.

Mientras llevábamos a cabo las síntesis de estos compuestos, en nuestro grupo de investigación se descubrió el ligando MaxPHOS. Esta sal de fosfonio, estable al aire, ofreció resultados preliminares muy prometedores para la hidrogenación enantioselectiva de derivados de aminoácidos cuando se complejaba con Rh (I).²⁶ El sistema [(COD) (S)-MaxPHOS] Rh(I)BF₄ fue usado como catalizador para la hidrogenación asimétrica de nuestros derivados de deshidroaminoácidos con excelentes resultados (Tabla S.1).

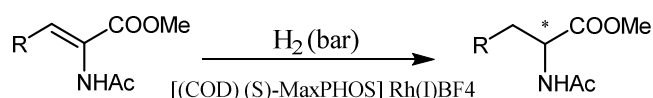


Tabla S.1. Síntesis de los acetamidoésterse de Msa, Tmp y Dfp enantioméricamente enriquecidos mediante una hidrogenación asimétrica usando el Rh(I)-MaxPHOS como sistema catalítico.^a

Entrada	R	Disolvente	T ^a	Presión	Rdto.	e.e.
1		MeOH	25 °C	40 bar	78 %	n.m.
2		MeOH	25 °C	60 bar	99 %	96 % ^b (S)
3		MeOH	25 °C	5 bar	99 %	98 % (S)
4		MeOH	25 °C	2 bar	99 %	99 % (S)
5		MeOH	25 °C	20 bar	99 %	95 % (S)
6		MeOH	25 °C	15 bar	99 %	96 % (S)
7		MeOH	25 °C	2 bar	< 5%	-
8		MeOH	25 °C	5 bar	99 %	97 % (S)

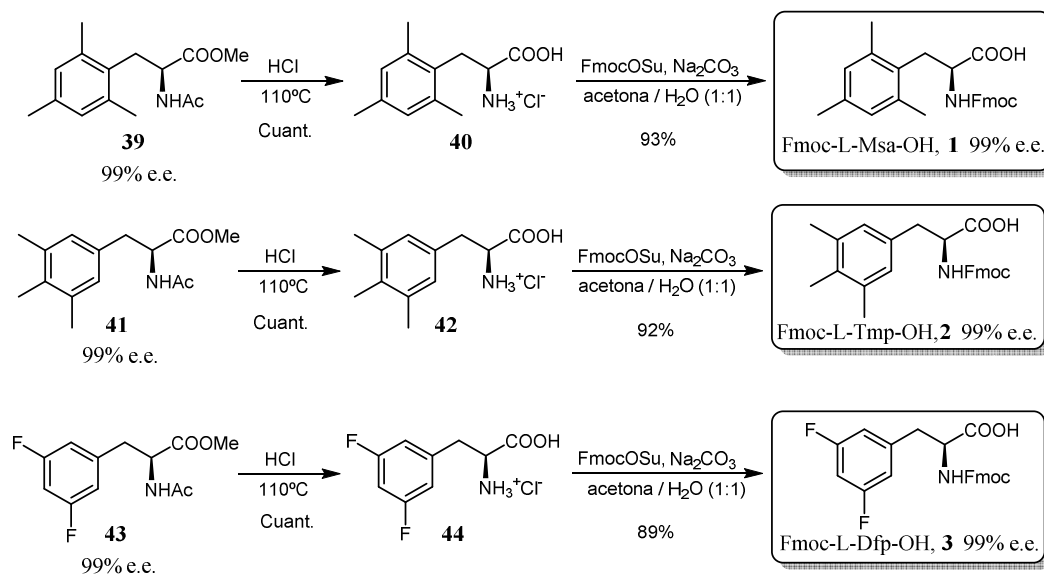
a: Todos los tiempos de reacción fueron 24 h. 3% cat. se usó en todos los casos. n.m.: no medido. b: 99% e.e. tras recristalización. De todas las probadas, sólo se muestran las condiciones más relevantes.

Hidrólisis y protección con Fmoc.

En todos los casos, la hidrólisis ácida y la posterior protección del grupo amino transcurrió con rendimientos excelentes y sin racemización. Esto nos permitió obtener los aminoácidos correspondientes a escala de multigramo, convenientemente

26 M. Reves, C. Ferrer, T. Leon, S. Doran, P. Etayo, A. Vidal-Ferran, A. Riera, X. Verdaguer, *Angew. Chem., Int. Ed.* **2010**, *49*, 9452-9455.

protegidos para su posterior uso en SPPS, en buenos rendimientos globales y con excelentes excesos enantioméricos (Esquema S.3).



Esquema S.3. Hidrólisis y protección con Fmoc.

Capítulo 3. Análogos de somatostatina que contienen residuos de Msa en su secuencia.

Para empezar a estudiar las interacciones aromáticas en análogos de somatostatina, preparamos diez péptidos conteniendo este aminoácido como modificación puntual. Elegimos este residuo por la alta hidrofobicidad y densidad electrónica que los tres grupos metilos aportan a su cadena lateral, y también por la baja movilidad conformacional de ésta en comparación con la de la Phe.²⁷ Preparamos tres grupos de análogos: en el primero, introdujimos un residuo de Msa en lugar de una de las fenilalaninas naturales, en posición 6, 7 u 11; en el segundo grupo, incluimos además una modificación extra, pues sustituimos el triptófano en posición 8 por su enantiómero D-Trp8; los péptidos del tercer grupo de análogos, por otra parte,

27 E. Medina, A. Moyano, M. A. Pericas, A. Riera, *Helv. Chim. Acta* **2000**, 83, 972-988.

contienen dos o tres residuos de Msa en su secuencia. La actividad biológica y estabilidad en suero humano de estos péptidos se resume en la Tabla S.2.

Tabla S.2. Tiempos de vida media en suero humano y valores de K_i (nM) de SRIF, [D-Trp8]-SRIF, octreótido y análogos para los receptores SSTR1-5.^a

	SSTR1	SSTR2	SSTR3	SSTR4	SSTR5	$t_{1/2}$ (h) ^b
Somatostatina, SRIF	0.43 ±0.08	0.0016 ±0.0005	0.53 ±0.21	0.74 ±0.07	0.23 ±0.04	2.75
[D-Trp8]-SRIF	0.32 ±0.11	0.0010 ±0.0007	0.61 ±0.02	5.8 ±0.4	0.46 ±0.24	19.7
Octreótido	300 ±85	0.053 ±0.011	15 ±6	>10 ³	11 ±1	200
[L-Msa6]-SRIF, 45	8.5 ±1.4	1.5 ±1.4	1.4 ±1.3	3.6 ±1.5	0.91 ±1.45	2.1
[L-Msa7]-SRIF, 46	4.2 ±1.5	0.019 ±0.009	>10 ³	28 ±6	>10 ³	5.2
[L-Msa11]-SRIF, 47	20 ±5	0.024 ±0.004	2.8 ±0.2	6.5 ±2.2	2.1 ±0.7	1.7
[L-Msa6_D-Trp8], 48	3.1 ±0.9	4.6 ±0.7	0.78 ±0.12	4.7 ±0.9	0.36 ±0.03	26
[L-Msa7_D-Trp8], 49	0.33 ±0.09	0.0024 ±0.0011	7.5 ±0.6	>10 ³	>10 ³	25
[L-Msa11_D-Trp8], 50	3.4 ±1.3	0.14 ±0.06	1.3 ±0.2	>10 ³	0.73 ±0.19	41
[L-Msa6,7]-SRIF, 51	>10 ³	14 ±1	>10 ³	>10 ³	>10 ³	43.9
[L-Msa6,11]-SRIF, 52	>10 ³	>10 ³	13 ±2	>10 ³	9.1 ±0.6	nm ^c
[L-Msa7,11]-SRIF, 53	105 ±30	1.4 ±0.3	>10 ³	>10 ³	>10 ³	10
[L-Msa6,7,11]-SRIF, 54	>10 ³	>10 ³	>10 ³	>10 ³	>10 ³	93.3

a: Las celdas sombreadas representan valores cercanos a los de la hormona natural. b: Tiempo de vida media en suero humano. c: No medido.

Estructura:

Compuestos con una única sustitución de Msa: Los espectros de NOESY de estos análogos mostraron que, en disolución, presentan una conformación mayoritaria. Esto nos permitió analizar la estructura de dichas conformaciones por técnicas computacionales y de RMN. Es la primera vez que se obtienen análogos de somatostatina de catorce aminoácidos lo suficientemente estructurados como para

obtener las estructuras de sus conformaciones mayoritarias. En todos los casos, se observó que una interacción aromática entre los residuos Ar6-Ar11 estabilizaba la conformación mayoritaria. Así pues, estos péptidos eran más estructurados que la hormona natural y, como resultado, tenían un perfil más selectivo frente a ciertos receptores.

Compuestos con Msa y D-Trp8: Tras descubrir que los análogos con un residuo de Msa en su secuencia poblaban una conformación mayoritaria en disolución, decidimos ir un paso más allá. Se sabe que la sustitución del triptófano por su enantiómero en posición 8 (D-Trp8) incrementa la estabilidad del péptido correspondiente mientras que no influye excesivamente en su perfil de actividad biológica (de ahí las similitudes tanto estructurales como relativas a la actividad biológica entre SRIF y su análogo [D-Trp8]-SRIF).²⁸ Por ello, introdujimos esta modificación extra en nuestros péptidos (**48-49**).

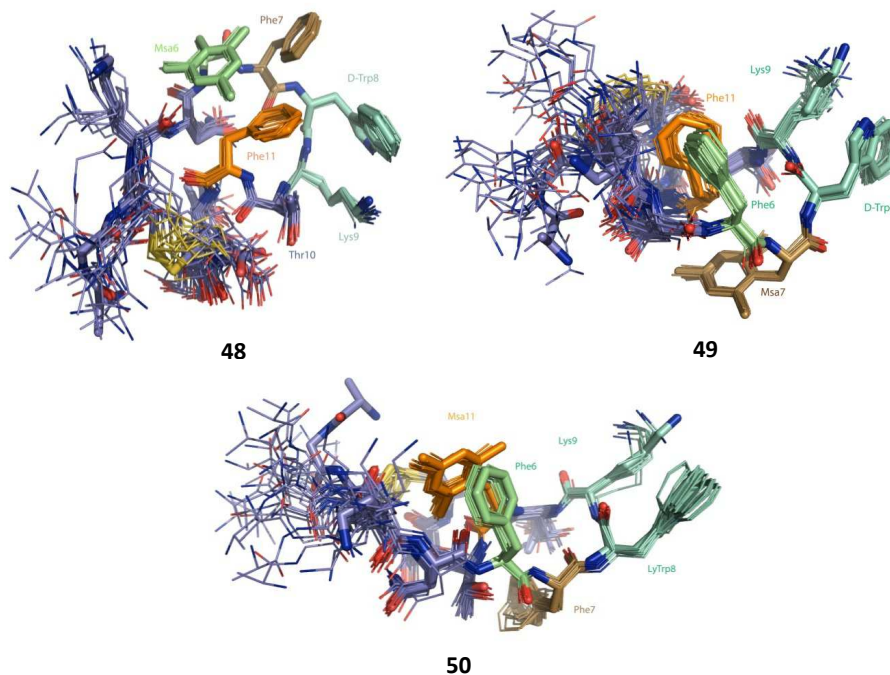


Figura S.5. Superimposición de los conformeros de menor energía que casan mejor con los datos experimentales de RMN de los péptidos [L-Msa6_D-Trp8]-SRIF (**48**), [L-Msa7_D-Trp8]-SRIF (**49**) y [L-Msa11_D-Trp8]-SRIF (**50**).

28 J. Rivier, M. Brown, W. Vale, *Biochem. Biophys. Res. Commun.* **1975**, 65, 746-75.

Estudios de RMN demostraron que estos péptidos tienen una mayor rigidez conformacional no sólo que la hormona natural, sino también que el primer grupo de análogos, aunque aquellos péptidos que contenían la Msa en las mismas posiciones (con L- ó D-Trp8) presentaban estructuras muy similares. Las estructuras de sus conformaciones mayoritarias en disolución fueron caracterizadas y estudiadas en detalle (Figura S.5).

El análogo **49** fue el más interesante de la serie, puesto que la Msa7 no se involucra en ningún tipo de interacción aromática, sino que se posiciona bajo la molécula favoreciendo la interacción (por repulsiones electrónicas y/ó estéricas) entre Phe6-Phe11. Éste fue el análogo más estructurado de este grupo de compuestos, y presentó una potente actividad y selectividad frente al receptor SSTR2, que es el receptor de somatostatina con mayor importancia farmacológica.

Compuestos con más de un residuo de Msa: Por técnicas de RMN pudimos comprobar como estos péptidos carecían prácticamente de estructura, probablemente por el conflicto estérico resultante de la introducción de más de uno de estos aminoácidos tan impedidos. Es importante destacar que, estos análogos tan poco estructurados, no presentaban buena afinidad por ninguno de los cinco receptores de somatostatina.

Capítulo 4. Análogos de somatostatina que contienen residuos de Tmp en su secuencia.

La introducción de un residuo de Msa en la secuencia de la hormona natural nos permitió obtener análogos con una gran rigidez conformacional, que hizo posible la caracterización de las estructuras de sus conformaciones mayoritarias. Además, estos péptidos, mucho más rígidos que SRIF y [D-Trp8]-SRIF, mostraron una alta actividad y selectividad frente a diferentes receptores. Nosotros consideramos que el impacto estructural causado por la Msa es debido a su alta hidrofobicidad y

densidad electrónica (y por ello intensifica ciertas interacciones aromáticas) y/ó a la rigidez intrínseca de su cadena lateral causada por la doble sustitución en *orto*- (lo que limita la movilidad de ésta, un efecto que podría extenderse a toda la arquitectura peptídica).

Sin embargo, no teníamos ningún tipo de cuantificación sobre cuál de los dos efectos (electrónicos o estéricos) contribuye en mayor medida a la rigidez conformacional de estos análogos. Para intentar responder esta cuestión, sintetizamos tres análogos de [D-Trp8]-SRIF conteniendo un residuo de Tmp en las posiciones 6, 7 u 11. Aparte de su diferente estructura, la hidrofobicidad y las propiedades electrónicas de este aminoácido aromático no natural son muy similares a las de la Msa, pero en este caso los metilos no limitan la movilidad de su cadena lateral (Figura S.6).

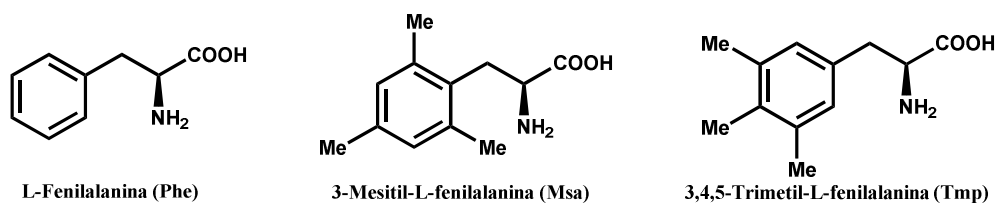


Figura S.6. Los aminoácidos aromáticos Phe, Msa y Tmp.

Los estudios de *binding* demostraron que aquellos análogos con Tmp o Msa en las mismas posiciones, tenían perfiles de selectividad muy similares frente a los cinco receptores de somatostatina (Tabla S.3).

No solo estos péptidos tenían perfiles de actividad muy similares a los análogos que contienen residuos de Msa, sino que además, las estructuras de sus conformaciones mayoritarias en disolución (que fueron determinadas por estudios de RMN y cálculos computacionales) eran muy semejantes. Como ejemplo, en la Figura S.7 se muestra la estructura del péptido **56**, que contiene un residuo de Tmp en posición 7. Esta conformación es muy similar a la del péptido **49**, que contienen una Msa en la misma posición.

Tabla S.3. Tiempos de vida media en suero humano y valores de K_i (nM) de SRIF, [D-Trp8]-SRIF, octreótido y análogos para los receptores SSTR1-5. ^a

	SSTR1	SSTR2	SSTR3	SSTR4	SSTR5	$t_{1/2}$ (h) ^b
Somatostatin, SRIF	0.43 ±0.08	0.0034 ±0.0006	0.53 ±0.21	0.74 ±0.07	0.23 ±0.04	2.75
[D-Trp8]-SRIF	0.32 ±0.11	0.0027 ±0.0020	0.61 ±0.02	5.8 ±0.4	0.46 ±0.24	19.7
Octreótido	300 ±85	0.029 ±0.012	15 ±6	>10 ³	11±2	200
[L-Msa6_D-Trp8]-SRIF, 48	3.1 ±0.9	4.6 ±0.7 ^c	0.78 ±0.10	4.7 ±0.9	0.36 ±0.03	26
[L-Msa7_D-Trp8]-SRIF, 49	0.33 ±0.09	0.0063 ±0.0011	7.5 ±0.6	>10 ³	>10 ³	25
[L-Msa11_D-Trp8]-SRIF, 50	3.4 ±1.3	0.14 ±0.06 ^c	1.3 ±0.2	>10 ³	0.73 ±0.19	41
[L-Tmp6_D-Trp8]-SRIF, 55	t.b.d.	2.8 ±1.1	0.64 ±0.18	t.b.d.	0.32 ±0.07	t.b. d
[L-Tmp7_D-Trp8]-SRIF, 56	t.b.d.	0.0086 ±0.0008	5.6 ±0.5	t.b.d.	49 ±6	t.b. d
[L-Tmp11_D-Trp8]-SRIF, 57	t.b.d.	0.74 ±0.32	9.7 ±2.6	t.b.d.	2.5 ±0.8	43

a: Las celdas sombreadas representan valores cercanos a los de la hormona natural. b: Tiempo de vida media en suero humano. c: Valores determinados por la Dra. M. A. Cortes en la Universidad de Alcalá de Henares. t.b.d.: Pendiente de ser determinado.

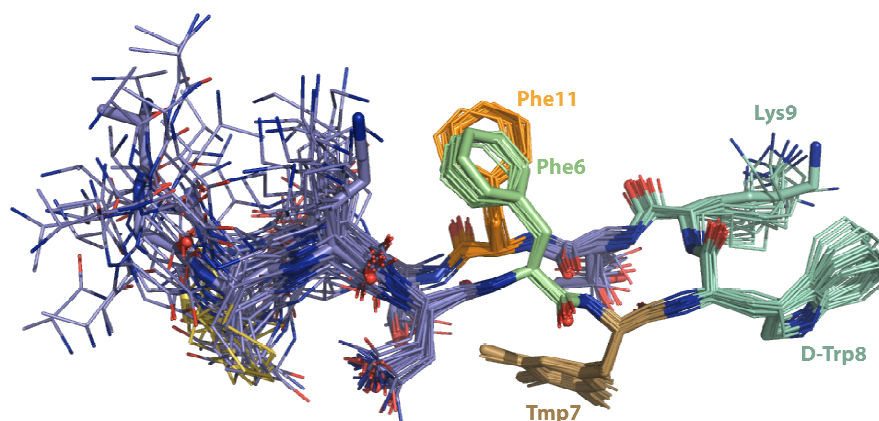


Figura S.7. Estructura de la conformación mayoritaria en disolución del análogo [L-Tmp7_D-Trp8]-SRIF (56), obtenida a partir de los datos experimentales de RMN.

Esto prueba que la introducción de un residuo altamente hidrofóbico y con una alta densidad electrónica en posición 7, desplaza el equilibrio conformacional de la hormona natural hacia una conformación mayoritaria en la que la cadena lateral de dicho residuo se coloca bajo la molécula estabilizando la estructura, mientras que las

dos Phe6-Phe11 están implicadas en una interacción aromática de tipo *edge-to-face*. Probablemente esta interacción no covalente es el factor es el que más contribuye a la rigidez conformacional de este análogo. Por otro lado, las cadenas laterales de D-Trp8 y Lys9 siempre se encuentran una cerca de la otra, debido al gran número de NOEs que se observan en todos los espectros de NOESY entre ellas. Esto prueba que, como es sabido, las cadenas laterales de D-Trp8 y Lys9 están implicadas en una interacción de tipo hidrofóbico que juega también un pequeño papel en la estabilización extra de la parte farmacofórica de la molécula. Al igual que su homólogo de Msa, este péptido ([L-Tmp7_D-Trp8]-SRIF, **56**) mostró una excelente selectividad y actividad frente al receptor SSTR2, lo que nos ha llevado a postular que la estructura mayoritaria que estos péptidos adoptan en disolución debería ser muy similar a la que adopta la hormona natural cuando se une a dicho receptor.

Capítulo 5. Análogos lineales de somatostatina que contienen el fragmento L-Msa7_D-Trp8.

Tras descubrir que los análogos tetradecapeptídicos de somatostatina que contenían un residuo de Msa ó Tmp en posición 7 (y D-Trp8) mostraban gran afinidad y selectividad por SSTR2, pensamos en estudiar este efecto en la ausencia del enlace disulfuro. Para ello, sintetizamos un péptido conteniendo el fragmento L-Msa7_D-Trp8 y dos residuos de alanina en posiciones 3 y 14 (péptido [L-Ala3,14_Msa7_D-Trp8]-SRIF (**58**)), sustituyendo a las dos cisteínas naturales. Por otro lado, y para seguir estudiando hasta qué punto una interacción entre dos fenilalaninas es capaz de estabilizar la estructura de análogos de somatostatina, sintetizamos un péptido conteniendo el fragmento L-Msa7_D-Trp8 incluyendo dos fenilalaninas en lugar de las cisteínas naturales (Phe3 y Phe14, péptido [L-Phe3,14_Msa7_D-Trp8]-SRIF (**59**)).

Estudios de RMN demostraron que, aun teniendo una alta flexibilidad conformacional, estos dos péptidos mantenían el β -turn, pues se identificaron bastantes NOEs entre residuos que se encuentran enfrentados. Estos estudios

también demostraron una mayor población en conformación de β -sheet del péptido **59** (Phe3,14) en comparación con **58** (Ala3,14). Esto sugiere que una interacción aromática extra entre Phe3 y Phe14 juega un cierto papel en la estabilización de **59**. Los estudios de *binding* demostraron que ambos péptidos son altamente selectivos y moderadamente activos frente al receptor SSTR2 (Tabla S.4). Esta alta actividad en SSTR2 ha sido atribuida al papel fundamental del fragmento L-Msa7_D-Trp8, que ejerce su papel de estabilización en la parte del farmacóforo incluso en ausencia del puente disulfuro. Por una parte, la Msa7 se posiciona debajo de la molécula ayudando a las dos Phe6-Phe11 a asociarse en una interacción aromática que estabiliza la conformación que hemos postulado como bioactiva en SSTR2. Por otra parte, el D-Trp8 posiciona su cadena lateral hacia la cadena alifática de la Lys9. Estos dos residuos estabilizan el *hairpin* vía una interacción hidrofóbica entre sus cadenas laterales. La alta actividad en SSTR2 de estos análogos tan flexibles también llevo a pensar que el residuo aromático en posición 7 podría estar involucrado en una interacción directa con dicho receptor.²⁹

Table S.4. Valores de K_i (nM) de SRIF, [D-Trp8]-SRIF, octreótido y análogos para los receptores SSTR1, SSTR3 y SSTR-5.^a

	SSTR2	SSTR3	SSTR5
Somatostatina	0.0034 ±0.0006	0.14 ±0.03	0.072 ±0.018
[D-Trp8]-SRIF	0.0027 ±0.0020	0.24 ±0.03	0.046 ±0.18
Octreótido	0.029 ±0.012	8.4 ±1.1	4.2 ±0.6
[L-Phe3,14_Msa7_D-Trp8]-SRIF, 59	0.069 ±0.013	> 10 ³	> 10 ³
[L-Ala3,14_Msa7_D-Trp8]-SRIF, 58	0.093 ±0.017	> 10 ³	> 10 ³

a: Las celdas sombreadas representan valores cercanos a los de la hormona natural

²⁹ La posibilidad de que el residuo en posición 7 esté implicado en una interacción directa con SSTR2 había sido propuesta anteriormente: S. Neelamkavil, B. Arison, E. Birzin, J. Feng, K. Chen, A. Lin, F. Cheng, L. Taylor, E. R. Thornton, A. B. Smith III, R. Hirschmann, *J. Med. Chem.* **2005**, *48*, 4025-4030.

Capítulo 6. Análogos tetradecapeptídicos de somatostatina que contienen el residuo Dfp.

En este capítulo, estudiamos la sustitución de las Phe naturales en posiciones 6, 7 u 11, por el aminoácido Dfp. Elegimos este residuo porque pensamos que su hidrofóbica cadena lateral aromática pobre en electrones podría asociarse eficientemente con las fenilalaninas restantes vía interacción aromática. Además, este residuo es prácticamente de igual tamaño que la Phe, por lo que el impacto estérico derivado de su introducción en la secuencia de SRIF debería ser mínimo.³⁰

Los ensayos de *binding* demostraron que estos péptidos tenían perfiles de actividad de gran interés, siendo bastante activos y selectivos frente a distintos receptores (Tabla S.5).

Tabla S.5. Valores de K_i (nM) de SRIF, [D-Trp8]-SRIF, octreótido y análogos para los receptores SSTR1-5.^a

	SSTR2	SSTR3	SSTR5
Somatostatin	0.0034 ±0.0006	0.14 ±0.03	0.072 ±0.018
[D-Trp8]-SRIF	0.0027 ±0.0020	0.24 ±0.03	0.046 ±0.018
Octreótido	0.029 ±0.012	8.4 ±1.1	4.2 ±0.6
[L-Dfp6_D-Trp8]-SRIF, 60	0.040 ±0.010	1.2 ±0.3	0.060 ±0.008
[L-Dfp7_D-Trp8]-SRIF, 61	0.18 ±0.07	0.58 ±0.12	0.18 ±0.05
[L-Dfp11_D-Trp8]-SRIF, 62	0.025 ±0.006	3.7 ±1.7	0.36 ±0.09

a: Las celdas sombreadas representan valores cercanos a los de la hormona natural.

Estudios de RMN bidimensionales demostraron que aquellos péptidos que tenían un residuo de Dfp y D-Trp8 tenían una gran rigidez conformacional y poblaban una conformación mayoritaria en disolución, lo que nos llevó a pensar que ciertas interacciones no covalentes habían sido intensificadas en comparación con la hormona natural. Esto nos permitió caracterizar sus estructuras tridimensionales por técnicas combinadas de RMN y computacionales (Figura S.8).

30 M. Salwiczek, E. K. Nyakatura, U. I. M. Gerling, S. Ye, B. Kokschi, *Chem. Soc. Rev.* **2012**, *41*, 2135-2171.

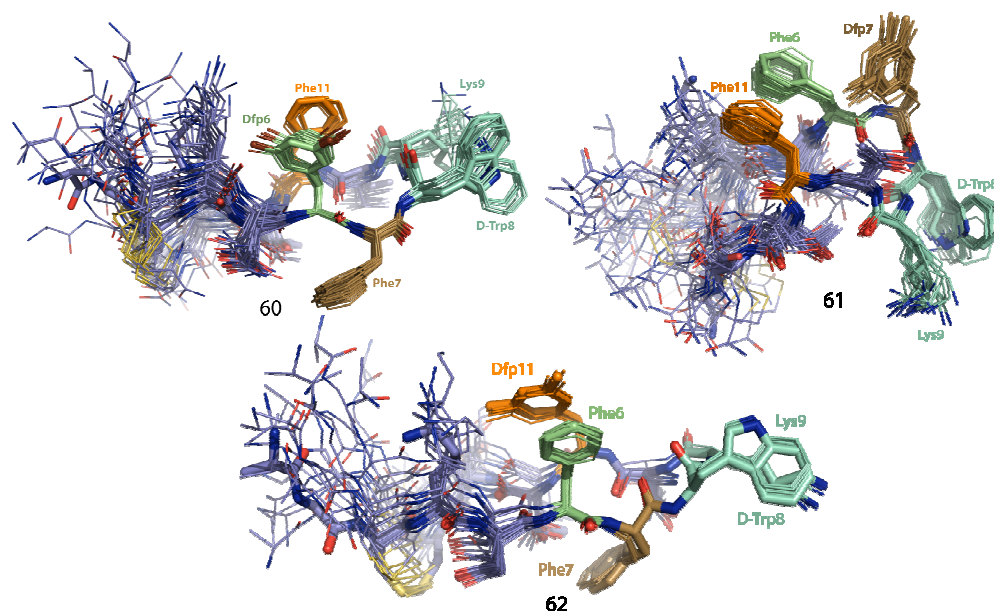


Figura S.8. Superimposición de los conformeros de menor energía obtenida a partir de los datos experimentales de RMN de los péptidos [L-Dfp6_D-Trp8]-SRIF (**60**), [L-Dfp7_D-Trp8]-SRIF (**61**) y [L-Dfp11_D-Trp8]-SRIF (**62**).

La geometría de las interacciones aromáticas entre los residuos Ar6-Ar11 han sido explicadas tanto en términos del modelo electrostático y “polar- π ” propuesto por Hunter y Sanders,³¹ y Cozzi y Siegel,³² respectivamente, como en términos del modelo de “interacción local-directa” descrito por Wheeler.³³

El primer modelo explica por qué se dan geometrías de tipo *face-to-face* cuando un residuo de Dfp está implicado en la interacción aromática: se considera que los ciclos aromáticos pobres en electrones favorecen interacciones de tipo π -stacking, debido a que los sustituyentes electroatrayentes disminuyen la densidad electrónica del anillo y por lo tanto atenúa las repulsiones electrónicas entre éstos. El segundo modelo podría explicar la orientación de la cadena lateral del Dfp (véase como ejemplo el péptido [L-Dfp6_D-Trp8]-SRIF, **60**), dado que los dos anillos se orientan de tal manera que los protones -parcialmente cargados positivamente- de la Phe solapan con los átomos de flúor que muestran una carga negativa parcial-.

31 C. A. Hunter, K. R. Lawson, J. Perkins, C. J. Urch, *J. Chem. Soc., Perkin Trans. 2* **2001**, 0, 651-669.

32 F. Cozzi, F. Ponzini, R. Annunziata, M. Cinquini, J. S. Siegel, *Angew. Chem., Int. Ed.* **1995**, 34, 1019-1020.

33 S. E. Wheeler, *J. Am. Chem. Soc.* **2011**, 133, 10262-10274.

El tetradecapéptido que contenía un aminoácido aromático pobre en electrones en posición 11, resultó ser mucho más estructurado que la hormona natural, debido a la intensificación de la interacción Phe6-Dfp11 vs. Phe6-Phe11 (de ahí su más que probable selectividad frente a los receptores SSTR2 y SSTR5). Este descubrimiento fue bastante interesante, puesto que se asumía que aminoácidos aromáticos pobres en electrones en esta posición conllevaban una gran pérdida de estabilidad conformacional, dado que es el residuo en 11 el que apantalla el aminoácido aromático en 6.³⁴

Capítulo 7. Análogos de somatostatina que contienen el aminoácido Cha.

En este punto ya habíamos demostrado que la introducción de ciertos aminoácidos aromáticos podían modular la estructura peptídica de la somatostatina al reforzar ciertas interacciones no covalentes. La intensificación de estas interacciones aromáticas incrementa la estabilidad conformacional de los análogos, pero el origen de ésta, que puede ser dependiente de efectos hidrofóbicos, electrostáticos o por fuerzas de van der Waals, es aún objeto de debate.

Con el fin de investigar, por separado, las contribuciones relativas de la hidrofobicidad y de los factores electrónicos a esta estabilización, estudiamos cuatro análogos de [D-Trp8]-SRIF que incluían residuos de Cha. Aunque es ligeramente mayor que la Phe (10%), este aminoácido no natural tiene una hidrofobicidad y polaridad similar, pero no tiene la capacidad de participar en interacciones aromáticas que sean promovidas por factores electrónicos (Figura S.9). De esta manera, si las interacciones aromáticas en SRIF son más de naturaleza electrostática que hidrofóbica, la sustitución de una o más fenilalaninas naturales por residuos de

34 S. Neelamkavil, B. Arison, E. Birzin, J. Feng, K. Chen, A. Lin, F. Cheng, L. Taylor, E. R. Thornton, A. B. Smith III, R. Hirschmann, *J. Med. Chem.* **2005**, *48*, 4025-4030.

ciclohexilalanina conllevaría una pérdida total o parcial de estructura, que debería reflejarse en los valores de actividad frente a los cinco receptores distintos.

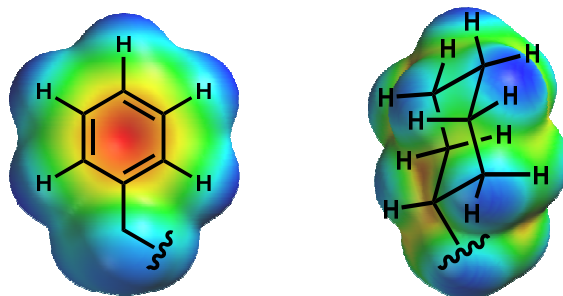


Figura S.9. Mapa de potencial electrostático para la Phe y Cha, en el que quedan claras las diferentes propiedades electrónicas a pesar de su tamaño similar. Las regiones ricas en electrones se observan en rojo. Spartan'10 modelo semiempírico PM3 (Wavefunction, Inc.).

Estudios de RMN demostraron que la estabilidad conformacional de estos análogos era ligeramente menor que la de [D-Trp8]-SRIF. Esta menor estabilidad conformacional era clara en la región farmacofórica, puesto que el desplazamiento a campos altos de los protones γ y de la Lys9 en estos péptidos era moderadamente menor que en [D-Trp8]-SRIF (y notablemente mayor que aquél en [L-Msa7_D-Trp8]-SRIF). El único análogo que mantiene un similar desplazamiento de los protones γ y de la Lys9 es el [L-Cha6_D-Trp8]-SRIF, que de hecho es el que retiene una mayor actividad frente a SSTR2.

Tabla S.6. Tiempos de vida media y valores de K_i (nM) de SRIF, [D-Trp8]-SRIF, octreótido y análogos para los receptores SSTR2, SSTR3 y SSTR5. ^a

	SSTR2	SSTR3	SSTR5	$t_{1/2}$ (h) ^b
Somatostatina	0.0034 ±0.0006	0.14 ±0.03	0.072 ±0.018	2.75
[D-Trp8]-SRIF	0.0027 ±0.0020	0.24 ±0.03	0.046 ±0.18	19.7
Octreótido	0.029 ±0.012	8.4 ±1.1	4.2 ±0.6	200
[L-Cha6_D-Trp8]-SRIF	0.096 ±0.004	4.62 ±1.46	6.00 ±1.40	10
[L-Cha7_D-Trp8]-SRIF	0.61 ±0.09	3.28 ±0.45	0.39 ±0.02	73
[Cha11_D-Trp8]-SRIF	3.3 ±0.3	6.56 ±1.55	4.39 ±1.32	40
[Cha6,11_D-Trp8]-SRIF	0.71 ±0.18	5.37 ±1.02	3.32 ±0.50	t.b.d.

a: Las celdas sombreadas representan valores cercanos a los de la hormona natural. t.b.d.: Pendiente de ser determinado.

Los estudios de afinidad frente a SSTR2, SSTR3 y SSTR5 (Tabla S.6), también mostraron que estos cuatro péptidos mantenían el perfil universal de actividad del compuesto madre, pero sin embargo los valores de sus K_i 's eran considerablemente mayores. Esto encaja con la ligera mayor flexibilidad conformacional de estos análogos. Además, nuestros resultados sugieren que los factores electrónicos son cruciales para dirigir y sostener las interacciones no covalentes entre los residuos aromáticos que estabilizan las conformaciones bioactivas de la hormona natural y sus análogos.

Capítulo 8. Análogos de somatostatina que contienen más de un aminoácido aromático no natural.

Puesto que la simple incorporación de residuos de Msa, Tmp ó Dfp desplazaba el equilibrio conformacional de la hormona natural hacia conformaciones mayoritarias bien definidas, pensamos en introducir más de uno de estos aminoácidos en la misma secuencia, y estudiar su efecto combinado en la estructura y actividad de los análogos correspondientes. Los buenos resultados obtenidos cuando introdujimos una Msa en posición 7 nos llevaron a mantener el fragmento L-Msa7_D-Trp8 en todos los análogos. De esta manera, sustituimos los residuos de fenilalanina en posiciones 6 y 11 por Tmp ó Dfp, para intentar fortalecer dicha interacción aromática. Las sustituciones que hicimos en la secuencia natural de la somatostatina y los péptidos resultantes se resumen en la Tabla S.7.

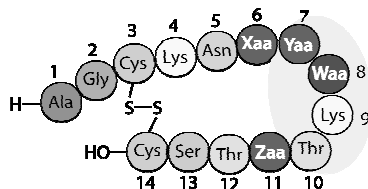


Tabla S.7. Análogos de [L-Msa7_D-Trp8]-SRIF obtenidos al reemplazar las Phe's en posiciones 6 y/6 11 por residuos de Dfp y Tmp.

6 ^a	7 ^a	8 ^a	11 ^a	Análogo
Dfp	Msa	D-Trp	Tmp	[L-Dfp6_Msa7_Tmp11_D-Trp8]-SRIF, 67
Tmp	Msa	D-Trp	Dfp	[L-Tmp6_Msa7_Dfp11_D-Trp8]-SRIF, 68
Dfp	Msa	D-Trp	Dfp	[L-Dfp6,11_Msa7_D-Trp8]-SRIF, 69

Los ensayos de *binding* probaron que, como era de esperar (debido a la presencia del fragmento L-Msa7_D-Trp8 y a la interacción 6-11), estos análogos tenían una alta afinidad y selectividad por el receptor SSTR2 (Tabla S.8).

Tabla S.8. Valores de K_i (nM) de SRIF, [D-Trp8]-SRIF, octreótido y análogos para los receptores SSTR2, SSTR3 y SSTR5. ^a

	SSTR2	SSTR3	SSTR5
Somatostatina	0.0034 ±0.0006	0.14 ±0.03	0.072 ±0.018
[D-Trp8]-SRIF	0.0027 ±0.0020	0.24 ±0.03	0.046 ±0.018
Octreótido	0.029 ±0.012	8.4 ±1.1	4.2 ±0.6
[L-Msa7_D-Trp8]-SRIF, 49	0.0063 ±0.0029	7.5 ±0.6 ^a	>10 ³ ^a
[L-Dfp6_Msa7_Tmp11_D-Trp8]-SRIF 67	0.0037 ±0.0015	19 ±5	11 ±2
[L-Tmp6_Msa7_Dfp11_D-Trp8]-SRIF 68	2.8 ±0.9	23 ±3	2.5 ±1.3
[L-Dfp6,11_Msa7_D-Trp8]-SRIF 69	0.0021 ±0.0006	>10 ²	>10 ²

a: Las celdas sombreadas representan valores cercanos a los de la hormona natural.

La gran rigidez conformacional de todos estos análogos fue comprobada por estudios de RMN. Posteriores cálculos computacionales nos permitieron caracterizar las conformaciones mayoritarias en disolución de estos péptidos, que resultaron ser muy similares a la conformación que hemos postulado como bioactiva en el receptor SSTR2.

Dos de estos análogos resultaron ser especialmente interesantes. El análogo de [L-Msa7_D-Trp8]-SRIF que incluía un Dfp6 y un Tmp11 (péptido **67**) mostró una gran afinidad y selectividad frente al receptor SSTR2. La estructura de su conformación mayoritaria (Figura S.10) expone una clara interacción aromática entre Dfp6 y Tmp11, probablemente fortificada por la posición inferior de la cadena lateral de la Msa7. Por otro lado, una interacción de tipo hidrofóbico entre Lys9-D-Trp8 estabiliza aún más esta conformación fortaleciendo el β -*hairpin*. La estabilidad en suero

humano de este análogo no ha sido aún medida, pero el péptido homólogo conteniendo los mismos aminoácidos no naturales en posiciones distintas (*i.e.* [L-Tmp6_Msa7_Dfp11_D-Trp8]-SRIF (**68**)) tiene un tiempo de vida media de 87 h. Este resultado nos lleva a esperar que el análogo (**67**) posea una gran estabilidad en suero, lo que le convertiría en un firme candidato como agonista del receptor de somatostatina SSTR2 en el mercado farmacéutico.

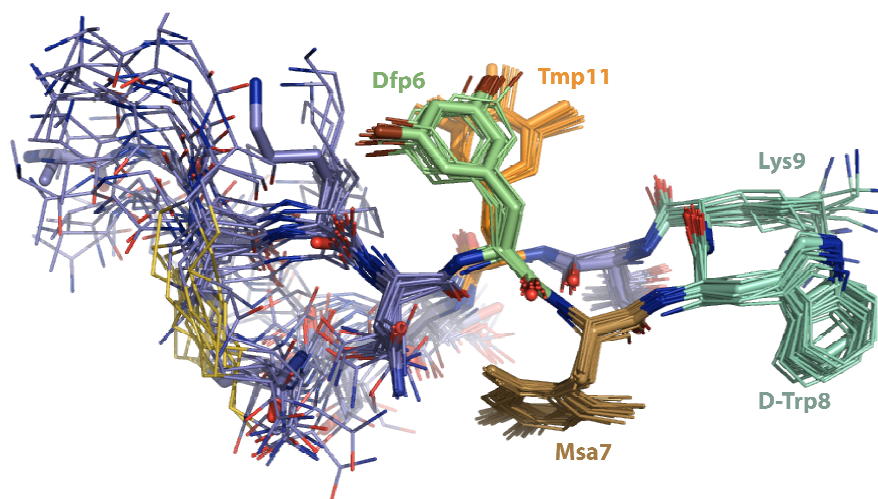


Figura S.10. Superimposición de los conformeros más estables [L-Dfp6_Msa7_Tmp11_D-Trp8]-SRIF (**67**) obtenida mediante cálculos computacionales utilizando los datos experimentales de RMN.

Otro de los análogos demostró tener una conformación muy similar, pero aún si cabe una mayor afinidad y sobre todo selectividad frente al receptor SSTR2. Se trata del péptido [L-Dfp6,11_Msa7_D-Trp8]-SRIF (**69**), que presumiblemente también debería de mostrar una gran estabilidad en suero debido a que contiene cuatro aminoácidos no naturales y muestra una rigidez conformacional excepcional. La estructura de su conformación mayoritaria se muestra en la Figura S.11, que presenta la típica conformación bioactiva en SSTR2 con una interacción aromática entre los dos residuos de Dfp6 y Dfp11 que jugaría un papel fundamental en la estabilización de esta conformación. Aunque la orientación de las cadenas laterales de los Dfp no ha podido ser refinada por RMN (al intercambiar cuatro de los protones aromáticos por átomos de flúor, perdemos una gran cantidad de información estructural, pues se pierden los NOEs entre ellos), una interacción de tipo *face-to-face* es la que mejor casa con los datos experimentales de resonancia

magnética nuclear. Esto coincide con el modelo electrostático^{31,32} que sostiene que una interacción entre dos residuos aromáticos pobres en electrones es más fuerte, puesto que los sustituyentes electroatrayentes disminuyen la densidad electrónica de los ciclos, haciendo mínimas las repulsiones entre ellos.

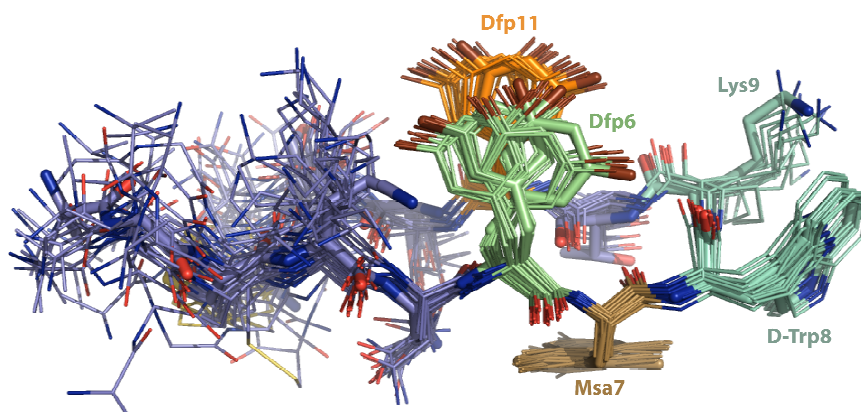
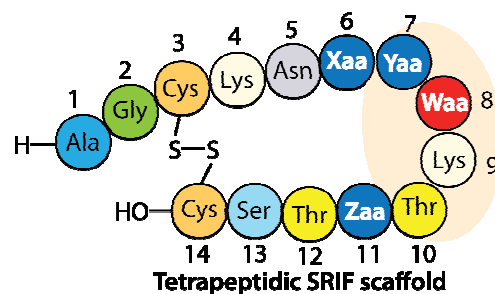


Figura S.11. Superimposición de los conformeros más estables [L-Dfp6,11_Msa7_D-Trp8]-SRIF (69) obtenida mediante cálculos computacionales utilizando los datos experimentales de RMN.

Los estudios con análogos tetradecapeptídicos de somatostatina nos han permitido obtener abundante información estructural que hasta ahora no había sido accesible tras décadas de estudios con octapéptidos. No sólo hemos obtenido éxito desde el punto de vista académico, sino que además, esperamos que estos análogos que muestran una gran actividad y selectividad frente a SSTR2 (mucho mejor que la que presentan los octapéptidos comerciales) y presumiblemente una alta estabilidad metabólica, podrán competir en el mercado con octreótido, lanreótido y vapreotide como agonistas de SSTR2.

Appendix II

**Index of SRIF analogs
(in order of appearance)**



Somatostatin analogs obtained by replacement of the Phe in positions 6, 7, 8 and 11 by non-natural aromatic amino acids.

Msa containing analogs
[L-Msa6]-SRIF, 45
[L-Msa7]-SRIF, 46
[L-Msa11]-SRIF, 47
[L-Msa6_D-Trp8]-SRIF, 48
[L-Msa7_D-Trp8]-SRIF, 49
[L-Msa11_D-Trp8]-SRIF, 50
[L-Msa6,7]-SRIF, 51
[L-Msa6,11]-SRIF, 52
[L-Msa7,11]-SRIF, 53
[L-Msa6,7,11]-SRIF, 54
Tmp containing analogs
[L-Tmp6_D-Trp8]-SRIF, 55
[L-Tmp7_D-Trp8]-SRIF, 56
[L-Tmp11_D-Trp8]-SRIF, 57
Linear analogs
[L-Ala3,14_Msa7_D-Trp8]-SRIF, 58
[L-Phe3,14_Msa7_D-Trp8]-SRIF, 59
Dfp containing analogs
[L-Dfp6_D-Trp8]-SRIF, 60
[L-Dfp7_D-Trp8]-SRIF, 61
[L-Dfp11_D-Trp8]-SRIF, 62
Cha containing analogs
[L-Cha6_D-Trp8]-SRIF, 63
[L-Cha7_D-Trp8]-SRIF, 64
[L-Cha11_D-Trp8]-SRIF, 65
[L-Cha6,11_D-Trp8]-SRIF, 66
Multiple incorporations
[L-Dfp6_Msa7_Tmp11_D-Trp8]-SRIF, 67
[L-Tmp6_Msa7_Dfp11_D-Trp8]-SRIF, 68
[L-Dfp6,11_Msa7_D-Trp8]-SRIF, 69

